universität wien

MASTERARBEIT

Titel der Masterarbeit

"Impact of *Alternaria* toxins on CYP1A1- and GST-expression in human tumour cells"

Verfasserin

Katharina Anna Domnanich Bakk. rer. nat.

angestrebter akademischer Grad

Master of Science (MSc)

Wien, 2012

Studienkennzahl lt. Studienblatt:	A 066 862
Studienrichtung lt. Studienblatt:	Chemie
Betreuerin / Betreuer:	Univ.-Prof. Dr. Doris Marko, Dr. Gudrun Pahlke

I am among those who think that science has great beauty.

A scientist in his laboratory is not only a technician:

he is also a child placed before natural phenomena

which impress him like a fairy tale.

Marie Curie (1867 - 1934)

Acknowledgement

First I want to thank Prof. Dr. Doris Marko for providing me the interesting topic.

I offer my sincerest gratitude to my supervisor, Dr. Gudrun Pahlke, who supported me throughout my thesis with her knowledge, whilst allowing me the room to work in my own way.

I would also like to thank the whole working group for their support and the pleasant atmosphere. In particular, I would like to thank Elisabeth Schwarz for reviewing my thesis and my fellow student Martina Dicker and Melanie Brunner. Both of them alleviated my day-to-day work in the laboratory with their cheerful mood and offered their assistance whenever needed.

The support and care of my friends helped me to overcome setbacks and stay focused on my studies. At this point I would like to thank Ann-Katrin Holik for the long discussions that helped me, to see a lot of things from another angle and Tina Dilhof, who always lent me an ear when I needed to talk.

Finally, none of this would have been possible without the patience and support of my family, who aided and encouraged me throughout all my studies at university and at school.

Table of Contents

List of Abbreviations

Ab	antibody
ABC-transporter	ATP-binding cassette transporter
Ago-2	argonaute 2
AhR	aryl hydrocarbon receptor
ALP	alkaline phosphatase
ALT	altenuene
AME	alternariol monomethyl ether
AOH	alternariol
APS	ammonium peroxide sulphate
ARE	antioxidant responsive element
Arnt	aryl hydrocarbon nuclear translocator
ARO	aroclor
ATP	adenosine triphosphate
ATX-I, -II, -III	altertoxin I, II, III
a_w	water activity
BaP	benzo(a)pyrene
Bax	Bcl-2 associated X protein
BfR	Bundesinstitut für Risikobewertung, Deutschland/ German Federal Institute for Risk Assessment
bHLH	basic helix-loop-helix
BSA	bovine serum albumin
BSA	bovine serum albumin
BSO	buthionine sulfoximine
cDNA	complementary DNA
CDNB	1-chloro-2,4- dinitrobenzene
CGA	chlorogenic acid
CSCF	Czech Scientific Committee on Food
C_T	threshold cycle
CYP	cytochrome P450 monooxygenase
CYP1A1	cytochrom P450 monooxygenase 1A1
df	dilution factor

DMEM	Dulbeccos´s Modified Eagle Medium
DMSO	dimethyl sulphoxide
DNA	desoxyribonucleic acid
DRE	dioxin responsive element
dsRNA	double-stranded RNA
EDTA	ethylenediaminetetraacetic acid
ER	estrogen receptor
EROD	ethoxyresorufin-*O*-deethylase
FAO	Food and Agriculture Organisation
FBS	fetal bovine serum
GSH	reduced glutathione
GST	glutathione-S-transferase
HAH	halogenated aromatic hydrocarbon
HPLC	High Performance Liquid Chromatography
HPRT	hypoxanthine-guanine phosphoribosyltransferase
HRP	horse radish peroxidase
I3C	indole-3-carbinol
IC_{50}	half maximal inhibitory concentration
ICZ	indolo-(3,2,-b) carbazole
IEP	isoelectric point
Kat	catalase
MEN	menadione
miRNA	micro RNA
MNF	3´-methoxy-4´-nitroflavone
8-MP	8-methoxypsoralen
mRNA	messenger RNA
MRP	multidrug resistance protein
NADH	nicotinamide adenine dinucleotide
NADPH	nicotinamide adenine dinucleotide phosphate
NES	nuclear export signal
α-NF	α-naphthoflavone
NLS	nuclear localisation signal

NQO1	NAD(P)H quinone oxidoreductase 1
nt	nucleotide
OATP 2	organic anion transporting polypeptide 2
P	passage
P/S	penicillin/ streptomycin
PAGE	polyacrylamide gel electrophoresis
PAH	polyaromatic hydrocarbon
PAS	Per, Arnt, Sim
PBS	phosphate buffered saline
PCB	polychlorinated biphenyl
PCDD	polychlorinated dibenzodioxin
PCR	polymerase chain reaction
P-gp	P-glycoprotein
PTGS	posttranscriptional gene silencing
qRT-PCR	quantitative real time PCR
Que	quercetin
RISC	RNA-induced silencing complex
RNA	ribonucleic acid
RNAi	RNA interference
rRNA	ribosomal RNA
RQ	relative quantity
RT	reverse transcription
SD	standard deviation
SDS	sodium dodecyl sulphate
SFN	sulforaphane
siRNA	short interfering RNA
spp.	*species pluralis*
SRB	sulforhodamine B
ssDNA	single-stranded DNA
T/C	test over control
Taq	*Thermus aquaticus*
tBHP	tert-butylhydroperoxide

tBHQ	tert-butylhydroquinone
TCDD	2,3,7,8- tetrachlorodibenzo-p-dioxin
TeA	tenuazonic acid
TEMED	*N,N,N´,N´*- tetramethylethylendiamine
TK	thymidine kinase
Tri	trigonelline
Tris	tris(hydroxymethyl)-aminomethan
TTS	Threshold of Toxicological Concern
tRNA	transfer RNA
UGT	UDP-glucuronosyl transferase
UPD	uridine diphosphate
UTR	untranslated region
XAP2	X-associated protein 2
XRE	xenobiotic responsive element

1. Introduction

Fungi are ubiquitous pathogens and represent a considerable health risk. A variety of different species are accountable for fungal diseases, allergies or have the ability of mycotoxin production. Mycotoxins are secondary metabolites, produced by diverse fungi. They are of diverse chemical structures and properties, which explains their various biological effects and toxicological endpoints.

Alternaria spp. belong together with *Penicillia*, *Fusaria* and *Aspergilla* to the groups of fungi producing mycotoxins. Many species are known to infest organic matter, furnishings and above all, they are common postharvest pathogens of diverse foodstuffs and can cause spoilage in the field and during storage (Barkai-Golan & Paster, 2008).

Especially mycotoxin contamination of agricultural commodities represents a serious problem. The “Food and Agriculture Organisation” (FAO) has recently pointed out that at least 25% of the world wide produced grain are infested with mycotoxins. Based on the ability of *Alternaria* to grow in tropic, subtropic and even temperate climate zones, they are most commonly involved in pathogenesis. Even more serious than economic loss due to infested foodstuffs, are diseases directly associated with mycotoxin contamination- the so called mycotoxicoses. In the 90-ies consumption of *Alternaria* contaminated grain has been associated with an increased incidence of oesophageal cancer in Linxian, China (Liu *et al.*, 1992). Furthermore, *Alternaria* extracts and single *Alternaria* toxins, like the main secondary metabolites alternariol (AOH) and alternariol monomethyl ether (AME) have shown considerable toxic potential (Pero *et al.*, 1973; Liu *et al.*, 1992).

Several reviews on *Alternaria* toxins have been published over the last few decades. However, the European Food Safety Authority (EFSA) has recently pointed out that there does not exist any relevant toxicity data for *Alternaria* toxins for identification of reference points for different toxicological effects. The Threshold of Toxicological Concern (TTC) approach has been applied on the data published about *Alternaria* toxins (including AME, AOH, TeA, TEN) so far. The estimated chronic dietary exposure to AME and AOH exceeds the relevant TTC value, indicating a need for additional compound-specific toxicity data (EFSA, 2011)

For a better risk assessment of xenobiotics such as mycotoxins, the metabolic pathway has to be elucidated. In the present thesis, the impact of AME and AOH with regard to the phase I enzyme cytochrome P450 CYP1A1 and the phase II enzyme glutathione-S-transferase in human oesophagus and colon carcinoma cells have been investigated.

2. Theoretical Background

2.1. *Alternaria* Toxins

Mycotoxins are secondary metabolites of fungi that are produced during the growth or storage of plant products. The synthesis of these secondary metabolites takes away energy from the growing fungi. Thus formation of mycotoxins occurs only if required for the fungal organism. The function of mycotoxins in fungi may be the suppression of bacterial growth or of other competing moulds. On the other hand mycotoxins cause toxic effects in other eukaryotic cells (Wexler *et al.*, 2005).

Mycotoxins of the genus *Alternaria* have recently received increasing attention, both in research programmes as well as in risk assessment studies. An example is the 4 year project “Safe organic vegetables and vegetable products by reducing risk factors and sources of fungal contaminants throughout the production chain: the carrot- *Alternaria* model” established by the European Union from 2000 to 2004. The objective was to develop detection methods, identifying *Alternaria* mycotoxin risks in the production chain and developing preventive measures. Since the carrot is one of the most popular vegetables of European consumers, it was chosen as model system. Based on the results of the study, *Alternaria* mycotoxins in organic carrots do not represent a hazard for consumers (EuropeanComission, 2003; Solfrizzo *et al.*, 2004).

2.1.1. The *Alternaria* Species

Alternaria is a genus of ascomycetes fungi and belongs to the class of Dothideomycetes. The genus of *Alternaria* was originally described in 1817 (Esenbeck & Daniel, 1817). According to a statement of the German Federal Institute of Risk Assessment (BfR) in 2003 depending on the source of information, *Alternaria spp.* are ubiquitous pathogens and saprophytes. They are among the most common postharvest pathogens of fruits and vegetables and can cause spoilage in the field as well (Ostry, 2008). Decaying wood, wood pulp, wall paper and compost are other known substrates of *Alternaria* (Gravesen *et al.*, 1994).

Alternaria alternata is regarded as the major mycotoxin producing species, although *A. citri, A. solani, A. longipes, A. tenuissima, A. arborescens* and *A. infectoria* are also able to produce characteristic *Alternaria* toxins (Barkai-Golan & Paster, 2008). *A. alternata* produces a variety of mycotoxins although the major compounds are alternariol, alternariol monomethyl ether, altenuene, tenuazonic acid and altertoxin I (Scott, 2001).

2.1.2. Morphology of *Alternaria*

The colonies of *Alternaria spp.* are black to olive-black or greyish and are suede-like to floccose. *Alternaria* species have septate, dark hyphae. The conidia may be observed singly or in acropental branched chains and may produce gem tubes. The end of the conidium is round, while it tapers at the apex (Murray *et al.*, 2007).

Figure 1: Morphology of *Alternaria alternata* (http://www.schadstofffrei.de/schimmelpilz-allergie.htm, http://www.mycology.adelaide.edu.au)

2.1.3. Significance of *Alternaria* Species & *Alternaria* Toxins as Pathogens of various Foodstuffs

Alternaria spp. are capable to produce more than 120 potentially toxic secondary metabolites. Most of them are phytotoxins, which play an important role in the pathogenesis of plants. However among them there are some mycotoxins which can be harmful for humans and animals (Panigrahi, 1997; Ostry, 2008).

The optimal growth conditions for *Alternaria spp*. are between 22 - 28°C, but they are also capable to grow at lower temperatures, with minimal temperatures as low as -3°C. Thus *Alternaria* species are involved in spoilage during refrigerated storage (Sommer, 1985). *Alternaria alternata* generally is not able to penetrate directly through the plant paring, lesions like injured tissue are required for infection. These injuries mostly happen during harvesting or handling. The initiation of infection often occurs at the stem scar of tomatoes (figure 2 A), peppers and eggplants. (Barkai-Golan, 2002). Cucumbers, squashes and melons are frequently infected after being weakened by sun-scald, chilling injury or over-ripeness (Snowdon, 1992). *A. alternata* is associated with the core rot in apples (figure 2 B). A recent study suggests that the major pathogen of Top Red apples in South Africa belongs to *A. tenuissima* (Serdani M., 2002).

A **B**

Figure 2: Tomatoes (A) and apples (B) infected with *Alternaria alternata* (http://www.extension.umn.edu and http://postharvest.tfrec.wsu.edu/)

The most important *Alternaria* toxins are alternariol (AOH), alternariol monomethyl ether (AME), altenuene (ALT), altertoxins I, II, III (ATX-I, -II, -III) and tenuazonic acid (TeA). They belong to three different classes of chemical structures, depictured in figure 3 (Ostry, 2008).

- dibenzopyrone derivatives: AOH, AME, ALT
- perylene derivatives: ATX-I, -II, -III
- tetramic acid derivatives: TeA

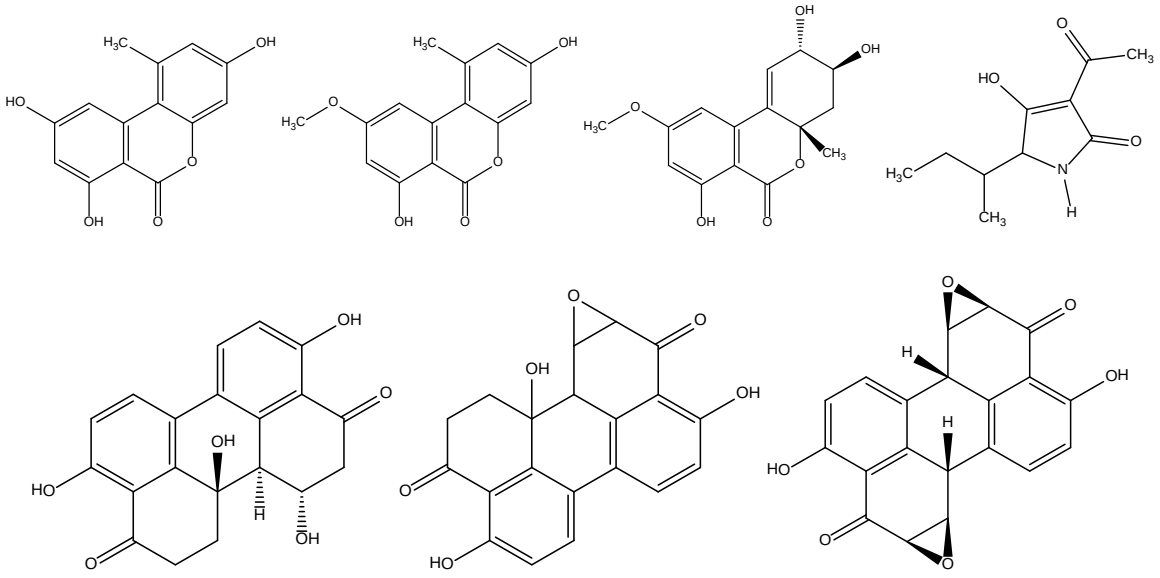

Figure 3: Chemical Structure of AOH, AME, ALT, TeA (upper row) and ATX-I, -II, -III (bottom row) (Ostry, 2008)

Scott (2011) reviewed the natural occurrence of *Alternaria* toxins in various fruits and vegetables visibly infected by *Alternaria spp*. High levels of AOH and TeA were found in apples, tomatoes, mandarins, peppers and olives, increased AME and ALT levels were detected in the latter two as well. The natural occurrence of *Alternaria* toxins in contaminated processed food is of even more interest for human health. TeA was found in tomato products, whereas AOH and AME were present in apple juice. Several other agricultural commodities, including grains, sunflower seeds, oilseed rape, sorghum and pecans were also found to be infested with various *Alternaria* toxins.

The maximum concentrations of *Alternaria* toxins in marketed products were reported to be in the range of 1 - 10^3 µg/kg. Higher levels were only found in samples visibly infected with *Alternaria spp*. (Ostry, 2008). Ackermann *et al.* (2011) developed a comparative enzyme immunoassay method for the determination of low levels of AOH in apple and tomato products. With this analytical system a rapid and easy method is available for the identification of AOH in foods and feeds. Since AOH was found to be very stable in apple juice, even at temperatures up to 80 - 100°C (Scott PM, 2001), and since tomatoes are a most common substrate for *Alternaria* species (da Motta S., 2000), the development of a suitable screening method was highly important. In apple (67%) and tomato products (93%) the alternariol concentration was found with high frequency to be in the range of 1 - 13 µg/kg. Apple and tomato products represent a significant part of the vegetable and fruit consumption in Germany, thus the regular consumption of alternariol contaminated products results in a long-term, low-level daily exposure in the ng/kg bodyweight range (Ackermann *et al.*, 2011).

Siegel *et al.* (2010) investigated the stability of AOH, AME and ALT at the process of bread baking. The results indicated that wet baking barely leads to the degradation of *Alternaria* toxins. However significant degradation occurs at dry baking with stability decreasing in the order of AME > AOH > ALT (Siegel *et al.*, 2010).

2.1.4. Factors affecting the Formation of *Alternaria* Toxins

Since mycotoxin production is influenced by several factors, the presence of fungi does not necessarily imply the presence of toxins. Conditions promoting fungal growth do not necessarily coincide with those responsible for mycotoxin production (Drusch & Ragab, 2003). *Alternaria alternata* is reported as the most important mycotoxin-producing species (Scott, 2001).

Alternaria spp. are flexible pathogens, capable of growing in both arid and humid areas. Factors known to affect production of mycotoxins in fruit include the fruit type, geographical location, climate, pre- and post-harvest treatment, method of harvest, presence of surface

injuries and storage conditions (Barkai-Golan & Paster, 2008). Nevertheless, the pre- and post-harvest key environmental determinants are water availability and temperature (Magan & Olsen, 2004).The water activity (a_w) and temperature limits for *A. alternata* for germination are lower than those for production of ALT, AOH and AME. The absolute a_w limit for germination is 0.86 a_w and for growth and mycotoxin production about 0.88 - 0.89 a_w. Conditions promoting the formation of all three mycotoxin moieties are at about 25°C and >0,97 a_w (Magan N., 1985).

2.1.5. Toxicity of *Alternaria* Toxins

Acute Toxicity

Alternaria Extracts

In the 1980-ies a retrospective survey of cancer mortality in China indicated areas of high-incidence for oesophageal cancer in Linxian country. The occurrence of *Alternaria alternata* contaminated grain in the area of high incidence was noted and a relationship between fungi and oesophageal cancer was proposed (Dong *et al.*, 1987; Liu *et al.*, 1991). The toxicity of the crude extract of *Alternaria spp*. towards mice was investigated by Pero *et al.* (1973). At concentrations of 300 mg/kg body weight the crude extract caused acute toxic effects (Pero *et al.*, 1973). Sauer *et al.* (1978) fed chicken and rats with corn-rice, containing cultures of four isolates of *Alternaria alternata* over a period of 21 days. Toxic symptoms and lethality are caused by culture media of *Alternaria* isolates synthesising TeA and ATX-I. Isolates producing AOH, AME and ALT in varying ratios did not show any deleterious effect (Sauer *et al.*, 1978).

Alternariol & Alternariol Monomethyl Ether

AOH and AME were first isolated from the dried mycelium of *A. tenius* in 1953 and a total synthesis of these substances was performed in 2005 by Koch *et al*. (Raistrick *et al.*, 1953; Koch *et al.*, 2005). The acute toxicity of AME was investigated in several studies and is assessed as low compared with other *Alternaria* toxins (Pero *et al.*, 1973; Sauer *et al.*, 1978). Pero *et al.* (1973) showed that mice treated with either AME or AOH get sedated, display dull eyes, occasional stomach spasms and periodic panting. When treating brine shrimp larvae with AOH-containing medium the 50% lethal concentration was about 100 µg/ml. However, AME was not found to cause any mortality in brine shrimp larvae, although these findings can be due to its poor solubility in the used solvents (Griffin & Chu, 1983).

Altertoxins

Altertoxin I, II and III were isolated the first time in 1973. ATX-I displayed toxic effects in rats, chicken and brine shrimp larvae (Sauer *et al.*, 1978; Griffin & Chu, 1983). ATX-I, -II and -III were found to be mutagenic even without the need of metabolic activation in the Ames test using *Salmonella typhimurium* TA98, TA100, and TA1537. Altertoxin III appeared to be the most mutagenic towards TA98, followed by ATX-II and ATX-I (Stack & Prival, 1986).

Cytotoxicity

The effect of AOH on the proliferation of human endometrial adenocarcinoma Ishikawa cells and Chinese hamster lung fibroblast cells (V79) was assessed by flow-cytometry and electronic cell counting, respectively. The cell number of Ishikawa cells treated with 10 µM AOH for 48 h and 72 h was reduced more than 50%. AOH at a concentration of 25 and 50 µM inhibited proliferation of V79 cells after 6 h of incubation but proliferation resumed when removing AOH (Lehmann *et al.*, 2006). Fehr *et al.* (2010) investigated the cytotoxic effects of AME and AOH toward the vulva carcinoma cell line A431 using the sulforhodamine B (SRB) assay. Concentration-dependent growth inhibitory effects were observed after 24 h and 72 h treatment with AME and AOH, respectively. AOH was more potent than AME, although relatively high concentrations were required.

The cytotoxic activity of AOH, AME, ALT, TeA, ATX-I and -II was investigated toward the human cervical adenocarcinoma cell line HeLa-S3 and *Bacillus mycoides* ATCC 6462. In HeLa-S3 cells ATX-II, AOH and AME were more toxic than in ATCC 6462 with ID_{50} values of 0.5, 6 and 8 - 14 µg/ml, respectively. On the other hand TeA, AOH and ALT displayed higher bacterial toxicity. Although a 1:1 mixture of AME and AOH elicited the most potent action for *Bacillus mycoides*, any synergistic effect was observed in HeLa-S3 cells (Pero *et al.*, 1973).

Teratotoxicity

Griffin & Chu (1983) investigated the teratogenic effects of AOH, AME, ALT and TeA using the chicken embryo assay. Yolk sac injection of *Alternaria* metabolites into 7-day old chicken embryos was performed. AOH, AME and ALT did not trigger any increase of mortality or malformation of hatched chicken, even at the maximum dose of 1 mg/egg. Although TeA displayed dose relevant mortality responses over the range of 0.15 - 1.5 mg/egg, the resulting 50% lethal dose calculated for this assay was 0.548 mg TeA/egg. The teratogenic effect of all tested substances was classified as low even at lethal or sublethal dose levels (Griffin & Chu, 1983). In another study Pero *et al.* (1973) indicated fetotoxic effects of AOH at 100 mg/kg. Although AME did not show any effects at 50 mg/kg, a synergism between AOH and AME was suggested since the co-administration of each 25 mg/kg yielded significant responses.

Mutagenicity

Statements concerning the mutagenicity of AME and AOH should be viewed critically, since controversial results were obtained with the Ames-test using different testing systems. AOH and AME presented mutagenic action independently of exogenous metabolic activation in the *Bacillus subtilis* rec assay and in the *Escherichia coli* ND160 revision test. AOH was found to be 4 - 8 times more potent than AME in both assays (Zhen *et al.*, 1991). Mutagenicity of AME towards the *E.* strain ND160 was supported by An *et al.* (1989). In the Ames *Salmonella* test using strains TA98 and TA100 similar results were obtained by Schrader *et al.* (2001), however AME and AOH were only weakly mutagenic in TA100. In contrast, Davis & Stack (1994) did not observe any mutagenic effects in TA98, TA100, TA1537 and TA1538 independent of previous metabolic activation.

On the other hand, the mutagenicity of AOH and AME was clearly confirmed in mammalian cells. AME treatment of hamster fibroblast cells (V79) induced persistent mutations, even without metabolic activation, indicating AME as a direct mutagen. Additionally, the mutagenic effect of AME was studied *in vivo* by injecting AME to sucking Wistar rats. The treatment increased the micronuclear rates of polychromatic erythrocytes of rat bone marrow (Liu *et al.*, 1992). AOH induced the hypoxanthine-guanine phosphoribosyltransferase (HPRT) gene locus in V79 cells and the thymidine kinase (TK) gene locus in mouse lymphoma L5178Y $tk^{+/-}$ cells in a concentration-dependent manner and in the lower micromolar range (Brugger *et al.*, 2006).

Dong *et al.* (1987) treated Chinese hamster lung fibroblast cells (V79) with an ether extract isolated from *Alternaria alternata* infested grain. The extract induced mutants, also in the absence of metabolic activation, indicating the presence of direct mutagens. Furthermore, treatment of mouse fibroblast cells (NIH/3T3) with the extract demonstrated its direct transforming activity. However, experiments with ether extracts isolated from *A. alternata* infested maize induced mutations in V79 cells only after metabolic activation, suggesting the existence of pre-mutagens, requiring previous metabolic activation (Liu *et al.*, 1991).

Genotoxicity

Liu *et al.* (1992) investigated the genotoxic effects of AOH and AME in primary rat hepatocytes and human embryonic fibroblast 2BS cells. Both mycotoxins induce DNA single strand breaks in both cell lines, however the AOH-mediated effect is 8 - 10 times stronger compared to AME (Liu *et al.*, 1992). Lehmann *et al.* (2006) investigated the genotoxic potential of AOH by using the induction of micronuclei, containing DNA fragments as indicator. A slight increase was observed in human Ishikawa cells and a pronounced increase in Chinese hamster cells (V79) (Lehmann *et al.*, 2006).

The DNA strand breaking activity of AME and AOH *in vitro* was investigated by Pfeiffer *et al.* (2007a) in cultured Chinese hamster V79 cells, human liver HepG2 cells and human colon HT29 cells using the method of alkaline unwinding. Treatment with AOH and AME for 1 h induced strand breaks in all three cell lines, whereas treatment for 24 h induced a higher increase of strand breaks in HepG2 cells than in HT29 cells. Since HT29 cells exhibited a higher UDP-glucuronosyl transferase (UGT) activity towards AOH and AME, the smaller number of strand breaks after 24 h suggests the formation of less genotoxic metabolites upon glucuronidation (Pfeiffer *et al.*, 2007a).

Fehr *et al.* (2009) further investigated the genotoxic properties of AOH and AME in terms of the underlying mechanism of action in human colon carcinoma HT29 cells and vulva carcinoma A431 cells. The DNA strand breaking effect was already observed at concentrations ≥ 1 µM. AOH had a substantial affinity to the minor groove of the DNA, which might contribute to its DNA-damaging properties. AOH was identified as a topoisomerase I and II inhibitor, with preference for the IIα isoform at concentrations ≥ 25 µM. AME did not affect topoisomerase IIβ activity up to 200 µM but was found to be equipotent to AOH with respect to the inhibition of topoisomerase IIα. Additionally, AOH also acted as topoisomerase I and II poison, stabilising the cleavable complex. Since topoisomerase poisoning and DNA strand breakage occurred in the same concentration range, absence of these enzymes might inhibit the unknotting of DNA. However, DNA unwinding is a crucible prerequisite for replication, transcription, recombination and DNA-repair. A failure in this highly complex system consequentially leads to DNA double strand breaks (Fehr *et al.*, 2009).

Carcinogenicity

Cultured human foetal oesophageal epithelium was exposed to AME and further cultivated for 7 days. The basal cells of oesophageal epithelium displayed papillary growth, disorderly arrangement and hyperplasia. The nuclei of the cells were larger, heavily stained and a nuclear karyokinetic phase was observed. Since the same effects were observed in groups treated with appropriate positive controls, AME was suggested to trigger human oesophageal cancer (Liu *et al.*, 1991). Additionally, the binding of AME and AOH toward human oesophageal DNA is assumed to be of ionic type, which may play an important role for mutagenicity and carcinogenicity. Oesophageal tissue of human embryos treated with AOH for 24 h were inoculated subcutaneously into nude mice. In one of three animals the tissue developed squamous cell carcinoma (Liu *et al.*, 1992). Furthermore, precancerous changes in mice oesophageal mucosa were observed after feeding the animals with 50 - 100 mg AME/kg body weight for 10 months. The oesophageal epithelium is inflamed and it is assumed that the generated cytokines and free-oxygen radicals might contribute to the observed dysplastic changes (Yekeler *et al.*, 2001).

Estrogenic Effects

Given that AOH is a diphenolic compound with a chemical structure similar to estrogen-mimicking substances, an estrogenic effect was suggested. The receptor binding assay showed a 10,000-fold lower binding affinity of AOH towards the estrogen receptor (ER)α but only a 2,500-fold lower affinity towards ERβ in comparison with the endogenous hormone 17β estradiol. Furthermore, AOH induced both, the alkaline phosphatase (ALP) activity and the corresponding ALP mRNA level. Thus, AOH acted as a pure ER agonist in the human endometrial adenocarcinoma Ishikawa cell line, with estrogenicity comparable to that of the phytoestrogen daidzein or the environmental estrogen bisphenol A (Lehmann *et al.*, 2006). However, any estrogenic potential of AOH in porcine endometrial cells could be detected (Wollenhaupt *et al.*, 2008).

2.1.6. Metabolism of AOH & AME

Pollock *et al.* (1982) administered ^{14}C labelled AME to adult male Sprague-Dawley rats and detected the majority excreted unabsorbed in the faeces, while urine excretion accounted for less than 10%. Nevertheless, an extensive amount of metabolites was detected in urine and incubation of rat liver post-mitochondrial supernatant showed the formation of AOH and several polar metabolites (Pollock *et al.*, 1982).

Pfeiffer *et al.* (2007b) incubated microsomes from rat, human and porcine liver with AME and AOH and detected seven oxidative metabolites of AME and five of AOH. The most common four aromatic hydroxylation products of AME were 2-, 4-, 8- and 10-hydroxy-AME. Further metabolites were monohydroxylated at the C-1 methyl group or dihydroxylated and demethylated to AOH. AOH was hydroxylated at each conceivable position of the molecule. All aromatic hydroxylation products of AME and AOH were prone to cytochrome P450-mediated hydroxylation at various positions, yielding either catechols or hydroquinones. The oxidative metabolism of AOH and AME is depicted in figure 4 and figure 5 (Pfeiffer *et al.*, 2007b). Since conjugation with glucuronic acid is a major pathway of detoxification and metabolic disposal, glucuronidation of AME and AOH was further investigated. Incubation of AOH with hepatic and intestinal microsomes of rat, pig and human in the presence of uridine diphosphate (UDP) glucuronic acid yielded equal amounts of AOH-3-*O*- and AOH-9-*O*-glucuronide. Incubation with AME led predominately to the formation of AME-3-*O*- with only small amounts of AME-7-*O*-glucuronide (Pfeiffer *et al.*, 2009).

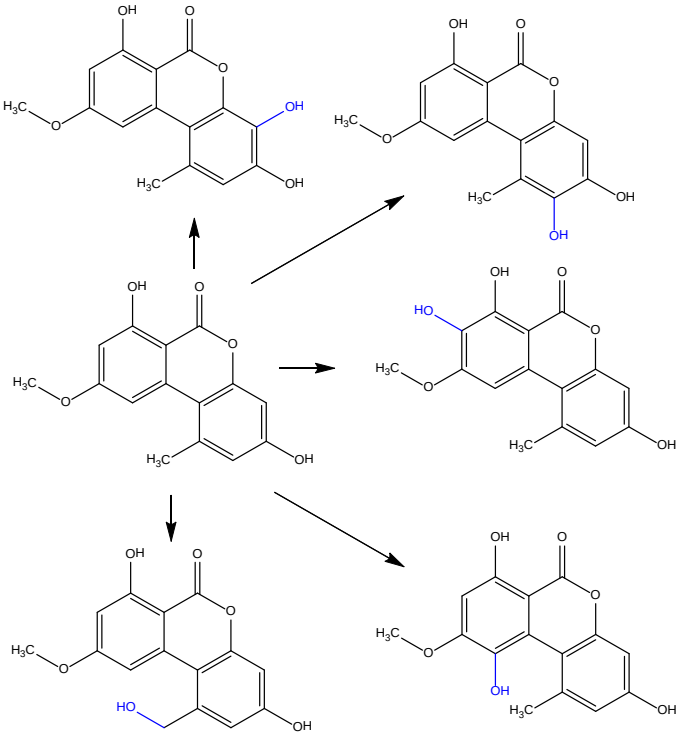

Figure 4: Oxidative metabolism of AME (Pfeiffer *et al.*, 2007b)

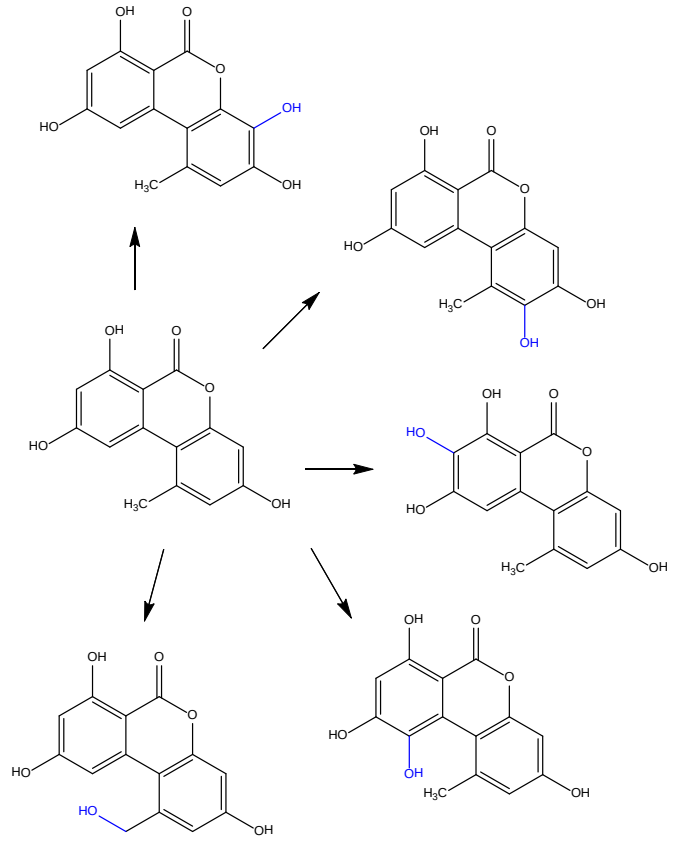

Figure 5: Oxidative metabolism of AOH (Pfeiffer *et al.*, 2007b)

Further investigations addressing the metabolism of AOH and AME were performed with human epithelial colorectal adenocarcinoma Caco2 cells grown in the Millicell® system. Their apical and basolateral sides faced different compartments, thus allowing mimicking the behaviour of metabolites in the intestines. Given that Caco2 cells lack cytochrome P450 activity, the formation of glucuronides and sulphates was studied. Based on the results of the experiment and the calculated permeability coefficients, AOH was expected to be rapidly absorbed from the intestinal lumen and reached the portal blood as aglycone, glucuronide and sulphate, whereas any AME aglycone was absorbed and only AME conjugates reached the portal blood (Burkhardt *et al.*, 2009).

To clarify whether hydroxylation of AOH and AME occured under *in vivo*-like conditions in the presence of conjugation reactions, the metabolism of these mycotoxins was studied in precision-cut rat liver slices of male Sprague Dawley rats. They were incubated with 50, 100 and 200 µM AOH or AME for 24 h. The formed conjugates accounted for 86% of the AOH and 74% of the AME metabolites. Several hydroxylation metabolites and their *O*-methylation products were detected, indicating that aromatic hydroxylation was performed under *in vivo*-like conditions allowing conjugation reactions. To investigate the formation of oxidative AOH metabolites *in vivo*, bile duct-cannulated male Sprague Dawley rats received a single dose of AOH and the collected bile was analysed with regard to oxidative metabolites. The pattern of *in vivo* metabolites was comparable with the one of *in vitro* metabolites of AOH, clearly confirming the relevance of oxidative metabolism *in vivo* (Burkhardt *et al.*, 2011).

2.2. Xenobiotic Metabolism

Xenobiotic metabolism consists of several metabolic pathways which are responsible for the modification of chemicals foreign to an organism´s biochemistry, for example drugs or poisons of anthropogenic or natural origin. During the biotransformation process xenobiotics are converted to more polar metabolites; their increased water solubility makes the excretion via urine or faeces easier (Klaassen & Watkins, 2003). The process relays on the action of drug metabolising enzymes, which belong to different enzyme families and catalyse phase I, II or III metabolising reactions (Xu *et al.*, 2005). Biotransformation can either result in detoxification of toxic xenobiotics to inactive metabolites or in activation of relatively harmless substances to reactive intermediates, whereat the latter process is known as metabolic activation (Rushmore & Kong, 2002; Klaassen & Watkins, 2003).

The metabolism of xenobiotics is divided in three phases: activation, conjugation and excretion. Phase I reactions, also known as activation reactions, introduce polar functional groups such as –OH, -SH, $-NH_2$ or -COOH, slightly increasing the hydrophilicity of the formed product. Enzymes performing these types of reactions primary belong to the cytochrome

P450 superfamily, which can be found predominantly in the liver, gastrointestinal tract, lung and kidneys (Mansuy, 1998; Guengerich, 2003). Enzymatic reactions of phase II, also known as conjugation reactions, conjugate xenobiotics with water soluble, charged biomolecules, creating a substantially more hydrophilic conjugate. Typical phase II enzymes are sulphotransferases, UDP-glucuronosyltransferases, epoxide hydrolases, glutathione-S-transferases and N-acetyltransferases (Rushmore & Kong, 2002). In the course of phase III reactions the formed metabolites are transported from the cell. Phase III transporters include P-glycoprotein (P-gp), multidrug resistance protein (MRP) and the organic anion transporting polypeptide 2 (OTAP2); all of them provide a barrier against drug penetration and are involved in drug absorption, distribution and excretion. P-gp and MRP belong to the family of ATP-binding cassette (ABC) transporters, utilising the energy required for the transport of the substrate through the cell membrane by hydrolysing ATP (Xu *et al.*, 2005).

2.3. The Aryl Hydrocarbon Receptor Pathway

The aryl hydrocarbon receptor (AhR), also known as dioxin receptor, is a transcription factor known to mediate the biochemical and toxic effects of dioxins, polyaromatic hydrocarbons (PAHs) and related compounds (Abel & Haarmann-Stemmann). It controls the regulation of drug metabolizing enzymes, predominantly the expression of the cytochrome P450 family genes and some phase II enzymes. The AhR pathway is not only a regulator of drug metabolism, it can be activated by endogenous ligands and influence cell cycle control, immune response and cell differentiation (Stejskalova *et al.*).

2.3.1. Gene Structure and Transcriptional Regulation of the AhR

The aryl hydrocarbon receptor is constitutively expressed in many cell types and tissues. Basal AhR expression is found in human and mouse lung, liver, kidney, spleen and placenta as well as in various primary and tumour-derived cells and cell lines (Abel & Haarmann-Stemmann). The chromosomal localisation of the human AhR gene is assigned to chromosome 7p15 with a length of about 50 kb, containing 11 exons. The overall intron/ exon structure of the human gene is homologous to the mouse gene, probably 20 kb longer (Bennett *et al.*, 1996).

Structure of the AhR & Arnt Protein

The human AhR gene encodes for a protein of 848 amino acids with a calculated mass of 96 kDa (Burbach *et al.*, 1992). The ligand-activated aryl hydrocarbon receptor is a basic helix-loop-helix (bHLH) protein that heterodimerises with the bHLH protein Arnt (aryl hydrocarbon nuclear translocator) and is localised in the cytoplasm of different cells (Gu *et al.*, 2000). The bHLH domain is required for protein dimerisation and DNA-binding. These processes are mediated by two sequences, the NLS (nuclear localisation signal) sequence is

important for AhR nuclear localisation and the NES (nuclear export signal) sequence contributes to the nuclear export. AhR and Arnt belong to two different classes of bHLH proteins. However, transcriptional activation of target genes by bHLH/PAS (further explanation concerning the PAS-domain see in the section below) factors requires association between a member of the AhR and the Arnt-class. The AhR-like component is responsible for interaction with gene promoters, whereas the Arnt-like component functions as a generic co-regulator. AhR and Arnt display different distribution patterns, suggesting diverse developmental roles (Wilson & Safe, 1998). The AhR PAS domain is involved in AhR/Arnt dimerisation (PAS A) and binding of AhR ligand and hsp90 (PAS B). These domains are designated as PAS because of their homology with the regulatory proteins known as Per, Arnt and Sim. The glutamine-rich transactivation domain is placed at the C-terminal end of the AhR (Whitelaw *et al.*, 1993). The domain structures of the AhR-protein are given in figure 6.

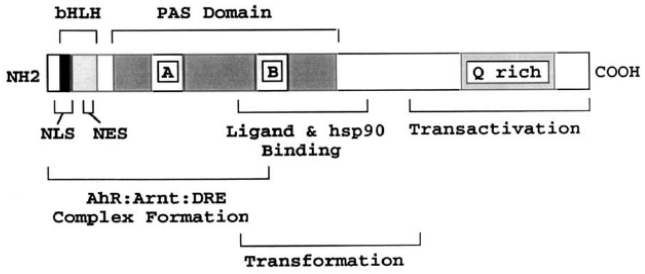

Figure 6: Domain structure of the AhR (Denison *et al.*, 2002), AhR: aryl hydrocarbon receptor, Arnt: aryl hydrocarbon nuclear translocator, bHLH: basic helix-loop-helix, DRE: dioxin responsive element, hsp90: heat shock protein (90k Da), NES: nuclear exposure signal, NLS: nuclear localisation signal, PAS: Per, Arnt, Sim

2.3.2. Aryl Hydrocarbon Receptor-mediated Signal Transduction

At least two different formations of AhR complexes are involved in the AhR-mediated signal transduction: the 9S and 6S form, which represent different sedimentation coefficients and also differ in their calculated molecular weight. In the absence of a ligand, the 9S aryl hydrocarbon receptor resides as a multi-protein complex in the cytosol (Rowlands & Gustafsson, 1997). It is associated with two molecules of hsp90, a heat shock protein of 90 kDa which is responsible for maintaining the receptor in a latent non-DNA binding state and the correct folding of the ligand binding domain, respectively. In the repressed state the PAS domain of the AhR is bound to the hsp90 proteins. Additional members of the complex are the X-associated protein 2 (XAP2) and p23, a co-chaperone protein of 23 kDa. XAP2 stabilises the whole complex and protects the AhR from ubiquitination and following proteosomal degradation. Ligand-binding induces a conformational change and a subsequent exposure of the nuclear localisation sequence (NLS). As a result of the exposed NLS the complex translocates into the nucleus, sheds hsp90, p23 and XAP2 and forms a

heterodimer with Arnt. Kazalauskas *et al.* (1999) report that Arnt is not needed for the nuclear translocation of the AhR, moreover it is assumed that hsp90 translocates with the ligand-bound receptor into the nucleus and dissociates as a result of the dimerisation with Arnt (figure 7) (Kazlauskas *et al.*, 1999).

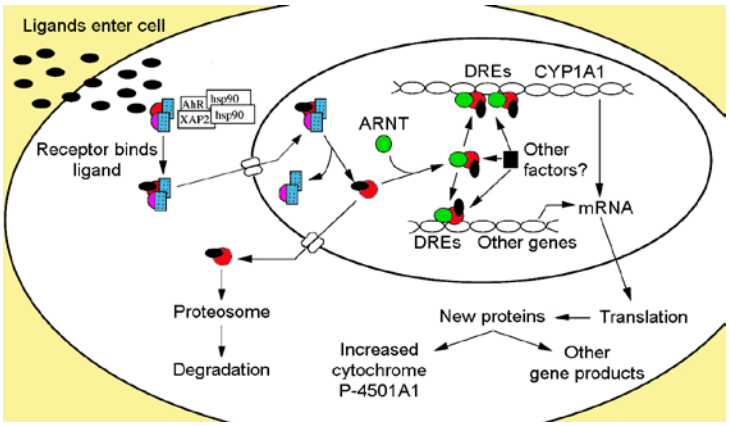

Figure 7: AhR-Signalling Pathway (Denison & Nagy, 2003), AhR: aryl hydrocarbon receptor, Arnt: aryl hydrocarbon nuclear translocator, CYP1A1: cytochrome P-4501A1, DRE: dioxin responsive element, hsp90: heat shock protein (90k Da), XAP2: X-associated protein 2

The molecular mass of the nuclear AhR/Arnt complex, also known as the 6S form, varies among species, strains and tissue types, ranging from 180 - 210 kDa. The 6S nuclear heterodimer is a transcription factor and binds to the core enhancer regulatory element known as xenobiotic or dioxin responsive element (XRE or DRE) which consists of the following sequence: 5´-T(C/T)GCGTG-3´. The AhR interacts with the 5´-half-site T(C/T)GC whereas the Arnt protein recognises the 3´-half-site (Wilson & Safe, 1998). Binding of the AhR/Arnt dimer leads to the recruitment of co-activators, which bind to the AhR/Arnt dimer and enhance transcription initiation. Furthermore, the binding of the AhR/Arnt dimer to the enhancer enables the binding of transcription factors to the promoter (Denison & Whitlock, 1995). Finally the RNA polymerase II assembles at the promoter and the elongation phase starts (Hankinson, 2005).

The AhR-signalling is quickly terminated upon elimination of the inducing xenobiotic. The exposure of the nuclear export signal (NES) sequence present in AhR by shedding of hsp90, p23 and XAP2, causes the activated aryl hydrocarbon receptor being transported from the nucleus into the cytoplasm. Since dimerisation with Arnt converts the AhR into its high affinity DNA-binding form, nuclear AhR complexes that fail to dimerise are shuttled into the cytoplasm. Subsequently the AhR is degraded via the 26S proteasome. The reasons for the degradation of AhR are wide ranging, in the first instance the process controls the duration and magnitude of the transcriptional activation by the AhR/Arnt dimer. The aryl hydrocarbon receptor-mediated signal transduction and termination process is shown in figure 7 (Davarinos & Pollenz, 1999).

2.3.3. AhR-regulated Genes

AhR-binding to dioxin response elements results in the increased transcription of several genes involved in xenobiotic metabolism, including phase I and phase II metabolising enzymes and several genes involved in proliferation, apoptosis, cell growth and differentiation. The most prominent example for phase I enzymes are monooxygenases of the CYP family. Several phase II enzymes, like glutathione-S-transferase A2 and NQO1 (NAD(P)H quinone oxidoreductase 1) are also up-regulated by the AhR pathway (Bock & Kohle, 2006). An example for the dependence of apoptosis towards AhR-signalling is the regulation of Bcl-2 associated X protein (Bax) which promotes apoptosis. Exposure towards polyaromatic hydrocarbons like benzo(a)pyrene (BaP) can lead to the induction of apoptotic cell death in murine oocytes. An explanation for the premature initiation of the menopause for female smokers might be the destruction of oocytes triggered by the BaP-induced AhR pathway (Matikainen *et al.*, 2001). Although numerous genes are regulated by the AhR pathway, the best studied is the induction of CYP1A1 which is also used as a model system to define the underlying gene regulation mechanism by AhR and other bHLH transcription factors (Denison & Whitlock, 1995).

2.3.4. Ligands and Inducers

Ligands of the aryl hydrocarbon receptor include a variety of structurally diverse chemicals, suggesting a promiscuous ligand-binding site. They can be separated into two major categories, anthropogenic-derived AhR ligands and naturally occurring ligands, formed in biological systems. HAHs (halogenated aromatic hydrocarbons) and PAHs belong to the first group, displaying a planar structure which accounts for the high AhR binding affinity. Both of them are usually referred as classical AhR ligands. The metabolically more stable HAHs are more potent than the PAHs, with binding affinities in the pM to nM range and nM to µM, respectively. Nevertheless, the most potent agonist known is 2,3,7,8-tetrachlorodibenzo-p-dioxin (TCDD, figure 8), often used as a model substance to induce CYP1A1 gene expression. Structure-activity relationship analysis suggests that the AhR binding pocket can accept planar ligands with maximal dimensions of 14 x 12 x 5 Å (Poland & Knutson, 1982; Waller & McKinney, 1995).

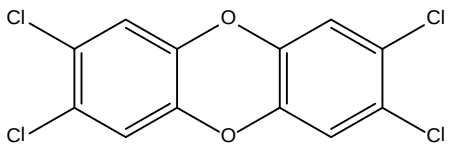

Figure 8: Structure of 2,3,7,8-tetrachlorodibenzo-p-dioxin (TCDD)

Recently a relatively large number of AhR ligands have been identified with completely diverse structural and physicochemical properties. Although the majority of these chemicals are relatively weak inducers, their identification as ligands supports a re-evaluation of the currently accepted view of AhR ligand structure. Within the naturally occurring ligands there are two subclasses: dietary and endogenous physiological AhR ligands (Denison *et al.*, 2002).

Naturally occurring dietary AhR Ligands

The greatest source of exposure for humans and animals to AhR ligands is the diet. Although they are very weak agonists, most of the natural occurring ligands can be found in food. Examples for dietary ligands are carotinoides, curcumin and indole-3-carbinol (I3C). It is reported that precursors with any or weak AhR binding activity can be converted to significantly more potent AhR ligands in the mammalian digestive tract, e.g. the conversion from I3C to indolo-(3,2,-b) carbazole (ICZ), which has perhaps the highest affinity of all naturally occurring agonists (Gillner *et al.*, 1993).

The largest group of dietary AhR ligands are flavonoids, including flavones, flavanols, flavanones and isoflavones. These chemicals are widely distributed in dietary plant products and the levels in human blood can reach the low µM range, concentration sufficient to interact with the AhR (Formica & Regelson, 1995). Flavanoids can exhibit agonistic and antagonistic effects, depending on their concentration, the investigated tissue or species (Denison *et al.*, 2002).

Synthetic AhR Ligands

3´-Methoxy-4´-nitroflavone (MNF)

The effect of 3´-methoxy-4´-nitroflavone (MNF, figure 9), a synthetic flavone, towards the expression of CYP1A1 mRNA, protein and enzyme activity was investigated in mouse hepatoma cells (Hepa.2DLuc.3A4-cells), using luciferase reporter gene assay and Western blot analysis. Cells treated with MNF displayed a dose-dependent induction of CYP1A1 protein expression, suggesting an agonistic effect for this protein. Otherwise any reporter protein was expressed, which may be due to a differential activation of gene transcription. An antagonistic effect of MNF was observed for Hepa.2DLuc.3A4-cells, co-incubated with 150 pM TCDD and increasing MNF concentrations. The TCDD-induced expression of the luciferase reporter and the CYP1A1 gene decreased in a MNF concentration-dependent manner. Further experiments addressed possible effects of posttranslational modulation of protein stability and regulation through diverse signal transduction pathways, but neither of them proved to be the explanation for the observed effects. The third possibility may be a primary mechanism accounting for the differential gene expression. Induction of CYP1A1 by

MNF depended on the CYP1A1 promoter sequence, which is a complex 2 kb spanning regulatory region, whereas p2DLuc has just a minimal promoter. Furthermore the obtained results suggested that MNF required a clustered DRE structure to enhance substantial gene transcription (Zhou & Gasiewicz, 2003). MNF acting as a low efficacy AhR ligand can act as an antagonist or agonist depending on its concentration as examined towards human breast cancer cells (MCF-7). MNF was reported to act as a pure antagonist in MCF-7 cells, suggesting species specific differences in AhRs, differences in the promoter regions between human and mouse CYP1A1 and thirdly, the species and tissue specific expression of co-activator/ co-repressor proteins (Lu *et al.*, 1995).

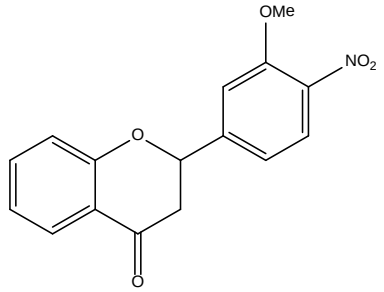

Figure 9: Structure of 3´-methoxy-4´-nitroflavone (MNF)

Alternaria Toxins as AhR Ligands

Alternaria toxins, like AME and AOH represent potential ligands of the AhR, naturally occurring and acting as agonists. The activation of the AhR pathway by appropriate agonists is followed by an induction of cytochrome P450 enzymes. The influence of AOH and AME towards the regulation of CYP1A1 in HepG2, KYSE510 and HT29 cells was investigated by M. Fehr (2008). He identified AME and AOH to induce CYP1A1 gene and protein expression in KYSE510 and HepG2 cells, whereas a greater response was detected in KYSE510 cells. Both mycotoxins did not trigger any CYP1A1 induction in HT29 cells (Fehr, 2008).

Schreck *et al.* investigated AME- and AOH-mediated expression of CYP1A1 in murine hepatoma cells differing in their AhR-signalling using Western blot analysis. Pfeiffer *et al.* (2008) reported for AOH and AME the highest activity of the AhR-regulated enzyme CYP1A1. The dependence of the mycotoxin-mediated CYP1A1 induction on AhR and Arnt was shown by comparison of wild type Hepa-1c1c7, Arnt-deficient Hepa-1c1c4 and AhR-deficient Hepa-1c1c12 cells. In AhR- and Arnt-expressing Hepa-1c1c7 cells, CYP1A1 protein-levels were already induced after 5 h of incubation with 40 µM AME, whereas 40 µM AOH-induced CYP1A1 expression only after 24 h. AME was a better substrate for CYP1A1 than AOH, suggesting it to be also a better AhR ligand. Any induction of CYP1A1 expression was detected after 24 h treatment with AOH or AME in AhR- and Arnt-deficient cells, supporting the hypothesis that the AhR-pathway is involved in AOH-/ AME-induced CYP1A1 expression in murine hepatoma cells (Schreck *et al.,* 2011).

Endogenous Ligands for the AhR

The existence of endogenous physiological AhR ligands has been suggested in numerous studies where the AhR signalling pathway in the absence of exogenous ligands (Denison & Nagy, 2003). Sadek & Allen-Hoffmann (1994) investigated the effect of semi-solid methylcellulose suspensions with human keratinocytes and dermal fibroblasts towards CYP1A1 gene expression without addition of any xenobiotics. Increase of steady state CYP1A1 mRNA is observed for human keratinocytes, whereas dermal fibroblasts are nonresponsive. Moreover, induction is also observed in kerationocyte suspension with medium (Sadek & Allen-Hoffmann, 1994).

The endogenous ligands are composed of a structurally diverse group of substances which are mainly relative weak agonists. They can be classified into different categories, comprising indoles, arachidonic acid metabolites, tetrapyroles and a variety of other ligands, whereby all of them are present in many species and tissues. Many of the toxic and biological effects of AhR ligands resulted from altered gene expression. The continuous and inappropriate expression of specific genes could be responsible for adverse effects of TCDD and other HAHs, which were usually observed after several days to weeks following exposure. This theory was consistent with endogenous ligands being relatively weak agonists and which could trigger only a transient activation of the AhR-signalling pathway (Denison & Nagy, 2003). Evidence for the AhR involved in normal development was described by Schmidt *et al.* (1996). They observed physiological changes and developmental defects in AhR-knockout mice like hypercellularity in liver tissue (Schmidt *et al.*, 1996).

2.3.5. Ligand-independent Activation of the AhR

Recently the hypothesis of a ligand-independent AhR activation was developed, based on the existence of substances, which cause AhR-mediated effects without meeting the requirements for AhR ligands or display any binding in ligand-binding assays. Both arguments were given in the case of primaquine, a reported anti-malaria agent. CYP1A1 gene expression and enzyme activity was induced in human hepatocytes and HepG2 cells. Furthermore, 8-methoxypsoralen (8-MP) and α-naphthoflavone (α-NF), both reported AhR antagonists, down regulate the primaquine-induced CYP1A1 induction. However, the absence of competitive binding of primaquine to the AhR suggests a probable not ligand-activated pathway, supported by the not polycyclic aromatic structure of primaquine (Fontaine *et al.*, 1999). Guigal *et al.* (2000) reported of 5- to 6-fold CYP1A1 mRNA increases after treatment of Caco2 cells with foetal or adult bovine and human serum. Furthermore, the induction observed with serum was suggested to be independent of the AhR pathway, because any reporter gene was expressed in serum-treated reporter gene transfected Caco2 cells (Guigal *et al.*, 2000).

2.4. The Cytochrome P450 System

The cytochrome P450 (CYP, P-450) system consists of the ubiquitous monooxygenase family which is present in plants, animals and prokaryotes. The human genome encodes 57 different CYPs, compared to more than 250 members of the plant *Arabidopsis*. The human P-450 genes are classified into 18 families and 42 subfamilies. Cytochrome P450s are hemoproteins and derive their name from the absorption maximum at a wavelength of 450 nm, elicited by the carbon monoxide derivate of reduced cytochrome (Stryer, 2002; Philip Wexler, 2005). One of the most important functions of cytochrome P450s are their role in drug metabolism. Despite their general protective role, the action of the P-450 system is not always beneficial since the toxicity of several substrates can be enhanced by metabolic activation (Tompkins & Wallace, 2007).

2.4.1. Enzyme Mechanism

Cytochrome P450s catalyse regio- and stereospecific oxygen attack of hydrocarbons at physiological temperatures. Without a catalyst such a reaction would occur at high temperatures and would not be specific. The reactions catalysed by cytochrome P450 enzymes generally are of following stoichiometry (Guengerich, 2003):

$$\text{Substrate} + O_2 + \text{NADPH} + H^+ \rightarrow \text{Product} + H_2O + NADP^+$$

The active catalytic centre of the enzyme is an iron-protoporphyrin IX (heme) with a thiolate group of a cysteine as fifth ligand. The sixth ligand of resting CYPs is a water molecule (Werck-Reichhart & Feyereisen, 2000). The catalytic mechanism of cytochrome P450 monooxygenases consists of four steps (figure 10). The first step includes substrate-binding by displacing the sixth ligand, the water molecule. The second step is a one-electron reduction of the complex from Fe^{3+} to Fe^{2+}. In the third step molecular oxygen binding results in the formation of a superoxide complex and the fourth step is a second reduction, leading to an activated oxygen species. Recent crystallographic analysis of the transiently activated oxygen species suggest the protonation of A^- leading to the formation of B^- and the formation of the oxoferryl species after cleavage of the O-O bond (Schlichting *et al.*, 2000). The oxoferryl species is apparently most abundant and catalyses the hydroxylation reaction (O insertion). The iron-hydroperoxo form (B^-) inserts OH^+, producing protonated alcohols. The oxygen free forms of the enzyme catalyse isomerisation, reduction and dehydration. The existence of various forms of enzymes together with the variety of apo-proteins explains the diversity of reactions catalysed by the P450 system (Mansuy, 1998).

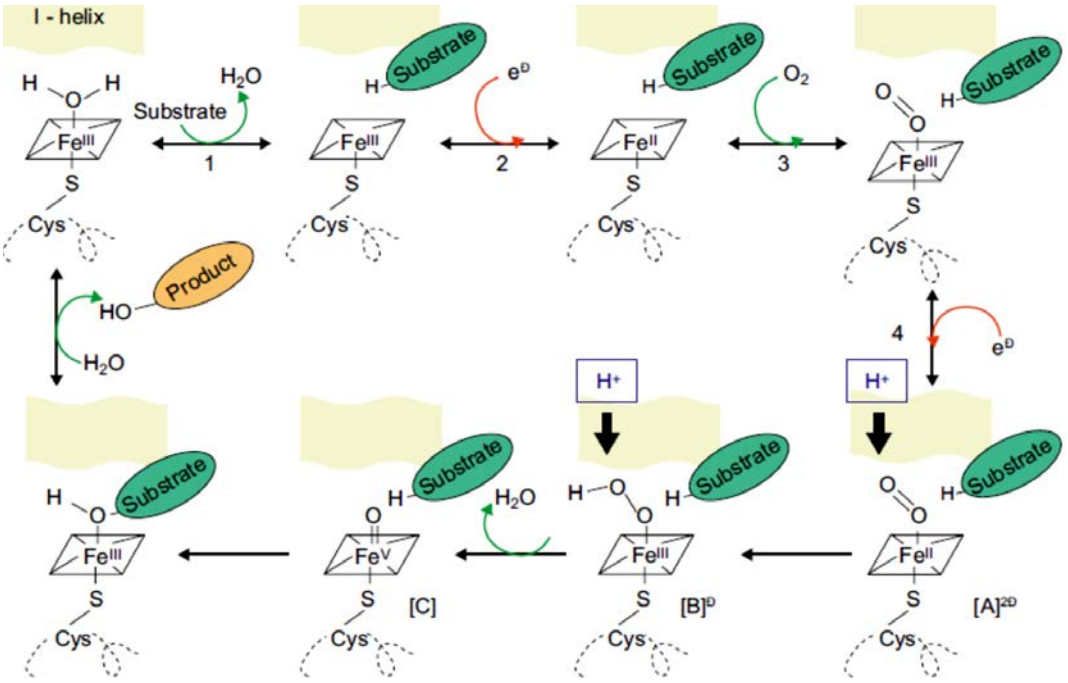

Figure 10: Catalytic mechanism of P-450 enzymes (Werck-Reichhart & Feyereisen, 2000)

2.4.2. Human Cytochrome P450 Genes

The organ expressing the highest levels of CYP enzymes is the liver, which plays a dominant role in the first-pass clearance of xenobiotics. Extrahepatic tissues also express xenobiotic metabolising CYPs, which can also influence the absorption of drugs and foreign chemicals. Since most therapeutic agents target extrahepatic tissues, the individual CYP profile may have a significant impact on the effectiveness of the treatment (Ding & Kaminsky, 2003).

Table 1: Human cytochrome P450 genes expressed in different tissues (Shimada *et al.*, 1994; Ding & Kaminsky, 2003; Choudhary *et al.*, 2005)

organ	expressed P-450 enzymes
oesophagus	1A1, 1A2, 2A, 2E1, 2J2, 3A5
small Intestine	1A1, 1B1, 2C9, 2C19, 2D6, 2E1, 2J2, 2S1, 3A4, 3A5
colon	1A1, 1A2, 1B1, 2J2, 3A4, 3A5
liver	1A1, 1A2, 2A6, 2B6, 2C8, 2C9, 2C19, 2D6, 2E1,3A

Oesophagus

Oesophageal cancer is the third common cancer of the gastrointestinal tract (GIT), reason enough to potentiate research concerning the underlying mechanism (Ding & Kaminsky, 2003). Lechevrel *et al.* (1999) investigated oesophageal tissue with regard to the pattern of CYP expression. They identified CYP2E1, an enzyme known to activate *N*-nitrosamines to DNA-damaging metabolites. Since smoking and alcohol consumption induce CYP2E1, they suggested CYP2E1 to contribute to the development of oesophageal cancer (Lechevrel *et*

al., 1999). This hypothesis was supported by the findings of Bergheim *et al.* (2007) who identified higher levels of CYP2E1, 3A4 and 3A5 mRNA in oesophageal tissue of squamous cell carcinoma. Higher CYP1A1 protein levels were expressed in tumour tissue compared to normal tissue (Bergheim *et al.*, 2007). M. Fehr (2008) reported a 500-fold CYP1A1 induction in KYSE510 cells treated with 1 µM AOH for 24 hours.

Liver

The liver plays a predominant role in xenobiotic metabolism mediated by cytochrome P450, resulting in an ubiquitous expression of these enzymes (Scripture *et al.*, 2005). Shimada *et al.* (1994) showed that CYP1A2, 2A6, 2B6, 2C, 2D6, 2E1 and 3A account for 72% of total CYP protein. Drahushuk et al. (1998) demonstrated a very weak constitutive expression of CYP1A1 protein in human microsomal liver samples, which could also be due to background exposure of polychlorinated dibenzodioxins (PCDDs) and related compounds. However, CYP1A1 was shown to be highly inducible by TCDD, resulting in significantly increased CYP1A1 protein and activity levels.

Colon

Colon and rectum cancer are responsible for the most cancer-related deaths in western countries. Despite this, few studies have been reported and very little information is available on the *in vivo* regulation of colonic CYPs (Ding & Kaminsky, 2003). The most prominently expressed CYPs are CYP3A3, CYP1A1 and CYP1A2. Expression of CYP3A3 and CYP1A1 was found to be site-specific, either higher in colon or rectum, whereas the mRNA levels of CYP1A2 were variable. Exposure to various xenobiotics and/ or genetic polymorphism may contribute to differential CYP expression (Mercurio *et al.*, 1995).

2.4.3. Human Cytochrome P450 Isoforms and Hydroxylation of AOH & AME

The *Alternaria* toxins AOH and AME undergo oxidative metabolism by cytochrome P450 enzymes, hence Pfeiffer *et al.* (2008) investigated the activities of twelve major human CYP isoforms for the hydroxylation of AME and AOH. CYP1A1 is the most active isoform in the hydroxylation of AOH, followed by CYP1A2, CYP2C8 and CYP3A5. The formed hydroxylation products in descending order are: 2-OH-AOH, 4-OH-AOH and small amounts 8-OH-AOH. CYP1A1 has been reported to have also the highest activity for aromatic hydroxylation of AME. Since most CYP isoforms display higher activities for AME than for AOH, it appears to be a better substrate (Pfeiffer *et al.*, 2008).

2.4.4. Regulation of CYP1A1 Expression

The AhR is involved in the induction of CYP1A1 transcription. Structure-activity studies indicate a correlation between receptor binding affinity of ligands and their potency as inducer. The binding of the heterodimeric AhR/Arnt complex to XRE or DRE is necessary for the subsequent expression of CYP1A1 protein (Fujisawa-Sehara *et al.*, 1987; Denison & Whitlock, 1995). However, Fujii-Kuriyama *et al.* (1992) reported an additional cis-acting DNA regulatory element to be responsible for the constitutive expression of the rat CYP1A1 gene. The element is known as basal transcription element and is located about -43 bp upstream of the TATA sequence (Yanagida *et al.*, 1990).

2.5. The Glutathione-S-Transferase Enzymes

Glutathione-S-transferases (GSTs) catalyse nucleophilic attack by reduced glutathione (GSH) on nonpolar compounds containing an electrophilic carbon, nitrogen or sulphur atom. GSTs catalyse conjugation reactions in phase II drug metabolism, a mechanism providing protection against a diverse spectrum of xenobiotics (Hayes & Pulford, 1995). Furthermore GSTs are also involved in protection against reactive oxygen species and in the biosynthesis of leucotrienes, prostaglandins, testosterone and progesterone. They are important targets for anti-asthmatic and antitumor drugs. They metabolise cancer chemotherapeutics, insecticides, herbicides, cancerogens and by-products of oxidative stress (Hayes *et al.*, 2005).

GST-Families

There are three different families which exhibit glutathione-S-transferase activity: cytosolic, mitochondrial and microsomal GSTs; every known GST isoform belongs to one family. All three families contain members that catalyse the conjugation of GSH with 1-chloro-2,4-dinitrobenzene (CDNB). Based on amino acid sequences, seven classes of GSTs are known in mammalians: GST α, GST μ, GST π, GST σ, GST θ, GST ω and GST ζ (Hayes & McLellan, 1999). The largest GSTs in humans are the cytosolic GSTs, consisting of 16 subunits (Hayes & Pulford, 1995). Their overlapping substrate specificity makes the identification of isoforms solely based on their catalytic properties very difficult. Beside catalysing conjugation, reduction and isomerisation reactions, cytosolic GSTs also bind hydrophobic ligands, essential in intracellular transport and elimination of xenobiotics (Hayes *et al.*, 2005).

Induction of GST

The expression level of GSTs can be increased in many species by exposure to xenobiotics, suggesting an important role in the adaptive response to chemical stress (Pickett *et al.*, 1984). Inducing substances of GSTs are mostly GST substrates or are transformed by cytochrome P450 enzymes to become GST substrates (Prochaska & Talalay, 1988). GSTs also modulate the induction of other enzymes, like quinone reductase, UDP-glucuronyl transferase, γ-glutamyl transferase and γ-glutamylcysteine synthetase. The modulation of other drug metabolising enzymes by GSTs suggests, that GST polymorphism influences other chemical defence mechanisms (Hayes & Wolf, 1990).

Substrates of GST

Substrates of GSTs are extremely diverse, PAHs, phenolic antioxidants, flavonoids, thiocarbamates and indoles have been reported as GST inducers in rats and mice (Hayes & Pulford, 1995). Structurally they do not seem to have a single feature in common. However, a parallel between GST inducers and Michael reaction acceptors, e.g. alkenes conjugated with electron withdrawing groups, or substances which are metabolised to Michael acceptors have been suggested (Prochaska & Talalay, 1988; Talalay *et al.*, 1988).

2.6. RNA Interference

RNA interference (RNAi) is a regulatory mechanism of many eukaryotic cells which can also be used for specific inhibition of gene expression. Posttranscriptional gene silencing (PTGS) was implemented in 1998 by Andrew Fire and Craig Mello, using double-stranded RNA molecules of the nematode *Caenorhabditis elegans* for specific gene silencing (Lottspeich, 2006). RNA interfering pathways are guided by small RNAs, including small interfering RNAs and micro RNAs (de Fougerolles *et al.*, 2007).

siRNA-Pathway

Long double-stranded RNA (dsRNA) is cleaved by RNase III endonuclease Dicer into small interfering RNAs (siRNA) in mammalian cells. siRNAs which have been synthesised previously by chemical methods, are used directly by Dicer. Dicer is complexed with RNA-binding proteins and the Argonaute 2 (Ago-2) domain of the RNA-induced silencing complex (RISC) (Zhang *et al.*, 2004, figure 11). The double-stranded siRNA is loaded into RISC, cleaved by Ago-2 and the sense, or passenger strand is released. The activated RISC contains a single-stranded anti-sense, or guide RNA molecule that recognizes complementary mRNA and performs intermolecular base pairing. The catalytic domain of Ago-2 cleaves the mRNA and exposes the cutting point without the protective poly(A) tail. Subsequently cellular RNases degrade the mRNA and inhibit its function as transcription template (Kim & Rossi, 2008).

In mammalian cells, double-stranded RNA with more than 30 nucleotides (nt) length activates interferons. The siRNA fragments used for gene silencing generally have a length of 21 - 23 nt (Lottspeich, 2006). The first nucleotide on the 5´-end is generally unpaired, followed by a 19 nt long base pair region (Elbashir *et al.*, 2001).

miRNA-Pathway

Another important part of RNAi involves microRNAs (miRNA, figure 11). These complexes trigger translational suppression due to imperfect completion with target mRNA, in contrast to siRNA, which requires a perfect complement with the targeted mRNA (Kim & Rossi, 2008).

miRNAs are endogenous substrates which are transcribed by RNA polymerase II into large primary miRNA (pri-miRNA) transcripts with poly(A) tail and 5´cap. They are processed by the microprocessor complex (containing Drosha and DGCR8) into pre-miRNA, consisting of 60 - 70 nt hairpins. Pre-miRNAs are exported from the nucleus to the cytoplasm by Exportin 5 and are processed by the Dicer enzyme complex for loading onto the Ago-2-RISC (Shan, 2010). When the RNA duplex loaded onto the RISC has imperfect sequence complementation, the antisense (or passenger) strand is unwound and the mature miRNA activates RISC. The mature miRNA recognises the target mRNA in the 3´untranslated region (3´-UTR) leading to translational inhibition (de Fougerolles *et al.*, 2007).

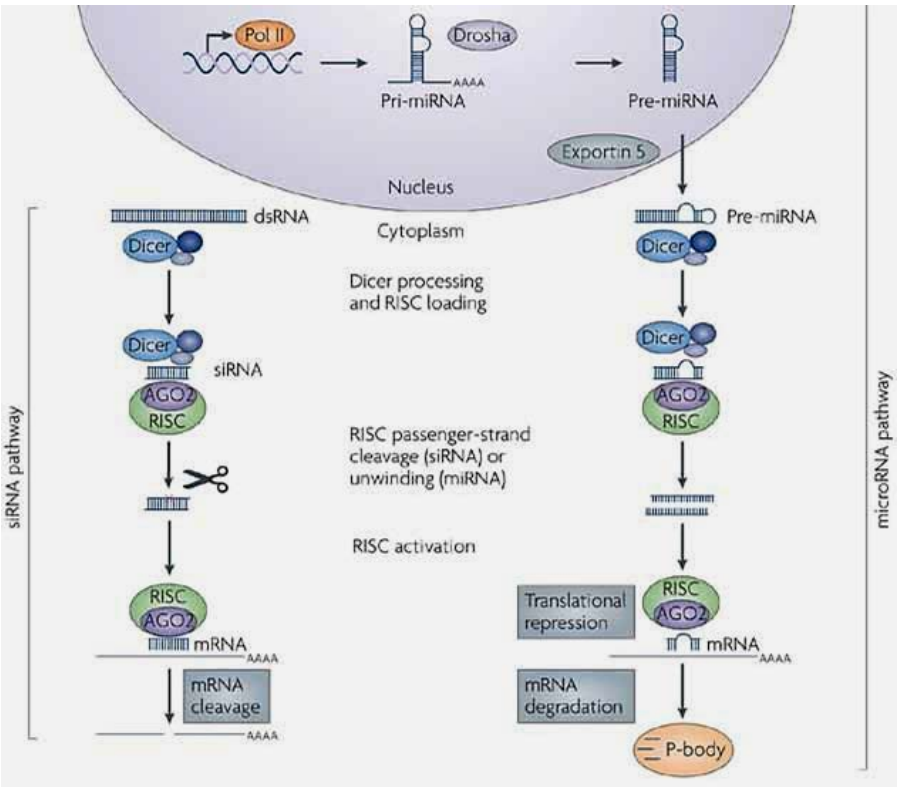

Figure 11: Mechanism of RNA interference (de Fougerolles *et al.*, 2007)

3. Aims and Objectives

Fungi of the genus *Alternaria* are ubiquitous pathogens. Many species are known to infest various food stuffs and produce diverse secondary metabolites- *Alternaria* mycotoxins. The consumption of *Alternaria* contaminated grain has been associated with an increased incidence of oesophageal cancer in Linxian, China (Liu *et al.*, 1992). Furthermore *Alternaria* extracts as well as single toxins such as alternariol (AOH) and its monomethyl ether (AME) have been described to possess genotoxic and mutagenic properties, however, the underlying mechanisms of action have not fully been elucidated so far (Dong et al., 1987; Liu et al., 1991, 1992; Schrader et al., 2001, 2006; Lehmann et al., 2005; Brugger et al., 2006; Fehr et al., 2009; Nitiss et al., 2006; Jackson, 2002; Maynard et al., 2009).

Even though several reviews on *Alternaria* toxins have been published over the last few decades, valid evidence is limited concerning their risk to health of man and animal. The EFSA has pointed out recently that there is an urgent need for further investigations on the toxicity of *Alternaria* toxins, because data published so far do not allow comprehensive risk assessment (EFSA, 2011).

In the present thesis the question was addressed whether AME and/ or AOH elicit CYP1A1 transcripts in human oesophageal carcinoma cells (KYSE510) and whether this dependents on AhR expression. The problem was approached in two different ways: firstly by posttranscriptional suppression of the Ah-receptor and secondly by using an AhR-specific inhibitor. The establishment of optimal transiently AhR-siRNA transfected KYSE510 cells, serving as test system for the investigations, represented a crucial part of the thesis. Benzo(a)pyrene (BaP) and aroclor (ARO), which is a mixture of polychlorinated biphenyls, are both known as potent CYP1A1 inducers. These compounds were used as a suitable positive control in oesophageal cells. 3´-Methoxy-4´-nitroflavone, a synthetic flavone and known AhR antagonist, was used for the specific blocking of the Ah-receptor in the second approach. Subsequent treatment with AOH or AME was expected to provide information about the AhR-dependence of CYP1A1 induction as well.

According to recent publication, AME and AOH are hydroxylated by cytochrome P450 monooxygenase CYP1A1 to catechols during phase I metabolism (Burkhardt *et al.*, 2011). To clarify whether both mycotoxins are subjected to phase II metabolism, the activity of glutathione-S-transferases (GST) was investigated in colon adenocarcinoma cells (HT29). Activity of glutathione-S-transferases was determined by the GST assay according to Habig *et al.* (1974), whereupon the implementation of the assay as a routine method had to be performed.

4. Results and Discussion

4.1. HPLC Purity of AOH and AME

Alternaria toxins used in the present thesis were purchased from Sigma-Aldrich, whereas the compounds used by M. Fehr (2008) were synthesised by Dr. K.-H. Merz, University of Kaiserslautern, Germany. The different mycotoxins were analysed by High Performance Liquid Chromatography (HPLC) prior the beginning of the experiment to assure comparable purity and thus cell response.

4.1.1. HPLC-Chromatogram of AME

The chromatogram of AME, purchased from Sigma-Aldrich, was recorded by C. Schwarz showing one main peak at a retention time of 17,866 min (figure 12), also depicted in the isoabsorbance plot (figure 13). The existence of a single main peak confirmed the purity of > 98% which is specified by the company.

In contrast the HPLC-chromatogram of the synthesised mycotoxin presented far more peaks for AME (figure 14). The strongest signal was observed at a retention time of 17.674 min and several smaller peaks at 12.727, 14.031, 18.963, 19.884, 20.424, 21.428 and 21.878 min were detected. The signal at 17.674 min was by far the most intense one. The retention time was closely related to the main peak of the Sigma-Aldrich product, thus it was identified as the AME-related signal. In addition, the isoabsorbance plot, a plot of retention time versus wavelength in figure 13, clearly showed the presence of impurities in the synthesised sample. The exclusive occurrence in the synthesised mycotoxin suspected them to be impurities or precursors potentially left from the process of synthesis.

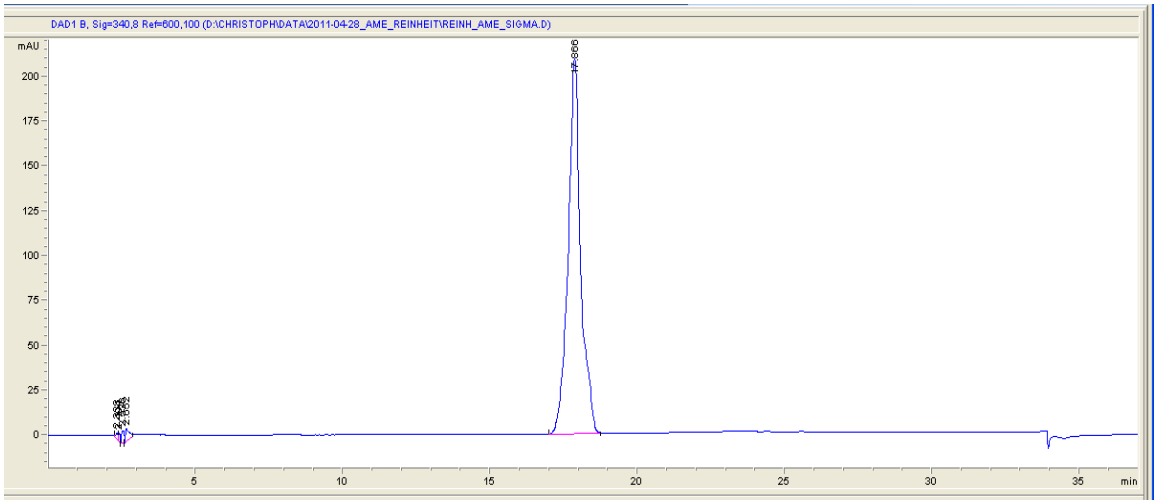

Figure 12: HPLC-Chromatogram of AME purchased from Sigma-Aldrich

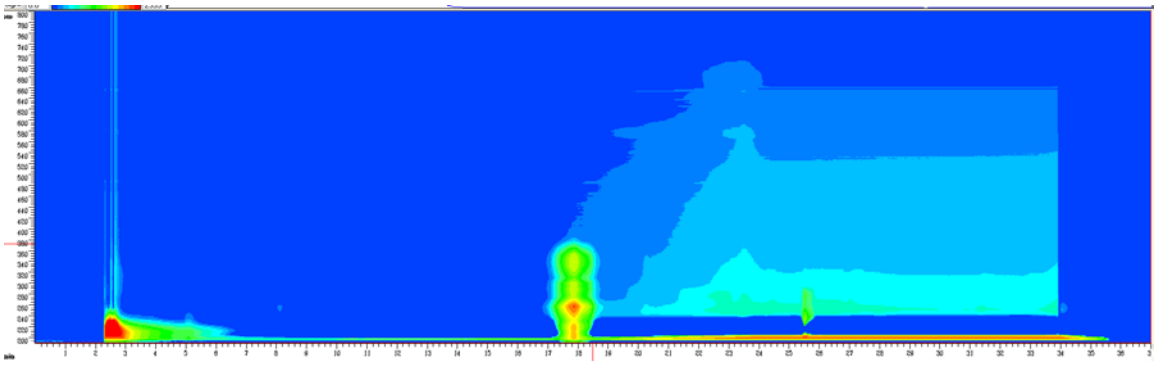

Figure 13: Isoabsorbance Plot of AME purchased from Sigma-Aldrich

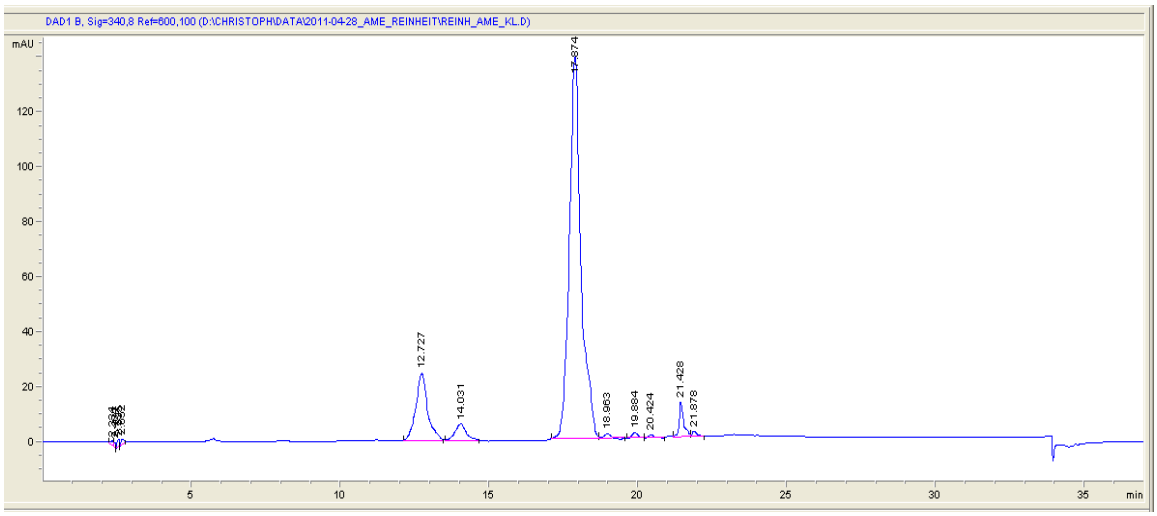

Figure 14: HPLC-Chromatogram of AME synthesised by Dr. K.-H. Merz, University of Kaiserslautern, Germany

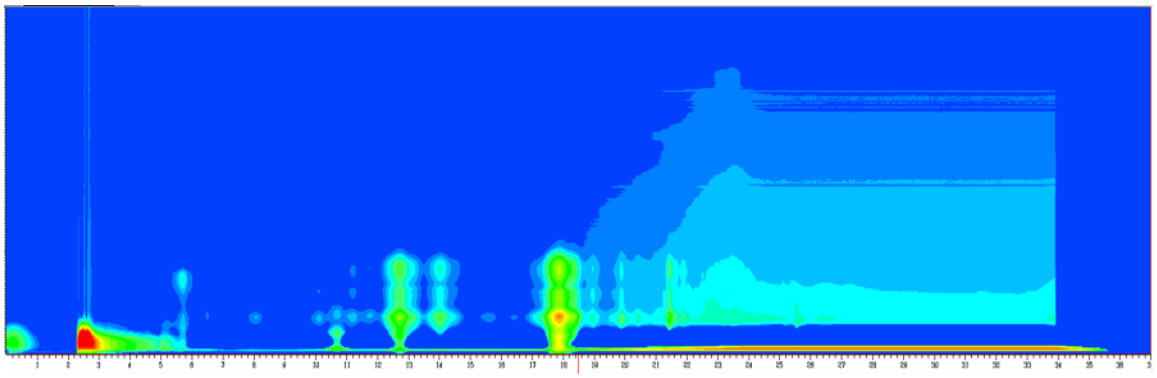

Figure 15: Isoabsorbance Plot of AME synthesised by Dr. K.-H. Merz, University of Kaiserslautern, Germany

4.1.2. HPLC-Chromatogram of AOH

Both HPLC-chromatograms of AOH, the product purchased from Sigma-Aldrich (figure 16) as well as the one of the synthesised compound (figure 17) were recorded by C. Tiessen. The retention times of the main peaks, which were annotated to be the AOH-related signals, differ slightly, 8.972 min were registered for the Sigma-Aldrich product and 9.154 min for the synthesised one. The chromatogram of the synthesised AOH showed several smaller peaks at 2.791, 3.334, 5.631, 11.083, 11.586, 12.273, 16.354 and 28.887 min. The impurity-derived peaks detected in synthesised AME (figure 14) are of stronger intensity, suggesting a higher purity of synthesised AOH. However, in both cases the identity of the impurities remained unknown.

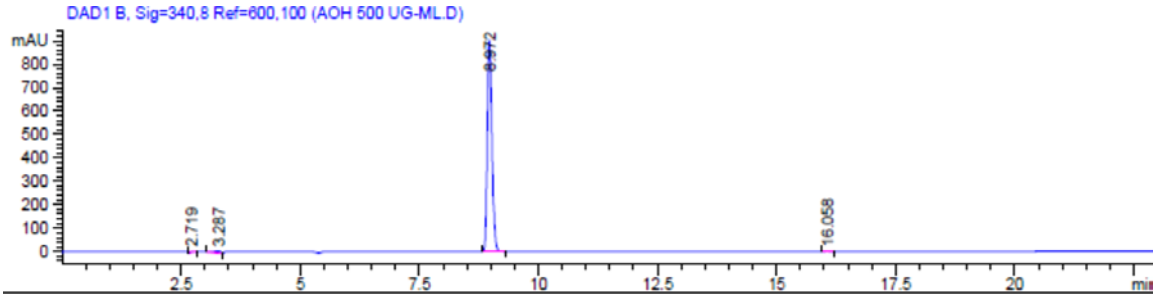

Figure 16: HPLC-Chromatogram of AOH purchased from Sigma-Aldrich

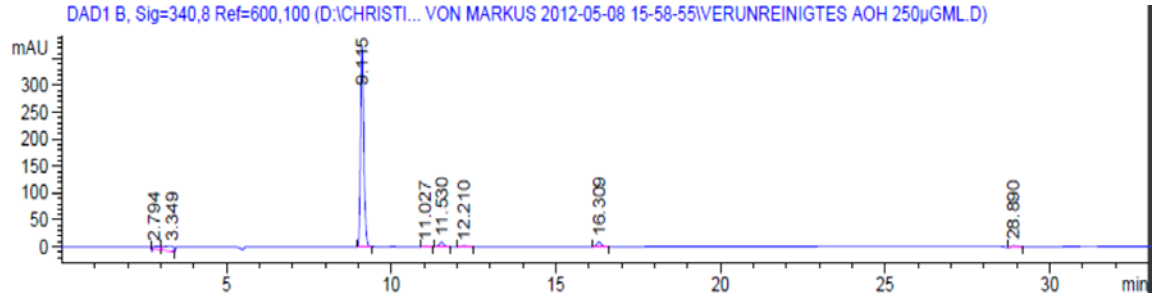

Figure 17: HPLC-Chromatogram of AOH synthesised by Dr. K.-H. Merz, University of Kaiserslautern, Germany

The experiments performed by M. Fehr (2008) addressed the mycotoxin-mediated modulation of CYP1A1 mRNA levels and activity as well as cytotoxicity in human oesophageal (KYSE510), liver (HepG2) and colon (HT29) carcinoma cells. The results, especially obtained for synthesised AME have to be viewed critically. The detected impurities potentially affected the metabolic activity of cells. Thus the results were expected not to be in compliance with those obtained with the Sigma-Aldrich products.

4.2. Cytotoxicity of AME and AOH

Prior to investigating gene modulating effects fostered by AME and AOH, the concentration range for testing had to be identified and determined to be suitable for the planned experiments. This implies that cell growth was not altered by cytotoxicity or other growth inhibitory effects.

The analysed parameter of the sulforhodamine B (SRB) assay is the total cellular protein, which is determined by binding of the dye sulforhodamine B. Shortly after removing excessive dye, the protein-bound fraction is dissolved under alkaline conditions and the concentration is determined spectrophotometrically at λ = 570 nm.

Briefly, 800 KYSE510 cells were seeded per well of a 96-well plate and grown for 72 hours. The medium was replaced by 0.1, 1 and 10 µM AME dissolved in DMSO, the final DMSO concentration in the medium being 1%. A 24 h treatment period followed and then the SRB assay was performed as described in chapter 6.2 “Sulforhodamine B (SRB) Assay”. After 24 h of incubation with 0.1, 1 and 10 µM AME no significant changes of protein amount were observed (figure 18). Even the highest concentration tested in the assay (10 µM AME) did not notably diminish cell growth.

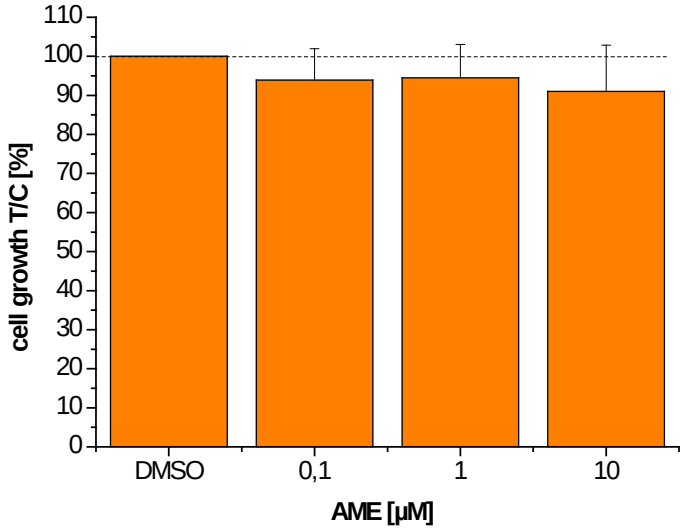

Figure 18: Cytotoxicity of AME in KYSE510 cells determined with the sulforhodamine B (SRB) assay. KYSE510 cells were incubated for 24 h with AME. Growth inhibition was calculated as the percent survival of treated cells over control cells (treated with the solvent 1% DMSO) x 100 (T/C %). The values given are the mean ± SD of at least three independent experiments. Calculation of the statistical significances are performed on the basis of underlying T/C [%] values.

M. Fehr (2008) already investigated the cytotoxicity of AME and AOH in KYSE510 cells, treating the cells for 24 h and 72 h with the mycotoxins. Both AME and AOH inhibited cell growth in a concentration-dependent manner. The IC_{50} could not be calculated for the 24 h incubation, as it exceeded 100 µM, the highest concentration used for the assay. Treatment for 72 h notably inhibited cell growth, yielding IC_{50} of 42 ±10 µM AOH and 48 ±3 µM AME, respectively. However, the SRB assay was performed with the toxins synthesised by Dr. Merz, hence the containing impurities and precursors might contribute to an altered cytotoxicity. AME used by M. Fehr did not inhibit cell growth up to a concentration of 10 µM, consequently the compound purchased from Sigma-Aldrich was also tested in the range of 0.1 - 10 µM (figure 18).

The cytotoxicity of AME and AOH purchased from Sigma-Aldrich was investigated by N. Kahle in 48 h pre-cultivated KYSE510 cells as well. Cells were treated with both mycotoxins in the concentration range of 0.01 - 60 µM for 24 h. AME in the concentration of 0.01 µM slightly inhibited cell growth, which turned into a weak cell proliferative effect at 0.1 µM AME. A significant cytotoxic effect was determined at concentrations ≥ 25 µM AME. Taken together, all the data concerning the cytotoxicity of AME, recorded in the course of the present thesis and by N. Kahle, suggested any significant cell growth inhibition in the concentration range of 0.1 - 10 µM AME and indicated the suitability for the planned gene modulation experiments (Kahle N., 2012).

In contrast to the data obtained by M. Fehr for AOH-mediated cytotoxicity, N. Kahle could show significant growth inhibitory effects in 48 h pre-cultivated KYSE510 cells at concentrations ≥ 50 µM. However, these results were obtained when the practical part of the present thesis was already finished. At the beginning of the present thesis, the only available data was the cytotoxicity profile of synthesised AOH, recorded by M. Fehr (2008). Since both HPLC-chromatograms, the one of AOH synthesised by Dr. K.-H. Merz and of the product purchased from Sigma-Aldrich mainly matched each other, comparable purity seemed to be given. Consequently, the cytotoxic potential of the compounds was believed to be similar as well. M. Fehr reported AOH to be less potent compared to AME; concentrations up to 50 µM AOH did not show any significant growth inhibitory effects. Therefore, 50 µM AOH were used as maximum concentration in CYP1A1 gene expression experiments in the present work.

4.3. Impact of AME and AOH on CYP1A1 and AhR Gene Transcription in KYSE510 Cells

CYPs are drug metabolising enzymes, catalysing the monooxygenation reaction during phase I metabolism. AME and AOH were identified as suitable substrates for human recombinant CYP enzymes, whereby CYP1A1 represented the most active isoform. Minor metabolic activities were described for CYP1A2, 2C19 and 3A4 (Pfeiffer *et al.*, 2008).

The question whether AOH and AME modulate gene transcription of CYP1A1 and AhR was investigated by M. Fehr in different human tumour cell lines of the gastrointestinal tract. The objective was, in case of an interference on transcription, to compare the results from KYSE510 (oesophagus), HepG2 (liver) and HT29 (colon) cells, to identify potential differences with respect to organ specificity. The induction of CYP1A1 mRNA transcripts was investigated using quantitative real time PCR (qRT-PCR) and CYP1A1 activity was determined by the ethoxyresorufin-*O*-deethylase (EROD) assay. A cell line-specific effect of AME and AOH was observed. The induction of CYP1A1 mRNA and CYP1A1 activity in KYSE510 cells was more potent compared to HepG2 cells, whilst any induction was observed in HT29 cells (Fehr, 2008). Thus the cell line KYSE510 was chosen for the comparative analysis of compounds synthesised and those purchased from Sigma-Aldrich. Additionally the impact of both mycotoxins on AhR transcription was investigated.

In the following, AME- and AOH-mediated CYP1A1 induction in oesophageal carcinoma KYSE510 cells should be tested, whether it is AhR dependent. Therefore the mRNA encoding AhR should be suppressed by using siRNA technology. AhR-suppressed cells were treated with the designated mycotoxins and the CYP1A1 transcripts were determined by qRT-PCR.

4.3.1. Effect of AME and AOH on AhR and CYP1A1 mRNA levels in KYSE510 Cells

To determine the effect of AME and AOH on CYP1A1 transcription, $3*10^4$ KYSE510 cells were seeded per well of a 24-well plate and cultivated for 24 h and 48 h, before incubation with the mycotoxins for 6 h, 12 h and 24 h. Cells were incubated with AME (0.1, 1, 10 µM) and AOH (0.1, 1, 10, 50 µM) under serum-containing conditions, with a final concentration of 1% DMSO. Benzo(a)pyrene (BaP) and aroclor (ARO), both potent inducers of CYP1-isoenzymes were used as positive controls at a concentrations of 5 µM (Whitlock, 1999; Almahmeed *et al.*, 2004). Total RNA was reverse transcribed with the QuantiTect® Reverse Transcription Kit from Qiagen®. The cDNA was amplified by qRT-PCR using gene-specific primers (QuantiTect® Primer Assay) and SybrGreen Master Mix from Qiagen®. Transcript levels of target genes were normalized by β-actin mRNA levels that served as endogenous control (see chapter 6.4 “Gene Expression Analysis of CYP1A1 and AhR using quantitative Real Time PCR”).

Optimisation of Pre-cultivation and Incubation Time in KYSE510 Cells

Cell pre-cultivated for 24 h

Short Time Incubation (6 h and 12 h) with AME

Treatment of 24 h pre-cultivated KYSE510 cells with 0.1 and 1 µM AME for 12 h fostered a marginal increase of CYP1A1, whereas a strong decline in CYP1A1 mRNA levels was observed at 10 µM AME (figure 19 A). 6 h of treatment with 1 µM and 10 µM AME induced a drop of CYP1A1 mRNA (figure 19 B). The positive controls strongly increased CYP1A1 levels, a 23.8-fold induction was observed after 12 h with ARO and a 28-fold induction after 6 h of incubation with BaP. The experiments with 12 h and 6 h of incubation were performed to screen for a significant CYP1A1 induction. Since no indication of such an effect was observed, the experiments were not repeated.

In summary the effects of AOH and AME on CYP1A1 induction in KYSE510 cells were marginal leading to the assumption, that the CYP1A1 induction fostered by AME may be time-dependent and would peak later in time. A time dependent induction of rat hepatic CYP1A1 and CYP1A2 expression after administration of the anti-angiogenic agent TSU-68 was described by Kitamura *et al.* (2008). Therefore further experiments with 24 hours of incubation were performed.

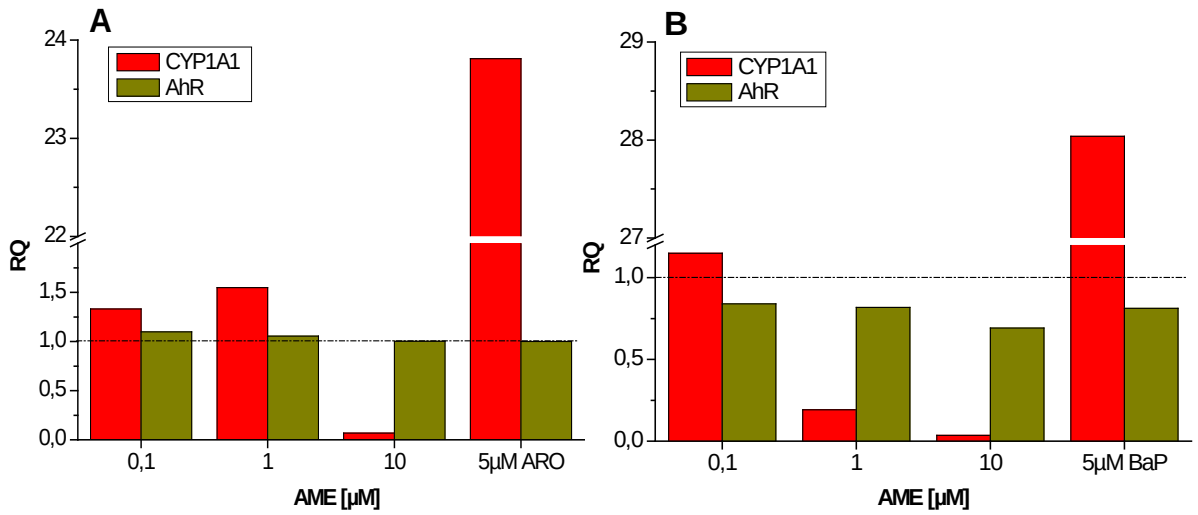

Figure 19: Effect of AME on the transcript level of CYP1A1 and AhR after 24 h pre-cultivation and subsequent treatment for 12 h (A) and 6 h (B). 5 µM ARO was used as positive control. CYP1A1 and AhR transcripts are normalised to β-actin and compared to respective DMSO (1%) treated control cells. The data are plotted as relative mRNA quantity (RQ) of a single experiment.

Incubation with AOH and AME for 24 h

After pre-cultivating KYSE510 cells for 24 h and subsequently incubating for 24 h with AME any increase of CYP1A1 transcripts at 0.1 µM and 1 µM was observed compared to the solvent control (figure 20).

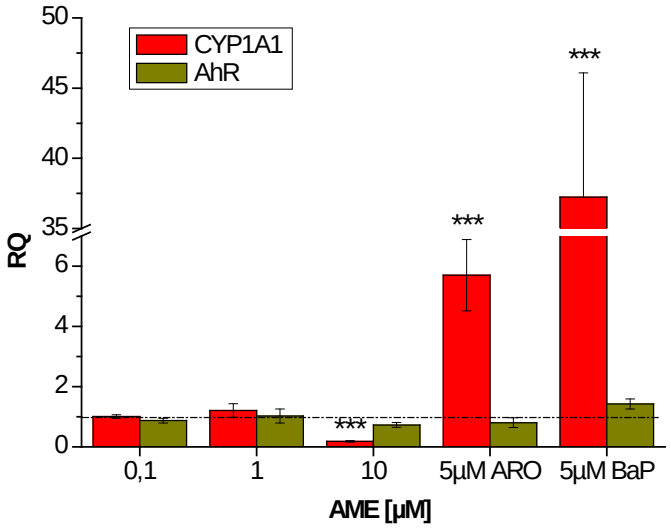

Figure 20: Effect of AME on the transcript level of CYP1A1 and AhR after 24 h pre-cultivation and subsequent treatment for 24 h. 5 µM ARO and 5 µM BaP were used as positive controls. CYP1A1 and AhR transcripts are normalised to β-actin and compared to respective DMSO (1%) treated control cells. The data are plotted as relative mRNA quantity (RQ) ± SD of at least three independent experiments. Calculation of statistical significances are performed on the basis of underlying ΔC_T-values (***=p<0.001).

At 10 µM AME the CYP1A1 transcript level significantly decreased 0.2-fold (± 0.02). The positive controls benzo(a)pyrene and aroclor raised the CYP1A1 level to 37.2 (± 8.8) - and 5.7-fold (± 1.2), respectively and thus demonstrated the inducibility of CYP1A1 in KYSE510 cells. The decreased CPY1A1 mRNA level at 10 µM AME potentially was not due to cytotoxic effects since 10 µM AME did not affect cell growth in the SRB assay (figure 18). 10 µM AME was the highest concentration tested, therefore it remained unclear whether the suppressing effect on transcription would be observed at any higher mycotoxin concentrations. Any of the tested AME concentrations and ARO did significantly influence cellular levels of AhR transcripts. Benzo(a)pyrene raised the cellular mRNA level of AhR to 1.4-fold (± 0.2), yet not significantly, however suggesting a potential impact of the compound on AhR mRNA levels.

In an orienteering experiment treatment of 24 h pre-cultivated KYSE510 cells with AOH for 24 h caused a 3.4- and 5.1-fold increase of CYP1A1 mRNA levels at 0.1 µM and 1 µM AOH, respectively (figure 21) whereas no substantial effect was observed when applying the same concentrations of AME (figure 20). 5 µM ARO induced CYP1A1 by about 16-fold, acting more potent compared to AME. However, the validity of the data was not supported by at least three independently performed experiments, thus any significant conclusion concerning the outcome could be drawn.

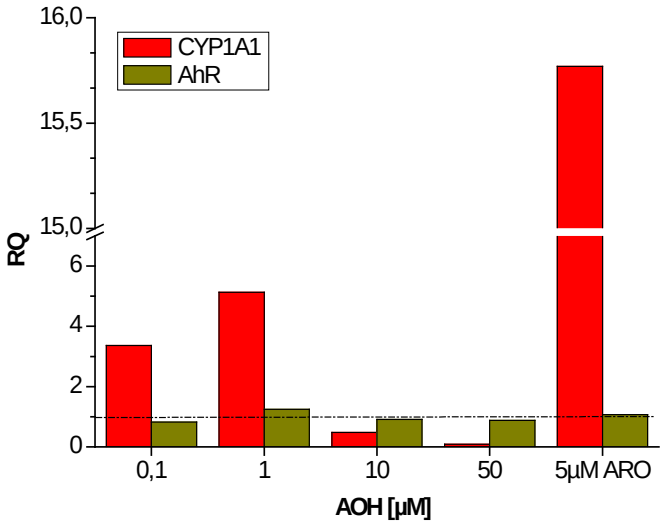

Figure 21: Effect of AOH on the transcript level of CYP1A1 and AhR after 24 h pre-cultivation and subsequent treatment for 24 h. 5 µM ARO was used as positive control. CYP1A1 and AhR transcripts are normalised to β-actin and compared to respective DMSO (1%) treated control cells. The data are plotted as relative mRNA quantity (RQ) of a single experiment.

Cells pre-cultivated for 48 h

Given that the mycotoxins did not significantly induce CYP1A1 at any of the tested incubation periods, further experiments with prolonged pre-cultivation were performed. A longer cultivation period is discussed to influence the inducibility of CYP1A1. Cytochrome P450 enzymes are an important part of the cell´s drug metabolising system, requiring fully developed cell morphology to ensure a well operating system. Thus the confluency of cells was to be considered. To ensure cell communication, which is required to trigger a homogenous and strong response toward xenobiotics, contact between neighbouring cells has to be established (Hamilton *et al.*, 2001). A confluent layer of cells can be reached by seeding more cells or prolonging the time of pre-experimental cell culture.

Figure 22 shows the morphology of KYSE510 cells after different times of cell culture. (A) 6 days after seeding, the cells already established their typical morphology whereas (B) after 24 h the cells are still round shaped and the contact between neighbouring cells is not given. In order to obtain the cell´s typical morphology at about 70 - 80% confluency more time for pre-cultivation and/ or increased numbers of cells appears to be of relevance. The pre-cultivation time for KYSE510 cells was therefore extended to 48 h and used in the following studies.

A **B**

Figure 22: Morphology of KYSE510 cells after a culture period of (A) 6 days (Fang *et al.*, 2003) and (B) after 24 h (Wang *et al.*, 2011)

Incubation with AME for 24 h

A significant 2.3-fold (± 0.2) increase of CYP1A1 transcripts after 24 h of incubation with 1 µM AME was observed in 48 h pre-cultivated KYSE510 cells (figure 23). Any induction was observed for 0.1 µM AME, identifying the concentration as the no effect level. A decreasing trend could be observed at 5 µM and 10 µM, causing 0.7 (± 0.05) - and 0.6-fold (± 0.08) drops compared to the solvent control. The suitability of the assay was proven by the very potent induction of BaP, raising the CYP1A1 level to 270-fold (± 18.9). The Ah-receptor transcripts did not experience great changes upon treatment with any AME concentration, whereas BaP raised the cellular AhR levels 1.8-fold (± 0.1).

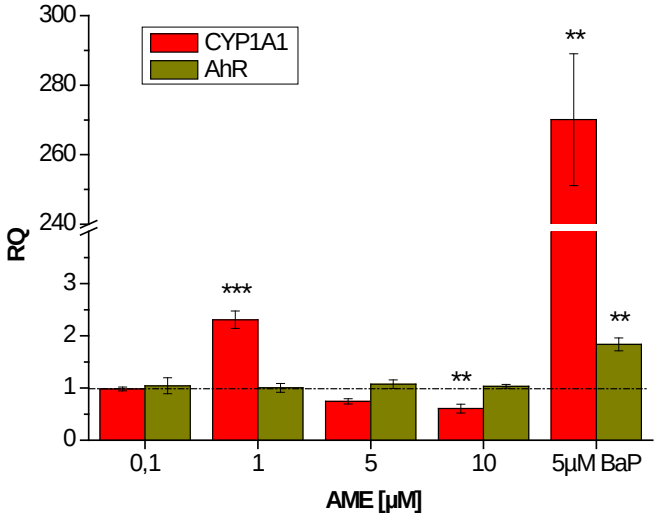

Figure 23: Effect of AME on the transcript level of CYP1A1 and AhR after 48 h pre-cultivation and subsequent treatment for 24 h. 5 µM BaP was used as positive control. CYP1A1 and AhR transcripts are normalised to β-actin and compared to respective DMSO (1%) treated control cells. The data are plotted as relative mRNA quantity (RQ) ± SD of at least three independent experiments. Calculation of statistical significances are performed on the basis of underlying ΔC_T-values (**=p<0.01; ***=p<0.001).

Incubation with AOH for 24 h

After 24 h of incubation, 1 µM AOH increased CYP1A1 levels in KYSE510 cells to 7.8-fold (± 0.4) (figure 24). AOH at a concentration of 10 µM fostered a nearly equal 7-fold (± 2.6) raise, whereas 0.1 µM AOH triggered a 1.9-fold (± 0.5) increase. This was in contrast to the experiment with AME, where any effects were observed at concentration as low as 0.1 µM. The pattern of AOH-triggered effects exhibited similarities compared to the AME effects. In both cases, at the highest AME (10 µM) and AOH (50 µM) concentration tested, CYP1A1 transcripts decreased to a similar magnitude. The positive control BaP strongly raised CYP1A1 mRNA levels (277-fold ±31.6) accompanied by a significant 1.7-fold (± 0.1) increase of AhR mRNA.

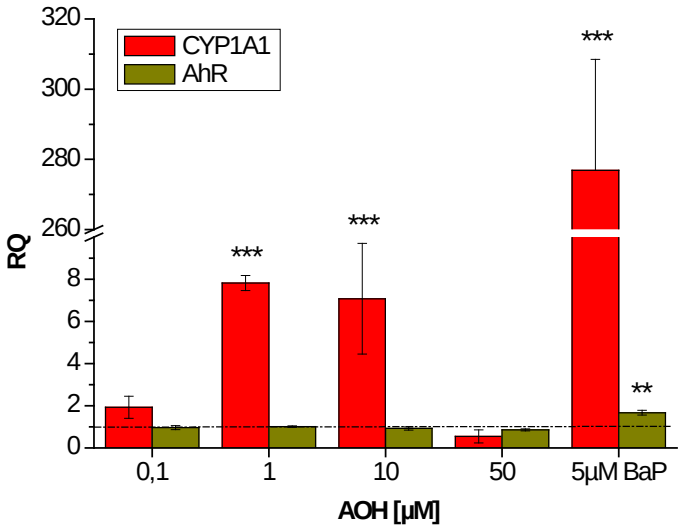

Figure 24: Effect of AOH on the transcript level of CYP1A1 and AhR after 48 h pre-cultivation and subsequent treatment for 24 h. 5 µM BaP was used as positive control. CYP1A1 and AhR transcripts are normalised to β-actin and compared to respective DMSO (1%) treated control cells. The data are plotted as relative mRNA quantity (RQ) ± SD of at least three independent experiments. Calculation of statistical significances are performed on the basis of underlying ΔC_T-values (**=p<0.01; ***=p<0.001).

It is hypothesized that the transcriptional induction of CYP1A1 by AME and AOH is mediated by the Ah-receptor. The CYP1A1 encoding gene is not constitutively expressed and it has been shown that the gene is negatively regulated under normal conditions (Guigal *et al.*, 2000). However, CYP1A1 is strongly substrate-inducible (Whitlock, 1999) which would be in accordance with the increase of relative amount of transcripts fostered by AME and AOH in oesophageal cells. Altogether, stronger effects of both mycotoxins on cellular CYP1A1 levels were observed in KYSE510 cells cultured for 48 h. Both, a prolonged cultivation time and higher cell density are important for the inducibility of CYP1A1. The former is responsible for the development of the cell´s morphology, ensuring an efficiently working metabolising cell system whereas the latter is crucial for the communication between neighbouring cells (Hamilton *et al.*, 2001). Several papers report of experiments on CYP1A1 induction performed with cells cultivated longer than 24 h. Dohr *et al.* (1995) treated nearly confluent MCF-7 and MDA-MB 231 human breast cancer cells with TCDD to observe a strong CYP1A1 mRNA induction. Hoivik *et al.* (1997) cultured MCF-7 and mouse hepatoma Hepa 1c1c7-cells for 48 h and 70 - 80% confluency were reported by El Gendy & El-Kadi for human hepatoma HepG2 cells. On the contrary, Jeong *et al.* (1995) cultured Hepa 1c1c7-cells for 24 h prior incubation with TCDD and observed strong CYP1A1-responds. However, since most papers report of culture periods longer than 24 h, the development of the cell´s morphology seems to be substantial for a strong CYP1A1 response. Nevertheless, the necessity of a certain cell density should not be neglected, given that increases in CYP1A1 mRNA were also observed at shorter cultivation periods.

4.3.2. Knockdown of AhR in KYSE510 Cells

The question was addressed whether CYP1A1 induction by AME and AOH is AhR-mediated in KYSE510 cells. The Ah-receptor pathway is believed to be the main contributor to CYP1A1 induction (Guigal *et al.*, 2000). However, Delescluse *et al.* (2000) pointed out, that some substances are potent CYP1A1 inducers without being agonists of the AhR. Their lack of structural requirements for ligand-binding can be compensated either by their metabolites being AhR ligands or by cross-talk with another pathway, for example the retinoic acid receptor, estrogen receptor, protein tyrosine kinases or a yet unknown signal transduction pathway. RNAi technology was used to investigate the role of the AhR in AOH- and AME-mediated CYP1A1 induction. The expression of AhR in human oesophageal KYSE510 cells was transiently suppressed by transfection with AhR-siRNA. Subsequently the effect of AME and AOH on CYP1A1 expression was analysed in these cells.

Prior working with AhR-suppressed cells, the conditions for transient siRNA transfection of KYSE510 cells had to be established, ensuring a maximum of knockdown of at least 70%. The development of optimal transfection conditions was an important part of the present thesis. The siRNA transfection was performed using HiPerFect Transfection Reagent from Qiagen®, two different siRNAs (siRNA 1 and siRNA 2), which encoded different AhR sequences, and a negative control siRNA (dsRNA). Both siRNAs and the dsRNA were kindly provided by Prof. C. Weiss from the Karlsruher Institute of Technology (KIT), Germany. The optimised transfection protocol for HepG2 cells, recommended by Prof. C. Weiss as well as the manufacturer's recommendations in section "Fast-Forward Transfection of Adherent Cells with siRNA/miRNA in 24-well Plates" (Qiagen®) served as an orienting procedure for the siRNA transfection of KYSE510 cells.

Transient siRNA Transfection

Two siRNAs differing in their sequence were analysed in order to identify the one with the higher AhR suppressing potential. The scrambled control siRNA (in the following referred to as dsRNA) does not affect the level of AhR mRNA. The whole transfection procedure was performed with dsRNA to encompass any change affecting cell culture conditions, cell viability or metabolism that could affect siRNA-transfected cells. Therefore dsRNA-treated cells were a suitable calibrator for monitoring the AhR-suppression by siRNA.

The potency of AhR suppression, indicative for transfection efficiency, was investigated using RT-PCR and Western blot analysis (see chapter 6.4 "Gene Expression Analysis of CYP1A1 and AhR using quantitative Real Time PCR" and chapter 6.5 "Western Blot Analysis of the Aryl Hydrocarbon Receptor"). Effects on the AhR mRNA levels were investigated while β-actin was co-amplified as endogenous control used for normalisation. The posttranscriptional

suppression of the Ah-receptor is given, when the level of AhR mRNA in transfected cells (siRNA 1 or siRNA 2) does not exceed a 0.3-fold level compared to cells transfected with control RNA (dsRNA). For Western blot analysis the total protein was extracted with RIPA buffer. The cell-lysates were disrupted, centrifuged and the supernatant as well as the cell pellet were dissolved in SDS-buffer. The samples were heated to 95°C assuring complete protein denaturation (see chapter 6.5 “Western Blot Analysis of the Aryl Hydrocarbon Receptor”.) Thereafter samples were stored at -20°C until performing electrophoresis.

Transient siRNA Transfection of HepG2 Cells

First the recommended transfection protocol of Prof. C. Weiss for HepG2 cells was performed to become familiar with the method and to prove reproducibility. The applied conditions are listed in table 2.

Table 2: Transfection conditions for HepG2 cells with HiPerFect Transfection Reagent (Qíagen®) according to Prof. Weiss (KIT), Germany

transfection conditions for HepG2 cells	
number of seeded HepG2 cells	$3*10^6$/well
volume of HiPerFect Transfection Reagent	3 µl/well
volume of siRNA (1 or 2), dsRNA	0.2 µl/well
transfection time	48 h

Figure 25 displays the membrane of the Western blot analysis for AhR, 48 h post-transfection with siRNA 1 and siRNA 2. In comparison to dsRNA-treated HepG2 cells, less intense bands were detected for siRNA 1 and siRNA 2 transfected cells. The weaker signal in siRNA 1 transfected cells suggested a more potent suppression of AhR-protein expression by this sequence.

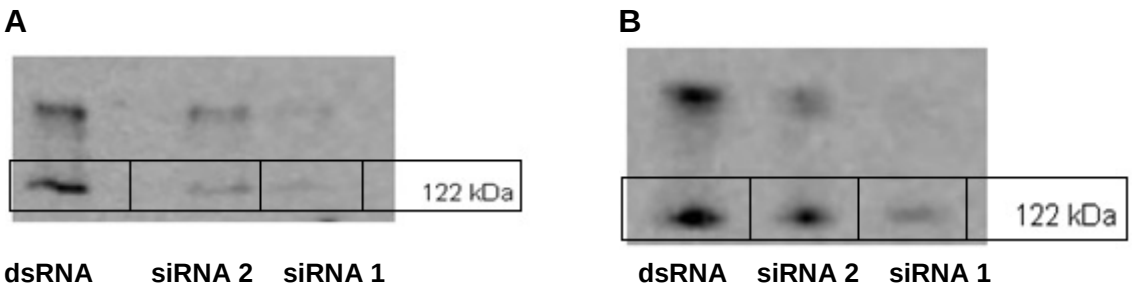

Figure 25: AhR expression in HepG2 cells 48 h post-transfection with two different siRNA sequences (siRNA 1 and siRNA 2) and the negative control (dsRNA) determined by Western blot analysis, performed with the (A) supernatant and (B) pellet of siRNA-transfected cells. Transfection conditions see table 2.

Since no endogenous control for sample loading was included, the diminished band intensities could be due to lower protein concentration as well. However, the loading of samples according to protein content was performed with great care for correctness, making the decreased band intensities solely due to a successful Ah-receptor suppression.

Transient siRNA Transfection of KYSE510 Cells

In general the confluency of cells should not exceed 60 - 70% at the time of transfection. Since the doubling time of KYSE510 cells with 30 hours is nearly one-half of HepG2 cells, which varies between 40 - 60 hours, the number of seeded KYSE510 cells was reduced from $1*10^6$ cells/well to $3*10^4$ cells/well and the volume of HiPerFect Transfection Reagent was increased from 3 µl to 4.5 µl. The transfection conditions used for KYSE510 cells are listed in table 3.

Table 3: Optimised siRNA-transfection protocol for KYSE510 cells (HiPerFect Transfection Reagent, Qíagen®)

optimised transfection protocol	
number of seeded KYSE510 cells	$3*10^4$/well
volume of HiPerFect Transfection Reagent	4.5 µl/well
volume of siRNA (1 or 2), dsRNA	0.2 µl/well
transfection time	48 h

Following the optimised transfection protocol, AhR mRNA levels in siRNA-transfected KYSE510 cells were reduced by 80% in comparison to dsRNA-treated cells (figure 26). In contrast, the level of AhR transcripts in siRNA 1 transfected cells was reduced only by about 20%. Thus transfection with siRNA 2 met the required at least 70% knockdown of Ah-receptor.

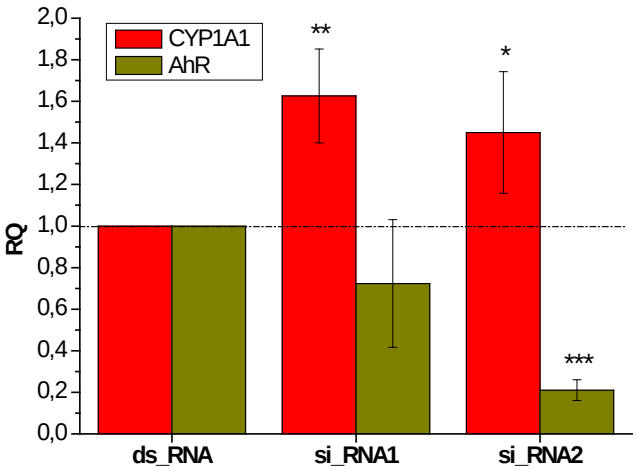

Figure 26: AhR and CYP1A1 transcripts of KYSE510 cells 48 h post-transfection with two different siRNA sequences (siRNA 1 & siRNA 2) and the control (dsRNA). CYP1A1 and AhR transcripts are normalised to β-actin and are compared to the control (dsRNA). The data are plotted as relative mRNA quantity (RQ) ± SD of at least three independent experiments. Calculation of statistical significances are performed on the basis of underlying ΔC_T-values (*=p<0.1; **=p<0.01; ***=p<0.001).

To test sufficient suppression of AhR at the protein level, Western blot analysis was performed using an AhR-specific antibody. Figure 27 represents the membrane after detection with the anti-AhR-antibody. Samples were lysed in Laemmli-buffer instead of RIPA-buffer to achieve complete protein degradation without labour intensive extraction.

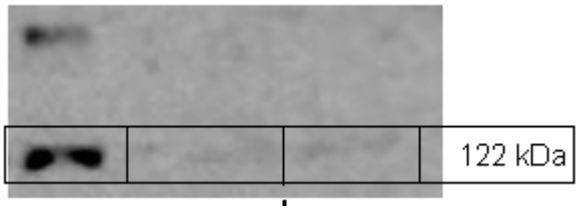

Figure 27: AhR expression in KYSE510 cells 48 h post-transfection with two different siRNA sequences (siRNA 1 and siRNA 2) and the negative control (dsRNA) determined by Western blot analysis with the whole cell lysate. Transfection conditions see table 3.

The signal for AhR at 122 kDa either in siRNA 1- or siRNA 2-transfected cells was notably lower in comparison to the signal for dsRNA-treated cells. Due to the absence of a loading control the attenuated signal in siRNA-transfected cells could not be ascribed exclusively to diminished AhR protein based on knockdown. However, the results corroborated the reduced levels of AhR mRNA in qRT-PCR.

4.3.3. Effect of AME and AOH on AhR and CYP1A1 mRNA levels in AhR-suppressed KYSE510 Cells

KYSE510 cells were cultivated for 48 h post-transfection with siRNA 2 enabling a sufficient suppression of Ah-receptor expression. The effect of AME (0.1 µM, 1 µM, 5 µM, 10 µM) and AOH (0.1 µM, 1 µM, 10 µM, 50 µM) on CYP1A1 and AhR mRNA levels was investigated in non-transfected, Ah-receptor suppressed and dsRNA-transfected KYSE510 cells. After 24 h of incubation, total RNA was isolated and used for gene transcription analysis (see chapter 6.4 “Gene Expression Analysis of CYP1A1 and AhR using quantitative Real Time PCR“).

Appropriate controls were implemented to assure correct evaluation of the performed experiments. Differently pre-treated cells (dsRNA-, siRNA- and non-transfected) were incubated with 1% DMSO and served as a calibrator with the ΔC_T-values set to 1. The reliability of the assay was monitored by using the positive control benzo(a)pyrene, applied at a concentration of 5 µM. To compare the effects of AOH and AME in siRNA-transfected cells with those in non-transfected and dsRNA-transfected KYSE510 cells, all three differently pre-treated cells were incubated with the same AME or AOH concentration. The successful suppression of AhR mRNA was monitored by pre-treating KYSE510 cells with dsRNA instead of siRNA.

AhR mRNA levels in dsRNA- and non-transfected KYSE510 Cells

A potential impact of AOH and AME on AhR transcript levels in non-transfected and dsRNA-transfected KYSE510 cells was controlled by qRT-PCR. Cells were incubated for 24 h with varying concentrations of AME and AOH. As shown in figure 28, AhR mRNA levels of non-transfected and dsRNA-treated cells were not altered by both mycotoxins. BaP fostered significant, yet marginal increases of AhR transcripts in non-transfected and dsRNA-transfected cells. The magnitude of the observed up-regulation was in the range of 1.7- to 1.9-fold. The results demonstrated that both mycotoxins as well as the transfection procedure, including the insertion of dsRNA into KYSE510 cells, did not affect the AhR transcript level.

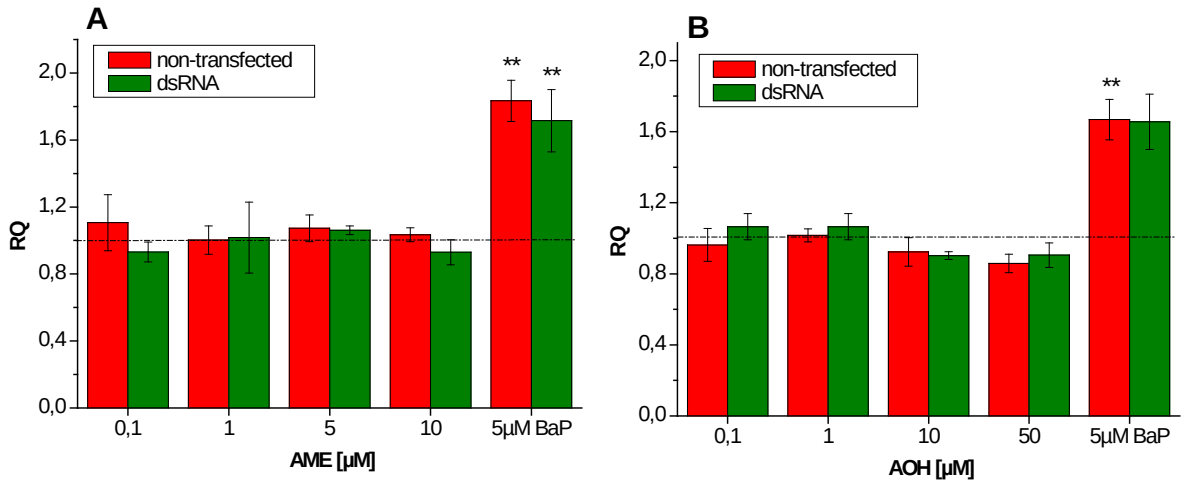

Figure 28: Effect of (A) AME and (B) AOH on the transcript level of AhR in non-transfected and negative control siRNA (dsRNA) transfected KYSE510 cells after treatment for 24 h. 5 µM BaP was used as positive control. AhR transcripts are normalised to β-actin and compared to respective DMSO (1%) treated control cells. The data are plotted as relative quantity of AhR transcripts (RQ) ± SD of at least three independent experiments. Calculation of statistical significances are performed on the basis of underlying ΔC_T-values (**=p<0.01; ***=p<0.001).

Transient Suppression of the Ah-Receptor in KYSE510 Cells

A sufficient and reproducible knockdown of AhR in KYSE510 cells is essential for correct analysis and proper interpretation of the results. Thus, AhR transcript levels were analysed in parallel to the CYP1A1 transcript levels, assuring a knockdown of at least 70%. Figure 29 displays the AhR mRNA levels in siRNA 2 transfected KYSE510 cells compared to dsRNA-treated cells 48 h post-transfection and subsequent 24 h of treatment with either (A) AME or (B) AOH. Cells dsRNA-transfected and treated with 1% DMSO were used as control.

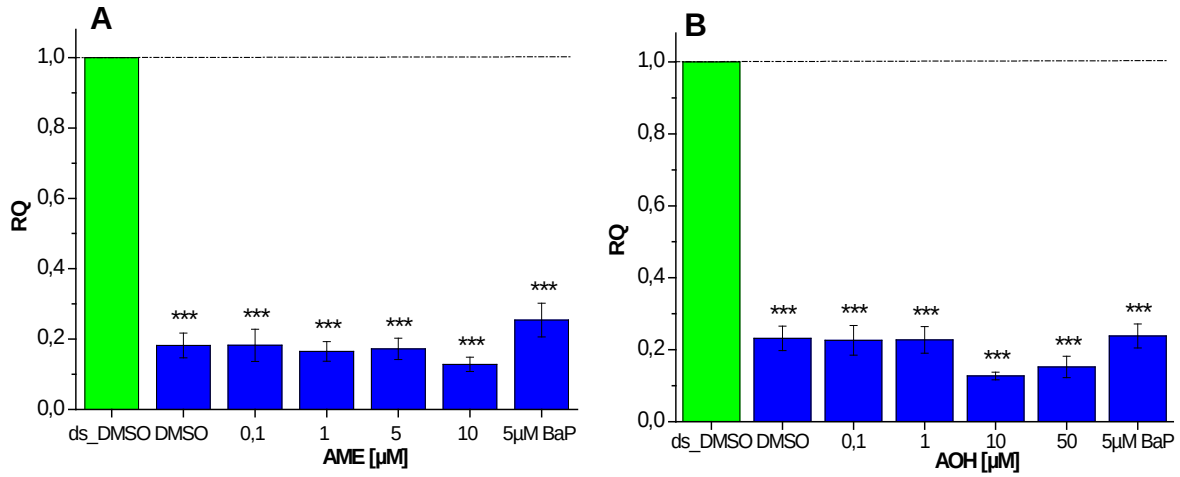

Figure 29: AhR transcripts in AhR-suppressed KYSE510 cells 48 h post-transfection and subsequent 24 h of treatment with (A) AME and (B) AOH. 5 µM BaP was used as positive control. AhR transcripts are normalised to β-actin and compared to negative control siRNA (dsRNA). The data are plotted as relative quantity of AhR transcripts (RQ) ± SD of at least three independent experiments. Calculation of statistical significances are performed on the basis of underlying ΔC_T-values (***=p<0.001).

The requirement of an at least 70% AhR-suppression was met for all siRNA-transfected KYSE510 cells, treated either with AME (figure 29 A) or AOH (figure 29 B). The AhR was even suppressed by about 80%. Thus, cells were analysed for CYP1A1 induction. The AhR transcript level was slightly less suppressed in cells incubated with 5 µM BaP for 24 h. Nevertheless, cellular AhR mRNA did not exceed the 0.3-fold level and the suppression was sufficient for the studies on CYP1A1 transcription.

Effect of AME on CYP1A1 mRNA levels in AhR-suppressed KYSE510 Cells

The investigation of AME-mediated changes in CYP1A1 transcription in AhR-suppressed KYSE510 cells required the implementation of two different controls. Firstly, successful suppression of AhR mRNA was monitored by pre-treating KYSE510 cells with dsRNA instead of AhR-siRNA, a more detailed description is given in the previous chapter. The second control was the use of differently pre-treated cells (non-transfected, AhR-siRNA and dsRNA-transfected KYSE510 cells) incubated with 1% DMSO. The CYP1A1 mRNA level in those cells represented the endogenous or basal level, which was set to 1, when calculating the AME-elicited changes in CYP1A1 transcripts.

A significant impact towards CYP1A1 transcripts was observed in non-transfected, dsRNA- and AhR-siRNA transfected KYSE510 cells after 24 h of incubation with ≥ 1 µM AME (figure 30). AME at a concentration of 0.1 µM did not affect CYP1A1 transcript levels in the tested cell types. A modest decrease was observed for dsRNA pre-treated cells in comparison to the respective DMSO (1%) control whereas CYP1A1 levels slightly increased in AhR-siRNA transfected cells. Yet the effects were not significant, thus 0.1 µM AME was referred as no effect concentration.

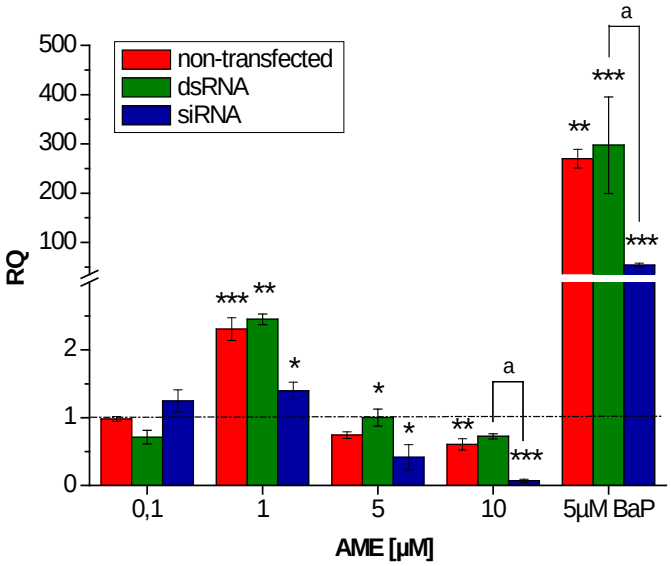

Figure 30: CYP1A1 mRNA levels in AhR-siRNA, negative siRNA control (dsRNA)-transfected and non-transfected KYSE510 cells 48 h post-transfection and subsequent 24 h of treatment with AME. 5 µM BaP was used as positive control. CYP1A1 transcripts are normalised to β-actin and compared to respective DMSO (1%) treated cells. The data are plotted as relative quantity of CYP1A1 transcripts (RQ) ± SD of at least three independent experiments. Calculation of statistical significances are performed on the basis of underlying ΔC_T-values (*/a=p<0.1; **/b=p<0.01; ***/c=p<0.001).

The induction of CYP1A1 transcripts in cells expressing AhR peaked at 1 µM AME with a maximum of 2.3 (± 0.2) - and 2.4-fold (± 0.08), respectively. In contrast, CYP1A1 mRNA in AhR-suppressed oesophageal cells was just slightly affected in comparison to the DMSO control. Given that the Ah-receptor, which is believed to be the main regulator of CYP1A1 transcription (Nebert *et al.*, 2004) is sufficiently suppressed (figure 29 A), it was expected that AME should not be able to elicit any induction of CYP1A1 transcripts. However, it has to be pointed out that, albeit the induction was significant, it was still marginal with 1.2-fold (±0.2).

The amount of CYP1A1 mRNA declined at 5 µM AME and the trend continued at 10 µM for all three different cell types. In AhR-suppressed cells CYP1A1 mRNA was diminished significantly to 0.4 (± 0.2) - and 0.07-fold (± 0.02). A minor, yet significant drop of CYP1A1 transcripts in comparison to the DMSO control was observed at 10 µM AME in non-transfected KYSE510 cells (figure 23). However, the decline in dsRNA-transfected KYSE510 cells was not significant. CYP1A1 transcription in AhR-suppressed cells should not be influenced by any AhR agonist purely acting via the Ah-receptor pathway. However, 5 µM benzo(a)pyrene, a substance which is only known to act by binding to the AhR (Whitlock, 1999; Almahmeed *et al.*, 2004), triggered a 54.3-fold (± 3.8) increase of CYP1A1 transcripts in AhR-suppressed KYSE510 cells. The remaining 30% of AhR mRNA, which were not suppressed by transient siRNA transfection and the fact that BaP is a very strong AhR-inducer, could account for the observed high CYP1A1 mRNA induction. The reduced levels of CYP1A1 at higher AME-concentrations are not accompanied by changes of AhR mRNA (figure 23), thus supporting the hypothesis of AhR playing a role in AME-mediated CYP1A1-induction.

Cytotoxicity has to be considered as a reason for the drop in CYP1A1 levels at ≥ 5 µM AME concentrations. However, cell viability of non-transfected KYSE510 cells was not significantly diminished in the range of 0.1 - 10 µM AME as shown by the SRB assay (figure 18). Given that the expression of CYP1A1 is mainly mediated by the Ah-receptor (Nebert *et al.*, 2004), its knockdown, as it is the case in AhR-suppressed KYSE510 cells, could potentially lead to a higher concentration of non-metabolised AME in the respective cells. This would make AhR-siRNA transfected oesophageal cells far more sensitive towards xenobiotic exposure. This argument is not supported by increased C_T-values of β-actin in siRNA-transfected cells in comparison to non-transfected cells. Higher C_T-values are obtained when the amount of template DNA at the beginning of the PCR-amplification process is low. It is reasonable to assume increased cytotoxicity would be accompanied by higher C_T-values. Since no such effect was observed, the role of cytotoxicity was considered to be of minor extend. However, a cytotoxicity assay, such as the SRB or MTT assay, with AhR-suppressed cells is necessary to verify the hypothesis.

The involvement of Ah-receptor in cell growth and differentiation should not be neglected. AhR-defective mouse hepatoma cells exhibited a slowed growth rate (Ma & Whitlock, 1996). A diminished cell growth, just as cytotoxicity, could be accountable for decreased CYP1A1 mRNA levels. Incubation with 10 µM AME decreased CYP1A1 transcripts by 0.6-fold (± 0.08) in non-transfected cells, a partial antagonistic effect of AME towards AhR at 10 µM would be a considerable explanation. However, any investigations addressing AME as partial Ah-receptor agonist/ antagonist have been performed by now, implying the necessity of further investigations.

Another explanation for plummeting CYP1A1 transcripts at ≥ 5 µM AME in AhR-suppressed KYSE510 cells might be the interference with another, yet unknown pathway. The induction of CYP1A1 by dioxin has already been shown to involve tyrosine kinases in human keratinocytes (Gradin *et al.*, 1994). CYP1A1 expression, triggered by the anti-ulcer drug omeprazole was believed to involve crosstalk of the Ah-receptor with protein tyrosine kinases (Backlund *et al.*, 1997). A suggested interfering pathway could be exclusively activated when signal transduction by the Ah-receptor was blocked, as it is the case in siRNA-suppressed Ah-receptor. However, CYP1A1 induction by a different pathway than the AhR would be of considerably weaker extend since transcripts decreased below the endogenous level. Additionally, concentrations of ≥ 5 µM AME were necessary for activation. Nevertheless, the existence of an interfering pathway was not proven and requires further investigations.

Effect of AOH on CYP1A1 mRNA levels in AhR-suppressed KYSE510 Cells

CYP1A1 transcripts in non-transfected, dsRNA- and AhR-siRNA transfected KYSE510 cells was determined after 24 h of incubation with AOH. AOH up to 10 µM fostered a concentration-dependent increase of CYP1A1 transcript levels in AhR-expressing cells (figure 31). Already 0.1 µM AOH triggered a considerable 2-fold (± 0.5) increase of CYP1A1 mRNA, while any alterations were observed for AME at the same concentration (figure 30). AOH raised CYP1A1 levels of non-transfected and dsRNA-transfected KYSE510 cells up to 7.8 (± 0.4) - and 7.4-fold (± 1.2), respectively at a concentration of 1 µM AOH. The effect on CYP1A1 was similar at 10 µM AOH and abolished when applying AOH concentrations of 50 µM.

The induction of CYP1A1 by 0.1 µM AOH in AhR-suppressed cells was still evident, albeit not significant. Even if classified as an all over weak induction, CYP1A1 mRNA exceeded the endogenous level. The very low, yet still present transcript level of AhR in knockdown cells might be sufficient to grant AhR-dependent CYP1A1 induction at low AOH concentrations (figure 31). In comparison to AhR-expressing cells, CYP1A1 induction was significantly diminished in AhR-suppressed cells at 1 µM and 10 µM AOH. However, the amount of CYP1A1 mRNA was still significantly increased at 1 µM AOH, yet to a minor extend

(4.1-fold ± 0.03), compared to AhR-expressing cells. The potent CYP1A1 induction at 10 µM AOH in non-transfected and dsRNA-transfected cells declined to a 0.6-fold (± 0.04) level in AhR-siRNA transfected cells, indicating the complete abolishment of AOH-mediated CYP1A1 expression. Incubation with 50 µM AOH reduced CYP1A1 mRNA levels in non-transfected, dsRNA- and AhR-siRNA transfected cells, indicating potential cytotoxic effects.

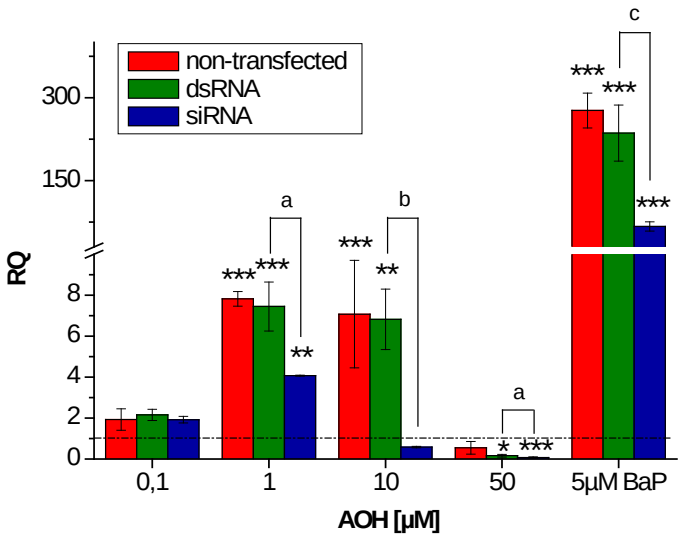

Figure 31: CYP1A1 mRNA levels in AhR-siRNA, negative siRNA control (dsRNA)-transfected and non-transfected KYSE510 cells 48 h post-transfection and subsequent 24 h of treatment with AOH. 5 µM BaP was used as positive control. CYP1A1 transcripts are normalised to β-actin and compared to respective DMSO (1%) treated cells. The data are plotted as relative quantity of CYP1A1 transcripts (RQ) ± SD of at least three independent experiments. Calculation of statistical significances are performed on the basis of underlying ΔC_T-values (*/a=p<0.1; **/b=p<0.01; ***/c=p<0.001).

While cytotoxicity was believed to play a minor role in the AME-fostered decrease of CYP1A1 transcripts at 10 µM, it is of greater importance when accounting for the AOH-mediated effects at 50 µM. The impurities in AOH used by M. Fehr were believed to be insignificant with respect to the quantity, hence the SRB assay was not performed with AOH purchased from Sigma-Aldrich. However, the cytotoxic effect of Sigma-Aldrich AOH in KYSE510 cells was analysed by N. Kahle post-finishing the experimental part of the present thesis. The data clearly showed the onset of cell growth inhibition at 50 µM AOH. Thus there was strong evidence, that decreased CYP1A1 transcript levels in all three different cell types were prone to cytotoxic activity.

Furthermore, at a concentration of 10 µM AOH potential cytotoxic effects in AhR-siRNA transfected cells cannot be excluded completely. Given that in AhR-suppressed KYSE510 cells less CYP1A1 mRNA is transcribed, the diminished amounts of CYP1A1 protein may not detoxify AOH to the same extend compared to AhR-expressing cells. This could lead to

similar accumulation effects as already postulated for AME. Again, the issue could only be addressed by performing a cytotoxicity-assay with AhR-suppressed KYE510 cells.

It might also be speculated that the suppression of the Ah-receptor could lead to the activation of a non AhR-mediated pathway at ≥ 10 µM AOH, affecting CYP1A1 transcription. Given that CYP1A1 transcripts decreased below the basal level, CYP1A1 expression via a putative pathway appeared to be considerably weaker than signalling via the Ah-receptor. As in the case of AME, the existence of an additional interfering pathway was just hypothesised and not proven by further experiments.

4.3.4. Ligand Inhibition of the AhR in KYSE510 Cells

In addition to the knockdown by AhR-siRNA, suppression of AhR function was approached by inhibition of ligand-binding in KYSE510 cells, using 3´-methoxy-4´-nitroflavone (MNF). In the literature, the synthetic flavone is described as a potent Ah-receptor antagonist in various cell systems. Lu *et al.* (1995) identified MNF as a pure AhR antagonist in human breast cancer cells (MCF-7). An antagonistic effect was also observed in human keratinocytes HaCaT by Schäfer, 2006.

In the present work, the modulation of CYP1A1 transcription by AME was investigated in AhR-inhibited KYKSE510 cells. Oesophageal cells were first incubated with MNF, subsequently with AME and then the amount of CYP1A1 mRNA was determined. Thus, additional information for a better understanding of the mode of action of AME-mediated CYP1A1 induction was expected. Briefly, $3*10^4$ KYSE510 cells were seeded per well of a 24-well plate and cultivated for 24 h. Then the cells were treated with 10 µM MNF for 15 minutes, enabling the adsorption of the molecules at the Ah-receptor binding site. Subsequently the MNF-containing medium was removed and complete medium (RPMI 1640 containing 10% FBS and 1% P/S) with varying concentrations of AME (0.1, 1, 5 and 10 µM) was added and left for 24 h. Additionally, appropriate controls were implemented: MNF pre-treated cells were incubated with 1% DMSO for 24 h serving as control for the AME-mediated effects. To investigate the purely MNF-elicited effects complete medium (RPMI 1640 containing 10% FBS and 1% P/S) was applied for 24 h onto 10 µM MNF pre-treated cells. A third control, which consisted of cells, pre-treated with 1% DMSO and a following 24 h incubation period with complete medium, was used to study MNF- and AME-mediated effects in KYSE510 cells only.

A concentration-dependent effect of AME was observed in MNF pre-treated KYSE510 cells after 24 h of incubation (figure 32). Treatment with 10 µM MNF increased the CYP1A1 transcript level about 11-fold (± 3.7) compared to 1% DMSO pre-treated control cells.

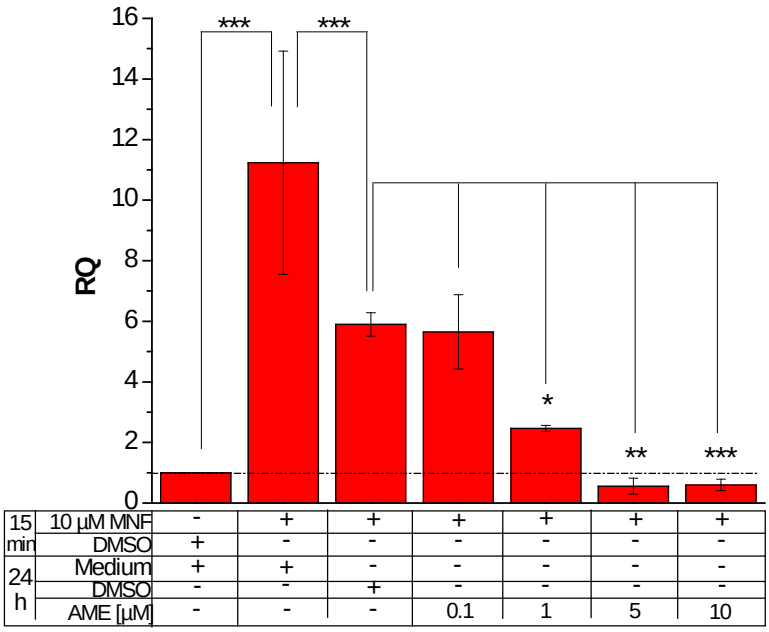

Figure 32: CYP1A1 mRNA levels in 15 minutes pre-treated KYSE510 cells (with 10 µM MNF or 1% DMSO) and subsequent 24 h treatment with AME, DMSO (1%) or medium. CYP1A1 transcripts are normalised to β-actin and compared to respective DMSO (1%) treated control cells. The data are plotted as relative quantity of CYP1A1 transcripts ± SD of at least three independent experiments. Calculation of statistical significances are performed on the basis of underlying ΔC_T-values (*=p<0.1; **=p<0.01; ***=p<0.001).

MNF is a known AhR antagonist, however some authors report of concentration-dependent agonistic and antagonistic effects. The antagonistic effect of MNF on TCDD-elicited luciferase gene induction in stably transfected Hepa.2DLuc.3A4-cells was observed at 0.1 µM and in the range of 1 - 10 µM a low level of reporter induction was observed (Zhou & Gasiewicz, 2003). Goergens (2009) showed a concentration-dependent MNF effect towards CYP1A1 transcription in the human promyelocytic leukaemia cell line HL-60. It acted as an antagonist in the concentration range of 1 - 10 µM by diminishing the curcumin-fostered CYP1A1 mRNA expression. An agonistic effect was observed for MNF concentrations smaller than 1 µM and higher than 10 µM (Goergens, 2009). Ah-receptor agonistic/ antagonistic effects of MNF seemed to be strongly concentration- and cell line-dependent.

Since an 11-fold increased CYP1A1 mRNA level was observed when applying 10 µM MNF, either an agonistic effect on the AhR or other potential responsive signal pathways, modulating CYP1A1 at that concentration need to be considered. However, subsequent incubation of MNF pre-treated cells with 1% DMSO for 24 h caused a minor, only 5.9-fold (± 0.4) increase of CYP1A1 mRNA compared to medium-treated cells. CYP1A1 transcripts even further decreased when applying increasing concentrations of AME.

The drop of CYP1A1 mRNA levels when replacing pure medium with 1% DMSO could be due to a potential displacement of Ah-receptor bound MNF by DMSO molecules. The strong AME concentration-dependent reduction of MNF-induced CYP1A1 transcripts supported a scenario of potential competitive properties of AME towards MNF at the AhR, implying binding to the receptor. Based on these results, it might be speculated that AME-mediated CYP1A1 induction was impeded by Ah-receptor bound MNF. This would support the role of AhR in AME-mediated CYP1A1 induction. However, an Ah-receptor antagonist, which did not induce CYP1A1 mRNA at certain concentrations, should be used to obtain a cell system, comparable to AhR-siRNA suppressed KYSE510 cells. MNF applied at a concentration of 10 µM clearly induced CYP1A1 transcripts, the addition of another inducer, like AME, would lead one to expect an additive effect. Instead, CPY1A1 mRNA levels declined concentration-dependently. The speculation of a potential displacement of MNF from the AhR binding site by AME could not be verified by the experiment conducted. Further investigations regarding the binding affinities and agonistic/ antagonistic effects of both substances in KYSE510 cells have to be performed to fully understand the underlying mechanism of action.

4.4. Impact of AOH and AME on Glutathione-S-Transferase Activity in HT29 Cells

Enzymes of the glutathione-S-transferase (GST) family are phase II drug-metabolising enzymes. They act by catalysing the reaction of glutathione with an acceptor molecule to form S-substituted glutathione (Hayes *et al.*, 2005). Xenobiotics are often activated by monooxygenases like cytochrome P450 enzymes which is followed by a nucleophilic attack of the thiol group of the reduced glutathione (Prochaska & Talalay, 1988). GSH-conjugates are subsequently eliminated via active transport systems (Ebert *et al.*, 2001). The photometrical determination of the change in absorbance occurring during the glutathione-S-transferase (GST)-catalysed reaction of glutathione and 1-chloro-2,4-dinitrobenzene (CDNB) is used for analysing GST activity. Nearly all GST isoenzymes can use CDNB as substrate for conjugation with glutathione (Habig *et al.*, 1974). GSTP1 is the predominant isoform in HT29 cells used in the present work (Ebert *et al.*, 2003).

Both A*lternaria* toxins tested in the present thesis, are prone to phase I drug metabolism (Pfeiffer *et al.*, 2008). Their impact on phase II drug metabolising enzymes GST in human colon carcinoma HT29 cells presented a further part of the present thesis. The colon carcinoma model was chosen due to published data by Pfeiffer *et al.* (2009) and Burkhardt *et al.* (2009), using the same, or comparable cell model. They demonstrated the formation of AOH- and AME-glucuronides by hepatic and intestinal microsomes. Both mycotoxins were also found to be readily conjugated to sulphates as well as to glucuronides in HT29 cells after 24 h incubation. The high glucuronidation activity coincided with a diminished DNA-strand breaking potential, indicating that the activity of a cell in forming AME- and AOH-glucuronides played a critical role in this context. Since glucuronidation and sulphation are both important detoxification reactions, the contribution of GSTs in colon tumour cells to the detoxification process should be analysed. The GST assay was established according to Habig *et al.* (1974) (see chapter 6.6 “Glutathione-S-Transferase (GST) Enzyme Activity“). Briefly, $1.2*10^6$ HT29 cells were seeded per Petri dish and cultivated for 48 h and 72 h, respectively. After 24 h of incubation with AME and AOH, cells were detached using trypsin/ EDTA solution. The results are plotted as test over control [%], whereas 1% or 0.1% DMSO- and 1% water-treated control cells, respectively were used.

4.4.1. GST Activity after 24 h of Incubation with AME and AOH

After 24 h of incubation with AME, any significant changes in GST activity compared to DMSO (1%) treated control cells were observed (figure 33 A). Although 0.1 µM AME fostered a marginal increase in GST activity up to 109% (± 16%), yet the change was not significant.

In figure 31 B a slight increase of GST activity was observed at higher AOH concentrations. AOH at a concentration of 0.1 - 10 µM elevated the activity to about 107 - 108%. However, the changes were too minor to differ significantly from 1% DMSO-treated control cells. Exclusively 50 µM AOH significantly increased GST activity to 113% (± 0.4%).

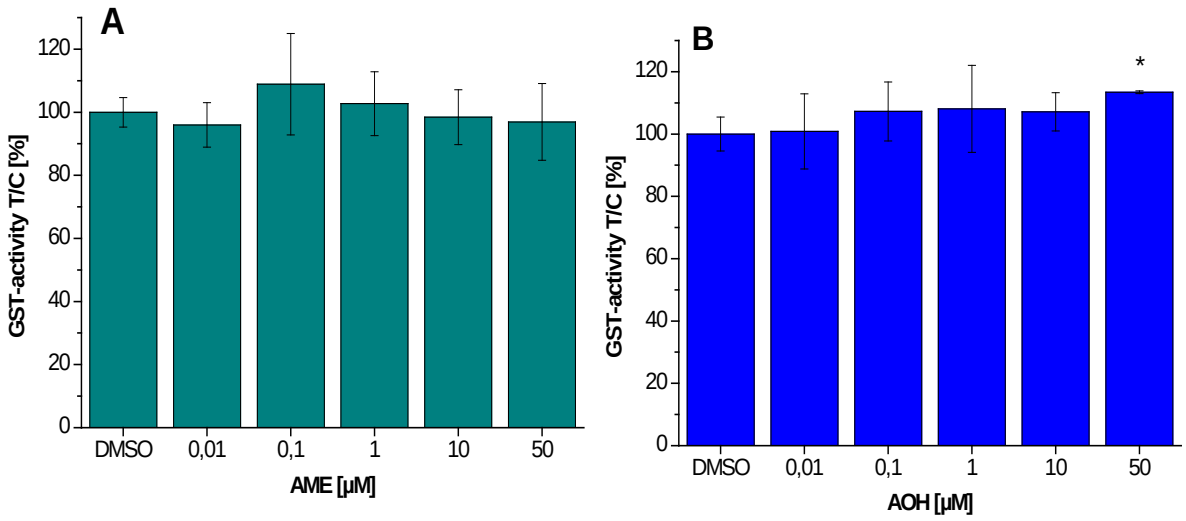

Figure 33: GST activity in HT29 cells determined in the GST assay according to Habig *et al.* (1974). Cells were pre-cultivated for 48 h and subsequently treated with either (A) AME or (B) AOH for 24 h, respectively. GST activities are calculated as the percent GST activity of treated cells over control cells (treated with the solvent 1% DMSO) x 100 (T/C%). The values given are the mean ± SD of at least three independent experiments. Calculation of statistical significances are performed on the basis of underlying T/C [%] values (*=p<0.1).

At the time GST activity experiments were performed, it was assumed, that based on the results of M. Fehr concerning cytotoxic effects of AOH in HT29 cells, no cytotoxic action at 50 µM AOH existed after 24 h incubation. However, later in according to results obtained by C. Tiessen, AOH purchased from Sigma-Aldrich already showed cell growth inhibitory effects at ≥ 50 µM in HT29 cells. Considering these results, the marginal, yet significant increase in GST activity at 50 µM AOH should be viewed critically.

Menadione (MEN) and tert-butylhydroperoxide (tBHP), described as inducers of GST activity in the literature (Dierickx *et al.*, 1999; Fehr, 2008), were tested in three independent experiments. Since tBHP was only available as aqueous solution, control cells were treated with 1% water-containing medium. However, any of the compounds fostered a significant increase of GST activity (figure 34 A, B).

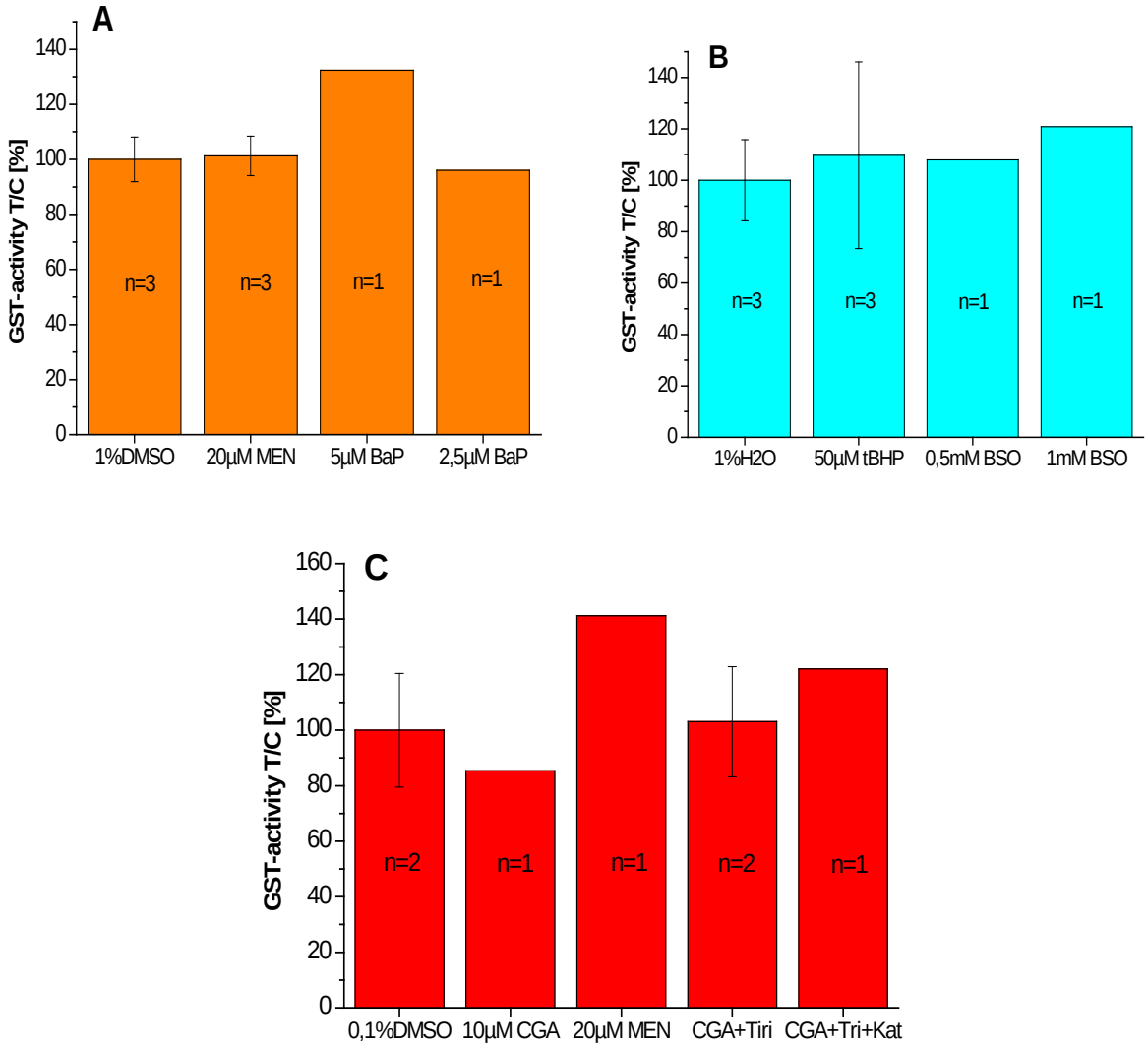

Figure 34: GST activity in HT29 cells determined in the GST assay according to Habig *et al.* (1974). Cells were pre-cultivated for 48 h and subsequently treated with MEN, BaP, tBHP, BSO, CGA, CGA+Tri and CGA+Tri+Kat for 24 h. HT29 cells were incubated with the designated substances dissolved in media, containing final DMSO-concentration of (A) 1% or (B) 0.1% or (C) 1% H_2O. GST activities are calculated as the percent GST activity of treated cells over control cells (treated with the solvent 0.1% and 1% DMSO and 1% H_2O, respectively) x 100 (T/C%). The number of replicates n is denoted in the bars, the mean ± SD is given for samples n ≥ 2.

Further compounds and combination of substances, which were reported to either induce GST mRNA, GST protein or GST activity such as benzo(a)pyrene (BaP) (Robertson *et al.*, 1986), 10 µM chlorogenic acid (CGA), co-incubation with 0.5 µM chlorogenic acid and 5.5 µM trigonelline (CGA+Tri), co-incubation with 0.5 µM chlorogenic acid, 5.5 µM trigonelline and 1000 U/ml catalase (CGA+Tri+Kat) (Volz, 2010) and buthionine sulfoximine (BSO), a reported suppressor of GST activity which acts by depleting the cell´s GSH pool (Dierickx *et al.*, 1999), were included in the testing for induction or suppression of GST activity (figure 34 A-C). However, none of the tested compounds caused a reproducible increase or decrease in GST activity in HT29 cells. The most impressive increase in GST activity was observed in cells treated with menadione in the presence of 0.1% DMSO. However, replicates were lacking. Thus, due to the high variation in the response of HT29 cells to GST inducers, the marginal induction of enzyme activity observed at 50 µM AOH, should be viewed critically and should not be overestimated.

4.4.2. Optimisation of Incubation Time for GST Activity

Induction of GST activity is considered to be time-dependent; hence the incubation time was modulated to achieve optimal induction of GST activity. Since neither treatment with known GST inducers (figure 34) nor with different AME or AOH concentrations (figure 33 A and B) triggered a significant or trustworthy increase of GST activity, the incubation time was reduced to 1 h, 6 h, 9 h and 16 h.

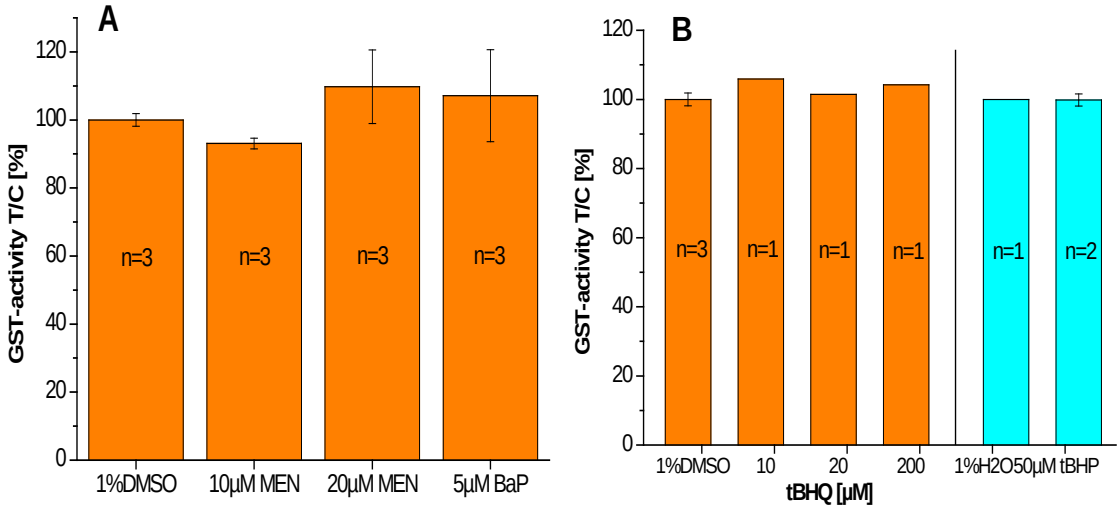

Figure 35**:** GST activity in HT29 cells determined in the GST assay according to Habig *et al.* (1974). Cells were pre-cultivated for 48 h and subsequently treated with (A) MEN, BaP and (B) tBHQ, tBHP for 1 h. GST activities are calculated as the percent GST activity of treated cells over control cells (treated with the solvent 1% DMSO) x 100 (T/C%). The number of replicates n is denoted in the bars, the mean ± SD is given for samples n ≥ 2.

M. Fehr (2008) observed in HT29 cells a significant increase in GST activity after 1 h of incubation with 20 µM menadione. The results of various experiments with HT29 cells, treated with substances known for their GST-inducing effects, including 5 µM benzo(a)pyrene (BaP), 10, 20 and 200 µM tert-butylhydroquinone (tBHQ) and 50 µM tert-butylhydroperoxide (tBHP) (Dierickx *et al.*, 1999) are shown in figure 35. MEN and BaP were tested in three independently performed experiments, whereas tBHP and tBHQ were tested just once. However, no significant increase in GST activity was observed for any of the tested compounds

Figure 36 shows the effect on GST activity after 6 h of incubation with various concentrations of AME, whereas 5 µM benzo(a)pyrene (BaP) and 200 µM tert-butylhydroquinone (tBHQ) (Jiang *et al.*, 2003) were used as positive controls. However, neither the mycotoxins nor the positive controls fostered significantly increased GST activity levels. The absence of any strong GST induction led to the decision to stop further experiments with incubation times as short as 6 h.

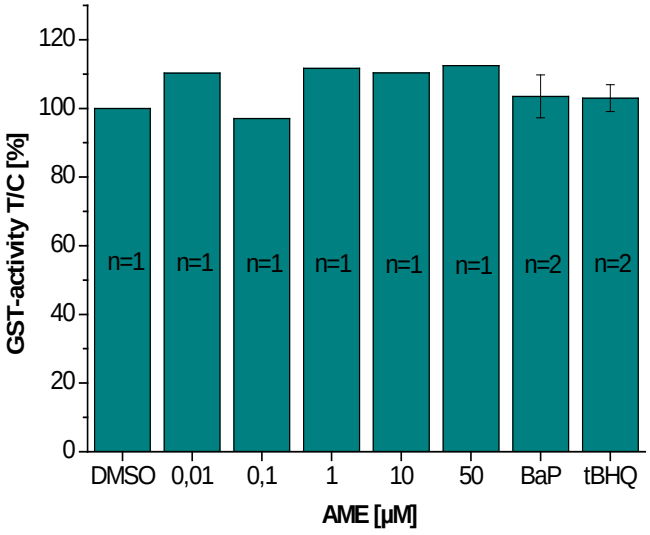

Figure 36: GST activity determined in the GST assay according to Habig *et al.* (1974). HT29 cells were pre-cultivated for 48 h and subsequently treated with AME and 5 µM BaP or 200 µM tBHQ for 6 h. GST activities are calculated as the percent GST activity of treated cells over control cells (treated with the solvent 1% DMSO) x 100 (T/C%). The number of replicates n is denoted in the bars, the mean ± SD is given for samples n ≥ 2.

Further investigations regarding the time-dependence of GST activity were performed by changing the time of incubation to 9 h (figure 37 A) and 16 h (figure 37 B). The increase in GST activity after 9 h of incubation with 10 µM and 20 µM sulforaphane (SFN) (Jiang *et al.*, 2003) and 20 µM menadione and after 16 h of incubation with 15 µM SFN, 20 µM MEN, 200 µM tBHQ and 5 µM BaP appeared too marginal, thus further investigations were stopped, particularly due to lack of time within the frame of the thesis.

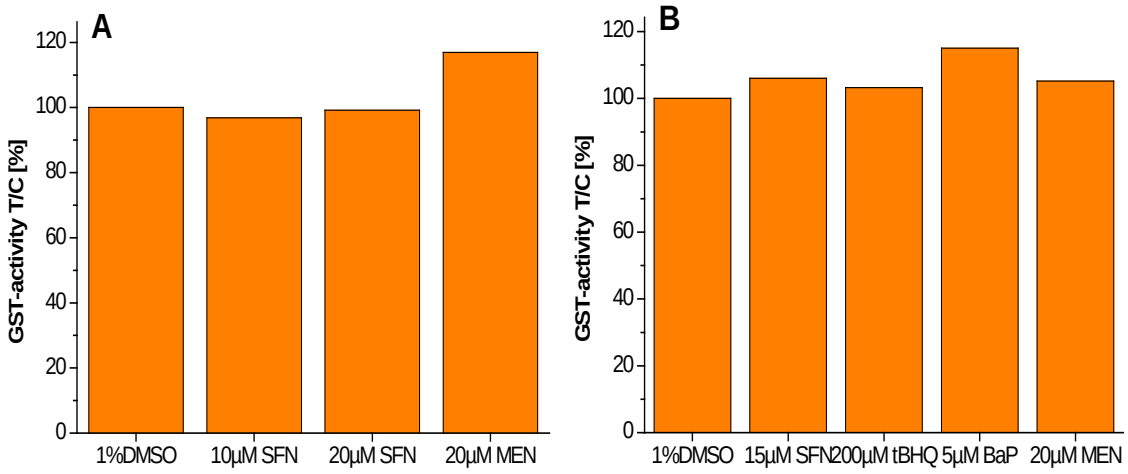

Figure 37: GST activity in HT29 cells determined in the GST assay according to Habig *et al.* (1974). Cells were pre-cultivated for 48 h and subsequently treated with (A) 10 µM or 20 µM SFN, 20 µM MEN for 9 h or with (B) 15 µM SFN, 200 µM tBHQ, 5 µM BaP, 20 µM MEN for 16 h. GST activities are calculated as the percent GST activity of treated cells over control cells (treated with the solvent 1% DMSO) x 100 (T/C%) of a single experiment.

In summary, the data on GST activity in HT29 cells obtained so far, did not show a significant induction of glutathione-S-transferases by known inducers, by AME and AOH with exception of a marginal, yet significant increase at 50 µM AOH. However, this concentration turned out to be already cytotoxic for HT29 cells, so the induced GST activity should be viewed critically.

4.4.3. Modulation of GSTA1,-A2,-T1 and P1 transcript levels in HT29 Cells

The analysis of mRNA levels was accomplished by qRT-PCR, which is a far more sensitive method than the photometric GST assay and technically preferred for screening. However, modulation of mRNA levels has to be verified always at the protein level. Since the induction of GST activity with known inducers was disappointing, orienting experiments on transcript levels of the GST isoenzymes, including GSTA1, -A2, -T1 and -P2 were performed in HT29 cells after incubation with GST inducers at different time points. It was expected to get more information why the response of HT29 cells at the protein level was so weak and unsteady.

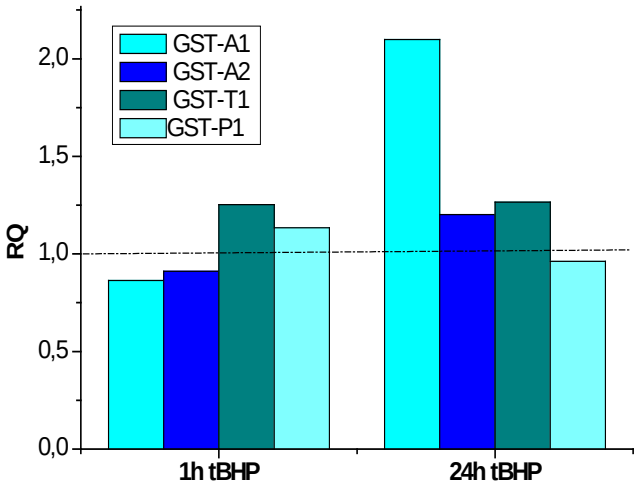

Figure 38: Effect of 50 µM tBHP on the transcript level of GSTA1, -A2, -T1 and –P1 in HT29 cells after 48 h pre-cultivation and subsequent treatment for 1 h and 24 h, respectively. GSTA1, -A2, -T1 and –P1 transcripts are normalised to β-actin and compared to respective H_2O (1%) treated control cells. The data are plotted as relative mRNA quantity (RQ) of a single orienting experiment.

Figure 38 displays the effect of 50 µM tBHP on the transcript level of various GST-isoenzymes in HT29 cells. Incubation for 1 h with tBHP did not affect GST transcript levels. After 24 h of incubation, GSTA1 mRNA was increased 2.1-fold, whereas the GSTA2,-T1 and -P1 transcript levels were not affected. Any increased GST activity was observed after 24 h of incubation with 50 µM tBHP (figure 34 B), indicating that the GSTA1 mRNA increase is too marginal to induce enhanced GST activities or the 2.1-fold increase may cause a too low induction of enzyme activity to be recorded by photometric determination in the GST enzyme assay.

Figure 39 displays the effect of 15 µM SFN, 20 µM MEN, 200 µM tBHQ and 5 µM BaP on GSTA1 and –A2 mRNA levels after 1 h of incubation. Among the tested substances, only 20 µM menadione fostered a 1.5-fold increase in GSTA1 mRNA and 5 µM BaP a 1.3-fold increase in GSTA2 mRNA. A maximum 1.2-fold induction of GSTA1 and GSTA2 mRNA was observed after incubation with all other substances.

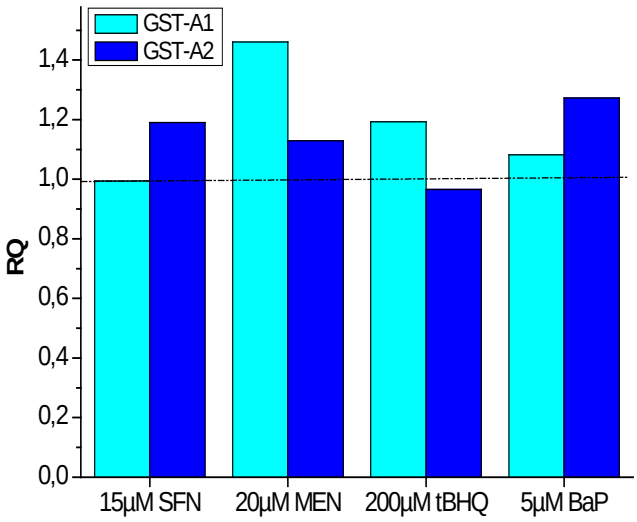

Figure 39: Effect of 15 µM SFN, 20 µM MEN, 200 µM tBHQ and 5 µM BaP on the transcript level of GSTA1 and -A2 in HT29 cells after 48 h pre-cultivation and subsequent treatment for 1 h. GSTA1 and -A2 transcripts are normalised to β-actin and compared to respective DMSO (1%) treated control cells. The data are plotted as relative mRNA quantity (RQ) of a single orienting experiment.

4.4.4. Glutathione-S-Transferase Activity in HepG2 Cells

Treatment of HT29 cells with various substances, described as inducers of GST activity in the literature at varying incubation times did not result in a significant induction. However, significant increases of GST activities in HT29 cells were reported previously by several authors (Ebert *et al.*, 2003; Nam & Shon, 2009). Thus, to exclude any problems in the responsiveness of the used HT29 cell clone (will be discussed in more detail at the end of chapter 4.4.5 “GST Activity in HT29 Cells cultivated for 72 h”) and to verify proper performance of the method, the assay was established in human liver carcinoma cells HepG2, known to express GST enzyme activity. This cell type not only represents most cellular features of normal human hepatocytes (Bouma *et al.*, 1989) but was also shown to retain many enzymes involved in xenobiotic metabolism (Roberts *et al.*, 1990).

Briefly, $3*10^6$ HepG2 cells were seeded per Petri dish and cultivated for 48 h and 72 h, respectively. An incubation period of 2 h with 40 µM quercetin (Que), a reported suppressor of GST activity (Wiegand *et al.*, 2009) and 5 µM BaP followed, whereas 15 µM SFN was applied for 24 h. Cells were trypsinised and the GST assay according to Habig *et al* (1974) was performed. The results were expressed as test over control [%], with 1% DMSO-treated cells as control.

Quercetin fostered a 50% decrease of GST activity independent of cultivation time (figure 40 A and B). However, any increase of GST activity was observed upon incubation with benzo(a)pyrene and sulforaphane.

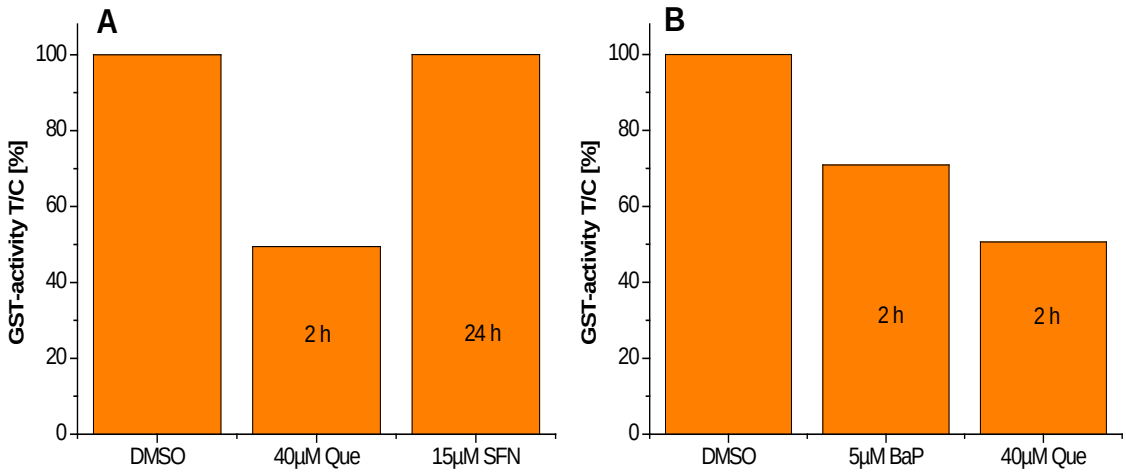

Figure 40: GST activity in HepG2 cells determined in the GST assay according to Habig *et al.* (1974). Cells were pre-cultivated for (A) 48 h and subsequently treated with 40 M Que for 2 h and 15 µM SFN for 24 h and (B) pre-cultivated for 72 h and subsequently treated with 5 µM BaP for 2 h and 40 µM Que for 2 h. GST activities are calculated as the percent GST activity of treated cells over control cells (treated with the solvent 1% DMSO) x 100 (T/C%) of a single orienting experiment.

Figure 41 shows the GST mRNA levels in HepG2 cells after 2 h of incubation with 5 µM BaP and 40 µM Que. BaP increased GSTP1 mRNA 8.7-fold, GSTA1, -A2 and -T1 levels remained nearly unchanged. However, this increase is only observed on the transcript level, different times of incubation (1 h see figure 35, 6 h see figure 36, 16 h see figure 37 B, 24 h see figure 34 C) did not enhance GST activity. GSTP1 mRNA is increased 3.1-fold after incubation with 40 µM Que. The enhanced GST mRNA level after Que treatment did not coincide with the observed diminishment in GST activity after 2 h (figure 40 A and B). However, since mRNA and protein isolation were performed both after 2 h of incubation, the minimum of mRNA transcripts was believed to be earlier in time, followed by an up-regulation after 2 h.

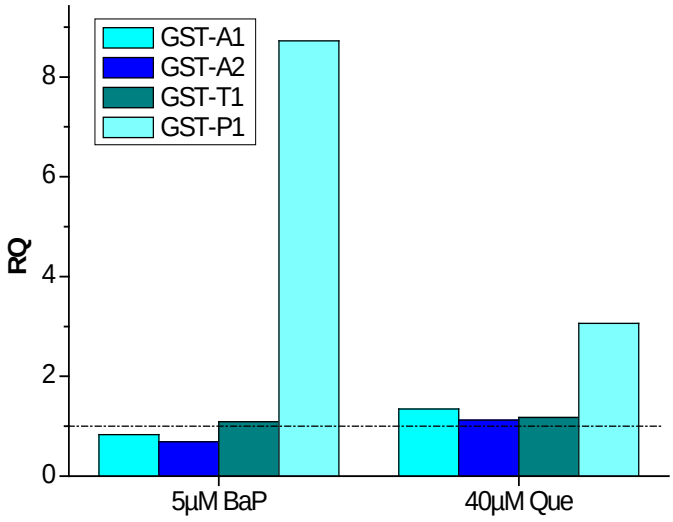

Figure 41: Effect of 5 µM BaP and 40 µM Que on the transcript level of GSTA1, -A2, -T1 and –P1 in HepG2 cells after 72 h pre-cultivation and treatment for 2 h. GSTA1, -A2, -T1 and –P1 transcripts are normalised to β-actin and compared to respective DMSO (1%) treated control cells. The data are plotted as relative mRNA quantity (RQ) of a single orienting experiment.

4.4.5. GST Activity in HT29 Cells cultivated for 72 h

Significant AME- or AOH-mediated increases of CYP1A1 transcripts in KYSE510 cells were observed only in cells cultivated for at least 48 h prior incubation with the mycotoxins. These results initiated the question, whether HT29 cells grown for 48 h are optimally developed for the expression of GST enzymes. However, the doubling time of HT29 cells, which varies between 40 - 60 h, is nearly twice as much as the 30 h doubling time of KYSE510 cells. HT29 cells, 48 h post-seeding were examined under the microscope. Their morphology was considered to be still in the developmental phase. Figure 42 A displays fully developed HT29 cells, which are clustered in complex groups and each cell is in tight contact with the neighbouring one. In contrast, freshly seeded cells are of spherical shape, mostly single individuals surrounded by wide areas of free space (figure 42 B). Since the morphology of HT29 cells after 48 h of culture corresponded more closely to the latter description, the time of cultivation was prolonged to 72 h.

A **B**

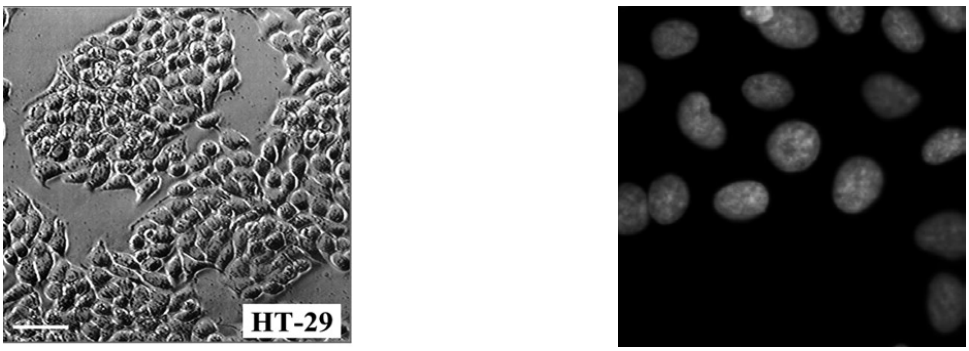

Figure 42: Morphology of HT29 cells which (A) already established their morphology [http://jcs.biologists.org/content/119/1/31/F1.expansion.html] and (B) HT29 cells seeded quite recently [http://www.cellprofiler.org/examples.shtml].

Even after increasing the time of pre-cultivation, any significant increase of GST activity by AME was apparent in HT29 cells (figure 43 A). The results were similar to the unchanged GST activity in cells cultivated for 48 h (figure 33 A).

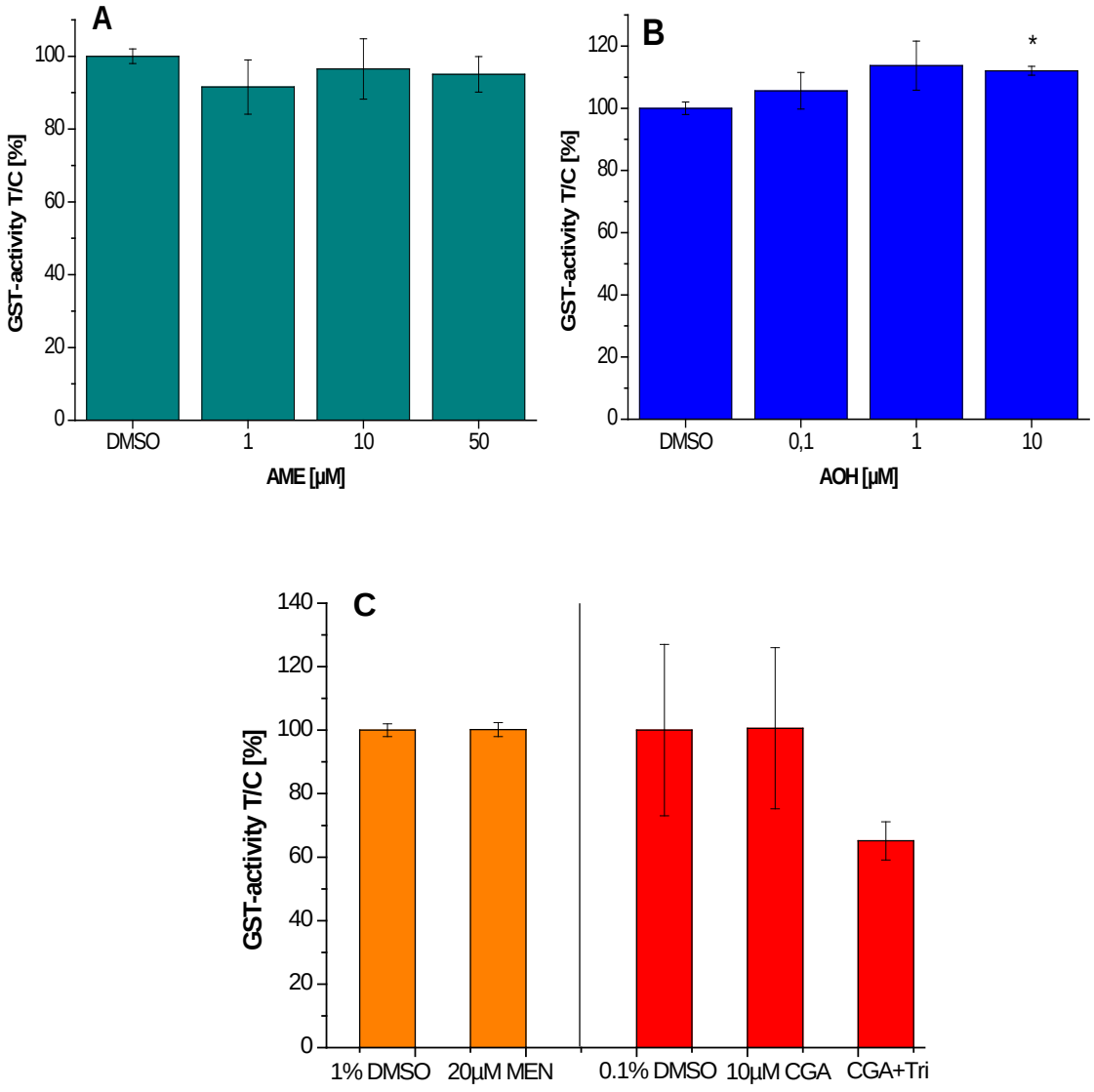

Figure 43: GST activity in HT29 cells determined in the GST assay according to Habig *et al.* (1974). Cells were pre-cultivated for 72 h and subsequently treated with (A) AME, (B) AOH and (C) 20 µM MEN, 10 µM CGA or 0.5 µM CGA + 5.5 µM trigonelline, respectively for 24 h. GST activities are calculated as the percent GST activity of treated cells over control cells (treated with the solvent 1% DMSO) x 100 (T/C%). The values given are the mean ± SD of three independent experiments. Calculation of statistical significances are performed on the basis of underlying T/C [%] values (*=p<0.1).

AOH at a concentration of 10 µM caused a minor, yet significant increase of GST activity to 112% (± 1.4%). Previous experiments with shorter cultivation periods (48 h) showed a significant increase of GST activity not before 50 µM AOH (figure 33 B). However, the observed induction at 50 µM AOH should be viewed critically, since the onset of cytotoxic effects was demonstrated. Any cell growth inhibition was observed at ≤ 10 µM AOH in 48 h pre-cultivated HT29 cells. So far any data for AOH elicited cytotoxicity in 72 h pre-cultivated cells had been available. Based on the results obtained with 48 h pre-cultivated HT29 cells, there would be just a minimal probability of cell growth inhibition by 10 µM AOH in 72 h pre-cultivated cells. However, due to changed culture conditions, cytotoxicity could not be completely excluded.

The positive controls 10 µM chlorogenic acid (CGA) and co-incubated 0.5 µM chlorogenic acid, 5.5 µM trigonelline and 1000 U/ml catalase (CGA+Tri+Kat) displayed any significant increase in GST activity (figure 43 C). The same result was obtained for 50 µM tBHP, which was tested just once. Since no induction was observed with the positive controls, the data for 50 µM AOH still needed to be viewed critically.

The use of appropriate concentrations of foetal bovine serum (FBS) and antibiotics is a required part of cell culture conditions. In retrospect, a fungal contamination of the used FBS was identified causing some trouble for cell cultivation and potentially also for cell response. The potential production of toxins by the contaminating fungi could influence the activity of drug metabolising enzymes in the different cell lines used. Thus it might be speculated that the basal cellular GST level for instance is up-regulated to a level allowing any further induction, resulting in already constantly increased GST activities in the cell. Thus the contaminating fungi might account for, or at least contribute to the problems in GST induction.

Taken together, despite several different approaches GST activity was neither in HT29 nor in HepG2 cells significantly increased after treatment with a number of different compounds, described as enhancers of GST activity in the literature. Nevertheless, GST activity was significantly increased by AOH in HT29 cells, albeit fairly weak. Doostdar *et al.* (1988) investigated GST activities in HepG2 cells cultivated in different media. Depending on the chosen medium, the obtained results differed up to 124% (Doostdar *et al.*, 1988). The results demonstrated, that a variety of different parameters despite contamination had a pivotal influence on GST activity and needed to be tested in detail prior any final conclusions.

5. Conclusion

Alternaria toxins, such as alternariol (AOH) and alternariol monomethyl ether (AME) are on the list of mycotoxins with an urgent need for further investigations of toxicity, permitting a better risk assessment for man and animal.

Based on the data reported by Fehr (2008) and Schreck *et al.* (2011) on the induction of CYP1A1 by *Alternaria* toxins, the role of the aryl hydrocarbon receptor (AhR) in AME- and AOH-mediated CYP1A1 expression was investigated in human tumour cells. The consumption of grain contaminated with *Alternaria spp.* has been associated with an increased incidence of oesophageal cancer in Linxian, China (Liu *et al.*, 1992), thus human oesophageal carcinoma cells KYSE510 were chosen as cell model.

Prior to the studies on CYP1A1 expression, the cytotoxic potential of alternariol monomethyl ether (AME) was investigated in KYSE510 cells. After 24 h of treatment with AME in the concentration range of 0.1 - 10 µM, no significant cytotoxic effects were observed in the SRB assay. Thus the tested concentration range seemed to be appropriate for studies on gene transcription. The cytotoxic potential of alternariol (AOH) based on available data, which suggested any cytotoxicity at 50 µM AOH. However, in retrospect growth inhibitory effects ≥ 50 µM AOH were detected. Thus, results in the present thesis with 50 µM AOH have to be rated critically.

Two approaches were used to investigate the question whether mycotoxin-induced CYP1A1 is AhR-dependent in oesophageal cells. Firstly, oesophageal AhR knockdown cells were generated by RNAi technology and served as an adequate model for studying the impact of *Alternaria* toxins on CYP1A1. Secondly, KYSE510 cells, pre-treated with the known AhR antagonist 3´-methoxy-4´nitroflavone (MNF) were used as cells with a reduced or either complete loss of functioning AhR. Hence knockdown of the Ah-receptor by transient siRNA transfection represented a major focus of the present thesis. Optimisation experiments for transient siRNA transfection, granting ideal transfection efficiency and knockdown of AhR of at least ≥ 70%, were performed with human oesophageal carcinoma cells (KYSE510). The optimised conditions for transfection of KYSE510 cells were: fast-forward protocol according to the manufacturer´s recommendations “Fast-Forward Transfection of Adherent Cells with siRNA/miRNA in 24-well Plates” (Qiagen®), $3*10^4$ KYSE510 cells/well, 0.2 µl AhR siRNA2, 4.5 µl HiPerFect Transfection Reagent from Qiagen® and 48 h post-transfection incubation with the mycotoxins for 24 h. The suppression of AhR in transfected cells was checked by qRT-PCR and by Western blot assuring a suppression of ≥ 70% at the transcription level and no signal for AhR at the protein level. Later on, suppression of AhR was routinely checked by qRT-PCR in all experiments conducted with the mycotoxins.

After 24 h treatment of non-transfected and dsRNA-transfected (negative control) KYSE510 cells with AME, CYP1A1 levels remained nearly unaltered at 0.1 µM and were induced at 1 µM up to 2.5-fold. At higher AME concentrations (5 µM and 10 µM) the transcript level of CYP1A1 was significantly reduced to about 60 - 70%. In contrast, AOH elicited a more potent CYP1A1 induction in oesophageal cells than AME. At 0.1 µM AOH the CYP1A1 induction was already 1.9-fold (± 0.5), at 1 µM and 10 µM the induction reached a maximum with about 8-fold. The results indicated, that non-transfected and dsRNA-transfected control cells respond similar to the mycotoxins. Thus the transfection procedure did not alter KYSE510 cells in their properties towards AME and AOH. In AhR-suppressed (AhR-siRNA transfected) KYSE510 cells the induction of CYP1A1 by AME as well as by AOH was significantly reduced up to complete abolishment, supporting the hypothesis of AhR-dependent CYP1A1 induction by both *Alternaria* toxins. However, CYP1A1 mRNA expression in AhR-deficient KYSE510 cells plummeted below the endogenous level, when applying high AME (≥ 5 µM) and AOH (≥ 10 µM) concentrations. The interference of another, yet unknown pathway had to be considered and required further experiments.

The results with KYSE510 cells inhibited by MNF (2nd approach) along general lines also supported a role of the AhR in modulation of CYP1A1 mRNA levels by AME. However, the picture is more complex. KYSE510 control cells pre-treated with 10 µM MNF for 15 minutes followed by incubation with 1% DMSO for 24 h, exhibited a significant, about 6-fold increase in CYP1A1 transcripts in comparison to non-treated cells. Thus suspecting MNF, when applied at 10 µM, to act potentially as Ah-receptor agonist in KYSE510 cells. Nevertheless, subsequent incubation with AME led to a significant and concentration-dependent reduction of CYP1A1 mRNA levels. Based on these results it might be speculated, that AhR inhibition by MNF impedes CYP1A1 induction by AME, emphasising the role of AhR in AME-mediated CYP1A1 induction. On the other hand the potent induction of CYP1A1 by MNF is reduced in the presence of AME allowing the assumption of a potential displacement of MNF from the AhR binding site. However, this hypothesis needs to be verified by receptor binding studies with labelled MNF.

Glutathione-S-transferases (GST) are important phase II drug metabolising enzymes, bearing a considerable role in the detoxification of xenobiotics by conjugation with a glutathione molecule. One aspects of the present thesis was the implementation of the GST assay according to Habig *et al.* (1973). The reliability of the assay was tested by a variety of positive control-substances reported in the literature. However, any of the tested substances reproducibly induced GST activity to an adequate extend. In this context, several potential parameters, impacting on GST activity, were investigated in orienting experiments. Despite the problem of identifying a proper positive control, human colon carcinoma HT29 cells were

treated with AME and AOH for 24 h in a concentration range of 0.01 - 50 µM. Previous studies in human colon carcinoma cells (HT29) and results obtained with hepatic and intestinal microsomes, demonstrated the formation of AOH- and AME-glucuronides and -sulphates. Thus, HT29 cells were considered to be a suitable test system to investigate the contribution of GST in the phase II detoxification process. Neither AME nor low concentrations of AOH significantly increased the GST activity, with exception of AOH at 10 µM and 50 µM. Since the induction was quite marginal and in the latter case cytotoxicity could be of not negligible influence, the involvement of GST in phase II detoxification and metabolic disposal was considered to be of minor extend.

The results of the present thesis on CYP1A1 expression in human oesophageal tumour cells showed a significant AME- and AOH-mediated increase of CYP1A1 transcripts and strongly suggested an Ah-receptor mediated induction of CYP1A1. Based on the existing data of dietary exposure, the EFSA Panel on Contaminants in the Food Chain (CONTAM) used the threshold of toxicological concern (TTC) approach to assess the relative level of concern for dietary exposure of humans. They recently pointed out, that the estimated chronic dietary exposure to AME (0.8 - 4.7 ng/kg body weight per day) and AOH (1.9 - 39 ng/kg body weight per day) exceeded the relevant TTC value, indicating a need for additional compound-specific data.

6. Materials and Methods

6.1. Cell Culture

Cell culture is a complex process by which cells are grown under controlled conditions. Culture conditions can vary widely depending on the type and origin of cells. The artificial environment in which the cells are cultivated contains the following: a medium that supplies the essential nutrients, growth factors, optimal grow conditions (37°C, 5% CO_2 and 95% relative humidity) and a regulated chemical environment (pH).

The supply of essential substances as well as the neutralisation of the degradation products by culture media is part of the *in vitro* conditions. To prevent bacterial growth in case of contamination, antibiotics (1% P/S) are added to the culture media (Lindl, 2000). Before use all media are warmed up to 37°C. Any handling with cells is performed under sterile conditions.

6.1.1. Cell Lines

KYSE510

KYSE510 cells were derived from an oesophageal squamous cell carcinoma, restricted from a 67-year-old Japanese woman after treatment with cisplatin and radiation. The cells are described as carrying a p53 mutation and amplification of MYC, HST1, CYCLIN D1. Furthermore they induce well-differentiated tumours in nude mice. The cells display epitheloid character, growing as monolayer with multilayer foci. The doubling time is about 30 hours and RPMI 1640 containing L-glutamine, 1% (v/v) penicillin (10000 units)/ streptomycin (10000 µg/ml) (P/S) and 10% (v/v) heat inactivated fetal bovine serum (FBS) is used as culture medium. Cells are grown in monolayers in tissue culture bottles at 37°C, 5% CO_2 and 95% relative humidity (DSMZ, Braunschweig).

HT29

The human colon adenocaricnoma cell line HT29 was established from the primary tumour of a 44-year-old Caucasian woman in 1964. The tumour is described to be heterotransplantable, forming well differentiated grade I tumours. The epitheloid HT29 cells grow adherent as a monolayer in large colonies with a doubling time of 40 - 60 hours. The culture medium used in the experiments is Dulbeccos´s Modified Eagle Medium (DMEM, with 4500 mg/l glucose, pyridoxine HCl, without sodium pyruvat) containing 1% (v/v) P/S and 10% (v/v) heat inactivated FBS. Cells are grown in monolayers in tissue culture bottles at 37°C, 5% CO_2 and 95% relative humidity (DSMZ, Braunschweig).

HepG2

HepG2 cells are human hepatoma cancer cells which were established from the tumour of a 15 year old Argentinean harbouring a hyperploid karyotype. They are adherent cells which grow in a monolayer with a doubling time of 40 - 60 h. The used culture medium is RPMI 1640, containing L-glutamine, 1% (v/v) penicillin/ streptomycin (P/S) and 10% (v/v) heat inactivated FBS. Cells are grown in monolayers in tissue culture bottles at 37°C, 5%CO_2 and 95% relative humidity (DSMZ, Braunschweig).

6.1.2. Re-culturing of Cells

Frozen cell stocks (stored at -80°C) are thawed quickly in a water bath at 37°C and transferred to 6 ml respective cell culture medium, containing 20% (v/v) heat inactivated FBS and antibiotics. The cell suspension is centrifuged at room temperature for 4 minutes at 450 x g, resulting in the formation of a cell pellet. The supernatant is discarded. The cell pellet is carefully resuspended in 6 ml medium (see above) and transferred to 4 ml medium already pipetted in a small tissue culture flask (25 cm^2) and the suspension is added. The cells are cultivated at the above mentioned conditions. Upon achieving 80% confluency, the cells are passaged into a medium size tissue culture flask (75 cm^2) and thereafter into a 175 cm^2 tissue culture flaks. The cells are maintained for at least one week in culture and 20% (v/v) FBS supplemented medium before attaining experimental competence.

6.1.3. Storage of Cells

Long term storage of cells takes place in the biofreezer at -80°C and as well as in liquid nitrogen. To prevent the formation of ice crystals and to counter act a partial dehydration of the samples, a defrosting agent like dimethyl sulphoxide (DMSO) is added. The protection by DMSO is due to the replacement of water (Lindl, 2000).

The cells are detached from the surface of the cell culture flask by trypsination as described in 6.1.5 “Sub-culturing of Cells”. 1 ml of the cell suspension is added to 500 µl of a mixture of 70% (v/v) heat inactivated FBS and 30% (v/v) DMSO in a cryo tube. The cell stocks are carefully stirred and stored at -20°C for 24 hours. The use of bubble wrap foil and storage in a styrofoam box should prevent too rapid cooling. For long term storage the cell stocks are transferred to the biofreezer at -80°C or to liquid nitrogen.

6.1.4. Changing of Cell Culture Medium

To ensure the growth of a uniform monolayer, the routinely change of medium is required. Due to metabolic processes, nutrient ingredients are degraded by the cells and eliminated metabolites accumulate in the cell culture media resulting in a change to more acidic pH, indicated by a change of the medium colour from red to yellow (Lindl, 2000).

The cell culture medium is aspirated and the cell monolayer is rinsed with 5 ml pre-warmed PBS (phosphate buffered saline) to remove dead cells. Subsequently the appropriate volume of pre-warmed cell culture medium (10 ml medium for 25 cm^2 culture flasks, 20 ml for 75 cm^2 and 40 ml for 175 cm^2 culture flask) is added and the flask is placed back into the incubator.

6.1.5. Sub-culturing of Cells

At a cell confluence of about 80 - 90% a proper monolayer growth is not granted anymore. Further cell growth is suppressed and the cell layer can detach from the bottom of the cell culture flask and thus the cells might die off. Therefore it is necessary to reduce the cell number by sub-culturing the cells (Lindl, 2000).

The depleted cell culture medium is aspirated and the cells are rinsed with 5 ml PBS to remove dead cells and residual cell culture medium. 2.5 ml pre-warmed trypsin solution is added and the cells are incubated at 37°C for 2.5 minutes by placing back the culture flask into the incubator. The culture flask is clapped several times to detach the cells. To stop the trypsin reaction 7.5 ml serum supplemented cell culture medium is added. Subsequently the cells are re-suspended by carefully pipetting up and down. Depending on the experimental setup, a certain volume of the cell suspension is transferred to the culture flask, 40 ml medium is added and the cells are further cultivated. After using the same culture flask for two times, it is replaced by a new, sterile one.

At high passage numbers during cell culture, the genotype of tumour cells can change potentially causing changes in their properties. To avoid this problem the cell line is replaced at a certain passage number (after about 30 passages) by a new, re-cultured cell stock.

6.1.6. Cell Counting

To ensure similar conditions for the experimental procedures, the same number of cells should be used. The cell number is determined by using a Neubauer counting chamber (haemocytometer). Shortly before the cells are detached from the bottom of the flask, the counting chamber is arranged as follows: the cover glass is breath-moistened and gently slid onto the counting chamber. A dilution of cell suspension with trypan blue is prepared in a test tube of 1.5 ml. The grid of the haemocytometer consists of nine squares, whereas each has an area of 1 mm^2. The depth is 0.1 mm, resulting in a volume of 0.1 µl/square and the entire counting grid has a volume of 0.9 µl. The counting chamber is loaded with 10 µl of the cell dilution by placing the tip of the pipette at the juncture between cover glass and counting chamber. As a result of the capillary effect, the suspension is drawn in between the cover glass and the chamber. The number of cells in the four squares is determined by counting (figure 44) and subsequently the arithmetic mean is calculated. Multiplication with the dilution factor and the volume factor of the haemocytometer (10^4) yields the number of cells/ ml. The

dye trypan blue (trypan blue solution 0.4%, Sigma) is used to distinguish between dead and living cells. The dye diffuses through the membrane into the cells. Living cells appear white, due to the fact that they are able to export the dye, whereas dead cells are not, thus remaining blue (Lindl, 2000).

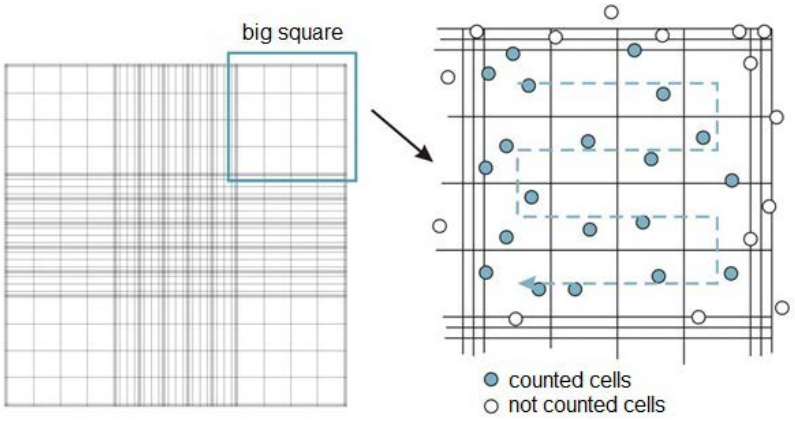

Figure 44: Depiction of the Neubauer counting chamber/ haemocytometer (Lindl, 2000)

Reagents

RPRMI 1640 medium	Gibco, Invitrogen
+ L-glutamine	
DMEM medium	Gibco, Invitrogen
+ 4.5 g glucose	
+ L-glutamine	
- pyruvate	
FBS (heat inactivated)	Gibco, Invitrogen
P/S (5000 units/ml penicillin, 5000 µg/ml streptomycin)	Gibco, Invitrogen
DMSO, for molecular biology (>99.5%)	Roth
trypan blue solution (0.4%)	Sigma

10x PBS (Phosphate Buffered Saline)

1710 mM NaCl	Roth
100 mM Na_2HPO_4	Roth
34 mM KCl	Roth
18 mM KH_2PO_4	Roth

The buffer is adjusted to pH 7.4 with conc. HCl and filled up to 1 l with bidest. water. The 1:10 diluted PBS (1x PBS) is autoclaved.

Trypsin Solution

500 mg trypsin bovine pancreas, 3.6 U/mg, Serva
250 mg EDTA Merck
100 ml 10x PBS

The solution is filled up to 1000 ml with bidest. water and stirred on ice over night. Thereafter the pH-value is adjusted to 7.0 - 7.4 and the solution is filtrated under sterile conditions (filter pore size: 0.2 µm), 5 ml aliquots are prepared and stored at -20°C.

6.2. Sulforhodamine B (SRB) Assay

The sulforhodamine B (SRB) assay is a test for cytotoxicity and was performed according to Skehan (1990). Living cells are fixed and stained with the anionic dye sulforhodamine B (figure 45), which binds to alkaline amino acids of cellular proteins at acidic conditions. Subsequently at alkaline conditions (pH 10) the dye is dissolved away from the affixed cells. The effect of the test substances on cell growth is evaluated by measuring the absorbance of the coloured solution photometrically at 570 nm, as the dye is only bound to living cells (Skehan, 1990).

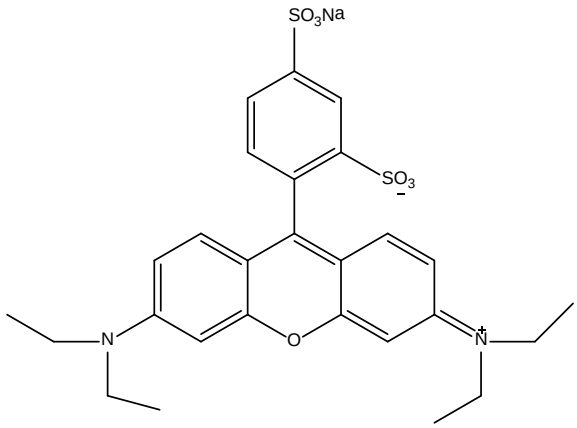

Figure 45: Structure of sulforhodamine B

Procedure

- 800 KYSE510 cells/200 µl complete RPMI 1640 medium are seeded per well of a 96-well plate and grown for 72 hours at 37°C, 5% CO_2 and 95% relative humidity.
- The cells are incubated for 24 hours with the test substances (AME in the present study at 0.1, 1 and 10 µM, originally dissolved in DMSO). A 1:100 dilution step with cell culture medium (containing 10% (v/v) FBS and 1% (v/v) P/S) yield incubation solutions with 1% (v/v) final DMSO concentration.
- At the end of substance incubation, cell monolayers are fixed by adding 20 µl trichloroacetic acid (50%) per well. The plate is stored at 4°C overnight.

- To remove cell- and medium-residues, the culture plate is rinsed carefully four times with bidest. water. Afterwards it is stored at room temperature until complete dryness.
- The fixed cells are stained with 50 µl SRB-solution (0.4 % w/v) per well and incubated for 1 hour at room temperature in the dark.
- The excess of dye solution is removed by rinsing the 96-well plate two times with bidest. water and two times with acetic acid (1% v/v).
- The plate is dried completely at room temperature in the dark. Subsequently the protein-bound dye is dissolved in 50 µl 10 mM Tris base solution (pH 10) per well and the absorbance is measured at 570 nm.

The absorbance values of treated cells are compared with the values of solvent control cells (1% DMSO) and presented as test over control [T/C] values, where the mean of the solvent control (1% DMSO) is set to 100%.

Reagents

- trichloroacetic acid (≥99%, Roth): 50% v/v solution in bidest. water
- acetic acid (≥96%, Roth): 1% v/v solution in bidest. water
- SRB-solution (Sigma-Aldrich): 0.4% w/v solution in 1% acetic acid
- Tris base (≥99.9%, Roth): 2.42 g Tris (10mM) are dissolved in 2 l bidest. water, pH 10

Data representation

The evaluation of the obtained spectrophotometrical data is demonstrated using the experiment performed on the 24/03/2011 with 1 µM AME. For the representation of the graphs eight absorbance values (ABS) are chosen (table 4, 2nd column). Due to unsteady growth of the cells at the edge of the 96 well-plate in comparison to the wells in the middle of the plate, the absorbance values obtained from the external wells are not used for further evaluation. The blank value is determined by measuring the absorbance of 50 µl 10 mM Tris base solution (pH 10) which is subsequently subtracted from the obtained absorbances (table 4, 3rd column). Then the arithmetic mean and the standard deviation of the obtained absorbance values are calculated according the following formulas:

$$\bar{x} = \frac{x_1 + x_2 + \ldots x_n}{n}$$

$$\sigma = \sqrt{\frac{\sum x^2 - \left(\sum x\right)^2}{n(n-1)}}$$

Table 4: Determined absorbance values in the SRB assay and calculated T/C [%] for 1 µM AME (experimental data recorded on the 24/03/2011)

Data point #	ABS	ABS-blank	T/C [%]
1	1.561	1.473	107.85
2	0.182	0.094	-
3	1.473	1.385	101.41
4	1.561	1.473	107.81
5	1.405	1.317	96.41
6	1.354	1.265	92.63
7	1.269	1.181	-
8	1.551	1.463	107.11
x		1.206	
σ		0.432	

ABS (blank)= 0.088

In order to detect and subsequently reject outliers, the Nalimov outlier test is used. Assuming a Gaussian distribution of the measured values, outliers are identified as such, when the test statistic q exceeds the critical threshold q_{crit}. ($q > q_{crit} \rightarrow$ outlier, table 5).

The test statistic q is calculated according the following formulas:

$$q = \frac{\bar{x} - x_n}{\sigma} * \sqrt{\frac{n}{n-1}} \quad or \quad q = \frac{x_n - \bar{x}}{\sigma} * \sqrt{\frac{n}{n-1}}$$

Table 5: Critical threshold q_{crit} values at a 95% confidence level

number of measured values	q_{crit}
n = 3	1.409
n = 4	1.645
n = 5	1.757
n = 6	1.814
n = 7	1.848
n = 8	1.870
n = 9	1.885

After rejecting the identified outliers, the test statistic q is calculated again by modifying n, x and σ to the correct value. After comparison with the respective q_{crit}, any existing outliers are rejected again. The Nalimov test is performed until at least three absorbance values are left. In the following experiment two outliers are identified and grey shaded in table 4. They are not used for further data evaluation.

Then the test over control (T/C) values are calculated according the following formula and are given in the 3rd column of table 4.

$$T/C\,[\%] = \frac{ABS}{\bar{x}\,(ABS_{DMSO})} \times 100$$

The arithmetic mean and standard deviation (σ) of the T/C [%] values are calculated for the respective concentrations (0.1 µM, 1 µM, 10 µM AME), including all replicate experiments. Both values are represented in the graph.

T/C [%] (DMSO): 100% (σ = 8.045)

T/C [%] (1µM AME) 96.33%(σ = 11.987)

Significant differences between AME- and solvent control (1% DMSO) treated cells are identified by the two tailed t-test. At first the degrees of freedom (f) are determined:

f = 2 x n -2= 8 n: number of independently performed experiments (n = 5)

Then the variances of 1 µM AME- and 1% DMSO-treated cells are calculated and used for the determination of the weighted variance (s^2).

$$s^2_{DMSO} = (\sigma_{DMSO})^2 = (8.045)^2 = 64.722$$

$$s^2_{1\mu M\ AME} = (\sigma_{1\mu M\ AME})^2 = (11.987)^2 = 143.69$$

$$s^2 = \frac{(n-1)s^2_{DMSO} + (n-1)s^2_{1\mu M\ AME}}{f} = \frac{(5-1)*64.722 + (5-1)*143.69}{8} = 104.206$$

If the t-value (t) exceeds the critical threshold t_{crit} ($t > t_{crit}$, table 6), the difference in arithmetic means is assigned to be significant. In the performed experiment, arithmetic means of all tested AME-concentrations (0.1 µM, 1 µM, 10 µM) do not significantly differ from DMSO-treated control cells.

$$t = \sqrt{\frac{n^2}{2*n}} * \frac{T/C_{DMSO}[\%] - T/C_{1\mu M\ AME}[\%]}{\sqrt{s^2}} = \sqrt{\frac{5^2}{2*5}} * \frac{100 - 96.33}{\sqrt{104.206}} = 0.568$$

Table 6: Critical threshold t_{crit} values at 95%, 99% and 99.9% confidence levels

confidence level	t_{crit}
95%	2.306
99%	3.355
99.9%	4.501

6.3. Gene Silencing by using siRNA

The expression of single genes can be suppressed by using siRNA technology. The introduction of short interfering RNA (siRNA) into the cell is a crucial requirement for the specific suppression of mRNA. siRNA is a short piece of double-stranded RNA, which is pried apart by the RNA-induced silencing complex (RISC), whereupon the antisense strand of RNA is responsible for the inactivation of mRNA and by extension the according gene. The whole process is known as RNA interference (RNAi) and an important part of the posttranscriptional gene silencing (PTGS) (Shan). In the present work the transfection reagent HiPerFect (Qiagen®) is used for siRNA transfection experiments. The aim was the suppression of AhR function in human oesophageal tumour cells (KYSE510).

AhR siRNA

Two siRNAs (siRNA 1 & siRNA 2) of different aryl hydrocarbon receptor (AhR) sequences were used. The exact sequences are not denoted by the supplier. Both siRNAs, a kind gift of Prof. C. Weiss (Karlsruher Institute of Technology, KIT Germany) are delivered as solutions in siRNA buffer with a concentration of 100 pmol/µl each.

Negative Control siRNA

The RNA used as negative control (dsRNA) has no homology to any known mammal gene. The dsRNA, also a kind gift of Prof. C. Weiss, is dissolved in siRNA buffer at a concentration of 20 pmol/µl. The sequence of the dsRNA is not specified by the supplier.

HiPerFect Transfection Reagent

HiPerFect Transfection Reagent (Qiagen®) consists of cationic liposomes. The liposomes bind siRNA and form complexes with high affinity toward cell membranes. The major mechanism involves endocytosis of the complexes, followed by disruption of the endosomal membrane. The optimal volume of transfection reagent and siRNA concentration depends on siRNA potency, cell type and the target gene (Qiagen, 2010).

6.3.1. Establishment of transient siRNA Transfection in KYSE510 Cells

The transient transfection of the KYSE510 cells is performed according to the manufacturers recommendations: “Fast-Forward Transfection of Adherent Cells with siRNA/miRNA in 24-well Plates”. The volumes of required transfection reagent and of AhR1-/ AhR2-siRNA in the optimised protocol are calculated for one well of a 24-well plate (Qiagen, 2010).

According to the manufacturer (Qiagen®) several factors have to be considered to meet optimal siRNA transfection:

- amount of siRNA
- ratio of HiPerFect Transfection Reagent to siRNA
- cell density at transfection
- choice of transfection protocol
- post-transfectional time of incubation

The used fast-forward protocol implies cell plating and transfection to be performed on the same day. Furthermore, it is recommended that the transfection master mix is added drop-wise onto the cells and not vice versa, since optimal mixing of cells and transfection complexes is desirable.

Post-transfection the gene silencing is verified by using quantitative real time PCR (qRT-PCR) and Western Blot analysis (see chapter 6.4 “Gene Expression Analysis of CYP1A1 and AhR using quantitative Real Time PCR” and chapter 6.5 “Western Blot Analysis of the Aryl Hydrocarbon Receptor”). The establishment of optimal siRNA-transfection conditions, including the number of seeded cells, volume of HiPerFect Transfection Reagent and siRNA is described in chapter 4.3.2 “Knockdown of AhR in KYSE510 Cells” and briefly summarised in table 7. The experimental setup for the transfection of KYSE510 cells in 24-well-plate format is displayed in table 8.

Procedure

Transfection experiments with AhR1- and AhR2-siRNA showed that a better suppression with the latter siRNA, thus all the following experiments are performed with AhR2-siRNA. More detailed information about the conducted experiments is given in the chapter "Transient siRNA Transfection of KYSE510 Cells".

- According to the optimised transfection protocol $3*10^4$ KYSE510 cells are seeded per well of a 24-well plate in 0.5 ml RPMI 1640 culture medium, containing 10% (v/v) heat inactivated FBS and 1% P/S.
- Subsequently cells are kept under normal growth conditions (37°C, 5% CO_2, 95% relative humidity).
- 0.2 µl of siRNA 2 and dsRNA, respectively are diluted in 50 µl serum free RMPI 1640 cell culture medium, containing 1% P/S. 4.5 µl HiPerFect Transfection Reagent are diluted in another volume of 50 µl serum free RPMI 1640 cell culture medium.

- The transfection solution is added to the AhR2-siRNA solution and mixed by vortexing. Then the mixture is incubated for 10 minutes at room temperature to allow the formation of transfection complexes.
- Afterwards the solution is added drop-wise onto the cells and gently swirling of the plate ensures uniform distribution of the transfection complexes. The cells are incubated under normal growth conditions for 48 h.

Table 7: Optimised transfection conditions for KYSE510 cells with HiPerFect Transfection Reagent (Qíagen®)

optimised transfection conditions	
number of seeded KYSE510 cells	$3*10^4$/well
volume of HiPerFect Transfection Reagent	4.5 µl/well
volume of siRNA (1 or 2), dsRNA	0.2 µl/well
transfection time	48 h

Table 8: Experimental setup for the transfection of KYSE510 cells with HiPerFect Transfection Reagent (Qiagen®) 24-well plate format

	A	B	C	D	E	F
1						
2	dsRNA	dsRNA	dsRNA	dsRNA	dsRNA	dsRNA
3	siRNA2	siRNA2	siRNA2	siRNA2	siRNA2	siRNA2
4						

6.4. Gene Expression Analysis of CYP1A1 and AhR using quantitative Real Time PCR (qRT-PCR)

The quantitative real time PCR (qRT-PCR) is a polymerase chain reaction technique which is commonly used in gene expression analysis to amplify and simultaneously quantify target DNA. Usually DNA templates are amplified by PCR; yet if RNA is the target of interest, it hast to be transcribed first into DNA with the help of a reverse transcriptase enzyme. This method is known as reverse transcription PCR. Quantification of amplicons using conventional end-point PCR is subjected to high deviations, thus real time PCR in which amplicons are monitored after each cycle is preferred. For quantification the fluorescent dye SYBR® Green is used. The compound intercalates with double-stranded DNA, allowing the determination of fluorescence correlating with the amount of amplicons and thus, with the amount of messenger RNA of a respective gene (Roche, 2008).

6.4.1. Incubation of Cells

$3*10^4$ KYSE 510 cells/0.5 ml RPMI 1640 medium, supplemented with 10% (v/v) heat inactivated FBS and 1% (v/v) P/S, are seeded into each well of a 24-well plate. The cells are grown for 24 h and 48 h respectively at 37°C, 5% CO_2 and 95% relative humidity. The experimental setup for incubation-experiments with transiently transfected cells is displayed in table 9 and table 10. The procedure for transient siRNA transfection in KYSE510 cells is described in chapter 6.3.1 “Establishment of transient siRNA Transfection in KYSE510 Cells”.

The test substances (AOH, AME, BaP, ARO) are dissolved in DMSO. Dilutions of 1:100 with cell culture medium, containing 10% (v/v) FBS and 1% (v/v) P/S, yield solutions with 1% DMSO as final concentration. The depleted cell culture medium is aspirated and the cells are rinsed with 500 µl pre-warmed PBS. Subsequently the cells are incubated with 500 µl of the respective chemicals in the appropriate concentration for 24 h. A solution containing 1% DMSO is used as solvent control. Due to unsteady growth of the cells at the edge of the 24 well-plate in comparison to the wells in the middle of the plate, these wells are avoided for incubation experiments.

Reagents

- AME from *Alternaria alternata* (*tenius*) Sigma-Aldrich
- AOH from *Alternaria spp.* (~96%) Sigma-Aldrich
- ARO kindly provided by Dr. Metzler, Karlsruher Institute of Technology (KIT), Germany
- BaP (≥96%) Sigma-Aldrich

Table 9: Experimental setup for the incubation of non-transfected, dsRNA- and siRNA 2-transfected KYSE510-cells with AME in 24-well plate format

	A	B	C	D	E	F
	non-transfected KYSE510 cells					
1	1% DMSO	0.1 µM AME	1 µM AME	5 µM AME	10 µM AME	5 µM BaP
	dsRNA-transfected KYSE510 cells					
2	dsRNA 1% DMSO	dsRNA 0.1 µM AME	dsRNA 1 µM AME	dsRNA 5 µM AME	dsRNA 10 µM AME	dsRNA 5 µM BaP
	siRNA 2-transfected KYSE510 cells					
3	siRNA 1% DMSO	siRNA 0.1 µM AME	siRNA 1 µM AME	siRNA 5 µM AME	siRNA 10 µM AME	siRNA 5 µM BaP
4						

Table 10: Experimental setup for the incubation of non-transfected, dsRNA- and siRNA 2-transfected KYSE510-cells with AOH in 24-well plate format

	A	B	C	D	E	F
	non-transfected KYSE510 cells					
1	1% DMSO	0.1 µM AOH	1 µM AOH	10 µM AOH	50 µM AOH	5 µM BaP
	dsRNA-transfected KYSE510 cells					
2	dsRNA 1% DMSO	dsRNA 0.1 µM AOH	dsRNA 1 µM AOH	dsRNA 10 µM AOH	dsRNA 50 µM AOH	dsRNA 5 µM BaP
	siRNA 2-transfected KYSE510 cells					
3	siRNA 1% DMSO	siRNA 0.1 µM AOH	siRNA 1 µM AOH	siRNA 10 µM AOH	siRNA 50 µM AOH	siRNA 5 µM BaP
4						

6.4.2. RNA Isolation

The RNA isolation is performed using the RNeasy® Mini Kit (Qiagen®) according to the RNeasy® Mini Handbook-Protocol: Purification of Total RNA from Animal Cells using Spin Technology.

The isolation of total RNA is performed according to the single step method as described in the manufacturer´s protocol (Qiagen®). The cells are first lysed and homogenised in the presence of a denaturating guanidine thiocyanate containing buffer, which immediately inactivates RNases assuring intact RNA. The addition of ethanol provides appropriate binding conditions to the silica membrane. Total RNA is obtained using solid phase extraction. Silica membranes are used, which allow the binding of RNA sequences longer than 200 nucleotides (nt). The procedure provides enrichment for mRNAs since most RNAs smaller than 200 nt (such as rRNA and tRNA) are selectively excluded (Qiagen, 2006).

Procedure

- The cell culture medium is aspirated and each well is rinsed twice with 500 µl ice-cold PBS.
- The cells are lysed directly by adding 300 µl Buffer RLT per well. Shortly before use 1% β-mercaptoethanol is added to the RLT-Buffer.
- The cell lysate is collected with a 1000 µl Eppendorf pipette and transferred into a 1.5 ml RNase-free test tube.
- Subsequently the lysate is homogenised by passing it five times through a blunt 20-gauge needle (0.9 mm diameter), fitted to a 1 ml RNase free syringe.
- 300 µl 70% ethanol is added to the lysate and mixed well by pipetting.

- The whole sample is transferred onto a RNeasy spin column placed in a 2 ml collection tube. The lid is closed, the sample centrifuged at 9600 x g for 60 seconds and the flow through discarded.
- 700 µl Buffer RW 1 is added to the RNeasy spin column and the centrifugation step is repeated as described above and the flow through discarded.
- Then the membrane of the spin column is washed twice with 500 µl Buffer RPE. The first time it is centrifuged for 60 seconds, the second time for 120 seconds at 9600 x g. After each centrifugation step the flow through is discarded.
- Thereafter the RNeasy spin column is placed into a new 2 ml collection tube. It is centrifuged at full speed (21500 x g) for 60 seconds and then the collection tube is discarded.
- The column is placed in a new 1.5 ml collection tube and 30 µl RNase-free water is added directly onto the membrane of the spin column. The sample is centrifuged at 9600 x g for 60 seconds.
- The obtained RNA is stored on ice and aliquots of 12 µl are prepared. Long term storage of RNA is performed in the biofreezer at -80°C.

Reagents

- PBS: see chapter 6.1.6 “Cell Counting”
- β-mercaptoethanol (99%): Roth
- lysis buffer: Buffer RLT with 1% β-mercaptoethanol
- washing buffer A: Buffer RW 1
- washing buffer B: Buffer RPE with 4 volumes of ethanol (96%, Roth)
- eluent: RNase-free water

6.4.3. Concentration and Purity of RNA

The concentration and purity of the isolated RNA is determined photometrically at λ = 260 nm using the NanoDrop 2000c Spectrophotometer (PeqLab). An absorbance of 1 unit at 260 nm corresponds to 44 µg of RNA per ml (A260 = 1 → 44 µg/ml). The ratio between the absorbance values at 260 and 280 nm gives an estimate RNA purity with respect to protein contaminants, which have an absorption maximum at λ = 280 nm. Pure RNA has an A_{260}/A_{280} ratio of 1.9 - 2.1.

Procedure

- The NanoDrop program is started and a new workbook is created.
- Prior the measurement the NanoDrop-System is initialised by pipetting RNase free water onto the pedestal of the device. RNase free water (1.5 µl) is also used as blank.

The arm of the device is closed and the blank button in the software program is pressed.

- Subsequently 1.5 µl of sample are transferred for measurement, using the measure button.
- After the measurement the liquid is removed with a clean tissue wipe and the next sample is loaded.
- After the measurement the workbook is saved and the pedestal of the device is cleaned with 1.5 µl RNase-free water.

6.4.4. Reverse Transcription

As the *Taq*-DNA polymerase used in PCR is not able to use RNA as template, it is necessary to transcribe the obtained RNA into complementary DNA (cDNA). Therefore an enzyme known as reverse transcriptase, usually obtained from RNA-containing retroviruses, is used. Reverse transcriptase is a multifunctional enzyme with three distinct enzymatic activities: a RNA-dependent DNA-polymerase, a hybrid-dependent exoribonuclease (RNase H), and a DNA-dependent DNA polymerase.

Oligo(dT)-primer, consisting of 12 - 18 nucleotides, specifically bind to the poly(A) tail at the 3´-end of eukaryotic messenger RNA (mRNA). The complementary DNA-strand is synthesised by the reverse transcriptase in 5´→ 3´direction. Additional short random primers with different sequences bind statistically to the template mRNA and yield a pool of cDNA with different lengths. After the synthesis of the first cDNA strand, the RNase H activity of reverse transcriptase degrades the RNA in RNA:DNA hybrids and replaces it with a second cDNA strand (Qiagen, 2009a). A schematic depiction of the reverse transcription process is given in figure 46.

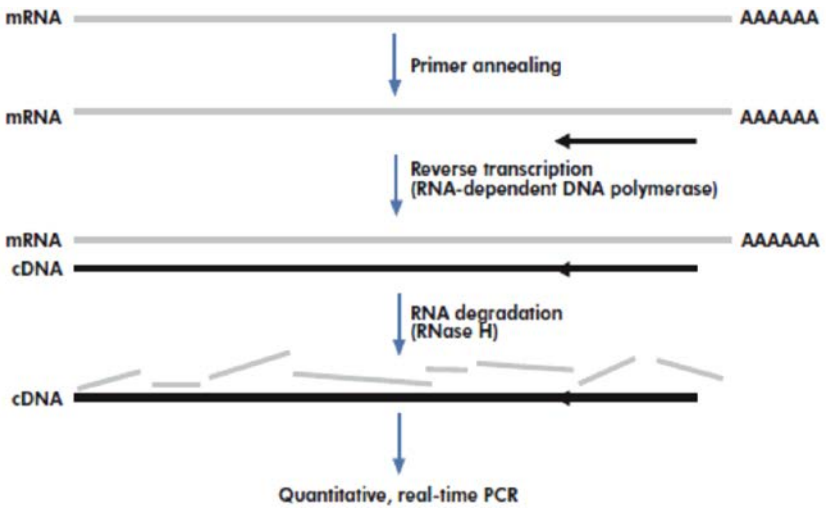

Figure 46: Schematic depiction of reverse transcriptase (QuantiTect® Reverse Transcriptase Handbook)

The reverse transcription is performed using the QuantiTect® Reverse Transcription Kit (Qiagen) according the QuantiTect® Reverse Transcription Handbook-Protocol: “Reverse Transcription with Elimination of Genomic DNA for Quantitative, Real-Time PCR”.

Procedure

- Total RNA, gDNA Wipeout Buffer, Quantiscript Reverse Transcriptase, Quantiscript RT Buffer, RT Primer Mix and RNase-free water are thawed on ice. Each solution is mixed by flicking the tube and briefly centrifuged to collect residual liquid from the sides and lid of the tubes.
- The genomic DNA elimination reaction mix is prepared on ice. For this purpose 500 ng of the isolated RNA are diluted with RNase-free water up to a volume of 6 µl and 1 µl gDNA Wipeout Buffer is added.
- The samples are incubated at 42°C for 2 minutes and put on ice immediately.
- 3 µl Master Mix are added, consisting of 2 µl 5x Quantiscript RT Buffer, 0.5 µl Quantiscript Reverse Transcriptase and 0.5 µl RT Primer Mix. Prior addition the Master Mix is stored on ice.
- Then the samples are incubated for 15 minutes at 42°C, followed by 3 minutes at 95°C to inactivate the Quantiscript Reverse Transcriptase.
- The obtained cDNA is stored on ice, respectively at -20°C or -80°C for long term storage.

Reagents

- 7x gDNA Wipeout Buffer
- Quantiscript Reverse Transcriptase
- 5x Quantiscript RT Buffer
- RT-Primer Mix

6.4.5. Real Time PCR

The polymerase chain reaction (PCR) is used to amplify gene specific DNA. The enzyme performing this reaction is the *Taq* polymerase, originally isolated from the bacteria *Thermus aquaticus*. The PCR is performed using the QuantiTect® SYBR Green PCR Kit, consisting of 2x QuantiTect SYBR Green PCR Master Mix, the respective cDNA templates and gene specific primers (QuantiTect Primer Assays) (Qiagen, 2009b).

A typical PCR-run is a cyclic process consisting of three different temperature steps which are repeated about 40 times. The reaction is started with a temperature increase to 92 - 98°C for about 5 - 10 minutes. As a consequence of this, the double-stranded DNA is denatured into single strands (figure 47 A), a requirement for the annealing of gene-specific primers. As

the DNA-polymerase is only able to amplify double-stranded DNA with a free 3´OH-end, the addition of DNA-fragments of about 20 nucleotides (known as primers) is required. This step is known as primer annealing (figure 47 B), achieved by cooling down the reaction to a temperature defined by the melting temperature of the primers. The oligonucleotides or primers bind to the single-stranded DNA. Thereafter the temperature is increased to 72°C, creating optimal conditions for the *Taq*-DNA-polymerase activity. The extension of the primers is now performed, yielding double-stranded DNA which is used as template for the next PCR-cycle (figure 47 C). After the extension step the newly formed DNA is denatured into two single strands at 92 - 95°C and a new PCR-cycle is started (Lottspeich, 2006; Mülhardt, 2009).

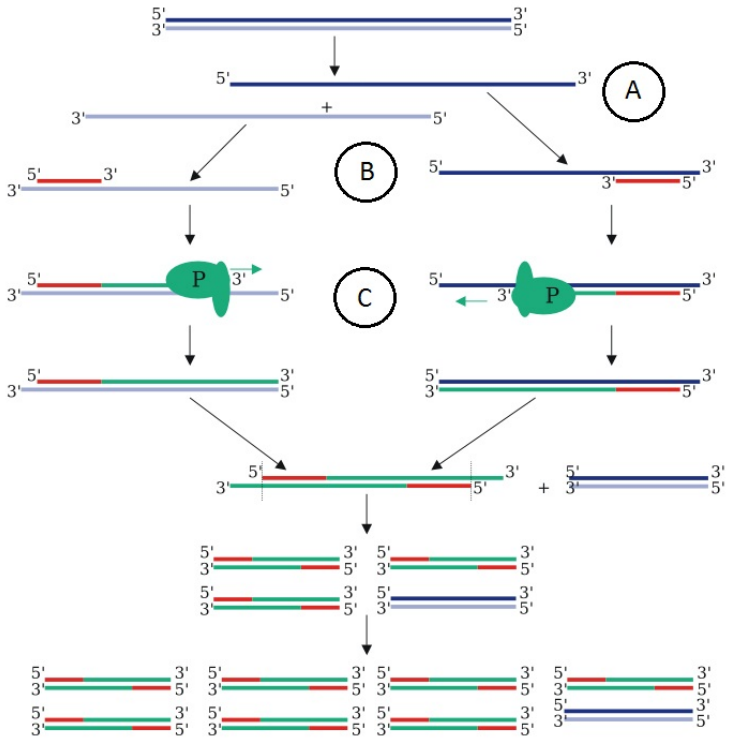

Figure 47: Mechanism of the polymerase chain reaction (PCR) (http://www.fsbio-hannover.de)

Procedure

- The template cDNA, 2x QuantiTect SYBR Green PCR Master Mix and the primers are thawed on ice and the individual solutions are mixed by vortexing.
- Then the reaction mix is prepared according to table 11.
- The reaction mix for one PCR determination is multiplied by the number of replicates, whereas the final reaction mix contains at least three reaction volumes in excess. Two excess reaction volumes are required for the no template controls and one to compensate the loss of volume due to pipetting.

Table 11: Reaction setup for the qRT-PCR

component	volume [µl]
2x QuantiTect SYBR Green PCR Master Mix	10
QuantiTect Primer Assay	2
RNase free water	7
total reaction volume	19

- The primer assays used for the PCR are CYP1A1 (QuantiTect® Primer Assay, HS_CYP1A1_1_SG) and AhR (QuantiTect® Primer Assay, HS_AHR_2_SG) as target genes and ß-actin (QuantiTect® Primer Assay, HS_ACTB_1_SG) as reference or endogenous control gene.
- The cDNA is diluted 1:2 by adding 10 µl RNase free water to 10 µl of the template solution. The concentration of the cDNA is estimated with 500 ng/10 µl, assuming that the efficiency of reverse transcription is 100%. Consequently the cDNA content of the diluted solution is estimated with 25 ng/µl.
- To each well of a 96-well PCR plate (MicroAmp® Optical 96-well Reaction Plate, Applied Biosystems) 19 µl of the reaction mix are dispensed and 1 µl of the diluted cDNA (~ 25 ng cDNA) is added. The determination of mRNA amount for each gene per sample is performed in duplicates respectively triplicates. Then the PCR plate is sealed with foil (MicroAmp® 96-well Optical Adhesive Film, Applied Biosystems). To remove any air bubbles the plate is centrifuged at 1000 x g for 5 minutes at room temperature.
- The PCR is performed with the StepOne Plus™ Instrument (96 wells, Applied Biosystems). Fluorescence is detected and quantified using the StepOneTM Software (version 2.1, © 2009 Applied Biosystems). Prior the PCR-run, the plate setup and run method are programmed (table 12).

Table 12: Real time PCR conditions of the QuantiTect SybrGreen protocol

QuantiTect SybrGreen				
Experiment Properties	StepOne Plus™ Instrument (96 wells)			
	Quantitation- Comparative C_T ($\Delta\Delta C_T$)			
	SYBR® Green Reagents			
	Standard (~ 2 h to complete a run)			
Run Method	Holding Stage	Step 1: 100%	95°C	15:00
	Cycling Stage	Step 1: 100%	94°C	00:15
		Step 2: 100%	55°C	00:30
		Step 3: 100%	72°C	00:30
	Melt Curve Stage	Step 1: 100%	95°C	00:15
		Step 2: 100%	60°C	01:00
		Step 3: +0,5°C	94°C	00:15
	Numbers of cycles		40	
	Reaction volume [µl]		20	
Plate Setup	Endogenous Control		ß-Actin	
	Dye as Passive Reference		ROX	

Quantification using the $\Delta\Delta C_T$-method

The amount of amplicons is detected at the end of each PCR-cycle by measuring the fluorescence in the sample, enabled by the fluorescent dye SYBR Green I, which binds to all double-stranded DNA molecules present in the PCR reaction mix. The excitation and emission maxima of SYBR Green I are at 494 nm and 521 nm, respectively. At the end of the PCR-amplification melting curve analysis is performed to verify the specificity and identity of PCR-products. One peak is normally recorded for each analysed gene. The appearance of two or more peaks indicates the formation of either primer dimers and/ or other nonspecific contaminating products, hampering a correct quantification of PCR-products (Qiagen, 2009b).

The real time amplification curves displays an exponential increase in fluorescence signal, necessary for the definition of a threshold for a constant fluorescence signal. For every amplification curve a threshold cycle (C_T-value) is assigned, which indicates the number of PCR-cycles necessary to reach this constant fluorescence signal (Pfaffl, 2004). The relative quantification of the formed transcripts is performed according the $\Delta\Delta C_T$-method. Relative quantification is based on the expression levels of a target gene versus one or more reference genes. For the $\Delta\Delta C_T$ calculation to be valid, the amplification efficiencies of the target and reference must be approximately equal (Livak & Schmittgen, 2001).

For relative quantification the amount for transcripts of the target gene is normalised with the amount of a non-regulated housekeeping gene such as β-actin, which is also used in the present work (A). An advantage of this method is the diminishment of variability in the expression results, due to tissue and matrix effects, different RNA isolation efficiencies and disturbances during the reverse transcription affecting the target as well as the housekeeping gene. Furthermore the relative transcription of a target gene in a sample, treated with the test compound, is related to an untreated control sample (B). The ratio for transcription is calculated according to C:

A. $\Delta C_T = C_T$ (target gene) - C_T (housekeeping gene)

B. $\Delta\Delta C_T = \Delta C_T$ (treated sample) – ΔC_T (control sample)

C. Ratio = $2^{-\Delta\Delta C_T}$

Data representation

The arithmetic mean and the standard deviation of CYP1A1 and AhR relative quantities (RQ) are calculated using the values of all replicate experiments. For the identification and rejection of outliers the Nalimov test is applied. The procedure and used formulas are explained previously in chapter 6.2 "Sulforhodamine B (SRB) Assay".

To assign significant differences between AME- and AOH- as well as solvent (1% DMSO) treated cells, the Student´s t-test is applied. Instead of using relative quantities, ΔC_T-values are used for the calculation. The respective ΔC_T-values of CYP1A1 and AhR relative quantities, already identified as outliers, are not used for the t-test. The calculation of the student´s t-test is performed using the function "TTEST" in Microsoft Excel 2007®. ΔC_T-values of 1% DMSO-treated cells are used as reference point and denoted as matrix 1, cells incubated with varying concentrations of the test substances as matrix 2.

=TTEST(Matrix1;Matrix2;2;2)

If the result of the t-test is smaller than the p-level, a significant difference is given. The smaller the p-level, the lower the probability of a coincidentally determined difference. The number of stars or small letters depicted in the graph, expresses the significance level (table 13).

Table 13: Depiction of significance levels in the graphs

p-level	assignment	
p<0.001	***	c
p<0.01	**	b
p<0.1	*	a

Reagents

2x QuanitTect SYBR Green PCR Master Mix

HotStar *Taq* DNA-Polymerase, QuantiTect SYBR Green PCR Buffer, SYBR Green I, ROX passive reference dye

10x QuantiTect Primer Assay

For reconstitution the vial is briefly centrifuged, 1.1 ml TE-buffer, pH 8.0 (10 mM Tris, pH 8.0 with conc. HCl, 1 mM EDTA) are added and mixed by vortexing. The reconstituted assay is frozen in aliquots of 100 µl at -20°C until use.

- CYP1A1 Primer Assay: QuantiTect® Primer Assay, HS_CYP1A1_1_SG, Qiagen, Lot no: 99640626
- AhR Primer Assay: QuantiTect® Primer Assay, HS_AHR_2_SG, Qiagen, Lot no: 99640627
- β-Actin Primer Assay: QuantiTect® Primer Assay, HS_ACTB_1_SG, Qiagen, Lot no: 97338266

Additional materials

- template cDNA
- RNase free water

6.5. Western Blot Analysis of the Aryl Hydrocarbon Receptor

Western Blot analysis consists of two major steps: first, the proteins are separated in an acrylamide gel by electrophoresis and second, thereafter they are transferred onto a membrane and detected by immune-detection. Electrophoresis is defined as the migration of charged particles in a uniformly charged electric field. In the electric field an accelerating force is applied on to charged particles, also known as field strength. The molecule moves to the opposite charged electrode, the resulting friction has a decelerating effect. This means, that the velocity of charged molecules is directly proportional to the field strength and their own charge, but inversely proportional to their radius and the viscosity of the surrounding medium. The separation occurs due to their different sizes and charges (Lottspeich, 2006).

SDS-PAGE

The purpose of SDS-PAGE (sodium dodecly sulphate polyacrylamide gel electrophoresis) is to separate proteins according to their size, and no other physical feature. In most proteins the binding of SDS to the polypeptide chains imparts an even distribution of charge per unit mass. The anionic detergent SDS (figure 48) covers the individual charge of single amino acids of a protein, thus creating a uniformly negative charged protein.

The addition of ß-mercaptoethanol causes the cleavage of disulfide bonds. Heating a protein together with SDS and ß-mercaptoethanol disintegrates its secondary and tertiary structure, yielding a mix of negatively charged polypeptide chains with a charge directly proportional to the size of the molecule (Lottspeich, 2006).

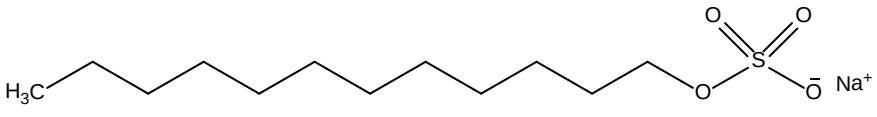

Figure 48: Structure of sodium dodecyl sulphate (SDS)

Disc (Discontinuous) Zone Electrophoresis

Discontinuous zone electrophoresis is the standard technique employed nowadays for the analysis of proteins. This technique permits a focusing of proteins in sharp bands, simultaneously counteracting the stacking of proteins and providing higher resolution than conventional electrophoresis. To implement the mentioned advantages, two different types of gels are used: a small mashed resolving gel and a highly porous stacking gel, both gels differ in their pH-value. Disc electrophoresis is also marked by the use of different types of charge carriers: the amino acid glycin as the main charge carrier in the electrophoresis buffer, and the chloride ions, that are prevalent in sample and gel. The chloride ions (fast and leading electrolyte) move with a high velocity creating an anion gradient in the gel. When glycine ions migrate into the stacking gel, their velocity is very low because the pH of 6.8 is close to the isoelectric point (IEP) of glycine (terminating electrolyte). The protein molecules align themselves between the fast chloride ions and the slow glycine ions, leading to the formation of stacks of proteins at the boundary of the stacking and resolving gel. As soon as the proteins enter the smaller mashed resolving gel at pH of 8.8, the glycine ions dissociate completely and move faster. They overtake the proteins, which are now the charge carriers, and get separated according to their size (Lottspeich, 2006).

Blotting

Immune-detection is a sensitive technique, which relies on the specificity of antibodies (Ab) to bind to single protein spots. In order to make the proteins accessible to antibody detection, they are transferred from within the acrylamide gel onto a nitrocellulose membrane. The membrane is placed between the gel and the anode and a stack of filter papers is placed on top of that. The entire stack is placed in a buffer solution and due to hydrophobic interactions the proteins get bound to the membrane. Specific antibodies are used to identify the proteins. To avoid non-specific binding of antibodies to the membrane, the binding sites are blocked with blocking reagent containing a dilute solution of protein, usually bovine serum albumin or non-fat dry milk. After incubation of the membrane with the primary antibody (1°Ab) the membrane is exposed to a secondary antibody (2°Ab), directed against a species specific

portion of the primary antibody. An enzyme, such as horse radish peroxidase (HRP) is linked to the secondary antibody, catalyzing the reaction of the respective substrate LumiGlo. The product formed is able to generate luminescence in correlation to the amount of protein (figure 49).

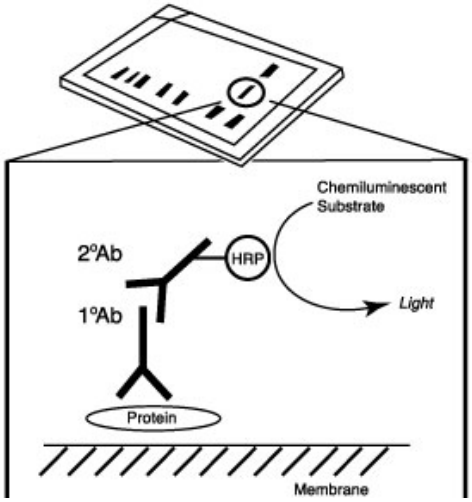

Figure 49: Schematic depiction of immune-blotting (http://www.cellsignal.com)

Procedure

Preparation of Protein Samples

- The cell culture medium of siRNA-transfected KYSE510 cells is aspirated and the cells are rinsed with 500 µl pre-warmed PBS per well. The previous transfection procedure is described in chapter 6.3 "Gene Silencing by using siRNA".
- The protein isolation is performed on ice. To each well 70 µl Laemmli buffer or RIPA-buffer, respectively are added and the cells are scraped of the plate-surface with the tip of the pipette. Then the cell lysate is transferred into a 1.5 ml reaction tube.
- Subsequently the protein samples are denatured at 95°C for 6 minutes in a heating block and sonificated for 1 minute.
- The obtained protein samples are stored at -20°C until required for electrophoresis. Before use all protein samples are heated for 6 minutes at 95°C.

Preparation of the Resolving and Stacking Gel

- The glass plates are degreased using 70% (v/v) ethanol and the gel caster is built up.
- At first the resolving gel is prepared first in a 15 ml tube according to table 14. The addition of APS (ammonium peroxide sulphate) as radical initiator and TEMED (N,N,N´,N´- tetramethylethylendiamine) as cross linking reagent is done shortly before filling the solution between two glass plates, separated by two spacers.

- Then the resolving gel is covered with a layer of n-butanol, causing the top of the gel to form a smooth surface. The gel polymerises at room temperature for about 30 minutes.
- Next, the n-butanol is removed precisely and the prepared stacking gel (table 14) is poured onto the resolving gel. A comb is placed into the stacking gel to create pockets for loading the samples. After the stacking gel is polymerised (about 30 minutes), the comb is removed and the gel is ready for electrophoresis.

Table 14: Preparation of the resolving and stacking gel (the volumes are calculated for two gels with 10 cm x 8 cm)

resolving gel (10%)		**stacking gel**	
component	**volume**	**component**	**volume**
bidest. water	2.05 ml	bidest. water.	1.2 ml
1.5 M Tris (pH 8.8)	1.23 ml	0.5 M Tris (pH 6.8)	0.5 ml
acrylamide (30%)	1.64 ml	acrylamide (30%)	0.25 ml
SDS (10%)	49.2 µl	SDS (10%)	20 µl
APS (10%)	24.6 µl	APS (10%)	20 µl
TEMED	2.46 µL	TEMED	2 µl

Electrophoresis

- First the acrylamide gel is fitted into the gel chamber and filled up with 1x electrophoresis buffer.
- The protein samples are heated at 95°C and centrifuged at 10,080 x g for 6 minutes.
- Then 20 µl of each sample are filled into the gel pockets (figure 50). Each sample is loaded in duplicates onto the gel, whereas the exact position of each one is noted. Additionally 5 µl of the "SeeBlue® Plus2 Pre-Stained Standard" marker is applied to one of the middle gel pockets. The exterior pockets are filled with 20 µl SDS-buffer (1x), as due to the smile effect at the border of the SDS gels the identification of the correct protein size would be problematical.

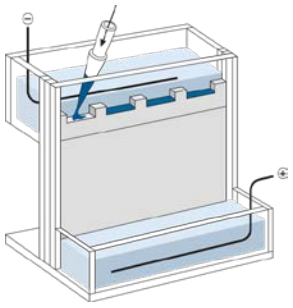

Figure 50: Loading the samples onto the gel

The electrophoresis apparatus is connected to the power supply, the voltage and current are set to 160 V, 1000 mA respectively and the run is performed for 1 h.

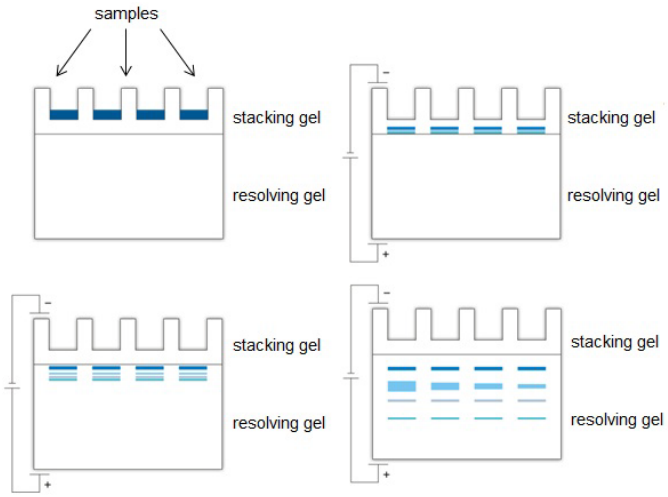

Figure 51: Separation of the proteins during electrophoresis

Protein Blotting

- Two pieces of Whatman-paper and one nitrocellulose membrane are cut in the size of the acrylamide gel and equilibrated in 1x blotting buffer for 30 minutes.
- Afterwards, a so called gel sandwich is prepared, which is shown in figure 52. The first piece of Whatman-paper is covered with a foam material pad and placed on the gray side of the cassette, which is the cathode of the transfer chamber. After the SDS-PAGE is completed, the gel is removed from the glass plate and transferred onto the pre-wet Whatman-paper. The gel is covered with the nitrocellulose membrane, another piece of Whatman-paper and a foam material pad. To avoid any air bubbles, a small cylinder is used to roll them out. The cassette is closed and locked with the white latch on the side.

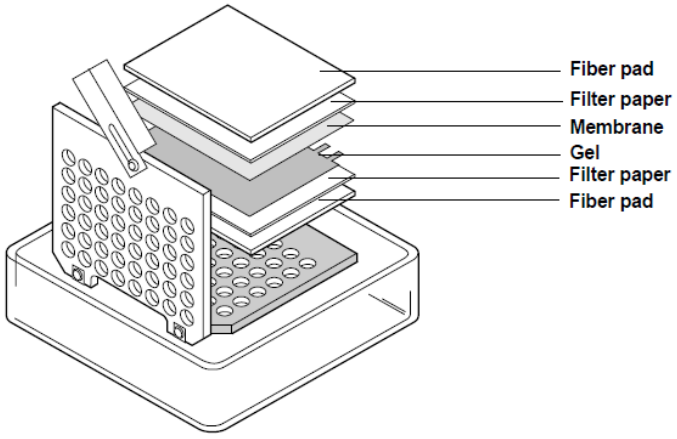

Figure 52: Schematic representation of a “wet blot” [Mini Trans Blot®- Electrophoretic Transfer Cell Instruction manual; BioRad]

- The cassette and the cooling loop are placed in the transfer tank, which is filled up to the mark with 1x blotting buffer. The hoses of the cooling unit are put in a beaker filled with ice water.
- Then the lid is attached to the tank, the cables and the pump of the cooling unit are connected and the blotting is performed at 1000 mA for 1 h 15 min.
- Upon completion of the transfer, the blotting unit is disconnected from the power supply, the blotting sandwich is disassembled and the membrane is removed for development with specific antibodies.

Detection with Specific Antibodies

- To block non-specific binding sites the membrane is shaken in a 5% (w/v) non-fat dry milk blocking reagent for 1 h at room temperature.
- Then the membrane is cut in the middle into two pieces. Since every sample is applied in duplicates, every sample is present on each piece. The primary antibodies (AhR, which was a kind gift of Prof. C. Weiss from the Karlsruher Institute of Technology, KIT Germany and α-tubulin, mouse monoclonal, Santa Cruz) are diluted 1:1000 with blocking reagent. The membrane is shrink-wrapped into a pocket filled with 1 ml of the diluted antibody solution and incubated over night at 4°C with agitation.
- Then the membrane is washed twice with washing buffer for 10 minutes on a shaker.
- The horse radish peroxidase (HRP) coupled secondary antibodies are diluted 1:5000 with blocking reagent. Goat anti-rabbit IgG-HRP antibody is used for the membrane previously incubated with AhR-antibody and goat anti-mouse IgG-HRP is used for the α-tubulin incubated membrane. Then the membranes are incubated for 1 h at room temperature on a shaking device.
- Then the membranes are rinsed two times with washing buffer for 10 minutes.
- To prepare the LumiGlo® solution 2 ml Enhanced Luminol Reagent and 2 ml Oxidizing Reagent are mixed and each membrane is incubated for exactly 1 minute under agitation. A luminescence signal is emitted due to the reaction of luminol with hydrogen peroxide, catalysed by the horse radish peroxidase enzyme (figure 53).

Each membrane is placed onto a tray and the detection is performed using the LAS-4000 Image Reader (Fujifilm).

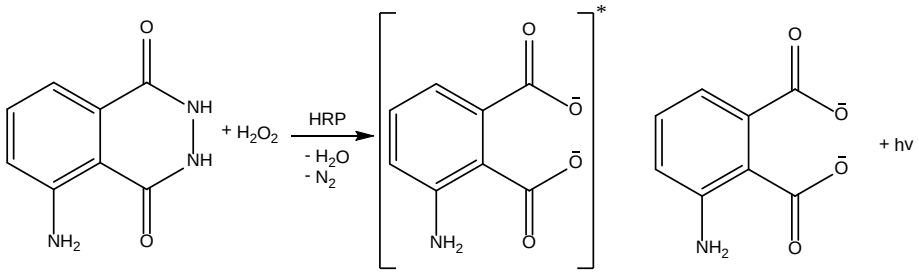

Figure 53: Reaction of LumiGlo® and HRP

Antibodies

- α-tubulin (B-7): mouse monoclonal, IgG2a, Santa Cruz, sc-5286, Lot no: D1808
- goat anti-mouse: HRP-conjugated, IgG-HRP, Santa Cruz, sc-2005, Lot no: J2910
- Anti-AhR (Aryl hydrocarbon receptor): rabbit polyclonal antibody, Enzo Life Science, Cat no: BML-SA210-0100
- goat anti-rabbit, HRP-conjugated, IgG-HRP, Santa Cruz

Reagents

1.5 M Tris buffer

36.4 g Tris(hydroxymethyl)-aminomethan (Tris) is dissolved in 200 ml bidest. water and the pH is set to 8.8.

0.5 M Tris buffer

12.1 g Tris (Roche) is dissolved in 200 ml bidest. water and the pH is set to 6.8.

6x SDS buffer

25 ml 0.5 M Tris buffer (pH 6.8)

20 ml glycerol	Sigma-Aldrich
620 mg SDS	Roth
80 mg bromophenol blue	Roth

The reagents are mixed together and dissolved in 50 ml bidest. water. Aliquots of 1 ml are prepared and stored at 4°C. Before use 52.6 µl ß-mercaptoethanol is added.

10x electrophoresis buffer

300 g glycin (2 M)	Sigma-Aldrich
60.57 g Tris (250mM)	Roche
1% SDS (20 g)	Roth

The reagents are dissolved in 2 l bidest. water and the pH is set to 8.3.

40x blotting buffer

234 g glycin	Sigma-Aldrich
466 g Tris	Roche
29.6 g SDS	Roth

The reagents are dissolved in 2 l bidest. water.

2x blotting buffer

2.9 l bidest. water and 2 l methanol (Sigma-Aldrich) are filled into a 5 l volumetric flask. 250 ml 40x blotting buffer are added and filled up with bidest. water.

10x Tris buffered saline with Tween-20 (10x TBST)

48.5 g Tris (200 mM)	Roche
160.1 g NaCl (1.37 M)	Roth

Both reagents are dissolved and the pH is set to 7.5. 20 ml Tween-20 (1%(v/v), Sigma-Aldrich) is added and filled up to 2 l with bidest. water.

Blocking reagent

5 g non-fat dry milk (5% (v/v), Roth) is dissolved in 1x TBST.

20x Tris buffered saline (20x TBS buffer)

96.6 g Tris (400 mM)	Roche
303.9 g NaCl (2.6 M)	Roth

The substances are dissolved in bidest. water, the pH of the solution is set to 7.6 and filled up to 2 l.

Washing buffer

250 ml 20x TBS buffer	
15 ml Tween-20 (0.3%)	Sigma-Aldrich

The reagents are mixed together and filled up to 5 l with bidest.water.

6.6. Glutathione-S-Transferase (GST) Enzyme Activity

The enzyme family of glutathione-S-transferases plays an important role in the detoxification of xenobiotics. GST enzymes catalyse the transfer of the thiol group of reduced glutathione to electrophilic molecules. In the course of this process, a lot of substances are converted to more hydrophilic metabolites, encompassing a better excretion (Volz, 2010).

The detection of GST enzyme activity is based on the GST-catalysed reaction of reduced glutathione (GSH) with 1-chloro-2,4-dinitrobenzene (CDNB) (figure 54). The formation of the corresponding thiolether conjugate is proportional to the enzyme activity. The formed product is determined photometrically at an absorption maximum of 340 nm. With this method the enzyme activity of all GST isoforms in the cytosol is detected (Immun Diagnostic, 2007).

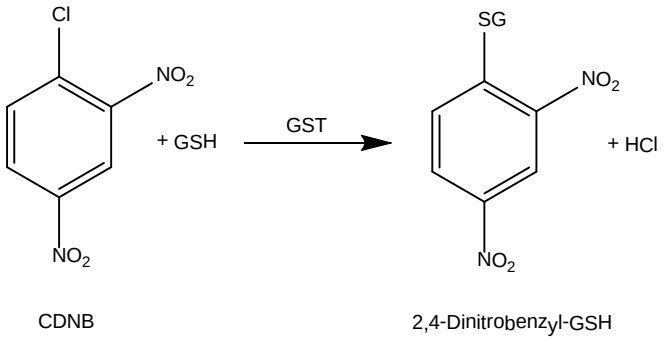

Figure 54: Reaction of 1-chloro-2,4-dinitrobenzene (CDNB) with glutathione (GSH), catalysed by glutathione-S-transferase enzymes (GST)

6.6.1. Procedure

Seeding Cells and Incubation of Cells

$1.2*10^6$ HT29 or $3*10^6$ HepG2 cells are seeded per Petri dish (d = 10 cm) using 10 ml DMEM medium and RPMI 1640 medium, respectively supplemented with 10% (v/v) heat inactivated FBS and 1% (v/v) P/S. The cells are grown for 48 h and 72 h, respectively at 37°C, 5% CO_2 and 95% relative humidity in the incubator.

The test substances are dissolved in DMSO and bidest. water, respectively; dilutions of 1:100 with cell culture medium (containing 10% (v/v) FBS and 1% (v/v) P/S) yield incubation solutions with a final concentration of 1% DMSO and 1% bidest. water. The depleted cell culture medium is aspirated and each dish is rinsed with 5 ml pre-warmed PBS. After removing the washing solution the cells are treated with 5 ml of the designated chemicals in the appropriate concentration for 24 h, 16 h, 9 h and 1 h. An incubation solution, containing 1% DMSO or 1% bidest. water, are used as solvent controls.

Sample Preparation

- After 24 h incubation time the cell culture medium is removed and the dish is rinsed with pre-warmed PBS.
- To each dish 1 ml trypsin solution is added and incubated for 2.5 minutes in the incubator. Then the cells are detached by slightly clapping the dish at the edge of a desk and the trypsin reaction is inhibited by adding 1 ml cell culture medium (containing 10% (v/v) FBS and 1% (v/v) P/S).
- The cells are rinsed carefully from the surface and the suspension is transferred into a 15 ml test tube. Additionally the dish is rinsed with 1 ml cell culture medium.
- 2 ml of the cell suspension is transferred into a 2 ml test tube and centrifuged at 500 x g at 4°C for 10 minutes.
- The cell culture medium is discarded, 1 ml PBS is added, the cell pellet is re-suspended and the test tube is centrifuged at 500 x g at 4°C for additional 10 minutes.
- The PBS is removed and the cell pellet is lysed in the biofreezer at -80°C overnight.
- Before starting with the GST assay, the cell pellet is thawed on ice and re-suspended in 500 µl potassium phosphate buffer. For proper cell disruption the lysate is passed 15 times through a blunt 20-gauge needle (0.9 mm diameter), fitted to a 1 ml RNase free syringe. The lysate is centrifuged for 10 minutes at 1000 x g and 4°C. The supernatant is transferred into a new 1.5 ml test tube and used for the GST assay.

Substrate Conversion

- 700 µl potassium phosphate buffer, 40 µl GSH-solution and 40 µl supernatant are incubated at 37°C for 5 minutes under shaking (300 rpm).
- 20 µl CDNB-solution is added, mixed by vortexing and 3 x 200 µl of the solution are pipetted into the wells of a 96-well plate. This step is accomplished in the dark, as the CDNB-solution is extremely light sensitive.
- The plate is transferred into the VICTOR^{3}V 1420 plate reader (Multilabel counter, Perkin Elmer) and the Wallac 1420 (version 3.0, revision 4) software is started. The absorption is monitored at 340 nm for 8 minutes, whereas a measurement is performed every 20 seconds.
- The volume of supernatant used for the assay depends on the absorbance values obtained. Absorbance values higher than 2.0 at the end of the reaction time are avoided, because the linearity according to Beer-Lambert´s law is not granted any more. Using less supernatant means, that the volume of potassium phosphate buffer has to be adjusted, so that after the addition of CDNB-solution the total volume of the reaction mixture yields 800 µl.

- To determine the absorbance of the blank, 740 µl potassium phosphate buffer and 40 µl GSH-solution are incubated at 37°C for 5 minutes under shaking (300 rpm). The increase of absorbance is measured after the addition of 20 µl CDNB-solution.
- After measuring the GST activity, the protein concentration of the supernatant is determined according the Bradford assay (see chapter 6.6.2 “Determination of Protein Concentration by Bradford)”.

Reagents

- 1 x PBS see chapter 6.1.6 “Cell Counting”
- trypsin solution see chapter 6.1.6 “Cell Counting”

Potassium Phosphate Buffer

50 ml 100 mM K_2HPO_4 (Roth) solution is prepared and the pH is adjusted to 7.4 by addition of 100 mM KH_2PO_4 (Roth) solution.

GSH-solution

20 mM reduced glutathione (GSH, Sigma-Aldrich) is dissolved in potassium phosphate buffer. For each analysis a fresh solution is prepared and stored on ice.

CDNB-solution

40 mM CDNB (Sigma-Aldrich) is dissolved in ethanol (96% v/v, Roth). Each time a fresh solution is prepared and due to the limited solubility of CDNB it is sonicated briefly. The light sensitive solution is stored in a black 1.5 ml test tube at room temperature.

Calculating GST activity

The calculation of the GST activity is demonstrated using the experiment performed on the 17/09/2011 with 1 µM AME. For calculating GST enzyme activity the measured absorbance is plotted against the time (table 15). The obtained absorbance values in the interval between the 1st and the 5th minute are used for calculating the slope, because linearity is granted in that range.

Table 15: Determined absorbance vs. time for 1 µM AME (recorded on the 17/09/2011)

time [min]	ABS
0.38	0.931
0.65	0.987
0.92	1.043
1.19	1.096
1.46	1.149
1.72	1.197
1.99	1.247
2.26	1.295
2.53	1.340
2.80	1.385
3.07	1.428
3.34	1.470
3.61	1.514
3.88	1.552
4.15	1.594

time [min]	ABS
4.42	1.630
4.68	1.668
4.95	1.701
5.22	1.743
5.49	1.781
5.76	1.814
6.03	1.848
6.30	1.875
6.57	1.914
6.84	1.951
7.11	1.979
7.38	2.013
7.64	2.026
7.91	2.071
8.18	2.108

The absorbance values used for the calculation of the slope [ΔA_{340}/min] are grey shaded in table 15. The plot of the recorded absorbance versus time confirms the linearity in the range which is used for further calculations (figure 55).

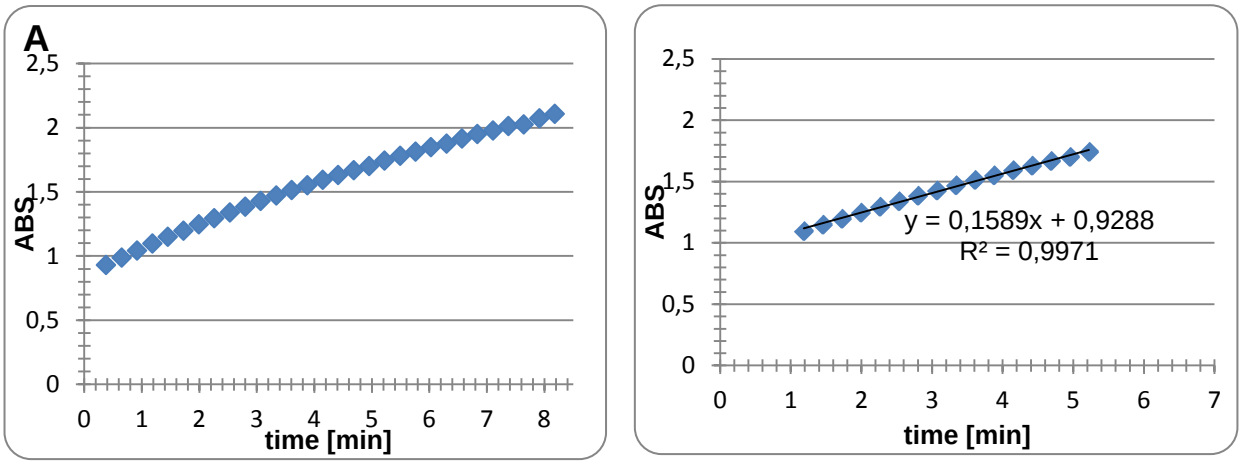

Figure 55: (A) Plot of absorbance vs. time of the 1 µM AME-sample, measurement recorded on the 17/09/2011, (B) the linear range between the 1st and the 5th minute is used for the calculation of the slope

Each absorbance determination is performed in triplicates, hence the slopes are determined independently three times and the arithmetic mean value is calculated.

- $[\Delta A_{340}/\min]_1 = 0.1589$
- $[\Delta A_{340}/\min]_2 = 0.1586$
- $[\Delta A_{340}/\min]_3 = 0.1588$

$$Arithmetic\ mean(GST-activity) = \frac{1}{3}\sum_{i=1}^{3}[\Delta A_{340}/\min] = \frac{0.1589+0.1586+0.1588}{3} = 0.1588$$

The background absorbance elicited by the solvent, is determined by measuring a blank solution. The slope obtained for the blank is subtracted from the arithmetic mean value of the sample slope and the result is used for further calculations.

- $[\Delta A_{340}/\min]_{blank} = 0.0530$

$$[\Delta A_{340}/\min]_{Sample} - [\Delta A_{340}/\min]_{blank} = 0.1588 - 0.0530 = 0.1058$$

The GST activity is calculated by applying Beer-Lambert´s law.

Following parameters are used for the calculation:

- absorption coefficient of the GST-CDNB-conjugate at λ = 340 nm: ε = 9,6 $mM^{-1}cm^{-1}$
- path length in the Victor V^3 plate reader for the 96-well plate: d = 0,45 cm

The dilution factor (*df*) is the ratio of total sample volume and the used volume of the cytosol:

- V (sample) = 800 µl
- V (cytosol) = 20 µl

$$df = \frac{V_{Sample}}{V_{Cytosole}} = \frac{800}{20} = 40$$

$$GST\ activity = \frac{[A_{340}/\min]}{\varepsilon * d} * df$$

$$GST\ activity = \frac{0{,}1058}{9{,}6 * 0{,}45} * 40 = 0{,}9799\ \mu mol * ml^{-1} * \min^{-1}$$

The activity of glutathione-S-transferases depends on the protein amount used for the analysis. Therefore GST activity is related to the protein concentration. The factor of 1000 is used for the conversion of µmol to nmol.

- protein concentration = 3.74 mg/ml

$$GST\ activity = \frac{0.9799}{3.74} * 1000 = 262.01\ nmol * ml^{-1} * mg^{-1}_{\mathrm{Pr}otein}$$

Double determination of the absorbance values is performed with every sample, hence arithmetic mean values of both measurements are calculated.

$$GST\ activity(1\mu M\ \ AME) = \frac{1}{2}\sum_{i=1}^{2}(GST - act.) = \frac{262.01 + 285.94}{2} = 273.97\ nmol * ml^{-1} * mg^{-1}_{\mathrm{Pr}otein}$$

Since GST activity expressed in [nmol x ml^{-1} x $mg_{protein}^{-1}$] represents absolute values, comparison of individual measurements is subjected to high variations. Furthermore, fluctuating absorbance background values due to individual lamp and spectrophotometer performances, are not taken into account. Therefore, the expression of test over control values (T/C) [%] is considered to be the better option.

$$T/C\ (1\%\ DMSO) = \frac{GST\ activity(1\%\ DMSO)}{arith.\ mean[GST\ act.(1\%\ DMSO)]} * 100 = \frac{269.82}{271.68} * 100 = 99.32\%$$

Calculated GST activity of samples is compared with solvent control-treated cells (1%, 0.1% DMSO and 1% bidest. water, respectively), facilitating following correlation:

$$T/C\ (1\mu M\ \ AME) = \frac{GST\ activity(1\mu M\ \ AME)}{arith.mean[GST\ act.(1\%\ DMSO)]} * 100 = \frac{273.97}{271.68} * 100 = 100.84\%$$

Student´s t-test is applied to assign significant differences between sample and solvent control-treated cells. The application of the "TTEST" function in Microsoft Excel 2007® is already described in chapter 6.4.5 "Real Time PCR". Solvent control cells are again used as reference point and designated as "Matrix 1", whereas cells incubated with diverse test substances are used as "Matrix 2".

6.6.2. Determination of Protein Concentration by Bradford

The method according to Bradford (1976) allows the detection of protein amounts as low as 0.5 µg. The dye Coomassie Brilliant Blue G-250 binds to basic amino acids under acidic conditions. Due to the formation of complexes, the absorbance maximum is shifted from 465 nm to 595 nm. A standard curve is necessary for the determination of the protein concentration. The protein used for the calibration should exhibit the same amount of basic amino acids as the unknown protein (Lottspeich, 2006).

Bovine serum albumin (BSA standard solution, 2 mg/ml) is used for calibration in the range of 0.2 - 1.6 mg/ml. A standard curve is obtained after plotting the standard concentration versus the corresponding absorption values. The protein concentration is determined after subtraction of the blank value (potassium phosphate buffer) using the linear regression standard curve.

Procedure

10 µl of the BSA standard solution, potassium phosphate buffer or diluted supernatant are added to 1 ml Bradford reagent and mixed by vortexing. The appropriate dilution factor of the supernatant is a consequence of the obtained absorption values, which should be in the middle range of the standard curve. Thus a reliable protein concentration is assured.

3 x 200 µl of every solution are pipetted into a 96-well plate, transferred to the VICTOR^{3}V 1420 plate reader (Multilabel counter, Perkin Elmer) and the absorption is determined photometrically at 595 nm.

Reagents

Bradford reagent

100 mg Coomassie Brillant Blue G-250	Roth
50 ml 96% v/v ethanol	Roth
100 ml 85% v/v phosphoric acid	Sigma-Aldrich

The solution is filled up to 1000 ml with bidest. water, stored in the dark for 4 weeks and filtered before use.

Additional reagents

- Bovine serum albumin (BSA) stock solution 2 mg/ml (Gibco^{TM}, Invitrogen)
- bidest. water

6.7. Materials

Laboratory Equipment	Company
casette & firbre pads	BioRad
cover glass (24 x 24 mm)	VWR
cryo tube vials (1.8 µl)	Nunc
duran flasks (250, 500, 1000 ml)	VWR/ Brand
diverse Eppendorf pipettes	0.1-2.5 µl, 0.5-10 µl, 2-20 µl, 10-100 µl, 20-200 µl, 100-1000 µl
diverse pipette tips:	2.5 µl, 10 µl, 100 µl, 200 µl, 1000 µl Sarstedt
diverse pipette tips with filter	2.5 µl, 10 µl, 100 µl, 200 µl, 1000 µl Sarstedt
diverse Eppendorf reaction tubes	0.2 ml, 1.5 ml, 2.0 ml
glass plates (10 x 8 x 0.1 cm)	BioRad
haemocytometer (0.0025 mm^2, depth 0.1 mm)	Marienfeld, Germany
micro test tube rack	Brand
needles (0.9 x 40 mm)	Neolus, Terumo
nitrocellulose membranes (pore size 0.2 µM)	Schleicher & Schuell Whatman
parafilm "M"	Pechiney Plastic Packaging
pasteur pipettes (length 230mm)	Roth
PCR-foil	MicroAmp® 96-Well Optical Adhesive Film, Applied Biosystems
PCR-plates	MicroAmp® Optical 96-well Reaction Plate, Applied Biosystems
syringe (1 ml)	Thermo
tissue culture flasks (25, 75, 175 cm^2)	Sarstedt
tissue culture dishes (100 x 20 mm)	Sarstedt
tubes (15, 50 ml)	Sarstedt
Whatman-paper (GB005)	Schleicher & Schuell Whatman
10 well comb (1.0 mm)	BioRad
24-well tissue culture plate	VWR
96-well tissue culture plate	Costar

Device	Model	Company
analytical balance	Atilon ATL-124-I	Acculab
autoclave	Systec DX-150	Bartelt
biofreezer	MDF-U53V	Sanyo
centrifuge	Mikro 220R V 1.02	Hettich
	Rotina 420R	Hettich
	Mikro 200 V 1.29	Hettich
electrophoresis power supply	EV231	Peqlab
electrophoresis unit	Mini-Protein Tetra Cell 552BR	BioRad
film sealing unit	Folio	Severin
fridge	Comfort Max Frost	Liebherr
incubator	Hera cell 240i	Thermo Scientific
laminar Air Flow	Hera Safe KS18	Thermo Scientific
luminescence image analyser	LAS-4000	Fujifilm
magnetic stiffer	IKAMAG RH64212	IKA-Labortechnik
microscope	Axiovert 40C	Zeiss
mini-centrifuge	Kinetic Energy-Galaxy Mini Centrifuge	VWR
ph-meter	Seven Easy	Mettler Toledo
pipetting aid	pipetus	Hirschmann Laborgeräte
plate reader	Victor3V 1420 Multilabel counter	Perkin Elmer
PCR	Step One Plus Real-Time PCR System	Applied Biosystems
shaker	Roto-Shake Genie	Scientific Industries
	Mini-Rocker MR-1	Peqlab
spectrophotometer	Nano Drop 2000c	Peqlab
suction system	Vacusafe Compfort V04 & Integra Vacuboy	IBS Integro Biosciences
thermo incubator	Thriller	Peqlab
thermo shaker	TS-100	Thermo
thermocycler	Dyad Disciple	BioRad
transfer tank & unit	Trans Blot Cell 49BR	BioRad
ultrasonic bath	USC 300T	VWR
ultraviolet sterilizing PCR workstation		Peqlab
vortex	Vortex Genie 2	Scientific Industries
	Bio Vortex V1	Peqlab
water purification system	Milli Q, Direct 8	Millipore

7. Referencesa

Abel J & Haarmann-Stemmann T An introduction to the molecular basics of aryl hydrocarbon receptor biology. *Biol Chem* 391, 1235-1248.

Ackermann Y, Curtui V, Dietrich R, Gross M, Latif H, Martlbauer E & Usleber E (2011) Widespread occurrence of low levels of alternariol in apple and tomato products, as determined by comparative immunochemical assessment using monoclonal and polyclonal antibodies. *J Agric Food Chem* 59, 6360-6368.

Almahmeed T, Boyle JO, Cohen EG, Carew JF, Du B, Altorki NK, Kopelovich L, Fang JL, Lazarus P, Subbaramaiah K & Dannenberg AJ (2004) Benzo[a]pyrene phenols are more potent inducers of CYP1A1, CYP1B1 and COX-2 than benzo[a]pyrene glucuronides in cell lines derived from the human aerodigestive tract. *Carcinogenesis* 25, 793-799.

An YH, Zhao TZ, Miao J, Liu GT, Zheng YZ, Xu YM & Van Etten RL (1989) Isolation, identification, and mutagenicity of alternariol monomethyl ether. *J. Agric. Food Chem.* 37, 1341–1343.

Backlund M, Johansson I, Mkrtchian S & Ingelman-Sundberg M (1997) Signal transduction-mediated activation of the aryl hydrocarbon receptor in rat hepatoma H4IIE cells. *J Biol Chem* 272, 31755-31763.

Barkai-Golan R (2002) An Annotated Check-List of Post-Harvest Fungal Diseases of Fruits and Vegetables in Israel [DoPSoF Produce, editor: Bet Dagan, Israel.

Barkai-Golan R & Paster N (2008) *Mycotoxins in Fruits and Vegetables*, 1st ed: Elsevier Inc.

Bennett P, Ramsden DB & Williams AC (1996) Complete structural characterisation of the human aryl hydrocarbon receptor gene. *Clin Mol Pathol* 49, M12-16.

Bergheim I, Wolfgarten E, Bollschweiler E, Holscher AH, Bode C & Parlesak A (2007) Cytochrome P450 levels are altered in patients with esophageal squamous-cell carcinoma. *World J Gastroenterol* 13, 997-1002.

Bock KW & Kohle C (2006) Ah receptor: dioxin-mediated toxic responses as hints to deregulated physiologic functions. *Biochem Pharmacol* 72, 393-404.

Bouma M-E, Rogier E, Verthier N, Labarre C & Feldmann G (1989) Further cellular investigation of the human hepatoblastoma-derived cell line HepG2: morphology and immunocytochemical studies of hepatic-secreted proteins. *In Vitro Cell Dev Biol.* 25, 9.

Brugger EM, Wagner J, Schumacher DM, Koch K, Podlech J, Metzler M & Lehmann L (2006) Mutagenicity of the mycotoxin alternariol in cultured mammalian cells. *Toxicol Lett* 164, 221-230.

BundesinstitutfürRisikobewertung(BfR) (2003) Stellungnahme des BfR vom 30. Juli 2003: Alternaria-Toxine in Lebensmitteln, pp. 2.

Burbach KM, Poland A & Bradfield CA (1992) Cloning of the Ah-receptor cDNA reveals a distinctive ligand-activated transcription factor. *Proc Natl Acad Sci U S A* 89, 8185-8189.

Burkhardt B, Pfeiffer E & Metzler M (2009) Absorption and metabolism of the mycotoxin alternariol and alternariol-9-methyl ether in Caco-2 cells in vitro. *Mycotox Res.* 25, 149-157.

Burkhardt B, Wittenauer J, Pfeiffer E, Schauer UM & Metzler M (2011) Oxidative metabolism of the mycotoxins alternariol and alternariol-9-methyl ether in precision-cut rat liver slices in vitro. *Mol Nutr Food Res* 55, 1079-1086.

Choudhary D, Jansson I, Stoilov I, Sarfarazi M & Schenkman JB (2005) Expression patterns of mouse and human CYP orthologs (families 1-4) during development and in different adult tissues. *Arch Biochem Biophys* 436, 50-61.

CSCF (2007) Scientific opinion of the Czech Scientific Commitee on Food to Alternaria mycotoxins, pp. 24. Brno, Czech Republic: http://www.chpr.szu.cz/.

da Motta S. LM, Soares V. (2000) A Method for the determination of two Alternaria toxins, Alternariol and Alternariol monomethyl ether, in tomato products. *Brazilian Journal of Microbiology* 31.

Davarinos NA & Pollenz RS (1999) Aryl hydrocarbon receptor imported into the nucleus following ligand binding is rapidly degraded via the cytosplasmic proteasome following nuclear export. *J Biol Chem* 274, 28708-28715.

Davis VM & Stack ME (1994) Evaluation of alternariol and alternariol methyl ether for mutagenic activity in Salmonella typhimurium. *Appl Environ Microbiol* 60, 3901-3902.

de Fougerolles A, Vornlocher HP, Maraganore J & Lieberman J (2007) Interfering with disease: a progress report on siRNA-based therapeutics. *Nat Rev Drug Discov* 6, 443-453.

Delescluse C, Lemaire G, de Sousa G & Rahmani R (2000) Is CYP1A1 induction always related to AHR signaling pathway? *Toxicology* 153, 73-82.

Denison MS & Nagy SR (2003) Activation of the aryl hydrocarbon receptor by structurally diverse exogenous and endogenous chemicals. *Annu Rev Pharmacol Toxicol* 43, 309-334.

Denison MS, Pandini A, Nagy SR, Baldwin EP & Bonati L (2002) Ligand binding and activation of the Ah receptor. *Chem Biol Interact* 141, 3-24.

Denison MS & Whitlock JP, Jr. (1995) Xenobiotic-inducible transcription of cytochrome P450 genes. *J Biol Chem* 270, 18175-18178.

Dierickx PJ, Nuffel GV & Alvarez I (1999) Glutathione protection against hydrogen peroxide, tert-butyl hydroperoxide and diamide cytotoxicity in rat hepatoma-derived Fa32 cells. *Hum Exp Toxicol* 18, 627-633.

Ding X & Kaminsky LS (2003) Human extrahepatic cytochromes P450: function in xenobiotic metabolism and tissue-selective chemical toxicity in the respiratory and gastrointestinal tracts. *Annu Rev Pharmacol Toxicol* 43, 149-173.

Dohr O, Vogel C & Abel J (1995) Different response of 2,3,7,8-tetrachlorodibenzo-p-dioxin (TCDD)-sensitive genes in human breast cancer MCF-7 and MDA-MB 231 cells. *Arch Biochem Biophys* 321, 405-412.

Dong ZG, Liu GT, Dong ZM, Qian YZ, An YH, Miao JA & Zhen YZ (1987) Induction of mutagenesis and transformation by the extract of Alternaria alternata isolated from grains in Linxian, China. *Carcinogenesis* 8, 989-991.

Doostdar H, Duthie SJ, Burke MD, Melvin WT & Grant MH (1988) The influence of culture medium composition on drug metabolising enzyme activities of the human liver derived Hep G2 cell line. *FEBS Lett* 241, 15-18.

Drahushuk AT, McGarrigle BP, Larsen KE, Stegeman JJ, Olson JR (1998) Detection of CYP1A1 protein in human liver and induction by TCDD in precision-cut liver slices incubated in dynamic organ culture. *Carcinogenesis* 19, 1361-1368.

Drusch S & Ragab W (2003) Mycotoxins in fruits, fruit juices, and dried fruits. *J Food Prot* 66, 1514-1527.

DSMZ (Braunschweig) Leibniz Institute DSMZ-German Collection of Microorganisms and Cell Cultures.

Ebert MN, Beyer-Sehlmeyer G, Liegibel UM, Kautenburger T, Becker TW & Pool-Zobel BL (2001) Butyrate induces glutathione S-transferase in human colon cells and protects from genetic damage by 4-hydroxy-2-nonenal. *Nutr Cancer* 41, 156-164.

Ebert MN, Klinder A, Peters WH, Schaferhenrich A, Sendt W, Scheele J & Pool-Zobel BL (2003) Expression of glutathione S-transferases (GSTs) in human colon cells and inducibility of GSTM2 by butyrate. *Carcinogenesis* 24, 1637-1644.

EFSA, European Food and Safety Authority (2011). Scientific Opinion on the risk for animal and public health related to the presence of Alternaria toxins in feed and food.

El Gendy MA & El-Kadi AO Harman induces CYP1A1 enzyme through an aryl hydrocarbon receptor mechanism. *Toxicol Appl Pharmacol* 249, 55-64.

Elbashir SM, Lendeckel W & Tuschl T (2001) RNA interference is mediated by 21- and 22-nucleotide RNAs. *Genes Dev* 15, 188-200.

Elbekai RH & El-Kadi AO (2007) Transcriptional activation and posttranscriptional modification of Cyp1a1 by arsenite, cadmium, and chromium. *Toxicol Lett* 172, 106-119.

Esenbeck N & Daniel CG (1817) *Das System der Pilze und Schwämme: ein Versuch* Würzburg: Stahel.

EuropeanComission (2003) Safe organic vegetables and vegetable products by reducing risk factors and sources of fungal contaminants throughout the production chain: The carrot - Alternaria model. In *Key Action: Food, Nutrition and Health* [R D'Amario, editor. Luxembourg:: European Commission - Quality of Life and Management of Living Resources.

Fang MZ, Wang Y, Ai N, Hou Z, Sun Y, Lu H, Welsh W & Yang CS (2003) Tea polyphenol (-)-epigallocatechin-3-gallate inhibits DNA methyltransferase and reactivates methylation-silenced genes in cancer cell lines. *Cancer Res* 63, 7563-7570.

Fehr M (2008) Mechanismen der genotoxischen Wirkung von Alternaria-Toxinen, Universität Karlsruhe.

Fehr M, Baechler S, Christopher K, Mielke C, Boege F, Pahlke G & Marko D (2010) Repair of DNA damage induced by the mycotoxin alternariol involves tyrosyl-DNA phosphodiesterase 1. *Mycotox Res* 26, 247-256.

Fehr M, Pahlke G, Fritz J, Christensen MO, Boege F, Altemoller M, Podlech J & Marko D (2009) Alternariol acts as a topoisomerase poison, preferentially affecting the IIalpha isoform. *Mol Nutr Food Res* 53, 441-451.

Fontaine F, Delescluse C, de Sousa G, Lesca P & Rahmani R (1999) Cytochrome 1A1 induction by primaquine in human hepatocytes and HepG2 cells: absence of binding to the aryl hydrocarbon receptor. *Biochem Pharmacol* 57, 255-262.

Formica JV & Regelson W (1995) Review of the biology of Quercetin and related bioflavonoids. *Food Chem Toxicol* 33, 1061-1080.

Fujii-Kuriyama Y, Imataka H, Sogawa K, Yasumoto K & Kikuchi Y (1992) Regulation of CYP1A1 expression. *Faseb J* 6, 706-710.

Fujisawa-Sehara A, Sogawa K, Yamane M & Fujii-Kuriyama Y (1987) Characterization of xenobiotic responsive elements upstream from the drug-metabolizing cytochrome P-450c gene: a similarity to glucocorticoid regulatory elements. *Nucleic Acids Res* 15, 4179-4191.

Gillner M, Bergman J, Cambillau C, Alexandersson M, Fernstrom B & Gustafsson JA (1993) Interactions of indolo[3,2-b]carbazoles and related polycyclic aromatic hydrocarbons with specific binding sites for 2,3,7,8-tetrachlorodibenzo-p-dioxin in rat liver. *Mol Pharmacol* 44, 336-345.

Goergens A (2009) Die Bedeutung des Arylhydrocarbon Rezeptors für die antileukämische Wirkung von Flavonoiden und Indolen, Heinrich-Heine-Universität Düsseldorf.

Gradin K, Whitelaw ML, Toftgard R, Poellinger L & Berghard A (1994) A tyrosine kinase-dependent pathway regulates ligand-dependent activation of the dioxin receptor in human keratinocytes. *J Biol Chem* 269, 23800-23807.

Gravesen S, Frisvad JC & Samson RA (1994) *Microfungi* Coppenhagen, Denmark: Munksgaard International Publishers.

Griffin GF & Chu FS (1983) Toxicity of the Alternaria metabolites alternariol, alternariol methyl ether, altenuene, and tenuazonic acid in the chicken embryo assay. *Appl Environ Microbiol* 46, 1420-1422.

Gu YZ, Hogenesch JB & Bradfield CA (2000) The PAS superfamily: sensors of environmental and developmental signals. *Annu Rev Pharmacol Toxicol* 40, 519-561.

Guengerich FP (2003) Cytochromes P450, drugs, and diseases. *Mol Interv* 3, 194-204.

Guigal N, Seree E, Bourgarel-Rey V & Barra Y (2000) Induction of CYP1A1 by serum independent of AhR pathway. *Biochem Biophys Res Commun* 267, 572-576.

Habig WH, Pabst MJ & Jakoby WB (1974) Glutathione S-transferases. The first enzymatic step in mercapturic acid formation. *J Biol Chem* 249, 7130-7139.

Hamilton GA, Jolley SL, Gilbert D, Coon DJ, Barros S & LeCluyse EL (2001) Regulation of cell morphology and cytochrome P450 expression in human hepatocytes by extracellular matrix and cell-cell interactions. *Cell Tissue Res* 306, 85-99.

Hankinson O (2005) Role of coactivators in transcriptional activation by the aryl hydrocarbon receptor. *Arch Biochem Biophys* 433, 379-386.

Hayes JD, Flanagan JU & Jowsey IR (2005) Glutathione transferases. *Annu Rev Pharmacol Toxicol* 45, 51-88.

Hayes JD & McLellan LI (1999) Glutathione and glutathione-dependent enzymes represent a co-ordinately regulated defence against oxidative stress. *Free Radic Res* 31, 273-300.

Hayes JD & Pulford DJ (1995) The glutathione S-transferase supergene family: regulation of GST and the contribution of the isoenzymes to cancer chemoprotection and drug resistance. *Crit Rev Biochem Mol Biol* 30, 445-600.

Hayes JD & Wolf CR (1990) Molecular mechanisms of drug resistance. *Biochem J* 272, 281-295.

Hoivik D, Willett K, Wilson C & Safe S (1997) Estrogen does not inhibit 2,3,7, 8-tetrachlorodibenzo-p-dioxin-mediated effects in MCF-7 and Hepa 1c1c7 cells. *J Biol Chem* 272, 30270-30274.

ImmundDiagnostic (2007) *Glutathion S-Transferase (GST) Assay Kit- Zur Bestimmung der GST-Aktivität in biologischen Proben*. Bensheim: Immun Diagnostic.

Jeong HG, Yun CH, Jeon YJ, Lee SS & Yang KH (1995) Suppression of cytochrome P450 (Cyp1a-1) induction in mouse hepatoma Hepa-1C1C7 cells by methoxsalen. *Biochem Biophys Res Commun* 208, 1124-1130.

Jiang ZQ, Chen C, Yang B, Hebbar V & Kong AN (2003) Differential responses from seven mammalian cell lines to the treatments of detoxifying enzyme inducers. *Life Sci* 72, 2243-2253.

Kahle N (2012) Einfluss von Alternariol und Alternariolmonomethylether auf die CYP1A1 Expression in humanen Tumorzellen, Universität Wien

Kazlauskas A, Poellinger L & Pongratz I (1999) Evidence that the co-chaperone p23 regulates ligand responsiveness of the dioxin (Aryl hydrocarbon) receptor. *J Biol Chem* 274, 13519-13524.

Kim D & Rossi J (2008) RNAi mechanisms and applications. *Biotechniques* 44, 613-616.

Kitamura R, Matsuoka K, Nagayama S & Otagiri M (2008) Time-dependent induction of rat hepatic CYP1A1 and CYP1A2 expression after single-dose administration of the anti-angiogenic agent TSU-68. *Drug Metab Pharmacokinet* 23, 421-427.

Klaassen CD & Watkins JB (2003) *Casarett and Doull's essentials of Toxicology*, 1st ed: McGraw-Hill Professional.

Koch K, Podlech J, Pfeiffer E & Metzler M (2005) Total synthesis of alternariol. *J Org Chem* 70, 3275-3276.

Kocher U (2007) Determination of 7 Alternaria toxins in edible oil and oilseeds by LC-MS/ MS. In *Gesellschaft für Mykotoxin Forschung (Ed.) Proceedings of the 29th mycotoxin workshop*. Stuttgart- Fellbach, Germany.

Lechevrel M, Casson AG, Wolf CR, Hardie LJ, Flinterman MB, Montesano R & Wild CP (1999) Characterization of cytochrome P450 expression in human oesophageal mucosa. *Carcinogenesis* 20, 243-248.

Lehmann L, Wagner J & Metzler M (2006) Estrogenic and clastogenic potential of the mycotoxin alternariol in cultured mammalian cells. *Food Chem Toxicol* 44, 398-408.

Lindl T (2000) *Zell- und Gewebekultur : Einführung in die Grundlagen sowie ausgewählte Methoden und Anwendungen*, 4., überarb. und erw. Aufl. ed. Heidelberg [u.a.]: Spektrum, Akad. Verl.

Liu GT, Qian YZ, Zhang P, Dong WH, Qi YM & Guo HT (1992) Etiological role of Alternaria alternata in human esophageal cancer. *Chin Med J (Engl)* 105, 394-400.

Liu GT, Qian YZ, Zhang P, Dong ZM, Shi ZY, Zhen YZ, Miao J & Xu YM (1991) Relationships between Alternaria alternata and oesophageal cancer. *IARC Sci Publ*, 258-262.

Livak KJ & Schmittgen TD (2001) Analysis of Relative Gene Expression Data Using Real-Time Quantitative PCR and the 2^{-ddCt} Method. *METHODS, Elsevier Science (USA)* 25, 402–408.

Lottspeich F (2006) *Bioanalytik*, 2. Auflage ed. Heidelberg: Spektrum Akademischer Verlag.

Lu YF, Santostefano M, Cunningham BD, Threadgill MD & Safe S (1995) Identification of 3'-methoxy-4'-nitroflavone as a pure aryl hydrocarbon (Ah) receptor antagonist and evidence for more than one form of the nuclear Ah receptor in MCF-7 human breast cancer cells. *Arch Biochem Biophys* 316, 470-477.

Ma Q & Whitlock JP, Jr. (1996) The aromatic hydrocarbon receptor modulates the Hepa 1c1c7 cell cycle and differentiated state independently of dioxin. *Mol Cell Biol* 16, 2144-2150.

Magan N & Olsen M (2004) *Mycotoxins in food- Detection and control*, 1st ed. Cambridge: Woodhead Publishing Ltd.

Magan N. LJ (1985) Interactions Between Field and Storage Fungi on Wheat Grain. *Trans. Br. Mycol. Soc.* 85, 29-37.

Magnani RF, De Souza GD & Rodrigues-Filho E (2007) Analysis of alternariol and alternariol monomethyl ether on flavedo and albedo tissues of tangerines (Citrus reticulata) with symptoms of alternaria brown spot. *J Agric Food Chem* 55, 4980-4986.

Mansuy D (1998) The great diversity of reactions catalyzed by cytochromes P450. *Comp Biochem Physiol C Pharmacol Toxicol Endocrinol* 121, 5-14.

Matikainen T, Perez GI, Jurisicova A, Pru JK, Schlezinger JJ, Ryu HY, Laine J, Sakai T, Korsmeyer SJ, Casper RF, Sherr DH & Tilly JL (2001) Aromatic hydrocarbon receptor-driven Bax gene expression is required for premature ovarian failure caused by biohazardous environmental chemicals. *Nat Genet* 28, 355-360.

Mercurio MG, Shiff SJ, Galbraith RA & Sassa S (1995) Expression of cytochrome P450 mRNAs in the colon and the rectum in normal human subjects. *Biochem Biophys Res Commun* 210, 350-355.

Mülhardt C (2009) *Molekularbiologie/ Genomics*, 6. Auflage ed. Heidelberg: Spektrum Akademischer Verlag.

Murray PR, Baron EJ & Jorgensen JH (2007) Bipolaris, Exophiala, Scedosporium, Sporothrix, and other dematiaceous fungi. In *Manual of Clinical Microbiology*, pp. 1898-1191. Washington, DC.: American Society for Microbiology.

Nam KS & Shon YH (2009) Chemopreventive effects of polysaccharides extract from Asterina pectinifera on HT-29 human colon adenocarcinoma cells. *BMB Rep* 42, 277-280.

Nebert DW, Dalton TP, Okey AB & Gonzalez FJ (2004) Role of aryl hydrocarbon receptor-mediated induction of the CYP1 enzymes in environmental toxicity and cancer. *J Biol Chem* 279, 23847-23850.

Ostry V (2008) Alternaria mycotoxins: an overview of chemical characterization, producers, toxicity, analysis and occurrence in foodstuffs. *World Mycotoxin Journal* 1, 175-188.

Panigrahi S (1997) Alternaria toxins. In *Handbook of Plant and Fungal Toxicants*, pp. 319–337. Boca Raton FL: CRC Press.

Pero RW, Posner H, Blois M, Harvan D & Spalding JW (1973) Toxicity of metabolites produced by the "Alternaria". *Environ Health Perspect* 4, 87-94.

Pfaffl MW (2004) Real-time RT-PCR: Neue Ansätze zur exakten mRNA Quantifizierung. *BIOspektrum* 1, 92- 94.

Pfeiffer E, Burkhardt B, Altemoller M, Podlech J & Metzler M (2008) Activities of human recombinant cytochrome P450 isoforms and human hepatic microsomes for the hydroxylation of Alternaria toxins. *Mycotox Research* 24, 117-123.

Pfeiffer E, Eschbach S & Metzler M (2007a) Alternaria toxins: DNA strand-breaking activity in mammalian cells in vitro. *Mycotoxin Research* 23, 152-157.

Pfeiffer E, Schebb NH, Podlech J & Metzler M (2007b) Novel oxidative in vitro metabolites of the mycotoxins alternariol and alternariol methyl ether. *Mol Nutr Food Res* 51, 307-316.

Pfeiffer E, Schmidt C, Burkhardt B, Altemoller M, Podlech J & Metzler M (2009) Glucuronidation of the mycotoxins alternariol and alternariol-9-methyl ether in vitro: chemical structures of glucuronides and activities of human UDP-glucuronosyltransferase isoforms. *Mycotox Res* 25, 3-10.

Philip Wexler BA, Ann de Peyster, Shayne Gad, P.J. Hakkinen, Michael Kamrin, Betty Locey, Harihara Mehendale, Carey Pope, Lee Shugart (2005) *Encyclopedia of Toxicology*, 2nd ed: Elsevier Inc. .

Pickett CB, Telakowski-Hopkins CA, Argenbright L & Lu AY (1984) Regulation of glutathione S-transferase mRNAs by phenobarbital and 3-methylcholanthrene: analysis using cDNA probes. *Biochem Soc Trans* 12, 71-74.

Poland A & Knutson JC (1982) 2,3,7,8-tetrachlorodibenzo-p-dioxin and related halogenated aromatic hydrocarbons: examination of the mechanism of toxicity. *Annu Rev Pharmacol Toxicol* 22, 517-554.

Pollock G, DiSabatino C, Heimsch R & Coulombe R (1982) The distribution, elimination, and metabolism of 14C-alternariol monomethyl ether. *J Environ Sci Health B.* 17, 109-123.

Prevette LE, Mullen DG & Holl MM Polycation-induced cell membrane permeability does not enhance cellular uptake or expression efficiency of delivered DNA. *Mol Pharm* 7, 870-883.

Prochaska HJ & Talalay P (1988) Regulatory mechanisms of monofunctional and bifunctional anticarcinogenic enzyme inducers in murine liver. *Cancer Res* 48, 4776-4782.

Quiagen (2006) *RNeasy® Mini Handbook*, 4th ed: Quiagen.

Quiagen (2009a) *QuantiTect® Reverse Transcription Handbook*: Quiagen.

Quiagen (2009b) *QuantiTect® SYBR® Green PCR Handbook*: Quiagen.

Quiagen (2010) HiPerFect Transfection Reagent Handbook. In *Handbook*, pp. 72: Quiagen.

Raistrick H, Stickings CE & Thomas R (1953) Studies in the biochemistry of microorganisms. 90. Alternariol and alternariol monomethyl ether, metabolic products of Alternaria tenuis. *Biochem J* 55, 421-433.

Roberts EA, Johnson KC, Harper PA & Okey AB (1990) Characterization of the Ah receptor mediating aryl hydrocarbon hydroxylase induction in the human liver cell line Hep G2. *Arch Biochem Biophys* 276, 442-450.

Robertson IG, Guthenberg C, Mannervik B & Jernstrom B (1986) Differences in stereoselectivity and catalytic efficiency of three human glutathione transferases in the conjugation of glutathione with 7 beta,8 alpha-dihydroxy-9 alpha,10 alpha-oxy-7,8,9,10-tetrahydrobenzo(a)pyrene. *Cancer Res* 46, 2220-2224.

Roche (2008) PCR: Eine ausgezeichnete Methode.

Rowlands JC & Gustafsson JA (1997) Aryl hydrocarbon receptor-mediated signal transduction. *Crit Rev Toxicol* 27, 109-134.

Rushmore TH & Kong AN (2002) Pharmacogenomics, regulation and signaling pathways of phase I and II drug metabolizing enzymes. *Curr Drug Metab* 3, 481-490.

Sadek CM & Allen-Hoffmann BL (1994) Cytochrome P450IA1 is rapidly induced in normal human keratinocytes in the absence of xenobiotics. *J Biol Chem* 269, 16067-16074.

Sauer DB, Seitz LM, Burroughs R, Mohr HE, West JL, Milleret RJ & Anthony HD (1978) Toxicity of Alternaria metabolites found in weathered sorghum grain at harvest. *J Agric Food Chem* 26, 1380-1393.

Schäfer C (2006) Die Rolle des Arylhydrokarbon-Rezeptors in der UVB-induzierten Signaltransduktion, Heinrich-Heine-Universität Düsseldorf.

Schlichting I, Berendzen J, Chu K, Stock AM, Maves SA, Benson DE, Sweet RM, Ringe D, Petsko GA & Sligar SG (2000) The catalytic pathway of cytochrome p450cam at atomic resolution. *Science* 287, 1615-1622.

Schmidt JV, Su GH, Reddy JK, Simon MC & Bradfield CA (1996) Characterization of a murine Ahr null allele: involvement of the Ah receptor in hepatic growth and development. *Proc Natl Acad Sci U S A* 93, 6731-6736.

Schrader TJ, Cherry W, Soper K, Langlois I & Vijay HM (2001) Examination of Alternaria alternata mutagenicity and effects of nitrosylation using the Ames Salmonella test. *Teratog Carcinog Mutagen* 21, 261-274.

Schreck I, Deigendesch U, Burkhardt B, Marko D & Weiss C The Alternaria mycotoxins alternariol and alternariol methyl ether induce cytochrome P450 1A1 and apoptosis in murine hepatoma cells dependent on the aryl hydrocarbon receptor. *Arch Toxicol*.

Scott PM (2001) Analysis of agricultural commodities and foods for Alternaria mycotoxins. *J AOAC Int* 84, 1809-1817.

Scott PM KSR (2001) Stability of Alternaria toxins in fruit juices and wine. *Mycotoxin Research* 17.

Scripture CD, Sparreboom A & Figg WD (2005) Modulation of cytochrome P450 activity: implications for cancer therapy. *Lancet Oncol* 6, 780-789.

Serdani M. KJC, Andersen B., Crous P.W (2002) Characterisation of Alternaria species-groups associated with core rot of apples in South Africa. *Mycol. Res.* 106, 561±569.

Shan G RNA interference as a gene knockdown technique. *Int J Biochem Cell Biol* 42, 1243-1251.

Shimada T, Yamazaki H, Mimura M, Inui Y & Guengerich FP (1994) Interindividual variations in human liver cytochrome P-450 enzymes involved in the oxidation of drugs, carcinogens and toxic chemicals: studies with liver microsomes of 30 Japanese and 30 Caucasians. *J Pharmacol Exp Ther* 270, 414-423.

Siegel D, Feist M, Proske M, Koch M & Nehls I (2010) Degradation of the Alternaria mycotoxins alternariol, alternariol monomethyl ether, and altenuene upon bread baking. *J Agric Food Chem* 58, 9622-9630.

Skehan (1990) New Colorimetric Cytotoxicity Assay for Anticancer-Drug Screening. *Articles* 82, 1107- 1112.

Snowdon AL (1992) *Post-Harvest Diseases and Disorders of Fruits and Vegetables*. Boca Raton: FL: CRC Press.

Solfrizzo M, De Girolamo A, Vitti C, Visconti A & van den Bulk R (2004) Liquid chromatographic determination of Alternaria toxins in carrots. *J AOAC Int* 87, 101-106.

Sommer NF (1985) Role of controlled environments in suppression of postharvest diseases. *Can. J. Plant Pathol.* 7, 331-339.

Stack ME & Prival MJ (1986) Mutagenicity of the Alternaria metabolites altertoxins I, II, and III. *Appl Environ Microbiol* 52, 718-722.

Stejskalova L, Dvorak Z & Pavek P Endogenous and exogenous ligands of aryl hydrocarbon receptor: current state of art. *Curr Drug Metab* 12, 198-212.

Stryer L (2002) *Biochemistry*, 5th ed: W.H.Freeman & Co Ltd.

Talalay P, De Long MJ & Prochaska HJ (1988) Identification of a common chemical signal regulating the induction of enzymes that protect against chemical carcinogenesis. *Proc Natl Acad Sci U S A* 85, 8261-8265.

Tompkins LM & Wallace AD (2007) Mechanisms of cytochrome P450 induction. *J Biochem Mol Toxicol* 21, 176-181.

Volz N (2010) Beeinflussung ARE-regulierter Phase-II-Enzyme durch Kaffee und ausgewählte Inhaltsstoffe, Universität Karlsruhe (TH), Universität Wien.

Waller CL & McKinney JD (1995) Three-dimensional quantitative structure-activity relationships of dioxins and dioxin-like compounds: model validation and Ah receptor characterization. *Chem Res Toxicol* 8, 847-858.

Wang ZJ, Zhang Q & Zhao XH (2011) Induced-differentiation of two flavones and two flavonols on a human esophageal squamous cell carcinoma cell line (KYSE-510). *Journal of Medicinal Plants Research* 5, 15.

Werck-Reichhart D & Feyereisen R (2000) Cytochromes P450: a success story. *Genome Biol* 1, REVIEWS3003.

Wexler P, Anderson B, Peyster Ad, Gad S, Hakkinen PJ, Kamrin M, Locey B, Mehendale H, Pope C & Shugart L (2005) *Encyclopedia of Toxicology*, 2nd ed: Elsevier Inc. .

Whitelaw ML, Gottlicher M, Gustafsson JA & Poellinger L (1993) Definition of a novel ligand binding domain of a nuclear bHLH receptor: co-localization of ligand and hsp90 binding activities within the regulable inactivation domain of the dioxin receptor. *Embo J* 12, 4169-4179.

Whitlock JP, Jr. (1999) Induction of cytochrome P4501A1. *Annu Rev Pharmacol Toxicol* 39, 103-125.

Wiegand H, Boesch-Saadatmandi C, Regos I, Treutter D, Wolffram S & Rimbach G (2009) Effects of quercetin and catechin on hepatic glutathione-S transferase (GST), NAD(P)H quinone oxidoreductase 1 (NQO1), and antioxidant enzyme activity levels in rats. *Nutr Cancer* 61, 717-722.

Wilson CL & Safe S (1998) Mechanisms of ligand-induced aryl hydrocarbon receptor-mediated biochemical and toxic responses. *Toxicol Pathol* 26, 657-671.

Wollenhaupt K, Schneider F & Tiemann U (2008) Influence of alternariol (AOH) on regulator proteins of cap-dependent translation in porcine endometrial cells. *Toxicol Lett* 182, 57-62.

Xu C, Li CY & Kong AN (2005) Induction of phase I, II and III drug metabolism/transport by xenobiotics. *Arch Pharm Res* 28, 249-268.

Yanagida A, Sogawa K, Yasumoto KI & Fujii-Kuriyama Y (1990) A novel cis-acting DNA element required for a high level of inducible expression of the rat P-450c gene. *Mol Cell Biol* 10, 1470-1475.

Yekeler H, Bitmis K, Ozcelik N, Doymaz MZ & Calta M (2001) Analysis of toxic effects of Alternaria toxins on esophagus of mice by light and electron microscopy. *Toxicol Pathol* 29, 492-497.

Zhang H, Kolb FA, Jaskiewicz L, Westhof E & Filipowicz W (2004) Single processing center models for human Dicer and bacterial RNase III. *Cell* 118, 57-68.

Zhen YZ, Xu YM, Liu GT, Miao J, Xing YD, Zheng QL, Ma YF, Su T, Wang XL, Ruan LR & et al. (1991) Mutagenicity of Alternaria alternata and Penicillium cyclopium isolated from grains in an area of high incidence of oesophageal cancer--Linxian, China. *IARC Sci Publ*, 253-257.

Zhou J & Gasiewicz TA (2003) 3'-methoxy-4'-nitroflavone, a reported aryl hydrocarbon receptor antagonist, enhances Cyp1a1 transcription by a dioxin responsive element-dependent mechanism. *Arch Biochem Biophys* 416, 68-80.

8. Appendix

8.1. Curriculum Vitae

Personal Details

Name:	Katharina Anna Domnanich
Address:	Wolfganggasse 42-46/1/4/9, A- 1120 Vienna
Mobile:	0043-664/88 46 97 64
e- mail:	katharina.domnanich@gmx.at
Date & Place of birth:	04/08/1989, A- 7350 Oberpullendorf

Education & Qualification

1995- 1999:	Bilingual Primary School Hauptstraße 29, A- 7304 Nebersdorf
1999- 2003:	Bilingual Secondary Modern School Schulstraße 3, A- 7304 Großwarasdorf
2003- June 2008:	Secondary School of Chemical Technology Specialising in Analytical Chemistry- Environmental Technology Rosensteingasse 79, A- 1170 Vienna
Final year project:	Analysis of primers in the face of further forensic applications
September 2008- 2009:	BSc Medicinal Chemistry and Pharmaceutical Science Dublin Institute of Technology School of Chemical and Pharmaceutical Sciences, Kevin Street
BSc thesis:	Investigation of the Ozone formation potential of different fuels
October 2009- 2012:	MSc Chemistry University Vienna, Faculty for Chemistry Währinger Straße 42, A- 1090 Vienna
MSc thesis:	Impact of *Alternaria* toxins on CYP1A1- and GST- expression in human tumour cells

8.2. Abstract

The *Alternaria* toxins alternariol (AOH) and alternariol monomethyl ether (AME) are, according to the EFSA, on the list of mycotoxins with an urgent need for further investigations of toxicity, permitting a better risk assessment for man and animal. The consumption of *Alternaria spp*. contaminated grain is associated with increased incidences of oesophageal cancer in Linxian, China (Liu *et al.,* 1992). Fehr (2008) and Schreck *et al.* (2011) reported the induction of CYP1A1 by *Alternaria* toxins, leading to investigations addressing the role of the aryl hydrocarbon receptor (AhR) in AME- and AOH-mediated CYP1A1 induction in human oesophageal carcinoma cells (KYSE510).

The question whether mycotoxin-induced CYP1A1 mRNA levels were AhR-dependent was investigated by two different approaches. Firstly, oesophageal AhR knockdown cells were generated by RNAi technology and were used for studying the impact of *Alternaria* toxins on CYP1A1. Secondly, the Ah-receptor of KYSE510 cells was inhibited in a pre-treatment with 10 µM MNF prior the incubation with the *Alternaria* toxins.

AOH and AME significantly induced CYP1A1 in a concentration dependent manner in AhR-expressing cells (non-transfected and dsRNA-transfected (negative control) KYSE510) after 24 h of incubation. Any changes in CYP1A1 transcript levels were observed at low mycotoxin concentrations (≤ 0.1 µM), whereas at higher concentrations (≥ 1 µM) CYP1A1 induction peaked by 2.5-fold for AME and 8-fold for AOH. Similar results for both cell types suggested, that the transfection procedure did not influence the response of KYSE510 cells towards AME and AOH. In AhR-suppressed (AhR-siRNA transfected) KYSE510 cells, CYP1A1 levels were significantly reduced after AME- as well as AOH-treatment in comparison to control cells, supporting the AhR-dependence of CYP1A1 induction by both mycotoxins. At high concentrations (10 µM AME, 50 µM AOH), CYP1A1 transcripts plummeted below the endogenous level, giving rise to consider the interference of a putative, yet unknown pathway.

The results obtained with MNF-inhibited cells were generally in line with those of transiently siRNA-transfected KYSE510 cells, suggesting a crucial role of the Ah-receptor in AME-mediated CYP1A1 induction.

Glutathione-S-transferases (GST) are important phase II drug metabolising enzymes, bearing a considerable role in the detoxification of xenobiotics. After establishment and optimisation of the GST assay according to Habig *et al.* (1973), the impact of AME and AOH on GST activities in human colon carcinoma cells (HT29) was investigated. Only a marginal, yet significant increase in GST activity at high AOH concentrations (10 µM, 50 µM) was observed, suggesting a minor role of GST in the detoxification of both *Alternaria* toxins.

8.3. Zusammenfassung

Die *Alternaria* Toxine Alternariol (AOH) und Alternariolmonomethylether (AME) wurden von der EFSA auf die Liste der Mykotoxine gesetzt, die noch einer weitgehenden toxikologische Untersuchungen bedürfen, um eine bessere Risikobewertung für Mensch und Tier zu ermöglichen. Der Konsum von *Alternaria spp.* kontaminierten Getreide wurde in Linxian, China in Verbindung mit Ösophaguskarzinom gebracht. In bereits veröffentlichten Daten von Fehr (2008) und Schreck *et al.* (2011) wurde die Induktion von CYP1A1 durch *Alternaria* Toxine beschrieben, was zu weiteren Untersuchungen über die Rolle des Arylhydrocarbon Rezeptors (AhR) in der AME- und AOH-vermittelten CYP1A1 Induktion in humanen Ösophagus Karzinomzellen (KYSE510) veranlasste.

Die Frage, ob die Induktion von CYP1A1 mRNA durch Mykotoxine Ah-Rezeptor vermittelt abläuft, wurde in zwei verschiedene Ansätze geklärt. Zuerst wurden AhR-supprimierte Ösophagus Karzinomzellen mithilfe der RNAi Technologie generiert, die ein geeignetes Modell für die Untersuchung des Einfluss der *Alternaria* Toxine auf CYP1A1 Genexpression darstellten. Zweitens wurde der Ah-Rezeptor in KYSE510 Zellen durch eine Vorbehandlung mit 10 µM MNF inhibiert.

Die signifikante Induktion von CYP1A1 in AhR-exprimierenden Zellen (nicht-transfizierte und dsRNA-transfizierte (Negativkontrolle) KYSE510) nach 24 h war abhängig von der applizierten AME- und AOH-Konzentration. Keine Änderungen der CYP1A1 Transkripte wurden bei geringen Mykotoxinkonzentrationen (≤ 0.1 µM) beobachtet, wobei höhere Konzentrationen (≥ 1 µM) eine maximale, 2.5-fache Induktion für AME und eine 8-fache Induktion für AOH hervor riefen. Vergleichbare Ergebnisse in beiden Zelltypen lassen auf keinerlei Veränderungen durch die Transfektion der KYSE510, in Hinblick auf ihre Reaktion auf AME und AOH, schließen. In AhR-supprimierten (AhR-siRNA transfizierten) KYSE510 Zellen waren die CYP1A1 mRNA Level nach der Inkubation mit AME und AOH im Vergleich zu den Kontrollzellen signifikant erniedrigt, was für die AhR-Abhängigkeit der CYP1A1 Induktion spricht. Das Absinken der CYP1A1 Transkripte unterhalb das endogene Level bei hohen Konzentrationen (10 µM AME, 50 µM AOH) lässt auf die Interferenz eines bisher unbekannten Signalweges vermuten.

Die Ergebnisse die mithilfe MNF-inhibierter KYSE510 Zellen ermittelt wurden, sind generell in Einklang mit denen, die mit transient siRNA-transfizierten Zellen erzielt wurden und sprechen für eine entscheidende Rolle des Ah-Rezeptors in der AME-vermittelten CYP1A1 Induktion.

Glutathion-S-Transferasen (GST) gehören zu den Phase II Enzymen und tragen einen beachtlichen Anteil zur Detoxifizierung von Xenobiotika bei. Nach der Etablierung und Optimierung des GST Assays nach Habig *et al.* (1973), wurde der Einfluss von AME und AOH auf die GST Aktivitäten in humanen Kolonkarzinomzellen (HT29) untersucht. Ein marginaler, aber doch signifikant erhöhter Anstieg der GST Aktivität bei hohen AOH Konzentrationen (10 µM, 50 µM) lässt auf einen minimalen Beitrag dieser Enzyme in der Detoxifizierung beider *Alternaria* Toxine schließen.

8.4. Data

In the following all measurement values are listed, used for the representation of the graphs. The dates refer to the day the measurement was performed. The calculation of the cytotoxicity of AME determined in the SRB assay is described in chapter 6.2. “Sulforhodamine B (SRB) assay” in more detail. The measurement values are given in tables 16 & 17 and represented in figure 18. Calculations of CYP1A1 & AhR relative quantities and the GST-activities are described in chapter 6.4.5. “Real Time PCR” and chapter 6.6. “Glutathione-S-Transferase (GST) Enzyme Activity”, respectively. CYP1A1 and AhR relative quantity (RQ)-values are given in table 18 – 34 (represented in figure 19 – 32) and GST-activities are listed in table 35 – 52 (represented in figure 33 – 43). Outliers identified by the Nalimov outlier test are grey-shaded in the following tables.

Table 16: Absorbance-values determined in the SRB assay at λ = 570 nm in KYSE510-cells, cultivated for 72 h and treated with AME for 24 h.

P (passage) 12 (2011/03/17)	**DMSO**	**0.1µM AME**	**1µM AME**	**10µM AME**
A1	1.026	1.000	0.833	0.941
A2	1.121	0.861	0.959	1.024
A3	0.945	0.907	0.952	0.944
A4	1.054	0.676	0.809	0.717
A5	1.077	0.729	0.772	0.786
A6	1.141	0.998	0.896	1.019
A7	0.905	0.973	0.865	0.750
A8	0.954	0.768	0.867	0.778
P14 (2011/03/24)				
A1	1.641	1.302	1.473	1.473
A2	1.366	1.370	1.385	1.465
A3	1.394	1.450	1.473	1.439
A4	1.234	1.360	1.317	1.447
A5	1.463	1.475	1.265	1.378
A6	1.146	1.349	1.463	1.189
A7	1.139	1.491	0.094	1.085
A8	1.545	1.452	1.181	1.529
P16 (2011/05/05)				
A1	0.648	0.585	0.725	0.766
A2	0.746	0.778	0.749	0.756
A3	0.682	0.776	0.746	0.643
A4	0.664	0.711	0.720	0.676
A5	0.738	0.713	0.766	0.810
A6	0.708	0.642	0.742	0.787
A7	0.734	0.650	0.632	0.606
A8	0.647	0.788	0.783	0.783
P23 (2011/05/05)	**DMSO**	**0.1µM AME**	**1µM AME**	**10µM AME**
A1	1.148	1.176	1.036	0.859
A2	1.034	0.953	1.096	1.156
A3	1.063	1.148	1.127	0.568
A4	1.022	0.903	0.824	0.888
A5	1.064	1.138	1.080	0.957
A6	1.151	0.794	1.144	1.185
A7	1.093	0.886	1.044	0.968
A8	0.991	0.941	0.844	0.454

P23 (2011/07/25)	DMSO	0.1µM AME	1µM AME	10µM AME
A1	0.706	0.701	0.676	0.692
A2	0.773	0.711	0.741	0.683
A3	0.844	0.790	0.732	0.661
A4	0.848	0.750	0.787	0.655
A5	0.707	0.794	0.696	0.663
A6	0.812	0.869	0.754	0.711
A7	0.763	0.855	0.734	0.760
A8	0.726	0.747	0.645	0.621

Table 17: Arithmetic mean and standard deviation (SD) of absorbance-values in KYSE510-cells. The absorbance values are given in table 16, whereas the grey shaded outliers are not used for the calculation of the arithmetic mean, depicted in figure 18 as T/C [%].

	DMSO	0.1µM AME	1µM AME	10µM AME
T/C [%]	100	96.33	95.91	93.43
SD	8.05	11.99	10.06	14.65

Table 18: CYP1A1 and AhR relative quantities (RQ) in KYSE510-cells, cultivated for 24 h and treated with AME for 12 h. The RQ-values are depicted in figure 19 A.

	β-Actin	CYP1A1			
	C_T	C_T	Δ C_T	ΔΔ C_T	RQ
P 12 (2011/07/07)					
DMSO	16.38	24.85	8.47	0.00	1.00
0.1 µM AME	16.69	24.75	8.06	-0.41	1.33
1 µM AME	16.71	24.55	7.84	-0.63	1.55
10 µM AME	16.90	29.22	12.33	3.86	0.07
5 µM BaP	16.50	20.40	3.90	-4.57	23.81
	β-Actin	**AhR**			
	C_T	C_T	Δ C_T	ΔΔ C_T	RQ
P 12 (2011/07/07)					
DMSO	16.38	22.36	5.98	0.00	1.00
0.1 µM AME	16.69	22.54	5.84	-0.13	1.10
1 µM AME	16.71	22.61	5.90	-0.08	1.06
10 µM AME	16.90	22.87	5.97	0.00	1.00
5 µM BaP	16.50	22.48	5.98	0.00	1.00

Table 19: CYP1A1 and AhR relative quantities in KYSE510-cells, cultivated for 24 h and treated with AME for 6 h. The RQ-values are depicted in figure 19 B.

	β-Actin	CYP1A1			
	C_T	C_T	Δ C_T	ΔΔ C_T	RQ
P 8 (2011/05/26)					
DMSO	17.64	26.74	9.10	0.00	1.00
0.1 µM AME	18.78	27.68	8.90	-0.20	1.15
1 µM AME	16.70	28.18	11.48	2.38	0.19
10 µM AME	16.26	30.15	13.89	4.79	0.04
5 µM BaP	16.88	21.17	4.29	-4.81	28.04
	β-Actin	**AhR**			
	C_T	C_T	Δ C_T	ΔΔ C_T	RQ
P 8 (2011/05/26)					
DMSO	17.64	22.84	5.20	0.00	1.00
0.1 µM AME	18.78	24.23	5.45	0.25	0.84
1 µM AME	16.70	22.18	5.49	0.29	0.82
10 µM AME	16.26	21.99	5.73	0.53	0.69
5 µM BaP	16.88	22.38	5.50	0.30	0.81

Table 20: CYP1A1 and AhR relative quantities in KYSE510-cells, cultivated for 24 h and treated with AME for 24 h.

	β-Actin	CYP1A1			
	C_T	C_T	Δ C_T	ΔΔ C_T	RQ
P29_1 (2011/05/16)					
DMSO	19.84	28.07	8.22	0.00	1.00
0.1 µM AME	19.13	27.44	8.31	0.09	0.94
1 µM AME	18.76	27.02	8.27	0.04	0.97
10 µM AME	18.55	29.41	10.87	2.64	0.16
5 µM ARO	18.93	24.73	5.80	-2.42	5.37
P29_2 (2011/05/16)					
DMSO	18.37	27.20	8.83	0.00	1.00
0.1 µM AME	19.14	27.51	8.36	-0.47	1.38
1 µM AME	19.42	27.82	8.40	-0.43	1.35
10 µM AME	18.74	29.81	11.07	2.24	0.21
5 µM ARO	20.44	26.40	5.96	-2.87	7.29
P7 (2011/05/19)					
DMSO	16.55	24.98	8.44	0.00	1.00
0.1 µM AME	16.46	24.78	8.31	-0.12	1.09
1 µM AME	17.12	24.98	7.86	-0.57	1.48
10 µM AME	16.65	28.93	12.28	3.84	0.07
5 µM ARO	16.88	23.17	6.28	-2.15	4.45
5 µM BaP	17.64	21.44	3.80	-4.63	24.82
P8 (2011/05/26)					
DMSO	16.82	25.81	8.98	0.00	1.00
0.1 µM AME	16.96	25.96	9.00	0.01	0.99
1 µM AME	16.82	26.01	9.19	0.21	0.86
10 µM AME	17.05	28.51	11.46	2.48	0.18
5 µM BaP	16.95	19.54	2.59	-6.39	84.09
P31_1 (2011/09/05)					
DMSO	16.11	25.48	9.37	0.00	1.00
1 µM AME	15.97	24.87	8.90	-0.47	1.39
5µM BaP	16.46	20.44	3.98	-5.40	42.18
P31_2 (2011/09/05)					
DMSO	16.17	25.55	9.38	0.00	1.00
1 µM AME	16.14	25.27	9.13	-0.25	1.19
5µM BaP	16.01	19.91	3.90	-5.48	44.72
	β-Actin	**AhR**			
	C_T	C_T	Δ C_T	ΔΔ C_T	RQ
P 29_1 (2011/05/16)					
DMSO	19,84	24,19	4,35	0,00	1,00
0.1 µM AME	19,13	23,83	4,69	0,34	0,79
1 µM AME	18,76	23,66	4,90	0,56	0,68
10 µM AME	18,55	23,58	5,03	0,69	0,62
5 µM ARO	18,93	23,96	5,02	0,67	0,63
P29_2 (2011/05/16)					
DMSO	18,37	23,76	5,39	0,00	1,00
0.1 µM AME	19,14	23,82	4,67	-0,72	1,64
1 µM AME	19,42	24,32	4,89	-0,50	1,41
10 µM AME	18,74	23,92	5,18	-0,21	1,16
5 µM ARO	20,44	26,23	5,79	0,40	0,76
P7 (2011/05/19)					
DMSO	16,55	22,47	5,92	0,00	1,00
0.1 µM AME	16,46	22,63	6,16	0,24	0,84
1 µM AME	17,12	22,74	5,62	-0,30	1,23
10 µM AME	16,65	22,88	6,23	0,31	0,81
5 µM ARO	16,88	22,78	5,89	-0,03	1,02
5 µM BaP	17,64	22,84	5,20	-0,72	1,65
P8 (2011/05/26)					
DMSO	16,82	21,97	5,14	0,00	1,00
0.1 µM AME	16,96	22,13	5,17	0,02	0,98
1 µM AME	16,82	22,04	5,23	0,08	0,94
10 µM AME	17,05	22,60	5,56	0,41	0,75
5 µM BaP	16,95	21,63	4,68	-0,46	1,38

	β-Actin	AhR			
	C_T	C_T	Δ C_T	ΔΔ C_T	RQ
P31_1 (2011/09/05)					
DMSO	16,11	22,52	6,41	0,00	1,00
1 µM AME	15,97	22,42	6,45	0,04	0,97
5µM BaP	16,46	22,99	6,52	0,11	0,93
P31_2 (2011/09/05)					
DMSO	16,17	22,81	6,64	0,00	1,00
1 µM AME	16,14	22,92	6,78	0,14	0,91
5µM BaP	16,01	22,34	6,32	-0,32	1,25

Table 21: Arithmetic mean and SD of CYP1A1 and AhR relative quantities in KYSE510-cells after 24 h AME-treatment. The RQ-values are given in table 20, whereas the grey shaded outliers are not used for the calculation of the arithmetic mean RQ, depicted in figure 20.

	CYP1A1		AhR	
	mean RQ	SD	mean RQ	SD
DMSO	1.00	0.00	1.00	0.00
0.1µM AME	1.01	0.06	0.87	0.08
1µM AME	1.21	0.22	1.02	0.24
10µM AME	0.18	0.02	0.73	0.08
5µM ARO	5.70	1.19	0.80	0.16
5µM BaP	37.24	8.84	1.42	0.17

Table 22: CYP1A1 and AhR relative quantities in KYSE510-cells, cultivated for 24 h and treated with AOH for 24 h. The RQ-values are depicted in figure 21.

	β-Actin	CYP1A1			
	C_T	C_T	Δ C_T	ΔΔ C_T	RQ
P29 (2011/05/10)					
DMSO	19.07	28.38	9.31	0.00	1.00
0.1 µM AOH	17.92	25.48	7.56	-1.75	3.37
1 µM AOH	18.84	25.80	6.95	-2.36	5.13
10 µM AOH	18.70	29.08	10.38	1.07	0.48
50 µM AOH	18.98	31.82	12.84	3.53	0.09
5 µM ARO	18.46	23.79	5.33	-3.98	15.77
	β-Actin	**AhR**			
	C_T	C_T	Δ C_T	ΔΔ C_T	RQ
P29 (2011/05/10)					
DMSO	19.07	24.75	5.69	0.00	1.00
0.1 µM AOH	17.92	23.89	5.97	0.29	0.82
1 µM AOH	18.84	24.21	5.37	-0.32	1.25
10 µM AOH	18.70	24.52	5.82	0.13	0.91
50 µM AOH	18.98	24.85	5.87	0.19	0.88
5 µM ARO	18.46	24.05	5.59	-0.09	1.07

Table 23: CYP1A1 and AhR RQ in KYSE510-cells, cultivated for 48 h and treated with AME for 24 h.

	β-Actin	CYP1A1			
	C_T	C_T	Δ C_T	ΔΔ C_T	RQ
P 12 (2011/06/09)					
DMSO	19.46	30.41	10.94	0.00	1.00
0.1 µM AME	19.96	30.96	11.00	0.06	0.96
1 µM AME	19.54	29.15	9.61	-1.33	2.51
10 µM AME	19.42	30.92	11.50	0.55	0.68
5 µM BaP	19.55	20.63	1.09	-9.86	928.41
P 14 (2011/06/24)					
DMSO	16.90	26.20	9.30	0.00	1.00
0.1 µM AME	17.54	28.33	10.79	1.49	0.35
1 µM AME	16.80	24.98	8.19	-1.11	2.16
5 µM AME	17.00	27.22	10.22	0.92	0.53
10 µM AME	16.96	27.67	10.71	1.42	0.37
5 µM BaP	16.96	17.54	0.58	-8.72	420.52

	β-Actin	CYP1A1			
	C_T	C_T	Δ C_T	ΔΔ C_T	RQ
P 15 (2011/07/08)					
DMSO	16.81	26.16	9.35	0.00	1.00
0.1 µM AME	16.92	26.68	9.76	0.41	0.75
1 µM AME	16.89	25.19	8.30	-1.05	2.07
5 µM AME	16.95	26.71	9.76	0.41	0.75
10 µM AME	16.81	27.13	10.32	0.97	0.51
5 µM BaP	17.10	18.33	1.23	-8.12	278.25
P 20_1 (2011/07/25)					
DMSO	17.06	26.53	9.47	0.00	1.00
0.1 µM AME	16.95	26.38	9.43	-0.05	1.03
1 µM AME	16.94	25.14	8.20	-1.27	2.42
5 µM AME	17.04	27.08	10.04	0.56	0.68
10 µM AME	16.93	27.31	10.38	0.90	0.53
5 µM BaP	17.16	18.71	1.54	-7.93	243.89
P 20_2 (2011/08/02)					
DMSO	16.81	22.93	6.12	0.00	1.00
0.1 µM AME	16.96	23.14	6.18	0.07	0.95
1 µM AME	16.89	21.76	4.87	-1.25	2.38
5 µM AME	16.83	23.27	6.44	0.33	0.80
10 µM AME	16.61	23.24	6.63	0.52	0.70
5 µM BaP	16.91	14.85	-2.05	-8.17	288.11
	β-Actin	**AhR**			
	C_T	C_T	Δ C_T	ΔΔ C_T	RQ
P 12 (2011/06/20)					
DMSO	19.23	24.34	5.11	0.00	1.00
0.1 µM AME	19.87	24.64	4.77	-0.34	1.27
1 µM AME	19.32	24.40	5.08	-0.03	1.02
10 µM AME	19.18	24.17	4.99	-0.12	1.09
5 µM BaP	19.33	23.73	4.39	-0.72	1.65
P 14 (2011/06/27)					
DMSO	16.87	21.81	4.94	0.00	1.00
0.1 µM AME	17.52	22.49	4.98	0.04	0.97
1 µM AME	16.72	21.87	5.15	0.21	0.86
5 µM AME	16.87	21.95	5.07	0.14	0.91
10 µM AME	16.98	21.89	4.91	-0.03	1.02
5 µM BaP	17.00	21.04	4.03	-0.91	1.87
P 15 (2011/07/08)					
DMSO	16.99	22.32	5.33	0.00	1.00
0.1 µM AME	17.14	22.59	5.45	0.12	0.92
1 µM AME	17.09	22.42	5.33	0.00	1.00
5 µM AME	17.22	22.52	5.29	-0.04	1.03
10 µM AME	16.99	22.35	5.35	0.02	0.98
5 µM BaP	17.36	21.68	4.32	-1.01	2.01
P 20_1 (2011/08/03)					
DMSO	16.97	22.35	5.38	0.00	1.00
0.1 µM AME	16.85	22.42	5.57	0.19	0.88
1 µM AME	16.92	22.30	5.38	0.00	1.00
5 µM AME	17.01	22.39	5.37	-0.01	1.01
10 µM AME	16.84	22.21	5.37	-0.01	1.01
5 µM BaP	17.12	21.68	4.56	-0.82	1.76
P 20_2 (2011/08/03)					
DMSO	16.69	21.72	5.04	0.00	1.00
0.1 µM AME	16.91	21.71	4.80	-0.23	1.18
1 µM AME	16.80	21.67	4.86	-0.17	1.13
5 µM AME	16.85	21.64	4.79	-0.25	1.19
10 µM AME	16.58	21.53	4.96	-0.08	1.06
5 µM BaP	16.79	20.92	4.13	-0.91	1.88

Table 24: Arithmetic mean and SD of CYP1A1 and AhR relative quantities in KYSE510-cells after 24 h AME-treatment. The RQ-values are given in table 23, whereas the grey shaded outliers are not used for the calculation of the arithmetic mean RQ, depicted in figure 23.

	CYP1A1		AhR	
	mean RQ	**SD**	**mean RQ**	**SD**
DMSO	1.00	0.00	1.00	0.00
0.1µM AME	0.98	0.04	1.04	0.15
1µM AME	2.28	0.20	1.00	0.08
10µM AME	0.74	0.05	1.03	0.10
5µM ARO	0.61	0.08	1.03	0.04
5µM BaP	270.08	18.96	1.83	0.12

Table 25: CYP1A1 and AhR RQ in KYSE510-cells, cultivated for 48 h and treated with AOH for 24 h.

	β-Actin	CYP1A1			
	C_T	**C_T**	**Δ C_T**	**ΔΔ C_T**	**RQ**
P20_1 (2011/08/08)					
DMSO	16.37	26.06	9.69	0.00	1.00
0.1 µM AOH	16.50	24.95	8.45	-1.24	2.37
1 µM AOH	16.59	23.29	6.70	-2.99	7.95
10 µM AOH	16.89	24.15	7.26	-2.44	5.41
50 µM AOH	17.25	27.52	10.27	0.58	0.67
5 µM BaP	17.10	18.53	1.43	-8.26	306.38
P20_2 (2011/08/08)					
DMSO	16.80	26.63	9.83	0.00	1.00
0.1 µM AOH	16.79	25.26	8.47	-1.36	2.57
1 µM AOH	16.82	23.71	6.89	-2.94	7.68
10 µM AOH	17.06	24.78	7.72	-2.11	4.32
50 µM AOH	16.98	27.19	10.21	0.38	0.77
5 µM BaP	17.42	19.13	1.71	-8.13	279.19
P23 (2011/08/22)					
DMSO	16.57	27.55	10.98	0.00	1.00
0.1 µM AOH	16.52	27.51	10.99	0.01	0.99
1 µM AOH	16.68	24.33	7.65	-3.33	10.06
10 µM AOH	16.96	24.00	7.04	-3.94	15.37
50 µM AOH	16.68	26.11	9.43	-1.55	2.92
5 µM BaP	16.85	17.94	1.09	-9.89	947.27
P24_1 (2011/08/09)					
DMSO	17.13	28.54	11.41	0.00	1.00
0.1 µM AOH	17.68	28.34	10.66	-0.75	1.68
1 µM AOH	17.20	24.30	7.10	-4.31	19.78
10 µM AOH	17.22	25.13	7.91	-3.50	11.32
50 µM AOH	16.66	28.04	11.37	-0.04	1.03
5 µM BaP	17.25	18.41	1.16	-10.25	1214.41
P24_2 (2011/08/17)					
DMSO	17.44	28.38	10.93	0.00	1.00
0.1 µM AOH	17.36	27.74	10.38	-0.55	1.47
1 µM AOH	17.14	23.63	6.50	-4.44	21.65
5 µM AOH	17.31	23.75	6.45	-4.48	22.38
10 µM AOH	17.55	25.32	7.78	-3.16	8.92
5 µM BaP	17.57	18.37	0.80	-10.13	1119.61
P27 (2011/08/17)					
DMSO	16.83	26.20	9.37	0.00	1.00
0.1 µM AOH	16.88	25.05	8.18	-1.19	2.28
1 µM AOH	16.95	23.26	6.31	-3.05	8.31
10 µM AOH	16.72	23.65	6.93	-2.43	5.41
50 µM AOH	16.43	27.18	10.75	1.38	0.38
5 µM BaP	16.92	18.48	1.55	-7.82	225.34
P32 (2011/08/31)					
DMSO	16.90	26.68	9.78	0.00	1.00
0.1 µM AOH	16.93	25.06	8.13	-1.64	3.12
1 µM AOH	16.92	23.82	6.90	-2.88	7.34
10 µM AOH	17.03	27.33	10.31	0.53	0.69
50 µM AOH	16.69	28.12	11.42	1.65	0.32
5 µM BaP	17.03	18.52	1.49	-8.28	311.82

	β-Actin	AhR			
	C_T	C_T	Δ C_T	ΔΔ C_T	RQ
P31 (2011/09/02)					
DMSO	17.41	26.82	9.41	0.00	1.00
0.1 µM AOH	17.34	25.64	8.31	-1.11	2.16
1 µM AOH	17.48	24.90	7.43	-1.99	3.97
10 µM AOH	17.08	28.04	10.96	1.55	0.34
50 µM AOH	16.83	29.45	12.61	3.20	0.11
5 µM BaP	17.54	18.92	1.38	-8.03	261.83
P20_1 (2011/08/08)					
DMSO	16.37	21.95	5.58	0.00	1.00
0.1 µM AOH	16.50	22.09	5.59	0.01	0.99
1 µM AOH	16.59	22.12	5.53	-0.05	1.04
10 µM AOH	16.89	22.49	5.60	0.01	0.99
50 µM AOH	17.25	22.93	5.68	0.09	0.94
5 µM BaP	17.10	21.82	4.72	-0.86	1.82
P20_2 (2011/08/08)					
DMSO	16.80	22.45	5.65	0.00	1.00
0.1 µM AOH	16.79	22.32	5.54	-0.12	1.09
1 µM AOH	16.82	22.54	5.72	0.06	0.96
10 µM AOH	17.06	22.95	5.88	0.23	0.85
50 µM AOH	16.98	22.87	5.90	0.24	0.85
5 µM BaP	17.42	22.47	5.05	-0.61	1.52
P23 (2011/08/22)					
DMSO	16.57	22.37	5.80	0.00	1.00
0.1 µM AOH	16.52	22.65	6.13	0.33	0.80
1 µM AOH	16.68	22.92	6.24	0.44	0.74
10 µM AOH	16.96	22.41	5.45	-0.35	1.28
50 µM AOH	16.68	22.55	5.87	0.07	0.95
5 µM BaP	16.85	21.67	4.83	-0.97	1.96
P24_1 (2011/08/10)					
DMSO	17.01	21.91	4.90	0.00	1.00
0.1 µM AOH	17.58	22.53	4.95	0.05	0.97
1 µM AOH	17.11	21.94	4.83	-0.06	1.05
10 µM AOH	17.12	22.08	4.96	0.06	0.96
50 µM AOH	16.57	21.65	5.08	0.18	0.88
5 µM BaP	17.24	21.43	4.19	-0.71	1.64
P24_2 (2011/08/25)					
DMSO	17.54	22.73	5.20	0.00	1.00
0.1 µM AOH	17.34	22.70	5.37	0.17	0.89
1 µM AOH	17.25	22.53	5.28	0.08	0.95
5 µM AOH	17.31	22.53	5.23	0.03	0.98
10 µM AOH	17.61	22.80	5.19	-0.01	1.01
5 µM BaP	17.57	21.85	4.29	-0.91	1.88
P27 (2011/09/16)					
DMSO	16.79	21.84	5.05	0.00	1.00
0.1 µM AOH	16.81	21.77	4.96	-0.09	1.06
1 µM AOH	16.89	21.86	4.97	-0.08	1.06
10 µM AOH	16.60	21.96	5.36	0.31	0.81
50 µM AOH	16.29	21.67	5.38	0.33	0.79
5 µM BaP	16.89	21.11	4.23	-0.82	1.77
P32 (2011/09/13)					
DMSO	17.27	22.41	5.15	0.00	1.00
0.1 µM AOH	16.94	22.22	5.28	0.13	0.91
1 µM AOH	17.10	22.23	5.13	-0.02	1.02
10 µM AOH	17.20	22.73	5.53	0.38	0.77
50 µM AOH	16.79	22.06	5.27	0.12	0.92
5 µM BaP	17.16	21.66	4.50	-0.65	1.57
P31 (2011/09/06)					
DMSO	16.83	22.66	5.83	0.00	1.00
0.1 µM AOH	16.80	22.71	5.91	0.08	0.94
1 µM AOH	17.46	22.90	5.44	-0.38	1.30
10 µM AOH	16.64	22.96	6.32	0.49	0.71
50 µM AOH	16.35	22.45	6.10	0.27	0.83
5 µM BaP	17.00	22.10	5.09	-0.73	1.66

Table 26: Arithmetic mean and SD of CYP1A1 and AhR relative quantities in KYSE510-cells after 24 h AOH-treatment. The RQ-values are given in table 25, whereas the grey shaded outliers are not used for the calculation of the arithmetic mean RQ, depicted in figure 24.

	CYP1A1		AhR	
	mean RQ	**SD**	**mean RQ**	**SD**
DMSO	1.00	0.00	1.00	0.00
0.1 µM AOH	1.93	0.52	0.96	0.09
1 µM AOH	7.82	0.35	1.02	0.04
10 µM AOH	7.08	2.63	0.98	0.15
50 µM AOH	0.55	0.31	0.86	0.05
5 µM BaP	276.91	31.56	1.67	0.11

Table 27: CYP1A1 and AhR relative quantities in KYSE510-cells, transfected with siRNA 1 and siRNA 2, respectively for 48 h.

	β-Actin	**CYP1A1**			
	C_T	**C_T**	**Δ C_T**	**ΔΔ C_T**	**RQ**
P15 (2011/03/29)					
ds_RNA	19.74	30.40	10.66	0.00	1.00
si_RNA 1	24.29	34.06	9.77	-0.89	1.85
si_RNA 2	21.04	30.97	9.92	-0.74	1.67
P17 (2011/04/04)					
ds_RNA	18.93	29.23	10.30	0.00	1.00
si_RNA 1	19.15	28.97	9.82	-0.49	1.40
si_RNA 2	18.69	28.93	10.25	-0.06	1.04
P17_1 (2011/04/04)					
ds_RNA	18.65	29.32	10.67	0.00	1.00
si_RNA 2	18.27	28.55	10.28	-0.39	1.31
P17_2 (2011/04/04)					
ds_RNA	18.14	29.01	10.87	0.00	1.00
si_RNA 2	19.90	29.94	10.04	-0.83	1.78
	β-Actin	**AhR**			
	C_T	**C_T**	**Δ C_T**	**ΔΔ C_T**	**RQ**
P15 (2011/03/29)					
ds_RNA	19.74	24.93	5.19	0.00	1.00
si_RNA 1	24.29	29.44	5.15	-0.04	1.03
si_RNA 2	21.04	28.37	7.32	2.13	0.23
P17 (2011/04/04)					
ds_RNA	18.93	24.42	5.49	0.00	1.00
si_RNA 1	19.15	25.90	6.75	1.26	0.42
si_RNA 2	18.69	26.62	7.93	2.45	0.18
P17_1 (2011/04/04)					
ds_RNA	18.65	24.41	5.76	0.00	1.00
si_RNA 2	18.27	26.78	8.51	2.75	0.15
P17_2 (2011/04/04)					
ds_RNA	18.14	24.05	5.91	0.00	1.00
si_RNA 2	19.90	27.64	7.74	1.83	0.28

Table 28: Arithmetic mean and SD of CYP1A1 and AhR relative quantities in KYSE510-cells after 48 h of transfection with siRNA 1 and siRNA 2, respectively. The RQ-values are given in table 27 and the arithmetic mean RQ is depicted in figure 24.

	CYP1A1		AhR	
	mean RQ	**SD**	**mean RQ**	**SD**
ds_RNA	1.00	0.00	1.00	0.00
si_RNA1	1.63	0.23	0.72	0.31
si_RNA2	1.45	0.29	0.21	0.05

Table 29: CYP1A1 and AhR relative quantities in KYSE510-cells, transfected for 48 h with siRNA_2 and ds_RNA, respectively and treated with AME for 24 h. The calculation of the RQ of the blue shaded measurement values is performed with another, also blue shaded reference point.

	β-Actin	CYP1A1			
	C_T	C_T	Δ C_T	ΔΔ C_T	RQ
P22_1 (2011/05/02)					
ds_DMSO	19.82	31.10	11.28	0.00	1.00
ds_10 µM AME	20.65	28.86	8.22	-3.06	8.34
si_DMSO	18.19	28.12	9.93	0.00	1.00
si_0.1 µM AME	19.65	28.86	9.22	-0.71	1.64
si_1 µM AME	18.74	26.93	8.20	-1.73	3.32
si_5 µM AME	20.87	30.03	9.16	-0.77	1.70
si_10 µM AME	16.65	26.55	9.90	-0.03	1.02
P22_2 (2011/05/02)					
ds_DMSO	18.58	29.61	11.03	0.00	1.00
ds_10 µM AME	19.83	27.56	7.73	-3.31	9.89
si_DMSO	21.36	30.86	9.50	0.00	1.00
si_0.1 µM AME	20.94	29.91	8.97	-0.53	1.44
si_1 µM AME	19.51	27.09	7.58	-1.92	3.78
si_5 µM AME	21.58	30.12	8.53	-0.97	1.96
si_10 µM AME	23.67	33.23	9.55	0.05	0.96
P24_1 (2011/05/18)					
ds_DMSO	17.57	27.92	10.35	0.00	1.00
ds_10 µM AME	17.09	25.89	8.80	-1.56	2.94
si_DMSO	17.34	26.55	9.21	0.00	1.00
si_0.1 µM AME	17.41	26.02	8.61	-0.60	1.52
si_1 µM AME	16.84	25.24	8.40	-0.81	1.75
si_5 µM AME	17.69	27.41	9.72	0.51	0.70
si_10 µM AME	16.73	26.95	10.22	1.01	0.50
P24_2 (2011/07/05)					
ds_DMSO	16.99	27.15	10.16	0.00	1.00
ds_10 µM AME	16.83	25.72	8.89	-1.27	2.41
si_DMSO	16.86	26.42	9.57	0.00	1.00
si_0.1 µM AME	17.30	26.84	9.55	-0.02	1.01
si_1 µM AME	16.75	25.64	8.89	-0.68	1.60
si_5 µM AME	16.88	27.53	10.65	1.08	0.47
si_10 µM AME	16.95	27.81	10.86	1.29	0.41
P 12 (2011/06/09)					
DMSO	19.46	30.41	10.94	0.00	1.00
0.1 µM AME	19.96	30.96	11.00	0.06	0.96
1 µM AME	19.54	29.15	9.61	-1.33	2.51
10 µM AME	19.42	30.92	11.50	0.55	0.68
5 µM BaP	19.55	20.63	1.09	-9.86	928.41
ds_DMSO	18.23	29.12	10.89	0.00	1.00
ds_0.1 µM AME	18.65	29.83	11.19	0.30	0.81
ds_1 µM AME	18.67	28.31	9.64	-1.25	2.37
P 12 (2011/06/09)					
ds_10 µM AME	19.07	30.37	11.30	0.41	0.75
ds_5 µM BaP	19.35	20.67	1.32	-9.57	757.95
si_DMSO	18.41	28.27	9.87	0.00	1.00
si_0.1 µM AME	18.50	27.98	9.48	-0.39	1.31
si_1 µM AME	18.88	28.28	9.40	-0.47	1.38
si_10 µM AME	18.34	32.90	14.56	4.69	0.04
si_5 µM BaP	19.36	22.77	3.42	-6.45	87.20
P 14 (2011/06/24)					
DMSO	16.90	26.20	9.30	0.00	1.00
0.1 µM AME	17.54	28.33	10.79	1.49	0.35
1 µM AME	16.80	24.98	8.19	-1.11	2.16
5 µM AME	17.00	27.22	10.22	0.92	0.53
10 µM AME	16.96	27.67	10.71	1.42	0.37
5 µM BaP	16.96	17.54	0.58	-8.72	420.52

	β-Actin	CYP1A1			
P 14 (2011/06/24)	**C_T**	**C_T**	**Δ C_T**	**ΔΔ C_T**	**RQ**
ds_DMSO	16.96	26.37	9.40	0.00	1.00
ds_0.1 µM AME	17.51	27.71	10.21	0.80	0.57
ds_1 µM AME	17.06	25.15	8.09	-1.32	2.49
ds_5 µM AME	16.94	26.53	9.59	0.19	0.88
ds_10 µM AME	17.39	27.60	10.20	0.80	0.57
ds_5 µM BaP	17.29	18.08	0.79	-8.61	392.04
si_DMSO	16.31	25.46	9.15	0.00	1.00
si_0.1 µM AME	17.42	26.35	8.93	-0.21	1.16
si_1 µM AME	16.90	25.45	8.55	-0.60	1.51
si_5 µM AME	16.80	27.83	11.03	1.88	0.27
si_10 µM AME	16.85	29.75	12.90	3.75	0.07
si_5 µM BaP	17.02	20.47	3.45	-5.70	52.06
P12 (2011/06/30)					
ds_DMSO	17.26	28.22	10.95	0.00	1.00
ds_0.05 µM AME	17.20	28.49	11.29	0.33	0.79
ds_1 µM AME	17.55	26.31	8.75	-2.20	4.59
ds_5 µM AME	16.82	26.45	9.63	-1.32	2.50
ds_5 µM BaP	17.11	18.73	1.62	-9.33	643.02
si_DMSO	16.20	26.12	9.92	0.00	1.00
si_0.05 µM AME	16.37	26.03	9.66	-0.25	1.19
si_1 µM AME	16.94	26.12	9.18	-0.74	1.67
si_5 µM AME	17.01	27.93	10.92	1.00	0.50
si_5 µM BaP	16.46	20.20	3.74	-6.17	72.17
P13 (2011/06/30)					
ds_DMSO	16.75	26.95	10.20	0.00	1.00
ds_0.05 µM AME	16.83	27.28	10.45	0.25	0.84
ds_1 µM AME	17.41	25.95	8.54	-1.66	3.15
ds_5 µM AME	16.92	26.59	9.67	-0.53	1.44
P13 (2011/06/30)					
ds_5 µM BaP	16.98	18.41	1.44	-8.76	434.01
si_DMSO	16.41	25.92	9.50	0.00	1.00
si_0.05 µM AME	16.43	25.86	9.42	-0.08	1.06
si_1 µM AME	17.33	26.48	9.15	-0.35	1.27
si_5 µM AME	16.87	27.83	10.96	1.46	0.36
si_5 µM BaP	16.84	20.45	3.60	-5.90	59.61
P15 (2011/07/08)					
DMSO	16.81	26.16	9.35	0.00	1.00
0.1 µM AME	16.92	26.68	9.76	0.41	0.75
1 µM AME	16.89	25.19	8.30	-1.05	2.07
5 µM AME	16.95	26.71	9.76	0.41	0.75
10 µM AME	16.81	27.13	10.32	0.97	0.51
5 µM BaP	17.10	18.33	1.23	-8.12	278.25
ds_DMSO	16.71	26.13	9.43	0.00	1.00
ds_0.1 µM AME	16.71	26.55	9.84	0.41	0.75
ds_1 µM AME	16.94	25.12	8.17	-1.25	2.38
ds_5 µM AME	16.87	26.12	9.25	-0.18	1.13
ds_10 µM AME	16.95	26.98	10.04	0.61	0.66
ds_5 µM BaP	17.55	18.95	1.40	-8.03	261.45
si_DMSO	16.42	25.78	9.35	0.00	1.00
si_0.1 µM AME	16.38	25.63	9.25	-0.10	1.07
si_1 µM AME	16.31	25.35	9.04	-0.31	1.24
si_5 µM AME	17.33	27.29	9.96	0.61	0.65
si_10 µM AME	16.23	28.95	12.72	3.37	0.10
si_5 µM BaP	16.83	20.50	3.67	-5.68	51.19
P 20_1 (2011/07/25)					
DMSO	17.06	26.53	9.47	0.00	1.00
0.1 µM AME	16.95	26.38	9.43	-0.05	1.03
1 µM AME	16.94	25.14	8.20	-1.27	2.42
5 µM AME	17.04	27.08	10.04	0.56	0.68
10 µM AME	16.93	27.31	10.38	0.90	0.53
5 µM BaP	17.16	18.71	1.54	-7.93	243.89

	β-Actin	CYP1A1			
	C_T	C_T	Δ C_T	ΔΔ C_T	RQ
ds_DMSO	16.94	26.51	9.57	0.00	1.00
ds_0.1 µM AME	17.16	26.59	9.43	-0.14	1.10
ds_1 µM AME	17.22	25.44	8.21	-1.36	2.56
ds_5 µM AME	16.67	26.07	9.40	-0.17	1.12
ds_10 µM AME	16.93	26.92	9.99	0.42	0.75
ds_DMSO	16.92	26.64	9.72	0.00	1.00
ds_5 µM BaP	17.00	18.87	1.87	-7.85	230.23
si_DMSO	16.29	25.51	9.22	0.00	1.00
si_0.1 µM AME	16.37	25.12	8.75	-0.47	1.39
si_1 µM AME	16.37	25.67	9.30	0.08	0.94
P 20_1 (2011/07/25)					
si_5 µM AME	16.62	27.94	11.32	2.10	0.23
si_10 µM AME	16.56	30.15	13.59	4.37	0.05
si_5 µM BaP	16.76	20.91	4.16	-5.06	33.40
P 20_2 (2011/08/02)					
DMSO	16.81	22.93	6.12	0.00	1.00
0.1 µM AME	16.96	23.14	6.18	0.07	0.95
1 µM AME	16.89	21.76	4.87	-1.25	2.38
5 µM AME	16.83	23.27	6.44	0.33	0.80
10 µM AME	16.61	23.24	6.63	0.52	0.70
5 µM BaP	16.91	14.85	-2.05	-8.17	288.11
ds_DMSO	16.69	22.76	6.08	0.00	1.00
ds_0.1 µM AME	16.74	22.78	6.04	-0.04	1.03
ds_1 µM AME	16.77	21.34	4.57	-1.51	2.84
ds_5 µM AME	16.88	23.15	6.27	0.19	0.87
ds_10 µM AME	16.60	23.11	6.51	0.43	0.74
ds_5 µM BaP	16.80	15.23	-1.58	-7.65	201.26
si_DMSO	16.40	22.45	6.04	0.00	1.00
si_0.1 µM AME	16.17	21.86	5.70	-0.35	1.27
si_1 µM AME	16.23	21.84	5.61	-0.44	1.35
si_5 µM AME	16.37	24.67	8.30	2.26	0.21
si_10 µM AME	16.25	25.89	9.64	3.60	0.08
si_5 µM BaP	16.93	17.54	0.61	-5.44	43.27
	β-Actin	**AhR**			
	C_T	C_T	Δ C_T	ΔΔ C_T	RQ
P22_1 (2011/05/02)					
ds_DMSO	19.82	24.92	5.09	0.00	1.00
ds_10 µM AME	20.65	25.85	5.20	0.11	0.93
si_DMSO	18.19	25.71	7.52	0.00	1.00
si_0.1 µM AME	19.65	27.38	7.74	0.22	0.86
si_1 µM AME	18.74	26.62	7.89	0.37	0.77
si_5 µM AME	20.87	28.39	7.52	0.00	1.00
si_10 µM AME	16.65	24.86	8.21	0.69	0.62
P22_2 (2011/05/02)					
ds_DMSO	18.58	23.31	4.74	0.00	1.00
ds_10 µM AME	19.83	24.54	4.71	-0.03	1.02
si_DMSO	21.36	28.07	6.71	0.00	1.00
si_0.1 µM AME	20.94	28.04	7.10	0.39	0.76
si_1 µM AME	19.51	25.94	6.43	-0.28	1.21
si_5 µM AME	21.58	28.94	7.36	0.65	0.64
si_10 µM AME	23.67	30.98	7.31	0.60	0.66
P24_1 (2011/05/18)					
ds_DMSO	17.57	22.26	4.69	0.00	1.00
ds_10 µM AME	17.09	22.12	5.03	0.34	0.79
si_DMSO	17.34	24.41	7.07	0.00	1.00
si_0.1 µM AME	17.41	24.40	6.99	-0.08	1.06
si_1 µM AME	16.84	23.79	6.95	-0.12	1.09
si_5 µM AME	17.69	24.62	6.93	-0.14	1.10
si_10 µM AME	16.73	24.04	7.31	0.24	0.85

	β-Actin	AhR			
	C_T	C_T	Δ C_T	ΔΔ C_T	RQ
P24_2 (2011/07/05)					
ds_DMSO	16.99	22.57	5.58	0.00	1.00
ds_10 µM AME	16.83	22.35	5.53	-0.05	1.04
si_DMSO	16.86	24.62	7.77	0.00	1.00
si_0.1 µM AME	17.30	24.81	7.52	-0.25	1.19
si_1 µM AME	16.75	24.50	7.75	-0.01	1.01
si_5 µM AME	16.88	24.81	7.93	0.16	0.89
si_10 µM AME	16.95	24.71	7.76	0.00	1.00
P 12 (2011/06/20)					
DMSO	19.23	24.34	5.11	0.00	1.00
0.1 µM AME	19.87	24.64	4.77	-0.34	1.27
1 µM AME	19.32	24.40	5.08	-0.03	1.02
10 µM AME	19.18	24.17	4.99	-0.12	1.09
5 µM BaP	19.33	23.73	4.39	-0.72	1.65
ds_DMSO	18.02	23.27	5.25	0.00	1.00
ds_0.1 µM AME	18.42	23.90	5.48	0.23	0.85
ds_1 µM AME	18.56	23.92	5.36	0.11	0.93
ds_10 µM AME	19.02	24.44	5.42	0.16	0.89
ds_5 µM BaP	19.24	23.86	4.61	-0.64	1.56
si_DMSO	18.29	26.41	8.11	0.00	1.00
si_0.1 µM AME	18.41	26.69	8.28	0.17	0.89
si_1 µM AME	18.70	26.81	8.11	0.00	1.00
si_10 µM AME	18.15	26.85	8.71	0.59	0.66
si_5 µM BaP	19.21	26.70	7.49	-0.63	1.54
P 14 (2011/06/27)					
DMSO	16.87	21.81	4.94	0.00	1.00
0.1 µM AME	17.52	22.49	4.98	0.04	0.97
1 µM AME	16.72	21.87	5.15	0.21	0.86
5 µM AME	16.87	21.95	5.07	0.14	0.91
10 µM AME	16.98	21.89	4.91	-0.03	1.02
5 µM BaP	17.00	21.04	4.03	-0.91	1.87
ds_DMSO	16.94	22.14	5.19	0.00	1.00
ds_0.1 µM AME	17.56	22.84	5.28	0.08	0.94
ds_1 µM AME	17.04	22.24	5.20	0.00	1.00
ds_5 µM AME	16.90	22.05	5.15	-0.04	1.03
P 14 (2011/06/27)					
ds_10 µM AME	17.35	22.58	5.23	0.04	0.97
ds_5 µM BaP	17.27	21.59	4.32	-0.88	1.83
si_DMSO	16.31	24.20	7.89	0.00	1.00
si_0.1 µM AME	17.34	25.42	8.08	0.20	0.87
si_1 µM AME	16.79	24.72	7.93	0.04	0.97
si_5 µM AME	16.70	24.73	8.03	0.14	0.91
si_10 µM AME	16.70	24.89	8.19	0.31	0.81
si_5 µM BaP	17.08	24.68	7.60	-0.28	1.22
P12 (2011/06/30)					
ds_DMSO	17.26	22.09	4.83	0.00	1.00
ds_0.05 µM AME	17.20	22.59	5.39	0.56	0.68
ds_1 µM AME	17.55	22.71	5.16	0.33	0.80
ds_5 µM AME	16.82	21.90	5.09	0.26	0.84
ds_5 µM BaP	17.11	21.46	4.35	-0.48	1.39
si_DMSO	16.20	24.48	8.28	0.00	1.00
si_0.05 µM AME	16.37	24.31	7.95	-0.33	1.26
si_1 µM AME	16.94	25.06	8.12	-0.16	1.11
si_5 µM AME	17.01	24.49	7.48	-0.80	1.74
si_5 µM BaP	16.46	23.81	7.36	-0.92	1.89

	β-Actin	AhR			
	C_T	C_T	Δ C_T	ΔΔ C_T	RQ
P13 (2011/06/30)					
ds_DMSO	16.75	22.24	5.49	0.00	1.00
ds_0.05 µM AME	16.83	22.58	5.74	0.25	0.84
ds_1 µM AME	17.41	22.75	5.34	-0.15	1.11
ds_5 µM AME	16.92	22.27	5.35	-0.14	1.11
ds_5 µM BaP	16.98	21.77	4.79	-0.70	1.62
si_DMSO	16.41	24.60	8.19	0.00	1.00
si_0.05 µM AME	16.43	24.01	7.58	-0.61	1.53
si_1 µM AME	17.33	25.30	7.97	-0.22	1.17
si_5 µM AME	16.87	24.61	7.74	-0.45	1.37
si_5 µM BaP	16.84	24.07	7.23	-0.96	1.95
P15 (2011/07/08)					
DMSO	16.99	22.32	5.33	0.00	1.00
0.1 µM AME	17.14	22.59	5.45	0.12	0.92
1 µM AME	17.09	22.42	5.33	0.00	1.00
5 µM AME	17.22	22.52	5.29	-0.04	1.03
10 µM AME	16.99	22.35	5.35	0.02	0.98
5 µM BaP	17.36	21.68	4.32	-1.01	2.01
ds_DMSO	16.90	22.43	5.53	0.00	1.00
ds_0.1 µM AME	16.96	22.49	5.53	0.00	1.00
ds_1 µM AME	17.13	22.56	5.43	-0.10	1.07
ds_5 µM AME	17.08	22.48	5.40	-0.13	1.10
ds_10 µM AME	17.17	22.62	5.45	-0.08	1.06
P15 (2011/07/08)					
ds_5 µM BaP	17.75	22.30	4.55	-0.98	1.97
si_DMSO	16.61	24.89	8.29	0.00	1.00
si_0.1 µM AME	16.64	24.71	8.07	-0.22	1.17
si_1 µM AME	16.53	24.62	8.10	-0.19	1.14
si_5 µM AME	17.63	25.88	8.25	-0.04	1.03
si_10 µM AME	16.53	24.90	8.37	0.08	0.95
si_5 µM BaP	17.08	24.48	7.40	-0.89	1.85
P 20_1 (2011/08/08)					
DMSO	16.97	22.35	5.38	0.00	1.00
0.1 µM AME	16.85	22.42	5.57	0.19	0.88
1 µM AME	16.92	22.30	5.38	0.00	1.00
5 µM AME	17.01	22.39	5.37	-0.01	1.01
10 µM AME	16.84	22.21	5.37	-0.01	1.01
5 µM BaP	17.12	21.68	4.56	-0.82	1.76
ds_DMSO	16.85	22.62	5.77	0.00	1.00
ds_0.1 µM AME	17.05	22.77	5.72	-0.05	1.03
ds_1 µM AME	16.13	22.88	6.75	0.98	0.51
ds_5 µM AME	16.56	22.27	5.71	-0.06	1.04
ds_10 µM AME	16.77	22.70	5.93	0.16	0.89
ds_5 µM BaP	16.94	21.92	4.98	-0.79	1.72
si_DMSO	16.21	24.24	8.03	0.00	1.00
si_0.1 µM AME	16.22	24.22	8.00	-0.03	1.02
si_1 µM AME	16.25	24.57	8.32	0.29	0.82
si_5 µM AME	16.50	24.92	8.42	0.38	0.77
si_5 µM BaP	16.63	24.66	8.03	-0.01	1.00
si_DMSO	16.27	25.78	9.51	0.00	1.00
si_10 µM AME	16.55	30.25	13.70	4.19	0.05
P 20_2 (2011/08/03)					
DMSO	16.69	21.72	5.04	0.00	1.00
0.1 µM AME	16.91	21.71	4.80	-0.23	1.18
1 µM AME	16.80	21.67	4.86	-0.17	1.13
5 µM AME	16.85	21.64	4.79	-0.25	1.19
10 µM AME	16.58	21.53	4.96	-0.08	1.06
5 µM BaP	16.79	20.92	4.13	-0.91	1.88

	β-Actin	AhR			
	C_T	C_T	Δ C_T	ΔΔ C_T	RQ
ds_DMSO	16.67	21.57	4.90	0.00	1.00
ds_0.1 µM AME	16.69	21.75	5.07	0.17	0.89
ds_1 µM AME	16.69	21.49	4.80	-0.10	1.07
ds_5 µM AME	16.87	21.67	4.80	-0.11	1.08
ds_10 µM AME	16.55	21.65	5.10	0.20	0.87
ds_5 µM BaP	16.81	21.21	4.39	-0.51	1.42
si_DMSO	16.42	23.91	7.49	0.00	1.00
si_0.1 µM AME	16.21	23.81	7.60	0.11	0.93
P 20_2 (2011/08/03)					
si_1 µM AME	16.11	23.82	7.70	0.21	0.86
si_5 µM AME	16.39	24.16	7.77	0.28	0.82
si_10 µM AME	16.17	23.98	7.81	0.32	0.80
si_5 µM BaP	16.93	24.07	7.14	-0.35	1.27

Table 30: Arithmetic mean and SD of CYP1A1 and AhR relative quantities in KYSE510-cells 48 h post-transfection and after 24 h AME-treatment. The RQ-values are given in table 29, whereas the grey shaded outliers are not used for the calculation of the arithmetic mean RQ, depicted in figure 28 A, 29 A and 30.

	CYP1A1					
	non-transfected		ds_RNA		si_RNA	
	mean RQ	SD	mean RQ	SD	mean RQ	SD
DMSO	1.00	0.00	1.00	0.00	1.00	0.00
0.1µM AME	0.98	0.04	0.71	0.10	1.25	0.16
1µM AME	2.28	0.20	2.45	0.08	1.39	0.13
5µM AME	0.74	0.05	1.00	0.13	0.42	0.19
10µM AME	0.61	0.08	0.72	0.04	0.07	0.02
5µM BaP	270.08	18.96	297.42	97.95	54.29	3.78
	AhR					
	non-transfected		ds_RNA		si_RNA	
	mean RQ	SD	mean RQ	SD	mean RQ	SD
DMSO	1.00	0.00	1.00	0.00	1.00	0.00
0.1µM AME	1.04	0.15	0.94	0.07	1.02	0.12
1µM AME	1.00	0.08	1.04	0.21	1.01	0.13
5µM AME	1.03	0.10	1.07	0.03	0.98	0.20
10µM AME	1.03	0.04	0.93	0.07	0.83	0.12
5µM BaP	1.83	0.12	1.69	0.18	1.47	0.34

Table 31: CYP1A1 and AhR relative quantities in KYSE510-cells, transfected for 48 h with siRNA_2 and ds_RNA, respectively and treated with AOH for 24 h.

	β-Actin	CYP1A1			
	C_T	C_T	Δ C_T	ΔΔ C_T	RQ
P20_1 (2011/08/08)					
DMSO	16.37	26.06	9.69	0.00	1.00
0.1 µM AOH	16.50	24.95	8.45	-1.24	2.37
1 µM AOH	16.59	23.29	6.70	-2.99	7.95
10 µM AOH	16.89	24.15	7.26	-2.44	5.41
50 µM AOH	17.25	27.52	10.27	0.58	0.67
5 µM BaP	17.10	18.53	1.43	-8.26	306.38
P20_2 (2011/08/08)					
DMSO	16.80	26.63	9.83	0.00	1.00
0.1 µM AOH	16.79	25.26	8.47	-1.36	2.57
1 µM AOH	16.82	23.71	6.89	-2.94	7.68
10 µM AOH	17.06	24.78	7.72	-2.11	4.32
50 µM AOH	16.98	27.19	10.21	0.38	0.77
5 µM BaP	17.42	19.13	1.71	-8.13	279.19
P23 (2011/08/22)					
DMSO	16.57	27.55	10.98	0.00	1.00
0.1 µM AOH	16.52	27.51	10.99	0.01	0.99
1 µM AOH	16.68	24.33	7.65	-3.33	10.06
10 µM AOH	16.96	24.00	7.04	-3.94	15.37
50 µM AOH	16.68	26.11	9.43	-1.55	2.92
5 µM BaP	16.85	17.94	1.09	-9.89	947.27

	β-Actin	CYP1A1			
	C_T	C_T	Δ C_T	ΔΔ C_T	RQ
P24_1 (2011/08/09)					
DMSO	17.13	28.54	11.41	0.00	1.00
0.1 µM AOH	17.68	28.34	10.66	-0.75	1.68
1 µM AOH	17.20	24.30	7.10	-4.31	19.78
10 µM AOH	17.22	25.13	7.91	-3.50	11.32
50 µM AOH	16.66	28.04	11.37	-0.04	1.03
5 µM BaP	17.25	18.41	1.16	-10.25	1214.41
ds_DMSO	17.12	28.37	11.25	0.00	1.00
ds_0.1 µM AOH	17.69	28.05	10.36	-0.89	1.86
ds_1 µM AOH	17.30	24.21	6.90	-4.35	20.37
ds_10 µM AOH	17.02	25.26	8.24	-3.01	8.07
ds_50 µM AOH	16.40	28.42	12.02	0.77	0.59
ds_5 µM BaP	17.26	18.54	1.28	-9.97	1001.58
si_DMSO	16.89	26.79	9.90	0.00	1.00
si_0.1 µM AOH	16.71	25.92	9.21	-0.69	1.61
si_1 µM AOH	16.86	24.72	7.86	-2.04	4.11
si_10 µM AOH	16.79	27.58	10.79	0.89	0.54
si_50 µM AOH	16.57	31.07	14.50	4.60	0.04
si_5 µM BaP	17.02	20.62	3.61	-6.29	78.43
P24_2 (2011/08/17)					
DMSO	17.44	28.38	10.93	0.00	1.00
0.1 µM AOH	17.36	27.74	10.38	-0.55	1.47
1 µM AOH	17.14	23.63	6.50	-4.44	21.65
5 µM AOH	17.31	23.75	6.45	-4.48	22.38
10 µM AOH	17.55	25.32	7.78	-3.16	8.92
5 µM BaP	17.57	18.37	0.80	-10.13	1119.61
ds_DMSO	16.92	27.66	10.74	0.00	1.00
ds_0.1 µM AOH	16.92	26.79	9.87	-0.87	1.83
ds_1 µM AOH	16.98	23.24	6.26	-4.48	22.29
ds_5 µM AOH	17.20	23.64	6.44	-4.30	19.69
ds_10 µM AOH	16.87	24.67	7.81	-2.94	7.65
ds_5 µM BaP	17.26	18.39	1.13	-9.61	782.27
si_DMSO	16.61	26.28	9.67	0.00	1.00
si_0.1 µM AOH	16.66	25.40	8.74	-0.94	1.91
si_1 µM AOH	16.56	24.01	7.45	-2.22	4.66
si_5 µM AOH	16.41	25.18	8.77	-0.90	1.87
si_10 µM AOH	16.39	26.87	10.47	0.80	0.57
si_5 µM BaP	17.26	20.93	3.68	-6.00	63.94
P27 (2011/08/17)					
DMSO	16.83	26.20	9.37	0.00	1.00
0.1 µM AOH	16.88	25.05	8.18	-1.19	2.28
1 µM AOH	16.95	23.26	6.31	-3.05	8.31
10 µM AOH	16.72	23.65	6.93	-2.43	5.41
50 µM AOH	16.43	27.18	10.75	1.38	0.38
5 µM BaP	16.92	18.48	1.55	-7.82	225.34
ds_DMSO	16.70	26.05	9.35	0.00	1.00
ds_0.1 µM AOH	16.60	24.63	8.03	-1.31	2.49
ds_1 µM AOH	16.74	22.93	6.20	-3.15	8.88
ds_10 µM AOH	16.65	23.75	7.10	-2.25	4.74
ds_50 µM AOH	16.22	27.58	11.36	2.01	0.25
ds_5 µM BaP	16.91	18.79	1.88	-7.47	177.13
si_DMSO	16.44	25.81	9.36	0.00	1.00
si_0.1 µM AOH	16.68	25.02	8.34	-1.02	2.03
si_1 µM AOH	16.48	23.83	7.35	-2.02	4.05
si_10 µM AOH	16.22	26.25	10.03	0.67	0.63
si_50 µM AOH	16.50	29.22	12.72	3.36	0.10
si_5 µM BaP	16.75	20.25	3.49	-5.87	58.51

	β-Actin	CYP1A1			
	C_T	C_T	Δ C_T	ΔΔ C_T	RQ
P32 (2011/08/31)					
DMSO	16.90	26.68	9.78	0.00	1.00
0.1 µM AOH	16.93	25.06	8.13	-1.64	3.12
1 µM AOH	16.92	23.82	6.90	-2.88	7.34
10 µM AOH	17.03	27.33	10.31	0.53	0.69
50 µM AOH	16.69	28.12	11.42	1.65	0.32
5 µM BaP	17.03	18.52	1.49	-8.28	311.82
ds_DMSO	16.85	26.30	9.45	0.00	1.00
ds_0.1 µM AOH	16.85	25.16	8.32	-1.13	2.20
ds_1 µM AOH	16.85	23.39	6.54	-2.91	7.51
ds_10 µM AOH	16.62	26.25	9.63	0.18	0.88
ds_50 µM AOH	16.49	28.72	12.23	2.78	0.15
ds_5 µM BaP	16.90	18.51	1.61	-7.84	229.26
si_DMSO	16.62	27.06	10.45	0.00	1.00
si_0.1 µM AOH	16.54	25.97	9.43	-1.02	2.02
si_1 µM AOH	16.76	25.19	8.43	-2.02	4.05
si_10 µM AOH	16.38	28.89	12.51	2.06	0.24
si_50 µM AOH	16.65	30.21	13.56	3.11	0.12
si_5 µM BaP	16.90	19.95	3.04	-7.41	169.57
P31 (2011/09/02)					
DMSO	17.41	26.82	9.41	0.00	1.00
0.1 µM AOH	17.34	25.64	8.31	-1.11	2.16
1 µM AOH	17.48	24.90	7.43	-1.99	3.97
10 µM AOH	17.08	28.04	10.96	1.55	0.34
50 µM AOH	16.83	29.45	12.61	3.20	0.11
5 µM BaP	17.54	18.92	1.38	-8.03	261.83
ds_DMSO	17.16	26.89	9.73	0.00	1.00
ds_0.1 µM AOH	17.02	25.48	8.46	-1.27	2.41
ds_1 µM AOH	16.98	24.14	7.15	-2.57	5.95
ds_10 µM AOH	16.80	27.36	10.56	0.83	0.56
ds_50 µM AOH	16.79	29.88	13.09	3.37	0.10
ds_5 µM BaP	17.39	18.89	1.49	-8.23	300.84
si_DMSO	17.02	27.39	10.37	0.00	1.00
si_0.1 µM AOH	17.07	26.43	9.36	-1.01	2.01
si_1 µM AOH	16.94	25.60	8.66	-1.71	3.27
si_10 µM AOH	16.64	29.84	13.19	2.83	0.14
si_50 µM AOH	17.17	31.84	14.67	4.30	0.05
si_5 µM BaP	17.21	20.61	3.41	-6.96	124.57
	β-Actin	**AhR**			
	C_T	C_T	Δ C_T	ΔΔ C_T	RQ
P20_1 (2011/08/08)					
DMSO	16.37	21.95	5.58	0.00	1.00
0.1 µM AOH	16.50	22.09	5.59	0.01	0.99
1 µM AOH	16.59	22.12	5.53	-0.05	1.04
10 µM AOH	16.89	22.49	5.60	0.01	0.99
50 µM AOH	17.25	22.93	5.68	0.09	0.94
5 µM BaP	17.10	21.82	4.72	-0.86	1.82
P20_2 (2011/08/08)					
DMSO	16.80	22.45	5.65	0.00	1.00
0.1 µM AOH	16.79	22.32	5.54	-0.12	1.09
1 µM AOH	16.82	22.54	5.72	0.06	0.96
10 µM AOH	17.06	22.95	5.88	0.23	0.85
50 µM AOH	16.98	22.87	5.90	0.24	0.85
5 µM BaP	17.42	22.47	5.05	-0.61	1.52
P23 (2011/08/22)					
DMSO	16.57	22.37	5.80	0.00	1.00
0.1 µM AOH	16.52	22.65	6.13	0.33	0.80
1 µM AOH	16.68	22.92	6.24	0.44	0.74
10 µM AOH	16.96	22.41	5.45	-0.35	1.28
50 µM AOH	16.68	22.55	5.87	0.07	0.95
5 µM BaP	16.85	21.67	4.83	-0.97	1.96

	β-Actin	AhR			
	C_T	C_T	Δ C_T	ΔΔ C_T	RQ
P24_1(2011(08/10)					
DMSO	17.01	21.91	4.90	0.00	1.00
0.1 µM AOH	17.58	22.53	4.95	0.05	0.97
1 µM AOH	17.11	21.94	4.83	-0.06	1.05
10 µM AOH	17.12	22.08	4.96	0.06	0.96
50 µM AOH	16.57	21.65	5.08	0.18	0.88
5 µM BaP	17.24	21.43	4.19	-0.71	1.64
ds_DMSO	16.99	22.17	5.17	0.00	1.00
ds_0.1 µM AOH	17.60	22.45	4.85	-0.32	1.25
ds_1 µM AOH	17.23	22.21	4.98	-0.19	1.14
ds_10 µM AOH	17.01	22.38	5.37	0.20	0.87
ds_50 µM AOH	15.97	21.80	5.83	0.65	0.64
ds_5 µM BaP	17.23	21.64	4.41	-0.76	1.69
si_DMSO	16.83	24.30	7.47	0.00	1.00
si_0.1 µM AOH	16.68	24.18	7.50	0.03	0.98
si_1 µM AOH	16.73	24.14	7.41	-0.06	1.04
si_10 µM AOH	16.71	24.78	8.07	0.60	0.66
si_50 µM AOH	16.39	24.81	8.42	0.95	0.52
si_5 µM BaP	16.92	24.21	7.28	-0.19	1.14
P24_2 (2011/08/25)					
DMSO	17.54	22.73	5.20	0.00	1.00
0.1 µM AOH	17.34	22.70	5.37	0.17	0.89
1 µM AOH	17.25	22.53	5.28	0.08	0.95
5 µM AOH	17.31	22.53	5.23	0.03	0.98
10 µM AOH	17.61	22.80	5.19	-0.01	1.01
5 µM BaP	17.57	21.85	4.29	-0.91	1.88
ds_DMSO	17.05	22.55	5.50	0.00	1.00
ds_0.1 µM AOH	17.04	22.53	5.49	-0.01	1.01
ds_1 µM AOH	17.01	22.47	5.45	-0.05	1.03
ds_5 µM AOH	17.23	22.69	5.46	-0.04	1.03
ds_10 µM AOH	16.96	22.59	5.63	0.13	0.91
ds_DMSO	16.94	22.56	5.62	0.00	1.00
ds_5 µM BaP	17.15	21.92	4.77	-0.86	1.81
si_DMSO	16.67	24.53	7.87	0.00	1.00
si_0.1 µM AOH	16.70	24.51	7.81	-0.06	1.04
si_1 µM AOH	16.66	24.54	7.88	0.01	0.99
P24_2 (2011/08/25)					
si_5 µM AOH	16.48	24.74	8.26	0.39	0.76
si_10 µM AOH	16.56	24.94	8.38	0.51	0.70
si_5 µM BaP	17.35	25.16	7.81	-0.06	1.04
P27 (2011/09/16)					
DMSO	16.79	21.84	5.05	0.00	1.00
0.1 µM AOH	16.81	21.77	4.96	-0.09	1.06
1 µM AOH	16.89	21.86	4.97	-0.08	1.06
10 µM AOH	16.60	21.96	5.36	0.31	0.81
50 µM AOH	16.29	21.67	5.38	0.33	0.79
5 µM BaP	16.89	21.11	4.23	-0.82	1.77
ds_DMSO	16.62	22.02	5.40	0.00	1.00
ds_0.1 µM AOH	16.63	21.96	5.33	-0.07	1.05
ds_1 µM AOH	16.69	21.86	5.17	-0.23	1.17
ds_10 µM AOH	16.55	22.06	5.51	0.12	0.92
ds_50 µM AOH	16.15	21.80	5.66	0.26	0.84
ds_5 µM BaP	16.80	21.42	4.62	-0.78	1.71
si_DMSO	16.32	23.63	7.30	0.00	1.00
si_0.1 µM AOH	16.87	23.97	7.10	-0.20	1.15
si_1 µM AOH	16.36	23.60	7.24	-0.06	1.04
si_10 µM AOH	16.17	24.73	8.56	1.25	0.42
si_50 µM AOH	16.39	24.24	7.85	0.54	0.69
si_5 µM BaP	16.60	23.82	7.22	-0.08	1.06

	β-Actin	AhR			
	C_T	C_T	Δ C_T	ΔΔ C_T	RQ
P32 (2011/09/13)					
DMSO	17.27	22.41	5.15	0.00	1.00
0.1 µM AOH	16.94	22.22	5.28	0.13	0.91
1 µM AOH	17.10	22.23	5.13	-0.02	1.02
10 µM AOH	17.20	22.73	5.53	0.38	0.77
50 µM AOH	16.79	22.06	5.27	0.12	0.92
5 µM BaP	17.16	21.66	4.50	-0.65	1.57
ds_DMSO	16.95	22.38	5.43	0.00	1.00
ds_0.1 µM AOH	16.96	22.37	5.41	-0.02	1.02
ds_1 µM AOH	16.95	22.35	5.40	-0.03	1.02
ds_10 µM AOH	16.76	22.36	5.60	0.17	0.89
ds_50 µM AOH	16.55	21.99	5.43	0.00	1.00
ds_5 µM BaP	17.00	21.90	4.90	-0.53	1.44
si_DMSO	16.76	24.04	7.28	0.00	1.00
si_0.1 µM AOH	16.59	24.34	7.75	0.47	0.72
si_1 µM AOH	16.75	24.57	7.81	0.53	0.69
si_10 µM AOH	16.46	24.70	8.24	0.95	0.52
si_50 µM AOH	16.78	24.76	7.98	0.70	0.62
si_5 µM BaP	17.05	23.90	6.85	-0.43	1.35
P31 (2011/09/06)					
DMSO	16.83	22.66	5.83	0.00	1.00
0.1 µM AOH	16.80	22.71	5.91	0.08	0.94
1 µM AOH	17.46	22.90	5.44	-0.38	1.30
10 µM AOH	16.64	22.96	6.32	0.49	0.71
50 µM AOH	16.35	22.45	6.10	0.27	0.83
5 µM BaP	17.00	22.10	5.09	-0.73	1.66
ds_DMSO	16.63	22.77	6.14	0.00	1.00
ds_0.1 µM AOH	16.57	22.72	6.15	0.01	0.99
ds_1 µM AOH	16.47	22.60	6.13	-0.01	1.01
ds_10 µM AOH	16.18	22.62	6.44	0.30	0.81
ds_50 µM AOH	16.01	22.34	6.33	0.18	0.88
ds_5 µM BaP	16.84	22.13	5.29	-0.86	1.81
si_DMSO	16.48	24.82	8.34	0.00	1.00
si_0.1 µM AOH	16.64	24.96	8.31	-0.03	1.02
si_1 µM AOH	16.43	24.10	7.68	-0.67	1.59
si_10 µM AOH	16.06	25.05	8.99	0.65	0.64
si_50 µM AOH	16.62	25.50	8.88	0.54	0.69
si_5 µM BaP	16.74	24.43	7.69	-0.65	1.57

Table 32: Arithmetic mean and SD of CYP1A1 and AhR relative quantities in KYSE510-cells 48 h post-transfection and after 24 h AOH-treatment. The RQ-values are given in table 31, whereas the grey shaded outliers are not used for the calculation of the arithmetic mean RQ, depicted in figure 28 B, 29 B and 31.

	CYP1A1					
	non-transfected		ds_RNA		si_RNA	
	mean RQ	SD	mean RQ	SD	mean RQ	SD
DMSO	1.00	0.00	1.00	0.00	1.00	0.00
0.1µM AOH	1.93	0.52	2.16	0.27	1.92	0.16
1µM AOH	7.82	0.35	7.45	1.20	4.07	0.03
10µM AOH	7.08	2.63	6.82	1.48	0.58	0.04
50µM AOH	0.55	0.31	0.16	0.06	0.08	0.03
5µM BaP	276.91	31.56	235.74	50.71	66.96	8.41
	AhR					
	non-transfected		ds_RNA		si_RNA	
	mean RQ	SD	mean RQ	SD	mean RQ	SD
DMSO	1.00	0.00	1.00	0.00	1.00	0.00
0.1µM AOH	0.96	0.09	1.07	0.07	0.93	0.16
1µM AOH	1.02	0.04	1.03	0.00	0.76	0.00
10µM AOH	0.92	0.08	0.90	0.02	0.68	0.02
50µM AOH	0.86	0.05	0.91	0.07	0.63	0.07
5µM BaP	1.67	0.11	1.66	0.16	1.08	0.04

Table 33: CYP1A1 and AhR relative quantities in KYSE510-cells, 15 min pre-treated with 10 µM MNF and subsequent AME-treatment for 24 h.

	β-Actin	CYP1A1				AhR			
	C_T	C_T	Δ C_T	ΔΔ C_T	RQ	C_T	Δ C_T	ΔΔ C_T	RQ
P17_1 (2011/04/01)									
DMSO	21.30	25.04	3.74	0.00	1.00	24.81	3.52	0.00	1.00
1µM AME	20.24	25.25	5.00	1.26	0.42	25.84	5.60	2.08	0.24
10µM AME	20.44	27.02	6.58	2.84	0.14	26.17	5.73	2.21	0.22
P17_2 (2011/04/01)									
DMSO	17.52	23.72	6.21	0.00	1.00	23.23	5.71	0.00	1.00
0.1µM AME	19.28	25.11	5.82	-0.38	1.30	25.27	5.99	0.27	0.83
1µM AME	18.00	23.63	5.63	-0.58	1.49	23.90	5.90	0.18	0.88
10µM AME	20.89	28.30	7.41	1.20	0.44	26.68	5.79	0.08	0.95
P19_1 (2011/04/18)									
DMSO	18.78	23.95	5.18	0.00	1.00	24.79	6.01	0.00	1.00
0.1µM AME	18.69	24.10	5.41	0.24	0.85	24.48	5.79	-0.22	1.16
1µM AME	18.95	26.50	7.56	2.38	0.19	24.97	6.03	0.02	0.99
5µM AME	19.13	27.95	8.82	3.65	0.08	24.94	5.81	-0.20	1.15
10µM AME	19.50	28.79	9.29	4.12	0.06	25.87	6.36	0.35	0.78
10µM AME-MNF	18.96	29.67	10.72	5.54	0.02	25.05	6.10	0.08	0.94
P19_2 (2011/04/18)									
DMSO	19.48	24.28	4.81	0.00	1.00	25.06	5.58	0.00	1.00
0.1µM AME	19.87	24.80	4.93	0.12	0.92	25.42	5.55	-0.03	1.02
1µM AME	19.18	25.31	6.13	1.32	0.40	24.69	5.50	-0.08	1.06
5µM AME	18.72	27.88	9.16	4.36	0.05	24.50	5.78	0.20	0.87
10µM AME	19.31	27.42	8.11	3.30	0.10	24.94	5.63	0.05	0.96
10µM AME-MNF	22.65	32.27	9.62	4.82	0.04	28.14	5.49	-0.09	1.07
P21_1 (2011/04/21)									
DMSO	19.19	24.04	4.85	0.00	1.00	25.98	6.79	0.00	1.00
0.1µM AME	28.88	36.92	8.04	3.19	0.11	36.01	7.13	0.34	0.79
1µM AME	18.85	25.00	6.15	1.30	0.41	25.08	6.23	-0.55	1.47
5µM AME	19.10	26.64	7.54	2.69	0.15	25.78	6.68	-0.10	1.07
10µM AME	19.37	28.05	8.68	3.83	0.07	26.16	6.79	0.01	1.00
10µM AME-MNF	19.95	28.85	8.90	4.05	0.06	26.93	6.99	0.20	0.87
P21_2 (2011/04/21)									
DMSO	29.65	35.53	5.89	0.00	1.00	35.05	5.40	0.00	1.00
0.1µM AME	21.82	26.39	4.57	-1.32	2.49	27.03	5.21	-0.20	1.15
1µM AME	19.76	25.64	5.88	-0.01	1.00	26.11	6.35	0.95	0.52
5µM AME	19.47	26.90	7.43	1.54	0.34	25.92	6.45	1.05	0.48
10µM AME	18.92	27.50	8.58	2.70	0.15	25.80	6.87	1.47	0.36
10µM AME-MNF	19.18	27.97	8.79	2.90	0.13	26.15	6.97	1.57	0.34
P28_2 (2011/05/12)									
DMSO-Med	19.77	29.61	9.84	0.00	1.00	23.94	4.16	0.00	1.00
MNF-Med	21.05	25.06	4.01	-5.83	56.83	25.03	3.98	-0.18	1.14
P28_2 (2011/05/12)									
DMSO-Med	20.55	30.78	10.23	0.00	1.00	24.94	4.39	0.00	1.00
MNF-Med	20.12	24.93	4.81	-5.41	42.65	24.45	4.34	-0.05	1.04
P29_1 (2011/05/13)									
DMSO-Med	18.41	27.69	9.28	0.00	1.00	23.31	4.90	0.00	1.00
MNF-Med	20.61	25.88	5.27	-4.00	16.04	25.78	5.17	0.28	0.83
P29_2 (2011/05/13)									
DMSO-Med	17.57	27.18	9.61	0.00	1.00	23.81	6.23	0.00	1.00
MNF-Med	17.26	24.13	6.87	-2.74	6.68	23.43	6.17	-0.06	1.05
P30_1 (2011/08/26)									
DMSO	16.29	23.01	6.72	0.00	1.00	22.37	6.07	0.00	1.00
0.1µM AME	18.95	24.70	5.75	-0.97	1.95	23.91	4.96	-1.11	2.17
10µM AME	16.35	26.46	10.11	3.39	0.10	22.51	6.16	0.09	0.94
DMSO-Med	16.14	25.42	9.28	0.00	1.00	22.58	6.45	0.00	1.00
MNF-Med	16.32	23.94	7.62	-1.66	3.16	22.68	6.36	-0.09	1.06
MNF-DMSO	16.29	23.01	6.72	-2.57	5.92	22.37	6.07	-0.37	1.29

	β-Actin	CYP1A1				AhR			
	C_T	C_T	Δ C_T	ΔΔ C_T	RQ	C_T	Δ C_T	ΔΔ C_T	RQ
P30_2 (2011/08/26)									
DMSO	16.27	22.95	6.68	0.00	1.00	22.26	5.98	0.00	1.00
0.1µM AME	16.38	23.45	7.07	0.40	0.76	22.32	5.93	-0.05	1.03
10µM AME	16.37	25.84	9.47	2.79	0.14	22.55	6.18	0.20	0.87
DMSO-Med	16.19	25.30	9.11	0.00	1.00	22.53	6.34	0.00	1.00
MNF-Med	16.23	22.62	6.39	-2.73	6.61	22.50	6.27	-0.07	1.05
MNF-DMSO	16.27	22.95	6.68	-2.44	5.42	22.26	5.98	-0.36	1.28
P30_1 (2011/08/29)									
DMSO-Med	18.38	27.86	9.49	0.00	1.00	23.81	5.43	0.00	1.00
MNF-Med	16.44	22.25	5.81	-3.67	12.76	23.05	6.61	1.17	0.44
P30_2 (2011/08/29)									
DMSO-Med	17.59	26.93	9.34	0.00	1.00	23.75	6.16	0.00	1.00
MNF-Med	16.55	22.00	5.44	-3.90	14.90	22.95	6.40	0.24	0.85
P31_1 (2011/09/05)									
DMSO	15.85	24.26	8.41	0.00	1.00	22.39	6.53	0.00	1.00
1µM AME	16.40	26.07	9.67	1.26	0.42	22.89	6.49	-0.04	1.03
DMSO-Med	15.90	25.54	9.64	0.00	1.00	22.62	6.73	0.00	1.00
MNF-Med	15.75	23.14	7.39	-2.26	4.77	22.66	6.91	0.18	0.88
MNF-DMSO	15.85	24.26	8.41	-1.23	2.35	22.39	6.53	-0.19	1.14
P31_2 (2011/09/05)									
DMSO	15.84	23.15	7.31	0.00	1.00	22.35	6.51	0.00	1.00
1µM AME	15.85	24.32	8.46	1.15	0.45	22.68	6.83	0.32	0.80
DMSO-Med	15.99	25.97	9.98	0.00	1.00	22.77	6.78	0.00	1.00
MNF-Med	16.00	22.60	6.60	-3.38	10.41	23.09	7.09	0.31	0.81
MNF-DMSO	15.84	23.15	7.31	-2.67	6.36	22.35	6.51	-0.27	1.21

Table 34: Arithmetic mean and SD of CYP1A1 relative quantities in KYSE510-cells 15 min pre-treated with 10 µM MNF and subsequently AME-treatment for 24 h. The RQ-values are given in table 33, whereas the grey shaded outliers are not used for the calculation of the arithmetic mean RQ, depicted in figure 32.

	mean RQ	SD
DMSO-Med	1.00	0.00
MNF-Med	11.23	1.90
DMSO	5.90	0.38
0.1 µM AME	5.65	1.22
1 µM AME	2.46	0.10
5 µM AME	0.56	0.26
10 µM AME	0.60	0.19

Table 35: GST activity determined in the GST assay according to Habig *et al.* in HT29-cells, cultivated for 48 h and treated with AME for 24 h.

	slope/ k	GST activity [µmol/ml*min]	β (protein) [mg/ml]	GST activity [nmol/min*mg]	mean GST act. [nmol/min*mg]	mean GST activity [%]
2011/06/03	dilution factor (df) = 20					
DMSO	0.0531	0.2457	0.850	289.23	290.42	107.15
	0.0535	0.2477	0.850	291.60		
DMSO (AOH)	0.0509	0.2356	0.850	277.36	285.31	105.26
	0.0538	0.2491	0.850	293.26		
0.01 µM AME	0.0549	0.2539	0.928	273.72	282.38	104.18
	0.0583	0.2700	0.928	291.04		
0.1 µM AME	0.0542	0.2508	0.857	292.48	293.78	108.39
	0.0546	0.2530	0.857	295.08		
1 µM AME	0.0593	0.2745	1.514	181.26	179.30	66.15
	0.0580	0.2685	1.514	177.33		
10 µM AME	0.0604	0.2796	0.993	281.57	293.05	108.12
	0.0653	0.3024	0.993	304.53		
50 µM AME	0.0498	0.2305	0.975	236.35	233.23	86.05
	0.0485	0.2245	0.975	230.11		
2011/06/08	df = 20					
DMSO	0.0566	0.2622	1.017	257.81	251.47	92.78
	0.0539	0.2493	1.017	245.13		
DMSO (AOH)	0.0662	0.3066	1.127	272.14	273.15	100.77
	0.0667	0.3089	1.127	274.16		

	slope/ k	GST activity [µmol/ml*min]	β (protein) [mg/ml]	GST activity [nmol/min*mg]	mean GST act. [nmol/min*mg]	mean GST activity [%]
0.01 µM AME	0.0568	0.2630	1.026	256.33	248.43	91.65
	0.0533	0.2468	1.026	240.53		
0.1 µM AME	0.0529	0.2451	0.981	249.82	259.35	95.68
	0.0570	0.2638	0.981	268.88		
1 µM AME	0.0621	0.2874	1.141	251.89	249.39	92.01
	0.0608	0.2817	1.141	246.89		
10 µM AME	0.0597	0.2764	0.985	280.74	238.21	87.88
	0.0416	0.1927	0.985	195.67		
50 µM AME	0.0626	0.2896	0.994	291.45	281.69	103.93
	0.0584	0.2702	0.994	271.94		
2011/06/17	df = 10					
DMSO	0.0691	0.1599	0.770	207.68	213.23	78.67
	0.0728	0.1684	0.770	218.78		
DMSO (AOH)	0.0723	0.3345	1.307	255.95	259.56	95.76
	0.0743	0.3440	1.307	263.17		
0.01 µM AME	0.0743	0.1720	0.768	223.88	235.12	86.74
	0.0818	0.1893	0.768	246.36		
0.1 µM AME	0.0756	0.1749	0.736	237.50	248.93	91.84
	0.0828	0.1917	0.736	260.36		
1 µM AME	0.0841	0.1947	0.773	251.96	248.38	91.64
	0.0817	0.1892	0.773	244.81		
10 µM AME	0.0791	0.1832	0.778	235.58	235.58	86.91
	0.0806	0.1866	0.816	228.73		
50 µM AME	0.0691	0.1599	0.770	207.68	228.73	84.39
2011/06/22	df = 20					
DMSO	0.0612	0.2833	0.916	309.12	306.48	113.07
	0.0601	0.2785	0.916	303.83		
0.01 µM AME	0.0686	0.3176	0.816	388.93	372.00	137.24
	0.0626	0.2899	0.816	355.07		
0.1 µM AME	0.0704	0.3257	0.915	356.00	355.81	131.27
	0.0703	0.3254	0.915	355.63		
1 µM AME	0.0638	0.2952	1.001	294.95	298.39	110.09
	0.0653	0.3021	1.001	301.82		
10 µM AME	0.0684	0.3165	1.073	294.80	294.64	108.70
	0.0683	0.3161	1.073	294.49		
50 µM AME	0.0703	0.3256	1.054	308.79	307.14	113.32
	0.0696	0.3221	1.054	305.49		
2011/06/28	df = 20					
DMSO	0.0607	0.2810	1.042	269.78	265.81	98.07
	0.0589	0.2727	1.042	261.84		
0.1 µM AME	0.0640	0.2965	0.812	364.88	351.62	129.72
	0.0594	0.2749	0.812	338.35		
1 µM AME	0.0575	0.2664	0.853	312.28	318.56	117.53
	0.0598	0.2771	0.853	324.83		
10 µM AME	0.0641	0.2966	1.107	267.82	274.43	101.25
	0.0672	0.3112	1.107	281.04		
2011/07/01	df = 20					
DMSO	0.0708	0.3280	1.191	275.41	271.64	100.22
	0.0689	0.3190	1.191	267.87		
0.01 µM AME	0.0652	0.3018	1.108	272.32	274.48	101.27
	0.0662	0.3066	1.108	276.65		
0.1 µM AME	0.0742	0.3437	1.334	257.66	261.40	96.44
	0.0764	0.3537	1.334	265.15		
1 µM AME	0.0782	0.3622	1.265	286.37	277.35	102.32
	0.0733	0.3394	1.265	268.33		
10 µM AME	0.0628	0.2907	1.146	253.57	264.83	97.70
	0.0684	0.3165	1.146	276.09		

Table 36: Arithmetic mean and SD of GST-activities in HT29-cells. The GST-activities are given in table 35, whereas the grey-shaded outliers are not used for the calculation of the arithmetic mean. In figure 33A the mean GST-activities of all experiments are depicted as T/C[%].

	mean GST activity [nmol/min*mg]	mean GST activity [%]	SD [%]
DMSO	271.05	100.00	4.68
0.01 µM AME	260.10	95.96	7.06
0.1 µM AME	295.15	108.89	16.10
1 µM AME	278.41	102.72	10.11
10 µM AME	266.79	98.43	8.68
50 µM AME	262.70	96.92	12.18

Table 37: GST activity determined in the GST assay according to Habig *et al.* in HT29-cells, cultivated for 48 h and treated with AOH for 24 h.

	slope/ k	GST activity [µmol/ml*min]	β (protein) [mg/ml]	GST activity [nmol/min*mg]	mean GST act. [nmol/min*mg]	mean GST activity [%]
2011/06/03	df = 20					
DMSO (AOH)	0.0509	0.2356	0.850	277.36	285.31	104.90
	0.0538	0.2491	0.850	293.26		
DMSO (AME)	0.0531	0.2457	0.850	289.23	290.42	106.78
	0.0535	0.2477	0.850	291.60		
0.01 µM AOH	0.0498	0.2305	0.928	248.50	243.83	89.65
	0.0479	0.2219	0.928	239.17		
0.1 µM AOH	0.0525	0.2430	0.857	283.43	290.88	106.95
	0.0553	0.2558	0.857	298.33		
1 µM AOH	0.0600	0.2777	1.146	242.22	242.22	89.06
10 µM AOH	0.0646	0.2990	0.993	301.09	300.26	110.40
	0.0642	0.2974	0.993	299.43		
50 µM AOH	0.0609	0.2819	0.975	288.96	309.98	113.97
	0.0697	0.3229	0.975	331.00		
2011/06/08	df = 20					
DMSO (AOH)	0.0662	0.3066	1.127	272.14	273.15	100.43
	0.0667	0.3089	1.127	274.16		
DMSO (AME)	0.0566	0.2622	1.017	257.81	251.47	92.46
	0.0539	0.2493	1.017	245.13		
0.01 µM AOH	0.0643	0.2975	0.901	330.37	319.87	117.61
	0.0602	0.2786	0.901	309.37		
0.1 µM AOH	0.0733	0.3394	1.032	328.73	323.61	118.98
	0.0710	0.3288	1.032	318.49		
1 µM AOH	0.0752	0.3480	1.069	325.58	331.82	122.00
	0.0780	0.3613	1.069	338.06		
10 µM AOH	0.0623	0.2884	1.029	280.20	305.75	112.42
	0.0737	0.3411	1.029	331.31		
50 µM AOH	0.0762	0.3529	1.123	314.22	308.41	113.39
	0.0734	0.3399	1.123	302.59		
2011/06/17	df = 20					
DMSO	0.0723	0.3345	1.307	255.95	259.56	95.43
	0.0743	0.3440	1.307	263.17		
0.01 µM AOH	0.0723	0.3349	1.300	257.60	259.24	95.31
	0.0733	0.3392	1.300	260.87		
0.1 µM AOH	0.0552	0.2556	1.112	229.89	260.67	95.84
	0.0700	0.3240	1.112	291.45		
1 µM AOH	0.0694	0.3214	1.068	301.01	307.81	113.17
	0.0726	0.3360	1.068	314.62		
10 µM AOH	0.0629	0.2914	1.134	257.07	268.08	98.57
	0.0683	0.3164	1.134	279.09		
50 µM AOH	0.0701	0.3245	1.049	309.46	307.16	112.93
	0.0690	0.3197	1.049	304.86		

Table 38: Arithmetic mean and SD of GST-activities in HT29-cells. The GST-activities are given in table 37, whereas the grey-shaded outliers are not used for the calculation of the arithmetic mean. In figure 33 B the mean GST-activities of all experiments are depicted as T/C [%].

	mean GST activity [nmol/min*mg]	mean GST activity [%]	SD [%]
DMSO	271.98	100.00	5.44
0.01 µM AOH	274.31	100.86	12.07
0.1 µM AOH	291.72	107.26	9.45
1 µM AOH	293.95	108.08	13.92
10 µM AOH	291.36	107.13	6.11
50 µM AOH	308.52	113.43	0.42

Table 39: GST activity determined in the GST assay according to Habig et al. in HT29-cells, cultivated for 48 h and treated with MEN, BaP, tBHP, BSO, CGA, CGA+Tri and CGA+Tri+Kat for 24 h.

	slope/ k	GST activity [µmol/ml*min]	β (protein) [mg/ml]	GST activity [nmol/min*mg]	mean GST act. [nmol/min*mg]	mean GST activity [%]
2011/06/03	df = 20					
1% DMSO	0.0531	0.2457	0.850	289.23	290.42	128.72
	0.0535	0.2477	0.850	291.60		
20 µM MEN (AME)	0.0514	0.2380	1.142	208.29	207.96	92.17
	0.0512	0.2372	1.142	207.62		
20 µM MEN (AOH)	0.0594	0.2750	1.142	240.68	247.27	109.60
	0.0626	0.2900	1.142	253.87		
2011/06/08	df = 20					
1% DMSO	0.0566	0.2622	1.017	257.81	251.47	111.46
	0.0539	0.2493	1.017	245.13		
20 µM MEN	0.0662	0.3066	0.990	309.54	307.24	136.17
	0.0652	0.3020	0.990	304.93		
5 µM BaP	0.0691	0.3200	1.050	304.65	298.65	132.37
	0.0664	0.3074	1.050	292.66		
2011/06/17	df = 10					
1% DMSO	0.0691	0.1599	0.770	207.68	213.23	94.51
	0.0728	0.1684	0.770	218.78		
2.5 µM BaP	0.0851	0.1970	0.909	216.71	216.71	96.05
2011/07/13	df = 10					
1% DMSO	0.0433	0.1001	0.484	206.80	212.17	94.04
	0.0455	0.1053	0.484	217.54		
20 µM MEN	0.0504	0.1167	0.507	230.42	230.14	102.00
	0.0503	0.1164	0.507	229.87		
0.1% DMSO	0.0279	0.0645	0.327	197.07	198.18	120.46
	0.0282	0.0652	0.327	199.29		
20 µM MEN	0.0364	0.0842	0.363	232.23	232.23	141.16
	0.0364	0.0842	0.363	232.23		
CGA+Tri_1	0.0275	0.0636	0.310	205.15	202.17	122.89
	0.0267	0.0618	0.310	199.20		
CGA+Tri_2	0.0543	0.1258	0.705	178.47	178.84	108.71
	0.0546	0.1263	0.705	179.20		
CGA+Tri+ Kat_1	0.0377	0.0872	0.447	195.19	200.79	122.05
	0.0398	0.0922	0.447	206.38		
CGA+Tri+ Kat_2	0.0343	0.0793	0.449	176.60	184.63	112.23
	0.0374	0.0866	0.449	192.65		
1% H_2O	0.0459	0.1063	0.488	218.00	219.48	121.20
	0.0465	0.1077	0.488	220.96		
0.5mM BSO	0.0377	0.0872	0.477	182.84	195.47	107.94
	0.0429	0.0993	0.477	208.10		
1mM BSO	0.0525	0.1215	0.566	214.68	218.82	120.83
	0.0545	0.1261	0.566	222.96		
2011/08/05	df = 10					
1% H_2O	0.0999	0.2313	1.356	170.59	172.67	95.35
	0.0994	0.2300	1.356	169.65		
	0.1041	0.2410	1.356	177.77		
50µM tBHP	0.0964	0.2231	1.378	161.89	168.38	92.98
	0.1000	0.2316	1.378	168.04		
	0.1043	0.2415	1.378	175.22		

	slope/ k	GST activity [µmol/ml*min]	β (protein) [mg/ml]	GST activity [nmol/min*mg]	mean GST act. [nmol/min*mg]	mean GST activity [%]
2011/08/20	df = 20					
1% H_2O	0.0610	0.2822	1.024	275.58	274.58	151.62
	0.0605	0.2802	1.024	273.57		
50µM tBHP_1	0.0658	0.3047	1.076	283.23	289.96	160.12
	0.0689	0.3192	1.076	296.69		
50µM tBHP_2	0.0596	0.2758	1.048	263.06	252.74	139.56
	0.0551	0.2552	1.048	243.38		
	0.0570	0.2640	1.048	251.77		
2011/09/09	df = 10					
0.1% DMSO	0.1414	0.3274	2.472	132.41	130.85	79.54
	0.1381	0.3197	2.472	129.29		
10µM CGA	0.1383	0.3201	2.301	139.10	140.48	85.39
	0.1373	0.3179	2.301	138.17		
	0.1439	0.3331	2.338	142.46		
	0.1436	0.3325	2.338	142.19		
CGA+Tiri	0.1563	0.3617	2.501	144.62	136.86	83.19
	0.1389	0.3215	2.501	128.53		
	0.1359	0.3146	2.267	138.77		
	0.1327	0.3072	2.267	135.49		
1% H_2O	0.1487	0.3442	2.289	150.39	151.13	83.46
	0.1502	0.3476	2.289	151.88		
50µM tBHP	0.1493	0.3455	2.304	149.99	137.82	76.10
	0.1405	0.3252	2.304	141.16		
	0.1393	0.3224	2.548	126.53		
	0.1470	0.3404	2.548	133.60		

Table 40: Arithmetic mean and SD of GST-activities in HT29-cells. The GST-activities are given in table 39, whereas the grey-shaded outliers are not used for the calculation of the arithmetic mean. In figure 34 A, B and C the mean GST-activities of all experiments are depicted as T/C [%].

	mean GST activity [nmol/min*mg]	mean GST activity [%]	SD [%]
1%DMSO	225.62	100.00	14.28
20µM MEN(1%)	228.46	101.26	18.86
5µM BaP	298.65	132.37	-
2.5µM BaP	216.71	96.05	-
0.1%DMSO	164.51	100.00	20.46
20µM MEN(0.1%)	232.23	141.16	-
10µM CGA	140.48	85.39	-
CGA+Tiri	169.52	103.04	19.85
CGA+Tri+Kat	200.79	122.05	-
1% H_2O	181.10	112.90	15.75
0.5mM BSO	195.47	107.94	-
1mM BSO	218.82	120.83	-
50µM tBHP	198.72	109.73	36.29

Table 41: GST activity determined in the GST assay according to Habig *et al.* in HT29-cells, cultivated for 48 h and treated with MEN, BaP, tBHP and tBHQ for 1 h.

	slope/ k	GST activity [µmol/ml*min]	β (protein) [mg/ml]	GST activity [nmol/min*mg]	mean GST act. [nmol/min*mg]	mean GST activity [%]
2011/06/17	df = 10					
DMSO	0.0691	0.1599	0.770	207.68	213.23	80.26
	0.0728	0.1684	0.770	218.78		
10 µM MEN	0.0792	0.1833	0.824	222.51	222.51	83.76
20 µM MEN	0.0653	0.1511	0.802	188.44	198.91	74.87
	0.0725	0.1679	0.802	209.37		
	df = 20					
DMSO	0.0723	0.3345	1.307	255.95	259.56	97.70
	0.0743	0.3440	1.307	263.17		
10 µM MEN	0.0698	0.3234	1.358	238.18	242.17	91.16
	0.0722	0.3342	1.358	246.17		
20 µM MEN	0.0736	0.3410	1.313	259.62	259.33	97.62
	0.0735	0.3402	1.313	259.04		

	slope/ k	GST activity [µmol/ml*min]	β (protein) [mg/ml]	GST activity [nmol/min*mg]	mean GST act. [nmol/min*mg]	mean GST activity [%]
2011/06/22	df = 20					
DMSO	0.0612	0.2833	0.916	309.12	306.48	115.36
	0.0601	0.2785	0.916	303.83		
10 µM MEN	0.0732	0.3391	1.321	256.71	247.29	93.08
	0.0679	0.3142	1.321	237.87		
20 µM MEN	0.0680	0.3148	0.924	340.54	329.16	123.90
	0.0635	0.2938	0.924	317.79		
5 µM BaP	0.0728	0.3372	0.996	338.35	335.19	126.17
	0.0715	0.3309	0.996	332.02		
2011/06/28	df = 20					
DMSO	0.0607	0.2810	1.042	269.78	265.81	100.05
	0.0589	0.2727	1.042	261.84		
10 µM MEN	0.0630	0.2918	1.148	254.22	252.25	94.95
	0.0620	0.2872	1.148	250.28		
20 µM MEN	0.0679	0.3144	1.081	290.75	286.23	107.74
	0.0658	0.3046	1.081	281.71		
10 µM tBHQ	0.0546	0.2529	0.968	261.23	281.27	105.87
	0.0630	0.2917	0.968	301.31		
20 µM tBHQ	0.0686	0.3178	1.189	267.26	269.59	101.47
	0.0698	0.3233	1.189	271.91		
2011/07/01	df = 20					
DMSO	0.0708	0.3280	1.191	275.41	271.64	102.25
	0.0689	0.3190	1.191	267.87		
5 µM BaP	0.0741	0.3428	1.198	286.06	262.27	98.72
	0.0617	0.2858	1.198	238.48		
5 µM BaP	0.0603	0.2790	1.096	254.66	256.23	96.44
	0.0610	0.2825	1.096	257.79		
200 µM tBHQ	0.0694	0.3211	1.350	237.83	231.50	87.14
	0.0676	0.3129	1.350	231.81		
	0.0656	0.3036	1.350	224.88		
200 µM tBHQ	0.0663	0.3069	1.166	263.26	276.85	104.21
	0.0705	0.3264	1.166	279.91		
	0.0690	0.3192	1.166	273.80		
2011/08/19	df = 10					
1% H_2O	0.0722	0.1672	0.839	199.27	289.53	100.00
	0.1041	0.2410	0.839	287.30		
	0.1010	0.2338	0.839	278.68		
50 µM tBHP	0.1027	0.2378	0.791	300.38	294.16	101.60
	0.0985	0.2279	0.791	287.94		
50 µM tBHP	0.1077	0.2494	0.842	296.22	284.00	98.09
	0.0988	0.2288	0.842	271.78		

Table 42: Arithmetic mean and SD of GST-activities in HT29-cells. The GST-activities are given in table 41, whereas the grey-shaded outliers are not used for the calculation of the arithmetic mean. In figure 35 A and B the mean GST-activities of all experiments are depicted as T/C [%].

	mean GST activity [nmol/min*mg]	mean GST activity [%]	SD [%]
1%DMSO	265.67	100.00	1.86
10µM MEN	247.24	93.06	1.55
20µM MEN	291.58	109.75	10.82
5µM BaP	284.56	107.11	13.51
10µM tBHQ	281.27	105.87	-
20µM tBHQ	269.59	101.47	-
200µM tBHQ	276.85	104.21	-
1% H_2O	289.53	100.00	-
50µM tBHP	294.16	99.85	1.75

Table 43: GST activity determined in the GST assay according to Habig *et al.* in HT29-cells, cultivated for 48 h and treated with AME for 6 h. In figure 36 the mean GST activity is depicted as T/C [%].

	slope/ k	GST activity [µmol/ml*min]	β (protein) [mg/ml]	GST activity [nmol/min*mg]	mean GST activity [nmol/min*mg]	GST activity [%]	mean GST act. [%]
2011/07/05	df = 10						
DMSO	0.0635	0.1469	0.751	195.48	196.02	100.00	
	0.0638	0.1477	0.751	196.55			
0.01 µM AME	0.0350	0.0811	0.367	220.69	216.11	110.25	
	0.0336	0.0777	0.367	211.53			
0.1 µM AME	0.0276	0.0639	0.373	171.59	190.27	97.07	
	0.0336	0.0778	0.373	208.95			
1 µM AME	0.0518	0.1200	0.578	207.54	218.82	111.63	
	0.0575	0.1330	0.578	230.11			
10 µM AME	0.0511	0.1182	0.541	218.51	216.31	110.35	
	0.0500	0.1158	0.541	214.12			
50 µM AME	0.0369	0.0854	0.383	223.31	220.50	112.49	
	0.0360	0.0833	0.383	217.69			
5 µM BaP_1	0.0287	0.0665	0.381	174.20	190.69	97.28	103.50 (±6.22)
	0.0341	0.0790	0.381	207.18			
5 µM BaP_2	0.0291	0.0674	0.304	221.52	215.08	109.72	
	0.0274	0.0635	0.304	208.64			
200 µM tBHQ_1	0.0328	0.0760	0.362	210.03	209.56	106.91	102.99 (±3.92)
	0.0327	0.0756	0.362	209.10			
200 µM tBHQ_2	0.0255	0.0590	0.297	198.83	194.21	99.08	
	0.0243	0.0563	0.297	189.60			

Table 44: GST activity determined in the GST assay according to Habig et al. in HT29-cells, cultivated for 48 h and treated with SFN and MEN for 9 h. In figure 37 A the mean GST activity is depicted as T/C [%].

	slope/ k	GST activity [µmol/ml*min]	β (protein) [mg/ml]	GST activity [nmol/min*mg]	mean GST act. [nmol/min*mg]	mean GST activity [%]
2011/08/04	df = 10					
1%DMSO	0.0696	0.1610	0.709	227.08	228.76	100.00
	0.0682	0.1579	0.709	222.78		
	0.0724	0.1676	0.709	236.43		
10µM SFN	0.0726	0.1681	0.771	217.94	221.50	96.82
	0.0708	0.1639	0.771	212.49		
	0.0780	0.1805	0.771	234.06		
20µM SFN	0.0711	0.1647	0.755	218.12	226.95	99.21
	0.0759	0.1758	0.755	232.86		
	0.0750	0.1736	0.755	229.88		
20 µM MEN	0.0635	0.1470	0.615	238.90	267.53	116.94
	0.0777	0.1798	0.615	292.26		
	0.0721	0.1670	0.615	271.42		

Table 45: GST activity determined in the GST assay according to Habig *et al.* in HT29-cells, cultivated for 48 h and treated with BaP, tBHQ, MEN and SFN for 16 h. In figure 37 B the mean GST activity is depicted as T/C [%].

	slope/ k	GST activity [µmol/ml*min]	β (protein) [mg/ml]	GST activity [nmol/min*mg]	mean GST act. [nmol/min*mg]	mean GST activity [%]
2011/08/13	df = 20					
1% DMSO	0.07665	0.35485	1.066	332.90	336.01	100.00
	0.07808	0.36148	1.066	339.12		
5 µM BaP	0.08240	0.38146	1.010	377.77	386.60	115.06
	0.08625	0.39931	1.010	395.44		
200 µM tBHQ	0.08430	0.39028	1.095	356.53	346.79	103.21
	0.07969	0.36895	1.095	337.04		
20 µM MEN	0.07554	0.34972	0.989	353.55	353.55	105.22
15 µM SFN	0.07864	0.36406	1.022	356.33	356.33	106.05

Table 46: GST-A1, -A2, -P1, and –T1 relative quantities in HT29-cells, cultivated for 24 h and treated with 50 µM tBHP for 1 h and 24 h, respectively. The RQ-values are depicted in figure 38.

	β-Actin	GST-A1				GST-A2			
	C_T	C_T	Δ C_T	ΔΔ C_T	RQ	C_T	Δ C_T	ΔΔ C_T	RQ
2011/08/22									
H_2O _1h	15.83	34.63	18.80	0.00	1.00	34.00	18.16	0.00	1.00
50 µM tBHP_1h	15.65	34.66	19.01	0.21	0.86	33.94	18.30	0.13	0.91
	β-Actin	**GST-P1**				**GST-T1**			
H_2O _1h	15.83	16.77	0.94	0.00	1.00	25.00	9.17	0.00	1.00
50 µM tBHP_1h	15.65	16.40	0.76	-0.18	1.13	24.49	8.84	-0.33	1.25
	β-Actin	**GST-A1**				**GST-A2**			
H_2O _24h	15.92	34.80	18.88	0.00	1.00	33.38	17.46	0.00	1.00
50 µM tBHP_24h	15.97	33.78	17.81	-1.07	2.10	33.17	17.20	-0.26	1.20
	β-Actin	**GST-P1**				**GST-T1**			
H_2O _24h	15.92	16.49	0.57	0.00	1.00	24.30	8.38	0.00	1.00
50 µM tBHP_24h	15.97	16.60	0.63	0.06	0.96	24.01	8.04	-0.34	1.27

Table 47: GST-A1 and -A2 relative quantities in HT29-cells, cultivated for 24 h and treated with SFN, MEN, tBHQ and BaP for 1 h. The RQ-values are depicted in figure 39.

	β-Actin	GST-A1				GST-A2			
	C_T	C_T	Δ C_T	ΔΔ C_T	RQ	C_T	Δ C_T	ΔΔ C_T	RQ
2011/08/12									
DMSO	15.88	34.51	18.63	0.00	1.00	33.76	17.88	0.00	1.00
15 µM SFN	16.10	34.75	18.64	0.01	0.99	33.74	17.63	-0.25	1.19
20 µM MEN	16.18	34.26	18.09	-0.55	1.46	33.89	17.71	-0.17	1.13
200 µM tBHQ	15.89	34.27	18.38	-0.25	1.19	33.83	17.93	0.05	0.97
5 µM BaP	16.01	34.53	18.52	-0.11	1.08	33.55	17.54	-0.35	1.27

Table 48: GST activity determined in the GST assay according to Habig *et al.* in HepG2-cells, cultivated for 48 h and treated with Que and SFN for 2 h and 24 h, respectively. In figure 40 A the GST activity is depicted as T/C [%].

	slope/ k	GST activity [µmol/ml*min]	β (protein) [mg/ml]	GST activity [nmol/min*mg]	GST-activity [%]
	df = 2.88				
DMSO	0.03714	0.02476	1.235	20.05	100.00
40 µM Que (2h)	0.01680	0.01120	1.13	9.91	49.44
	df = 4				
DMSO	0.02878	0.02664	1.795	14.84	100.00
15 µM SFN (24 h)	0.03260	0.03018	2.035	14.83	99.91

Table 49: GST activity determined in the GST assay according to Habig *et al.* in HepG2-cells, cultivated for 72 h and treated with BaP and Que for 2 h. In figure 40 B the GST activity is depicted as T/C [%].

	slope/ k	GST activity [µmol/ml*min]	β (protein) [mg/ml]	GST activity [nmol/min*mg]	GST-activity [%]
	df = 4				
DMSO	0.03644	0.03375	2.020	16.71	100.00
5 µM BaP	0.02840	0.02630	2.220	11.85	70.91
40 µM Que	0.01973	0.01827	2.160	8.46	50.63

Table 50: GST-A1, -A2, -P1, and –T1 relative quantities in HepG2-cells, cultivated for 72 h and treated with Que and BaP for 2 h. The RQ-values are depicted in figure 41.

	β-Actin	GST-A1				GST-A2			
	C_T	C_T	Δ C_T	ΔΔ C_T	RQ	C_T	Δ C_T	ΔΔ C_T	RQ
2011/08/22									
DMSO	16.19	30.85	14.65	0.00	1.00	31.92	15.73	0.00	1.00
40 µM Que	16.59	30.81	14.23	-0.43	1.34	32.14	15.56	-0.17	1.12
5 µM BaP	16.27	31.20	14.92	0.27	0.83	32.54	16.27	0.54	0.69
	β-Actin	**GST-P1**				**GST-T1**			
DMSO	16.19	31.59	15.39	0.00	1.00	23.03	6.84	0.00	1.00
40 µM Que	16.59	30.36	13.78	-1.62	3.06	23.19	6.61	-0.23	1.17
5 µM BaP	16.27	28.54	12.27	-3.13	8.73	22.98	6.71	-0.13	1.09

Table 51: GST activity determined in the GST assay according to Habig *et al.* in HT29-cells, cultivated for 72 h and treated with AME, AOH, MEN, CGA and CGA+Tri for 24 h.

	slope/ k	GST activity [µmol/ml*min]	β (protein) [mg/ml]	GST activity [nmol/min*mg]	mean GST act. [nmol/min*mg]	mean GST activity [%]
2011/09/07	df = 10					
0.1%DMSO	0.1269	0.2938	2.105	139.56	139.56	62.04
10µM CGA 1	0.1428	0.3306	2.511	131.68	131.68	58.53
10µM CGA 2	0.1399	0.3238	2.416	134.00	134.00	59.57
CGA+Tri 1	0.1402	0.3246	2.442	132.92	132.92	59.09
CGA+Tri 2	0.1515	0.3508	2.191	160.08	160.08	71.16
2011/09/14	df = 40					
1%DMSO 1	0.1145	1.0600	3.630	292.02	300.11	110.46
	0.1208	1.1187	3.630	308.21		
1 µM AME	0.0921	0.8526	3.479	245.06	247.83	91.22
	0.0942	0.8719	3.479	250.60		
10 µM AME	0.0977	0.9044	3.882	232.96	230.62	84.89
	0.0957	0.8863	3.882	228.29		
50 µM AME	0.0926	0.8571	3.548	241.59	242.37	89.21
	0.0932	0.8626	3.548	243.15		
0.1 µM AOH	0.0885	0.8195	3.149	260.26	264.79	97.46
	0.0916	0.8480	3.149	269.31		
1 µM AOH	0.1039	0.9619	3.100	310.32	337.01	124.05
	0.1218	1.1274	3.100	363.71		
10 µM AOH	0.0921	0.8528	3.140	271.61	300.49	110.60
	0.1117	1.0341	3.140	329.37		
20 µM MEN 1	0.0862	0.7979	3.684	216.57	224.70	82.71
	0.0926	0.8579	3.684	232.83		
20 µM MEN 1_2	0.1081	1.0012	3.684	271.73	267.34	98.40
	0.1046	0.9688	3.684	262.95		
20 µM MEN 2	0.0783	0.7248	3.132	231.39	238.87	87.92
	0.0833	0.7717	3.132	246.35		
0.1% DMSO	0.0761	0.7046	3.120	225.80	259.65	115.42
	0.0891	0.8250	3.120	264.38		
	0.0871	0.8061	3.172	254.08		
	0.1008	0.9337	3.172	294.33		
10 µM CGA 1	0.0860	0.7960	3.191	249.46	270.36	120.18
	0.1004	0.9294	3.191	291.27		
10 µM CGA 1a	0.0901	0.8346	3.112	268.18	283.70	126.11
	0.1006	0.9311	3.112	299.21		
10 µM CGA 2	0.0775	0.7176	3.544	202.50	219.01	97.36
	0.0901	0.8347	3.544	235.53		
10 µM CGA 2a	0.0963	0.8918	3.303	270.02	259.02	115.14
	0.0885	0.8192	3.303	248.03		
2011/09/14	df = 40					
1% DMSO 1	0.1019	0.9436	3.728	253.08	266.12	97.95
	0.1124	1.0408	3.728	279.15		
1 µM AME	0.0967	0.8957	3.991	224.41	224.39	82.59
	0.0967	0.8955	3.991	224.37		
10 µM AME	0.0980	0.9073	3.317	273.50	275.01	101.22
	0.0991	0.9173	3.317	276.51		
50 µM AME	0.0983	0.9099	3.544	256.70	257.27	94.69
	0.0987	0.9139	3.544	257.83		
0.1 µM AOH	0.0960	0.8888	3.167	280.59	293.97	108.20
	0.1051	0.9735	3.167	307.34		
1 µM AOH	0.0961	0.8900	3.191	278.89	304.81	112.19
	0.1140	1.0555	3.191	330.74		
10 µM AOH	0.1021	0.9449	3.261	289.75	308.34	113.49
	0.1151	1.0662	3.261	326.93		
20 µM MEN 1a	0.0902	0.8356	3.185	262.36	273.10	100.52
	0.0976	0.9041	3.185	283.84		
20 µM MEN 2a	0.0940	0.8703	3.341	260.45	275.28	101.32
	0.1047	0.9694	3.341	290.12		

	slope/ k	GST activity [µmol/ml*min]	β (protein) [mg/ml]	GST activity [nmol/min*mg]	mean GST act. [nmol/min*mg]	mean GST activity [%]
2011/09/17	df = 40					
DSMO 1	0.1133	1.0494	3.876	270.76	297.68	109.57
	0.1359	1.2581	3.876	324.60		
DMSO 2	0.1175	1.0881	3.871	281.08	269.82	99.32
	0.1081	1.0010	3.871	258.57		
DMSO 2 (neu)	0.1173	1.0866	3.871	280.67	279.11	102.73
	0.1160	1.0745	3.871	277.54		
1 µM AME	0.1058	0.9799	3.740	262.01	273.97	100.84
	0.1155	1.0694	3.740	285.94		
10 µM AME	0.1091	1.0104	3.704	272.79	281.05	103.45
	0.1157	1.0716	3.704	289.31		
50 µM AME	0.1079	0.9994	3.805	262.67	274.95	101.20
	0.1180	1.0929	3.805	287.24		
0.1 µM AOH	0.1238	1.1467	3.700	309.91	302.05	111.18
	0.1176	1.0885	3.700	294.19		
1 µM AOH	0.1122	1.0393	3.789	274.29	285.05	104.92
	0.1210	1.1208	3.789	295.80		
10 µM AOH	-0.0530	-0.4905	4.331	-113.26	-113.26	-41.69
	-0.0530	-0.4905	4.331	-113.26		
20 µM MEN 1	0.1131	1.0469	3.990	262.36	264.27	97.27
	0.1147	1.0621	3.990	266.18		
20 µM MEN 1a	0.1068	0.9892	4.052	244.13	252.81	93.05
	0.1144	1.0596	4.052	261.49		
20 µM MEN 2	0.1011	0.9364	3.959	236.53	228.59	84.14
	0.0943	0.8736	3.959	220.66		
20 µM MEN 2a	0.1045	0.9678	3.490	277.30	281.07	103.46
	0.1074	0.9941	3.490	284.84		
0.1% DMSO	0.1018	0.9428	3.557	265.03	275.66	122.54
	0.1100	1.0185	3.557	286.30		
10 µM CGA_1	0.0976	0.9033	3.767	239.80	242.43	107.77
	0.0997	0.9232	3.767	245.07		
10 µM CGA_2	0.1068	0.9889	3.671	269.36	270.46	120.23
	0.1077	0.9969	3.671	271.55		

Table 52: Arithmetic mean and SD of GST-activities in HT29-cells. The GST-activities are given in table 51, whereas the grey-shaded outliers are not used for the calculation of the arithmetic mean. In figure 43 A, B and C the mean GST-activities of all experiments are depicted as T/C [%].

	mean GST activity [nmol/min*mg]	mean GST activity [%]	SD [%]
1%DMSO	271.68	100.00	2.01
1µM AME	248.73	91.55	7.45
10µM AME	262.23	96.52	8.27
50µM AME	258.20	95.04	4.90
0.1µM AOH	286.94	105.61	5.89
1µM AOH	308.96	113.72	7.88
10µM AOH	304.42	112.05	1.45
20µM MEN	272.21	100.19	2.18
0.1%DMSO	224.96	100.00	27.00
10µM CGA	226.33	100.61	25.36
CGA+Tri	146.50	65.12	6.04